

7-12-2010

The Nature of the O-2/O-5 Cooperative Effect and Its Role in Chemical Glycosylation

Laurel Kathryn Mydock

University of Missouri-St. Louis, lmydock@yahoo.com

Follow this and additional works at: <https://irl.umsl.edu/dissertation>



Part of the [Chemistry Commons](#)

Recommended Citation

Mydock, Laurel Kathryn, "The Nature of the O-2/O-5 Cooperative Effect and Its Role in Chemical Glycosylation" (2010).
Dissertations. 473.

<https://irl.umsl.edu/dissertation/473>

This Dissertation is brought to you for free and open access by the UMSL Graduate Works at IRL @ UMSL. It has been accepted for inclusion in Dissertations by an authorized administrator of IRL @ UMSL. For more information, please contact marvinh@umsl.edu.

**THE NATURE OF THE O-2/O-5 COOPERATIVE EFFECT
AND ITS ROLE IN CHEMICAL GLYCOSYLATION**

By

LAUREL K. MYDOCK

Master of Science (Chemistry), May 2008

Bachelor of Science (Mathematics), May 2002

A DISSERTATION

Submitted to the Graduate School of the

UNIVERSITY OF MISSOURI – ST. LOUIS
in Partial Fulfillment of the Requirements for the degree of

DOCTOR OF PHILOSOPHY

in

CHEMISTRY

April 9th 2010

Dissertation Committee

Prof. Alexei V. Demchenko, Ph.D. (Chair)

Prof. Stephen M. Holmes, Ph.D.

Prof. Christopher D. Spilling, Ph.D.

Prof. Rudolph E. K. Winter, Ph.D.

ABSTRACT

The Nature of the O-2/O-5 Cooperative Effect and Its Role in Chemical Glycosylation

Laurel K. Mydock

Doctor of Philosophy

University of Missouri – St. Louis

Prof. Alexei V. Demchenko, Advisor

Since carbohydrates were first discovered, understanding the structure, reactivity, and function of these bioorganic compounds has remained of great priority. However, as the appreciation for the biological roles of carbohydrates intensifies, a growing demand for efficient and scalable methods towards the synthesis of these challenging molecules has become even more imperative. While modern synthetic techniques have allowed us to readily achieve most glycosidic linkages, it is the inability to effectively predict and control the stereoselectivity of the glycosylation reaction that has remained the synthetic hurdle.

Herein, much effort has been placed in the investigation of “mixed-patterned” glycosyl donors as they have shown some interesting behaviors in glycosylation. Initial findings revealed that the behavior of these particular donors could be rationalized by a theory developed in our laboratory, entitled the “O-2/O-5 cooperative effect,” wherein the energetic consequences associated with particular protecting group patterns were analyzed. As a result, the work of this doctoral dissertation is centered upon the exploration of glycosyl donor protecting groups, and their effect on both the reactivity and stereoselectivity with which the glycosylation reaction proceeds.

ACKNOWLEDGEMENTS

I would like to express my gratitude to my Ph.D. Advisor, Dr. Alexei V. Demchenko for all of his support. I originally came to University of Missouri – St. Louis with the intention of getting a second Bachelor's Degree (my first was in mathematics). However, my second semester here, I found myself in undergraduate Organic Chemistry II, taught by Dr. Demchenko. It was he who recognized that I had an aptitude for chemistry, and strongly encouraged me to directly pursue graduate studies here at UMSL, without the need for a second Bachelor's Degree. I wasn't even aware that this was an option, and so without his belief in my abilities, I would not have aimed as high, nor made it as far academically. I would also like to thank the various faculty members that have provided valuable chemistry (as well as life) knowledge along the way. Dr Spilling not only served on my dissertation committee, but he helped me to design organic synthesis strategies and his insight proved to be indispensable. Additionally, Dr. Mannino (who I had as a teacher for Advanced Organic, and Medicinal Chemistry classes) instilled confidence in my chemistry abilities and inspired my future direction upon completion of my Ph.D.

Of course, any acknowledgement would not be complete without thanking my family and friends for their continued love and support. My dad and mom, Jim and Linda Roberts, have always had high expectations for me, and have encouraged me to pursue my academic interests to the fullest extent, supporting me 100% of the way. Additionally, I would like to thank my fiancé, Scott, for his infinite patience and understanding, while I was working the long hours necessary to complete my degree.

LIST OF ABBREVIATIONS

Å.....	Angstrom
Ac.....	Acetyl
AgBF ₄	Silver tetrafluoroborate
AgClO ₄	Silver perchlorate
AgNO ₃	Silver nitrate
AgOTf.....	Silver trifluoromethanesulfonate
AgOTs.....	Silver <i>p</i> -toluenesulfonate
AgOMs.....	Silver methanesulfonate
AgPF ₆	Silver hexafluorophosphate
Bn.....	Benzyl
Bz.....	Benzoyl
BF ₃ (OEt) ₂	Boron trifluoride etherate
Bu ₄ NBr.....	Tetrabutylammonium bromide
Cp.....	Cyclopentyl
Cu(OTf) ₂	Copper trifluoromethanesulfonate
d.....	Doublet
DCE.....	1,2-Dichloroethane
DCM.....	Methylene chloride
dd.....	Doublet of doublets
DFT.....	Density functional theory
DMF.....	<i>N,N</i> -Dimethylformamide

DMTST	Dimethyl(methylthio)sulfonium trifluoromethanesulfonate
E _A	Activation energy
Et	Ethyl
EtAc	Ethyl acetate
Et ₂ O	Diethyl ether
EtOH	Ethanol
Gal	Galactose
Glc	Glucose
h	Hour(s)
HR-EI MS	High Resolution Electron Ionization mass spectrum
HR-FAB MS	High Resolution Fast Atom Bombardment mass spectrum
HSEt	S-Ethyl
HSTol	S-Tolyl
Hz	Hertz
<i>i</i> Pr	Isopropyl
KOH	Potassium hydroxide
m	Multiplet
MAN	Mannose
min	Minute
<i>m/z</i>	Mass to charge ratio
Me	Methyl
MeOTf	Methyl trifluoromethanesulfonate
MeI	Methyl iodide

MeCN.....	Acetonitrile
MeOH	Methanol
Me ₃ OBF ₄	Trimethyloxonium tetrafluoroborate
MS.....	Molecular sieves
NaOH	Sodium hydroxide
NaOMe.....	Sodium methoxide
NIS	<i>N</i> -Iodosuccinimide
NMR	Nuclear magnetic resonance
<i>p</i> -TolSCl.....	<i>p</i> -Toluenesulfonyl chloride
Ph	Phenyl
PLC	Preparative layer chromatography
ppm	Parts per million
R _f	Retention factor
rt	Room temperature
SBox.....	<i>S</i> -Benzoxazolyl
s.....	Singlet
t	Triplet
TBDMS.....	tert-Butyldimethylsilyl
TFA.....	Trifluoroacetic acid
TfOH.....	Trifluoromethanesulfonic (triflic) acid
TLC.....	Thin layer chromatography
TMSOTf.....	Trimethylsilyl trifluoromethanesulfonate

CONTENTS

CHAPTER 1

Revisiting the Basic Mechanisms of Glycosylation	17
1.1 Project Background	18
1.2 General Considerations and Basic Mechanisms of Glycosylation	21
1.3 Historical Perspective and Important Lessons from Early Work	22
<i>1.3.1. Development of the glycosylation reaction</i>	22
<i>1.3.2. Discovery of neighboring group participation</i>	25
1.4 Glycosylation Kinetics	29
<i>1.4.1. General energy profile</i>	29
<i>1.4.2. Anomeric effect</i>	33
<i>1.4.3. Halide ion-catalyzed glycosylation</i>	35
1.5 References	37

CHAPTER 2

Current Mechanistic Theories	43
2.1 Current Theories behind Glycosyl Donor Reactivity	44
<i>2.1.1. Protecting groups – electronic effects</i>	44
<i>Armed-disarmed theory</i>	
<i>Expansions of the armed-disarmed theory</i>	
<i>2.1.2. Protecting groups – axial vs. equatorial</i>	47
<i>2.1.3. Pyranose ring conformation (of the glycosyl donor)</i>	49

Conformational superarming

Conformational disarming

2.2	Current Theories behind Glycosylation Stereoselectivity	52
2.2.1	<i>Pyranose ring conformation (of the glycosyl donor) and its influence on the anomeric effect</i>	53
2.2.2	<i>Oxocarbenium ion conformation – approach of the acceptor</i>	54
2.2.3	<i>Oxocarbenium ion conformation – protecting group influence</i>	56
2.3	Exploration of Anomeric Inversion and Participation–Assisted Mechanistic Pathways	60
2.3.1	<i>Displacement of counter-anions (glycosyl triflate)</i>	61
2.3.2	<i>Intramolecular participation</i>	65
2.4	Conclusions and Future Implications	69
2.5	References	70

CHAPTER 3

Discovery of a Superarmed S-Benzoxazolyl Glycosyl Donor	74	
3.1	Introduction	75
3.1.1	<i>Armed-disarmed strategy revisited</i>	75
3.1.2	<i>The O-2/O-5 cooperative effect</i>	77
3.2	Utilization of the O-2/O-5 Cooperative Effect in Superarming Methodology	80
3.2.1	<i>Synthesis of superarmed S-benzoxazolyl glycosyl donors</i>	81
3.2.2	<i>Glycosylation results</i>	82

3.3	Conclusions	86
3.4	Experimental	87
3.5	References	97
CHAPTER 4		
Application of the Superarmed Glycosyl Donor to Chemoselective Oligosaccharide Synthesis		102
4.1	Introduction	103
4.1.1	<i>Chemoselective oligosaccharide synthesis strategy</i>	104
4.2	Application of the Superarmed Glycosyl Donor in Chemoselective Glycosylation	106
4.2.1	<i>Chemoselective activation</i>	106
4.2.2	<i>One-pot trisaccharide synthesis</i>	108
4.2.3	<i>Competitive glycosylations</i>	109
4.3	Conclusions	110
4.4	Experimental	111
4.5	References	122
CHAPTER 5		
Investigation of Sulfonium Species as Key Intermediates in Chemical Glycosylation		125
5.1	Introduction	126
5.2	Discovery of an Anomeric β -Sulfonium Glycoside	129

5.2.1	<i>Initial observation</i>	129
5.2.2	<i>Isolation and characterization</i>	133
5.2.3	<i>Mechanistic rationalization via the O-2/O-5 cooperative effect</i>	135
5.2.4	<i>Investigating other classes of thioglycosides</i>	137
5.3	Investigation of the Counter-anion	137
5.3.1	<i>Methodology for β-sulfonium ion generation</i>	137
5.3.2	<i>Characterization of the silver catalyzed β-sulfonium salts</i>	140
5.3.3	<i>Diastereomer investigation</i>	142
5.4	Glycosylation Results	148
5.5	Expanding Upon the Methodology	154
5.5.1	<i>Dimethyl(methylthio)sulfonium triflate (DMTST) generated sulfonium ion</i>	154
5.5.2	<i>Investigation of superdisarmed α-S-ethyl glycosyl donor</i>	157
5.6	Rationalization	160
5.7	Experimental	165
5.8	References	176
 CHAPTER 6		
Appendix (selected NMR spectral data)		179

LIST OF FIGURES**CHAPTER 1**

- Figure 1.1** Products of intramolecular reaction pathways 26
- Figure 1.2** Anomeric effect 34

CHAPTER 2

- Figure 2.1** Substituent effect and conformational preferences of substituted piperidines 48
- Figure 2.2** (a) Relative reactivities of *O*-pentenyl glycosides (b) electronic effect of the C-6 orientation on glycosyl donors reactivity 52
- Figure 2.3** Alternative participating groups 67

CHAPTER 3

- Figure 3.1** Classic armed and disarmed glycosyl donors 76
- Figure 3.2** SBox glycosyl donors with varying protecting group arrangements 76

CHAPTER 4

- Figure 4.1** Superarmed glycosyl donors 103

CHAPTER 5

- Figure 5.1** Mixed patterned glycosides 126
- Figure 5.2** Ethyl thioglycosyl donors with varying protecting group arrangements 129
- Figure 5.3** ¹H NMR of (a) starting material **5.4**, (b) β-sulfonium ion **5.4a**, (c) hydrolysis product **5.12a** 135
- Figure 5.4** Simplified energy diagram of a glycosylation reaction 136

Figure 5.5	Additionally investigated superdisarmed thioglycoside donors	137
Figure 5.7	(a) Reaction of glycosyl donor 5.4 with MeI/AgClO ₄ , (b) ¹ H NMR spectrum of glycosyl donor 5.4 ; (c) ¹ H NMR spectrum of resulting diastereomeric β-sulfonium ions 5.4d^a and 5.4d^b	141
Figure 5.8	Formation of diastereomeric β-sulfonium ions 5.4d^a and 5.4d^b	145
Figure 5.9	Spectra of β-sulfonium salt 5.4c (a) 20 min, crude; (b) 1 h, after PLC; (c) 3 h, after workup followed by PLC	146
Figure 5.10	Possible preferred rotamers (5.4^x , 5.4^y , 5.4^z) of glycosyl donor 5.4 , and methylated β-sulfonium diastereomers 5.4a^a and 5.4a^b	148
Figure 5.11	(a) Proposed thiomethylated β-sulfonium ion 5.4j , (b) starting material 5.4 , (c) <i>in situ</i> NMR of 5.4j	155
Figure 5.12	Possible structures and conformations of 5.4j	156
Figure 5.13	α-SEt 5.22 and sulfonium salt 5.22c ; (a) ¹ H NMR of α-SEt starting material 5.22 ; (b) ¹ H NMR of diastereomeric salt formation 5.22c	158
Figure 5.14	Geometry of S _N 1 intermediate vs. S _N 2 transition state	160
Figure 5.15	Examples of reactions not occurring through their expected inversion pathways, (a) anomeric dimethyl sulfonium species, Yoshida <i>et. al.</i> , (b) intramolecular glycosyl sulfonium species, Woerpel <i>et. al.</i> , (c) possible reaction pathways of acyloxonium ion intermediates, Whitfield <i>et. al.</i>	163

LIST OF SCHEMES

CHAPTER 1

- Scheme 1.1** General glycosylation mechanism 21
- Scheme 1.2** Glycosylation reactions developed by (a) Michael, (b) Fischer, and (c) Koenigs–Knorr 23
- Scheme 1.3** (a) Walden inversion, (b) inversion at the anomeric center 25
- Scheme 1.4** Rate-determining ionization pathways for (a) S_N1 and (b) S_N2 mechanisms 27
- Scheme 1.5** Bimolecular mechanism of the Koenigs–Knorr reaction (a) 1,2-*cis* glycoside, (b) 1,2-*trans* glycoside 28
- Scheme 1.6** General mechanism of glycosylation (with a non-participating group at C-2) 30
- Scheme 1.7** General mechanisms of glycosylation (with a participating group at C-2) 32
- Scheme 1.8** Mechanism of Lemieux's *in situ* anomerization procedure 36

CHAPTER 2

- Scheme 2.1** Arming and disarming effects of protecting groups 45
- Scheme 2.2** Conformationally modified glycosyl donors (a) 1C_4 chair conformation of TIPS-protected β -D-xylopyranoside (b) application of conformationally superarmed TBS-protected glucosyl donor 50
- Scheme 2.3** Attempts to reverse the anomeric effect with conformationally inverted glycosyl donors. (a) influence of conformation on the 53

	anomeric effect, (b) glycosylation using conformationally inverted D-galactosyl donor, (c) steric factors affecting transition state of a ring inverted D-glucosyl donor	
Scheme 2.4	(a) Reaction profile of oxacarbenium ion transition-state, (b) plausible reaction pathways of 4,6- <i>O</i> -benzylidene-2,3-di- <i>O</i> -methyl-mannopyranosyl cation	56
Scheme 2.5	Investigation with C-4 substituted tetrahydropyrans (a) intermediates corresponding to the various trajectories of nucleophilic attack (b) stereoselectivity of C-glycoside formation (c) preferred substituent orientations	57
Scheme 2.6	Proposed participation–dissociation pathway in a glycosylation reaction: glycosyl triflates. (a) continuum of ionic species, (b) preferred oxacarbenium ion species for 4,6- <i>O</i> -benzylidene protected D-mannosyl donor, (c) preferred oxacarbenium ion species for 4,6- <i>O</i> -benzylidene protected D-glucosyl donor	63
Scheme 2.7	Plausible mechanism of neighboring group-assisted formation of 1,2- <i>trans</i> glycosides	66
Scheme 2.8	Model study of the neighboring group participation	69
CHAPTER 3		
Scheme 3.1	Mechanistic depiction of the O-2/O-5 cooperative effect in SBox glycosyl donors of the D-gluco series; Figures 3.1-3.3 show experimentally determined relative reactivities; Figures 3.1a-3.3a illustrate the cooperative arming and disarming effects	78

Scheme 3.2 Stabilization from the O-2 position via participation	79
Scheme 3.3 Proposed superarming mechanism	80
Scheme 3.4 Synthesis of the SBox Glycoside 3.4 and its analogues	82

CHAPTER 4

Scheme 4.1 Oligosaccharide synthesis strategies; a) linear approach, b) chemoselective activation approach	105
Scheme 4.2 Chemoselective sequential synthesis of trisaccharides 4.17 and 4.18	109
Scheme 4.3 Competitive glycosidations of glycosyl donors 4.1 and 4.4 with glycosyl acceptor 4.16 in the presence of DMTST	110

CHAPTER 5

Scheme 5.1 Plausible <i>S</i> -ethyl glycosylation mechanism	128
Scheme 5.2 Synthesis of the superdisarmed ethyl thioglycoside 5.4	130
Scheme 5.3 Sulfonium salt formation in the absence of a glycosyl acceptor	133
Scheme 5.4 <i>In situ</i> promoter formation and glycosyl donor activation	138
Scheme 5.5 Continuum of ionic species upon dissociation of anomeric triflate	161
Scheme 5.6 Possible reaction pathways of β -sulfonium salt dissociation	162

LIST OF TABLES

CHAPTER 2

Table 2.1 Torsional angle values (and change) from α -glycosyl triflates to their likely oxacarbenium conformers	64
-----------------------------------------------------------------------------------------------------------------------------------	----

CHAPTER 3

Table 3.1	Comparative glycosidations of glycosyl donors 3.1-3.4 and 3.7-3.12 in the presence of DMTST	83
------------------	-----------------------------------------------------------------------------------------------------------	----

CHAPTER 4

Table 4.1	Chemoselective activation of superarmed donors 4.1-4.3 over glycosyl acceptors 4.4-4.8	107
------------------	------------------------------------------------------------------------------------------------------	-----

CHAPTER 5

Table 5.1	Comparative glycosidations of glycosyl donors 5.1-5.4 with acceptor 5.7 in the presence of (a) MeOTf (3 equiv) at rt	131
Table 5.2	β -Sulfonium ion formation using <i>in situ</i> generated methylating promoters	139
Table 5.3	Diastereomer investigation	143
Table 5.4	Glycosidation of thioglycoside donor 5.4 and acceptor 5.7 using various methylating promoters	150
Table 5.5	Glycosylation of thioglycoside donor 5.4 with low weight alcohol acceptors under preactivation conditions.	151
Table 5.6	Comparative glycosidation of thioglycoside donor 5.4 with various acceptors under varied promoter conditions	153
Table 5.7	DMTST promoted glycosylations	157
Table 5.8	α -SEt glycosylations	159

CHAPTER 1

Revisiting the Basic Mechanisms of Glycosylation

Mydock, L. K.; Demchenko, A. V. “Mechanism of chemical *O*-glycosylation: from early studies to recent discoveries,” *Org. Biomol. Chem.* **2010**, 8, 497–510.

1.1 Project Background

Since the first glycosylation reactions were performed in the late 1800s, carbohydrate chemistry has continued to evolve, expanding into a broad area of research that persistently captures the interest of the scientific community. As carbohydrates are easily the most abundant class of organic compounds, they are also involved in a myriad of life-sustaining and life-threatening processes.¹ However, understanding the structure, reactivity, and function of these bioorganic compounds has proven to be a remarkable challenge, even for the most adept of scientist. Therefore, the unique complexities associated with these molecules have attracted just as much attention as their biological significance. However, in order to utilize the full potential of these natural compounds, it is essential that we are able to first reproduce them.

In nature, monosaccharide units are flawlessly and repeatedly coupled together via the glycosylation reaction, effortlessly yielding complex poly- and oligosaccharides.² Unfortunately, the chemical installation of the glycosidic linkage still remains cumbersome, even with the aid of modern technologies. The extensive number of free hydroxyls and the multiple chirality centers inherent in these molecules, thereby translates into a host of possible configurational outcomes, which, if not exactly replicated can have significant biological ramifications. Nonetheless, despite these complexities, many recent breakthroughs in the field have allowed for most glycosidic bonds to be readily achieved.³⁻¹⁶ However, it is the inability to effectively predict and control the stereoselectivity of the reaction that has proven to be the synthetic hurdle.

This is in part due to the lack of mechanistic understanding regarding a few key steps and intermediates within the glycosylation reaction. As recent advances in the rapidly expanding field of glycobiology¹⁷ have increased the demand for more reliable and stereocontrolled glycosylation methodologies, the need to optimize this reaction and improve our synthetic capabilities has accordingly elevated in priority.

Over the last three decades, much scientific effort was directed toward refining the glycosylation reaction through optimization of general reaction conditions, such as the influence of the leaving group,¹⁸⁻²² temperature,²³⁻³⁰ pressure,^{31, 32} promoter/additives³³⁻³⁵ or reaction solvent^{28, 35-41} as they are all known to significantly affect the glycosylation outcome.^{3, 4, 10, 42-44} However, as these enhancements were not able to adequately control the reaction, subsequent studies have now turned their focus toward gaining a better understanding of the underlying mechanisms and energies controlling the reaction. While studies in this area are often neglected due to the inherent difficulties in quantifying and interpreting the resulting data, they are becoming ever more common, as previous efforts have fallen short.

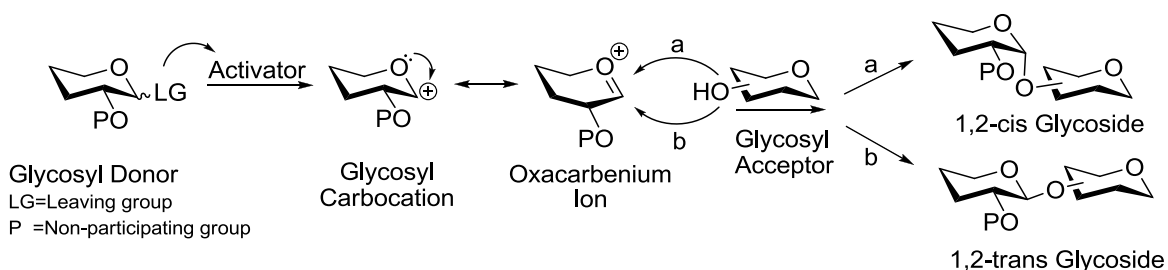
Accordingly, it was from this perspective that the investigation into the peculiar reactivity of “mixed-patterned” glycosyl donors was approached. Initial findings revealed that the behavior of these particular donors could be rationalized by a theory developed in our laboratory, entitled “the O-2/O-5 cooperative effect,” wherein the energetic consequences associated with particular protecting group patterns were analyzed. As a result, the work of this doctoral dissertation is centered upon the exploration of glycosyl donor protecting

groups, and their effect on both the reactivity and stereoselectivity with which the glycosylation reaction proceeds. Subsequently, the investigation evolved into three different areas of research: the development and application of a methodology whereby glycosyl donors could be “superarmed” through the strategic placement of common protecting groups (chapter 3); the discovery and characterization of an unusually stable anomeric β -sulfonium glycoside (chapter 4); and lastly, the potential application of the β -sulfonium glycoside in stereoselective 1,2-*cis* glycosylations (chapter 5).

However, before the experimental finding of this research can be discussed, it is first important to establish the mechanistic foundations whereby the particulars of my research can be easily discussed and understood. Therefore, the first chapter will be spent revisiting the basic history of the glycosylation mechanism; taking a look at how early pioneering studies helped to shape our modern understanding of the reaction. The following chapter will then relate how this knowledge has branched out into the current areas of interest. As such, the main focus in chapter 2 will be to outline how the intrinsic properties of the glycosyl donor can affect the glycosylation reaction. This includes glycosyl donor traits, such as: the conformation of the pyranose ring, the orientation of the attached substituents (axial *vs.* equatorial), and the type, number and location of the protecting groups.

1.2 General Considerations and Basic Mechanisms of Glycosylation

Although there are many complexities to consider when depicting the mechanism of the glycosylation reaction, it is often illustrated as a unimolecular S_N1 type reaction (Scheme 1.1)¹⁸. Leaving groups employed at the anomeric (hemiacetal) carbon are nucleophilic in nature, therefore upon addition of an electrophilic activator (promoter), the leaving group will complex with the promoter, thus assisting in the departure of the anomeric substituent. This, in turn, results in a glycosyl carbocation, which is subsequently stabilized by a neighboring lone electron pair on the endocyclic O-5 oxygen to form the oxacarbenium ion. The vacancy of the sp^3 orbital at the anomeric center causes a geometric transformation, wherein the resulting sp^2 hybridization indiscriminately allows for nucleophilic attack from both the top (pathway a) and bottom (pathway b) face of the sugar. This results in the formation of two possible diastereomeric linkages, which in reference to the configuration of the substituent at C-2, are aptly termed 1,2-*trans* or 1,2-*cis* glycosides.



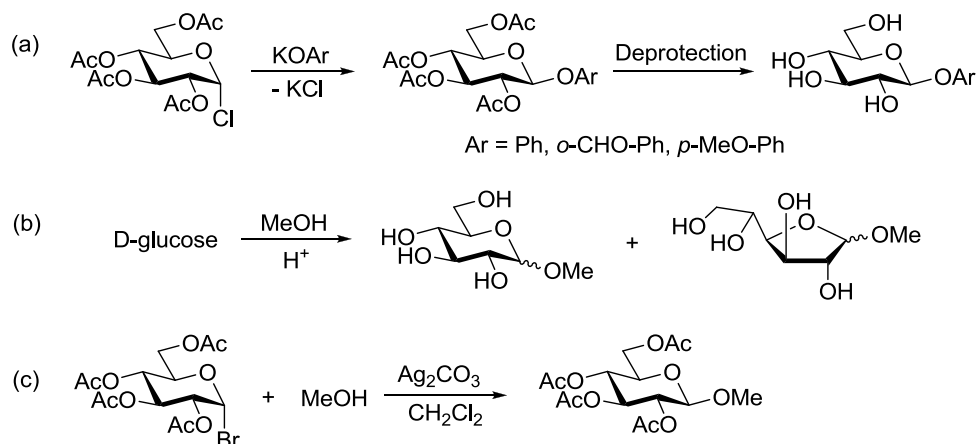
Scheme 1.1 General glycosylation mechanism

To make matters more complex, the new chiral center created by the glycosylation can either be defined as α or β , according to the configurational relationship between the anomeric center and a designated reference atom. For our investigations of glycopyranosides of the D-series, the reference atom is C-5. Therefore, the anomeric substituent can easily be defined as β when it is on the same side of the ring as the C-5 arm, and α when opposite.

1.3 Historical Perspective and Important Lessons From Early Work

1.3.1 Development of the glycosylation reaction

The first chemical glycosylation was reported by Arthur Michael some 130 years ago.⁴⁵ Just as in many modern methodologies, this reaction proceeded by the nucleophilic displacement of an anomeric chlorine leaving group (Scheme 1.2a). Although there was still very little known about the structure and reactivity of carbohydrates, Michael's vision of how the anomeric substitution should proceed was fundamentally accurate. Inconveniently however, it was deemed necessary to first convert the glycosyl acceptor into its respective potassium salt. Then, in 1893, Emil Fischer took a different approach to the glycosylation reaction.⁴⁶ In sharp contrast to the earlier protocol, Fischer perceived the unprotected monosaccharide unit as a hemiacetal. As such, the reaction was carried out under harsh acidic conditions in an excess of the desired low weight alcohol acceptor (Scheme 1.2b). Being conceptually the simplest way to obtain glycosides, the Fischer method commonly leads to an equilibrium of inter-converting species, all of which are formed in addition to the product formation.



Scheme 1.2 (a) Michael, (b) Fischer and (c) Koenigs-Knorr glycosylation reactions

While these pioneering approaches were not broad in their applicability, some of the fundamentals necessary for carrying out a successful glycosylation reaction had already emerged. First, in order to give the product a definite ring size, the use of temporary protecting groups appeared as a relatively simple and practical solution. Secondly, Michael's displacement of an anionic leaving group became prototypical in many modern glycosylation techniques. Third, it became clear that the glycosylation could not simply be regarded as a typical acetal formation. Combined, these elements created a solid base for developing a more practical and versatile glycosylation approach.

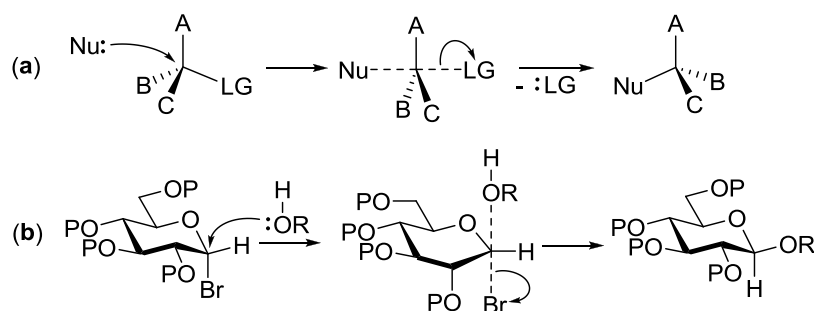
In 1901 Koenigs and Knorr⁴⁷ (and independently Fischer and Armstrong)⁴⁸ took the chemical glycosylation approach a step further by reacting glycosyl halides with conventional alcohol acceptors in the presence of Ag_2CO_3 or Ag_2O (Scheme 1.2c). While the latter were used as mild bases with the primary intent of scavenging the hydrogen

halide byproduct, it was not until the early 1930s that it was realized that the silver salts actually play an active role by assisting in leaving group departure.⁴⁹ However, there were also downsides to this methodology. With the addition of these silver salts came an appreciable amount of yield loss resulting from donor hydrolysis (due to the release of an H_2CO_3 byproduct). Additionally, the insolubility of these salts also resulted in heterogeneous reaction mixtures which made the acquisition of kinetic data near-impossible and severely limited the ability to consistently replicate the reaction outcomes.

As such, these findings led to a series of new investigations by Helferich et al.,⁵⁰⁻⁵² and independently Zemlen and Gerces,⁵³ wherein they began exploring the use of more effective heavy-metal-based catalysts. The most famous improvement to the classic Koenigs-Knorr reaction utilized mercury(II) cyanide in a polar solvent, such as nitromethane or acetonitrile, and is commonly referred to as the Helferich Modification. Furthermore, to address the issue of the unwanted water byproduct, Helferich implemented the use of dehydrating additives and/or molecular sieves, which further increased the reaction yield. As a result of these investigations, both the addition of a reaction catalyst (promoter) to assist with leaving group departure, and the addition of a desiccant; became standard protocol in glycosylation methodology. In addition, it was noticed that the Koenigs-Knorr glycosylation was often very stereoselective. Thus, research efforts continued toward gaining a better understanding of the glycosylation reaction mechanism.

1.3.2 Discovery of neighboring group participation

As aforementioned, the Koenigs–Knorr glycosylation reaction often provides a complete inversion of stereochemistry at the anomeric center, and was thus rationalized by the occurrence of Walden inversion⁵⁴ (otherwise known as concerted nucleophilic substitution).⁵⁵ Mechanistically, this requires an opposite face attack, meaning that the incoming nucleophile must approach from the reverse side of the departing leaving group (Scheme 1.3a). Therefore, it was commonly assumed that the nucleophilic displacement at the anomeric center also proceeded *via* this mechanism (Scheme 1.3b).⁵⁶



Scheme 1.3 (a) Walden inversion, (b) inversion at the anomeric center

Later on, however, several research groups began to notice that the ester protecting group at C-2 seemed to effect both the stereochemical outcome and the byproduct formation of the glycosylation reaction.⁵⁷ For instance, Pigman and Isbell observed that the 1,2-*trans* configuration was a prerequisite to both 1,2-anhydro and 1,2-orthoester formation (Figure 1.1),⁵⁸ and insightfully drew upon this information to re-evaluate the mechanistic pathway of the Koenigs–Knorr reaction.⁵⁹ At the time, the mechanistic details of how and why orthoesters formed were still sketchy;⁶⁰ however, their existence helped to validate the intramolecular reaction pathways within the sugar ring. This in turn, provided a solid

mechanistic scaffold for which the fundamental theories of C-2 participation could be built upon, ultimately providing further insight into understanding and rationalizing the end products of the glycosylation reaction.

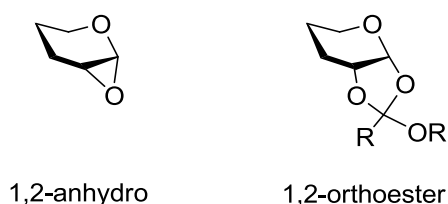
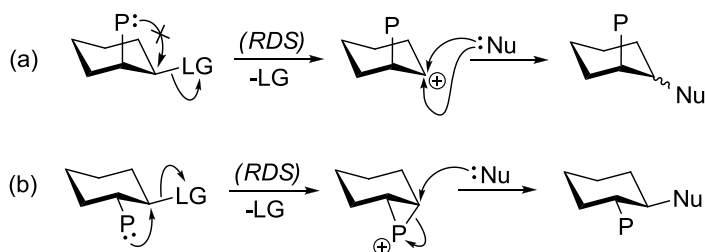


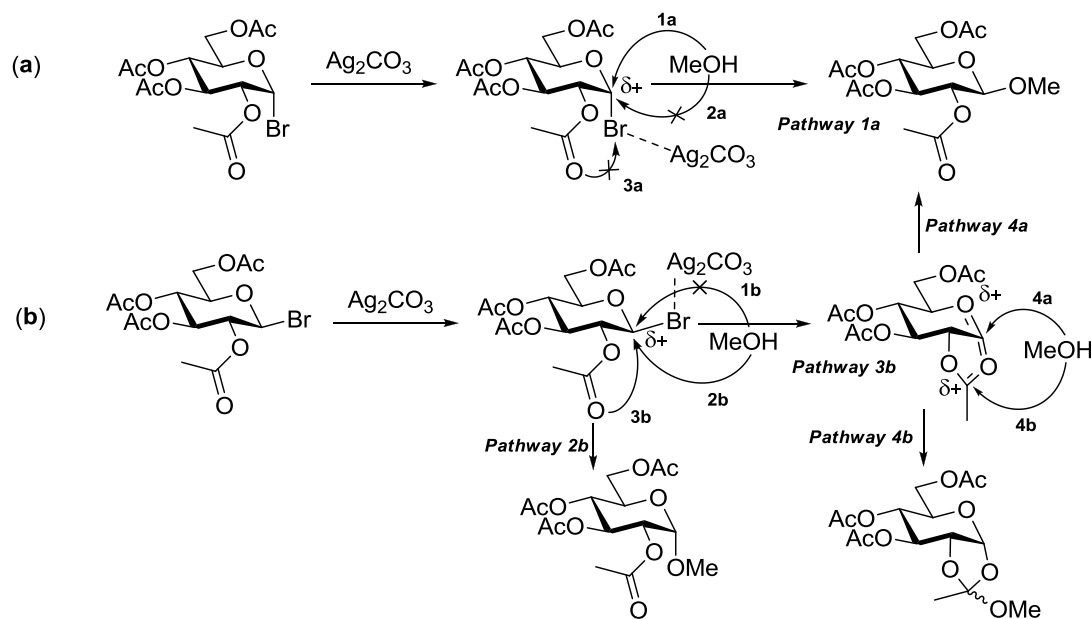
Figure 1.1 Products of intramolecular reaction pathways

Isbell's findings were further substantiated through Winstein's kinetic studies on neighboring group participation. This approach involved calculating the energy required for a nucleophilic substitution to occur in the absence or presence of participation in various 1,2-disubstituted cyclohexanes. Ultimately, this led to the conclusion that the unassisted departure of a leaving group to yield a free ion species (S_N1 mechanism, Scheme 1.4a), would require much more energy than a concerted nucleophilic displacement that occurs *via* intramolecular participation (S_N2 mechanism, Scheme 1.4b).^{61, 62} As a consequence, 1,2-*trans* species were found to react efficiently through concerted S_N2 mechanisms, while their analogous 1,2-*cis* counterparts were forced to proceed *via* the higher energy S_N1 pathway, making them sluggish in comparison. Although these model studies were not conducted at the anomeric center, this acquired knowledge proved invaluable in application to carbohydrates, ultimately giving rise to the current standard protocol for introducing a 1,2-*trans* linkage through utilization of neighboring group participation.



Scheme 1.4 Rate-determining ionization pathways for (a) S_N1 and (b) S_N2 mechanisms

As a result of these findings, Isbell was also able to propose two distinct pathways of glycosylation based upon the relationship between the C-1 and C-2 substituent, being either 1,2-*cis* or 1,2-*trans* (Scheme 1.5).⁵⁹ The activation pathway is initially the same for both configurations; the anomeric bromide complexes with the silver salt, which decreases the electron density at the anomeric center, making it more susceptible to nucleophilic attack. Subsequent to this point, however, the pathways diverge. In the case of the 1,2-*cis* glycosyl donor, wherein both the anomeric bromide and the 2-*O*-acetyl substituent are on the same side of the ring, only the inversion product was obtained (pathway 1a). The lack of the 1,2-orthoester formation (pathway 3a), was rationalized by the fact that the approach of the 2-*O*-acetyl group is blocked, making participation impossible. It would then follow, that the 1,2-*cis* glycoside is not observed because there is no plausible mechanism that would lead to this product (pathway 2a). *The high stereoselectivity and lack of an observed 1,2-orthoester byproduct from 1,2-cis bromides, serves as evidence that the Koenigs–Knorr reaction is one of the rare examples wherein a concerted bimolecular displacement (S_N2 mechanism) occurs.*



Scheme 1.5 Bimolecular mechanism of the Koenigs–Knorr reaction

(a) 1,2-*cis* glycoside, (b) 1,2-*trans* glycoside

Conversely, the 1,2-*trans* glycosyl donor yielded three distinct products: two diastereomeric glycosides and an orthoester. Following activation, the expected 1,2-*cis* product was obtained *via* direct nucleophilic displacement from the bottom (opposite) face of the ring (pathway 2b). Additionally, the intramolecular attack from the adjacent carbonyl oxygen leads to the formation of a reactive acyloxonium (*i.e.* dioxalenium) intermediate (pathway 3b). Then, depending on the site of nucleophilic attack on the acyloxonium intermediate, two products are possible; a 1,2-*trans* glycoside (pathway 4a) and a 1,2-orthoester (pathway 4b). It should be noted that the 1,2-*trans* glycoside cannot be obtained directly (pathway 1b).

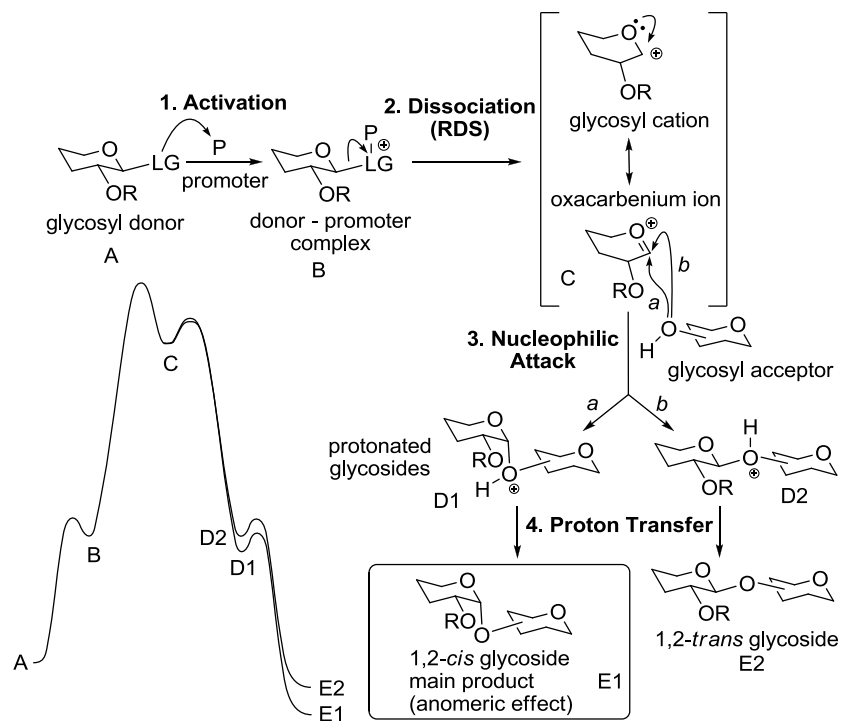
1.4 Glycosylation Kinetics

1.4.1 General energy profile

There are many complexities to consider when depicting the mechanism of the glycosylation reaction, and often a clear delineation between S_N1 and S_N2 nucleophilic substitution reactions is obscured.⁶³ Nevertheless, nowadays it is generally presumed that the reaction conditions favor that of a unimolecular S_N1 mechanism, as simply depicted in Section 1.2 (however, one can *always* find counterarguments; for example, Paulsen's glycosyl donor–acceptor match–mismatch concept⁶⁴ that was recently explored by Fraser-Reid and Lopez *et al.*,⁶⁵⁻⁶⁹ and the double stereodifferentiation phenomenon⁷⁰). Theoretically speaking, an S_N1 mechanism implies that the rate determining step (RDS) is unimolecular, and is therefore independent of the glycosyl acceptor. As such, this also implies that there is at least one intermediate prior to product formation. Consequently, the reaction is thought to proceed through a total of four distinct steps:⁶³ (1) formation of the donor–promoter complex, which can be reversible or irreversible depending on the system involved; (2) ionization of the glycosyl donor, a typically irreversible act, and the slowest step (RDS) of the reaction; (3) nucleophilic attack by the glycosyl acceptor; and (4) proton transfer to give a neutral glycoside. Thus, Scheme 1.6 provides an in depth profiling of these four steps.

(Step 1) Generally, the leaving group (LG) employed at the anomeric carbon of a glycosyl donor (A, *herein and below is pertained to the D-glucopyranose series*) is nucleophilic in nature (halogen, SR, OR, *etc.*). Therefore, upon adding an electrophilic

promoter (activator, *P*), it will activate the leaving group to form donor–promoter complex B.



Scheme 1.6 General mechanism of glycosylation

(with a non-participating group at C-2)

(Step 2) This step is considered to be the unimolecular RDS, wherein the transformation of complex B into the glycosyl carbocation occurs. This intermediate exists in its stabilized resonance form, oxacarbenium ion (C). As a consequence, the anomeric carbon is sp^2 -hybridized, which results in a flattened half chair conformation.

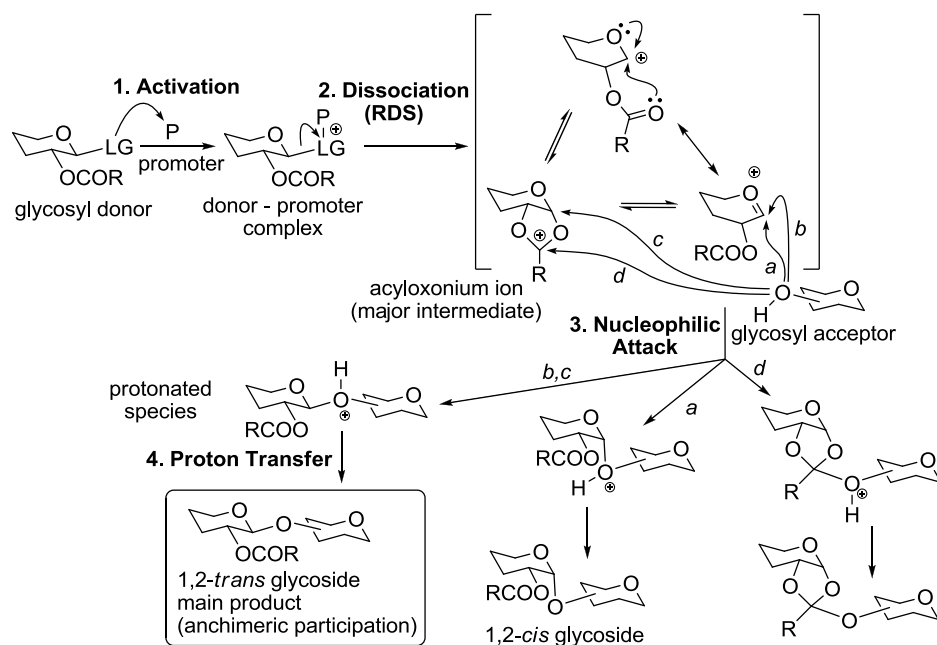
(Step 3) At this stage, the subsequent nucleophilic attack of the glycosyl acceptor is possible from both the bottom (pathway a) and the top (pathway b) face of the sugar ring,

leading to the formation of α -(1,2-*cis*) or β -(1,2-*trans*) linkages, respectively. Given that this step occurs after the RDS, it is not the rate with which this step proceeds, but rather the selectivity of this step that is of significance. In other words, it is the facial preference of the approaching nucleophile that is largely responsible for the observed stereoselectivity, as reflected in intermediate D, and is then presumed to be carried through to the glycosidic product E, to form the kinetic product. This preferential attack is thought to arise from the stability of the transition state associated with each approach (α or β). Additional product selectivities can arise from the stabilization provided by the anomeric effect (chapter 1.4.2), which is thought to be responsible for the thermodynamic product of the reaction. We are also aware of the existence of the non-kinetically controlled glycosylations, in which the initially formed β -glycoside is then anomerized into its thermodynamically more stable α -counterpart. Without diminishing the importance and versatility of this approach, we choose to direct the reader to the recent authentic publications.^{71,72}

(Step 4) Finally, the loss of the proton results in the formation of the neutral 1,2-*cis* and 1,2-*trans* glycosides E1 and E2. Once proton transfer occurs, the formation of the glycosidic bond is irreversible, and as such can be thought of as the termination step in the glycosylation reaction. It should be noted that step 4 is often neglected in mechanistic discussions with the belief that it has no effect on the outcome of glycosylation. However, there has been accumulating evidence that this simple assumption is inaccurate,⁷³ and that the effects of hydrogen bonding and proton transfer may have great influence. For example, H-bonding has been found to occur at or near the transition state

associated with the approach of the nucleophile, and as such, can affect the transition state energy corresponding to a specific facial approach. Furthermore, it has been proposed that intramolecular proton transfer may also be involved in the mechanism by which neighboring group participation proceeds.

The glycosylation mechanism becomes slightly more complicated however, when a glycosyl donor bearing a participating group at C-2 is utilized (Scheme 1.7). While the underlying philosophy dictating product formation remains the same, the number of potential intermediate species and plausible mechanistic pathways increases (addressed more thoroughly in Chapter 2.3.2).



Scheme 1.7 General mechanisms of glycosylation

(with a participating group at C-2)

As before, a promoter is first employed to assist in leaving group departure. Upon dissociation of the leaving group, a short lived positively charged species is formed and it is generally assumed that an intramolecular attack immediately occurs to form the more stable, lower-energy acyloxonium ion. From this point, it is unclear whether the incoming nucleophile directly attacks this species (in an S_N2 fashion), or if a more complex pathway involving additional intermediates is followed. However, it is generally presumed that the direct nucleophilic attack on C-1 is the route to the 1,2-*trans* glycoside product (pathway c), and that direct attack at the carbonyl carbon is responsible for the formation of the orthoester product (pathway d).

At this point, it also seems appropriate to draw attention to the points of this reaction mechanism that will be further discussed in Chapter 2. As such, Section 2.1 will cover *Steps 1 and 2 (Activation and Dissociation)*, wherein the focus will be on the reactivity of the glycosyl donor. Additionally, Section 2.2 will expand upon *Step 3 (Nucleophilic Attack)*, wherein the factors affecting the stereoselectivity of the glycosylation reaction will be addressed.

1.4.2 Anomeric Effect

As studies on the unique reactivity of sugars continued, it was further revealed that there exists an unconventional inclination for anomeric substituents to reside in an axial configuration. This phenomenon was first observed by Edward⁷⁴ and later defined as the *anomeric effect* by Lemieux.⁷⁵ Although the anomeric effect is well recognized in the field, its rationalization is often the subject of much deliberation. Typically, in cyclic six-

membered hydrocarbons, *equatorial* substituents are energetically preferred over *axial* substituents, due to the unfavorable 1,3-diaxial interactions that arise (Figure 1.2a). With sugar structures, however, the six-membered ring differs in that it contains an endocyclic oxygen atom adjacent to C-1. As the attached leaving group is also a heteroatom, the combined inductive effects produce a considerable electron deficiency at C-1, leading to some unique electronic characteristics.

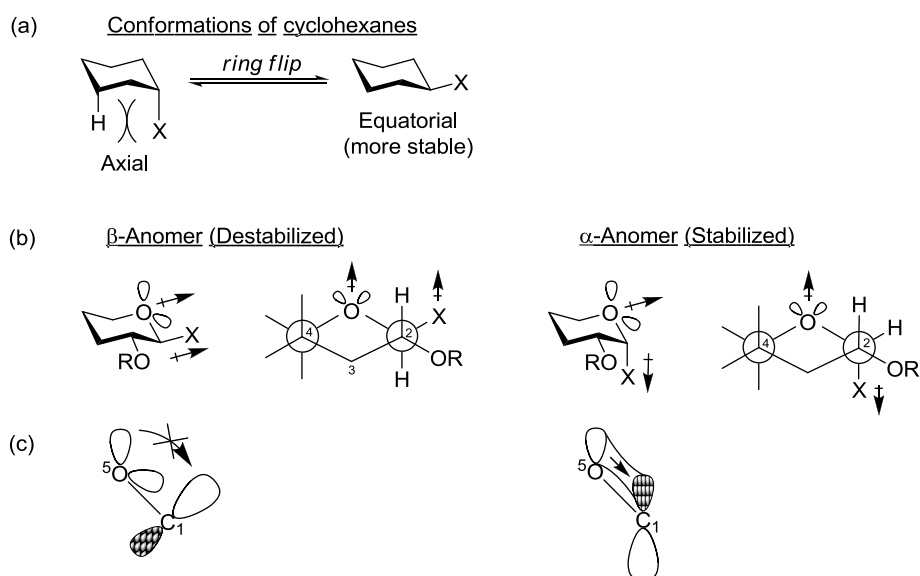


Figure 1.2 Anomeric Effect.

The rationale for the observed phenomenon, is often a unification of both electrostatic and hyperconjugation effects. Electrostatically, the anomeric effect is explained in terms of dipole–dipole interactions (Figure 1.2b). Thus, when the leaving group (X) resides equatorially, the lone pair electrons on its heteroatom exhibit strong repulsive electrostatic interactions with electrons on the ring oxygen (O-5). These destabilizing electrostatic interactions do not exist when X is in the axial orientation. Additionally,

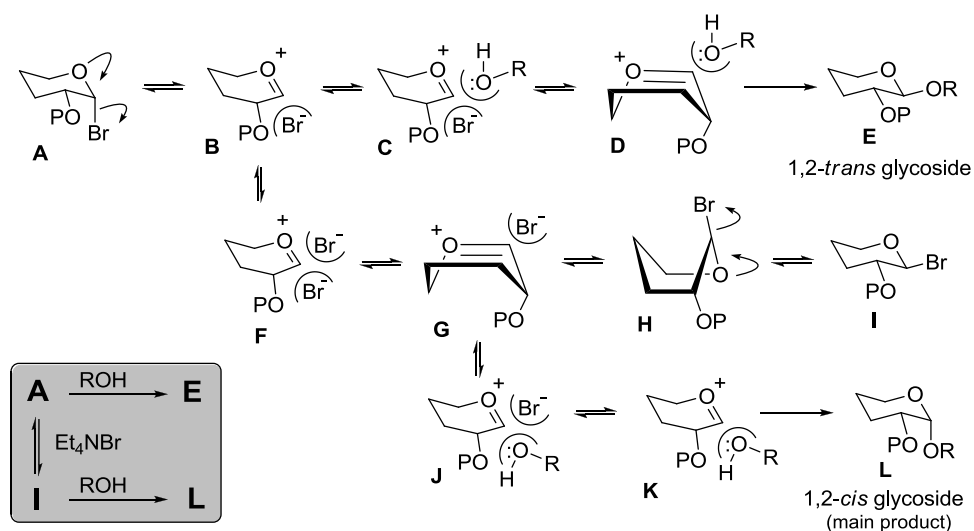
electron-withdrawing axial substituents are further stabilized through hyperconjugation (Figure 1.2c), as the lone-pair electrons at O-5 and the antibonding orbital of C-1 are in an *anti*-periplanar alignment. This stabilization cannot be achieved when X is equatorial, as the respective orbitals of O-5 and C-1 are in different planes. It then follows, that as the electronegativity of X increased, so does its axial proclivity.⁷⁶ This rationalization is supported by the observed shortening of the C-1–O-5 bond and a concomitant lengthening of the C-1–X bond.

In terms of the reactivity of the anomeric center, it has often been observed that one anomer is often more reactive than the other. While several theories have emerged to justify this, the *anti*-periplanar lone pair hypothesis, also known as the kinetic anomeric effect, is the most well known.^{77, 78} This theory expounds upon the hyperconjugation model (Figure 1.2c), owing a greater lability of axial glycosides to a lengthening, and therefore weakening, of the axial C-1–X bond. However, often the opposite reactivity is also encountered, and so alternative theories, namely the *syn*-periplanar lone pair hypothesis⁷⁹ and the principle of least nuclear motion,⁸⁰ have been developed to explain this contradictory observation.

1.4.3 Halide ion-catalyzed glycosylation

The first application of this accrued mechanistic and kinetic knowledge was the halide ion-catalyzed glycosylation developed by Lemieux *et al.*⁸¹ Through careful consideration of the reaction intermediates and conformations thereof, and through extensive theoretical studies, it was found that a rapid equilibrium could be established between a

relatively stable α -halide **A** and its far more reactive β -counterpart **I**, by adding tetraalkylammonium bromide (Et_4NBr , Scheme 1.8). Initially, the expulsion of the α -halide **A** results in the formation of ion-pair **B**. Since no inverted product (**E**) is formed herein, it can be concluded that the ion-pair **F** leading to the anomerized β -linked bromide **I** is a more energetically favorable pathway. Note the existence of alternative conformations for intermediates **G** and **H**. These are presumed to be necessary in order to form/activate the equatorial bond, and are in accordance with the *syn*-periplanar lone pair hypothesis,⁷⁹ wherein an axial-like stabilization is achieved when the sugar ring adopts a conformation where the equatorial anomeric substituent becomes axial (or pseudo-axial).



Scheme 1.8 Mechanism of Lemieux's *in situ* anomerization procedure

At this point, the highly unstable β -halide dissociates back into its ion pair (**I**→**G**), whereupon it quickly undergoes nucleophilic attack (**G**→**K**) to form the 1,2-*cis* product **L**. As an end result, nucleophilic substitution of the β -bromide **I** occurs favorably,

whereas the α -bromide **A** quickly anomerizes before glycosylation can occur. The observed stereoselectivity is additionally reinforced by the Curtin–Hammett principle⁸² in that when two compounds are in rapid equilibrium, the ratio of product formation is often controlled by the standard Gibbs energies of the respective transition states, and is not a reflection of their respective equilibrium populations; as equilibrium favors the α -bromide and would therefore yield the 1,2-*trans* glycoside.

1.5 References

1. Varki, A., *Glycobiology* **1993**, 3 (2), 97-130.
2. Hehre, E. J., *Carbohydr. Res.* **2001**, 331, 347-368.
3. Nicolaou, K. C.; Mitchell, H. J., *Angew. Chem. Int. Ed.* **2001**, 40 (9), 1576-1624.
4. Davis, B. G., *J. Chem. Soc., Perkin Trans. 1* **2000**, (14), 2137-2160.
5. Whitfield, D. M.; Douglas, S. P., *Glycoconjugate J.* **1996**, 13 (1), 5-17.
6. Toshima, K.; Tatsuta, K., *Chem. Rev.* **1993**, 93 (4), 1503-1531.
7. Seeberger, P. H.; Werz, D. B., *Nature* **2007**, 446 (7139), 1046-1051.
8. Galonic, D. P.; Gin, D. Y., *Nature* **2007**, 446 (7139), 1000-1007.
9. Smoot, J. T.; Demchenko, A. V., *Adv. Carbohydr. Chem. Biochem.* **2009**, 62, 161-250.
10. Demchenko, A. V., *Curr. Org. Chem.* **2003**, 7 (1), 35-79.
11. Seeberger, P. H.; Haase, W. C., *Chem. Rev.* **2000**, 100 (12), 4349-4393.
12. Plante, O. J.; Palmacci, E. R.; Seeberger, P. H., *Science* **2001**, 291 (5508), 1523-1527.

13. Plante, O. J.; Palmacci, E. R.; Seeberger, P. H., *Adv. Carbohydr. Chem. Biochem.* **2003**, *58*, 35-54.
14. Carrel, F. R.; Geyer, K.; Codée, J. D. C.; Seeberger, P. H., *Org. Lett.* **2007**, *9*, 2285-2288.
15. Seeberger, P. H., *Chem. Soc. Rev.* **2008**, *37*, 19-28.
16. Oberli, M. A.; Bindschadler, P.; Werz, D. B.; Seeberger, P. H., *Org. Lett.* **2008**, *10*, 905-908.
17. Varki, A.; Cummings, R. D.; Esko, J. D.; Freeze, H. H.; Bertozzi, C. R.; Stanley, P.; Hart, G. W.; Etzler, M. E., *Essentials of Glycobiology*. Second ed.; CSH Laboratory Press: New York, 2009.
18. Demchenko, A. V., *Handbook of Chemical Glycosylation: Advances in Stereoselectivity and Therapeutic Relevance*. Wiley-VCH: Weinheim, 2008; p 1-21.
19. Garcia, B. A.; Poole, J. L.; Gin, D. Y., *J. Am. Chem. Soc.* **1997**, *119*, 7597-7598.
20. Garcia, B. A.; Gin, D. Y., *J. Am. Chem. Soc.* **2000**, *122*, 4269-4279.
21. Nguyen, H. M.; Chen, Y. N.; Duron, S. G.; Gin, D. Y., *J. Am. Chem. Soc.* **2001**, *123*, 8766-8772.
22. Boebel, T. A.; Gin, D. Y., *J. Org. Chem.* **2005**, *70*, 5818-5826.
23. Andersson, F.; Fugedi, P.; Garegg, P. J.; Nashed, M., *Tetrahedron Lett.* **1986**, *27* (33), 3919-3922.
24. Wegmann, B.; Schmidt, R. R., *J. Carbohydr. Chem.* **1987**, *6* (3), 357-375.
25. Nishizawa, M.; Shimomoto, W.; Momii, F.; Yamada, H., *Tetrahedron Lett.* **1992**, *33* (14), 1907-1908.

26. Shimizu, H.; Ito, Y.; Ogawa, T., *Synlett* **1994**, 535-536.
27. Chenault, H. K.; Castro, A.; Chafin, L. F.; Yang, J., *J. Org. Chem.* **1996**, *61* (15), 5024-5031.
28. Manabe, S.; Ito, Y.; Ogawa, T., *Synlett* **1998**, 628-630.
29. Schmidt, R. R.; Rucker, E., *Tetrahedron Lett.* **1980**, *21* (15), 1421-1424.
30. Dohi, H.; Nishida, Y.; Tanaka, H.; Kobayashi, K., *Synlett* **2001**, (9), 1446-1448.
31. Klimov, E. M.; Malysheva, N. N.; Demchenko, A. V.; Makarova, Z. G.; Zhulin, V. M.; Kochetkov, N. K., *Dokl. Akad. Nauk* **1989**, *309* (1), 110-114 and references therein.
32. Sasaki, M.; Gama, Y.; Yasumoto, M.; Ishigami, Y., *Tetrahedron Lett.* **1990**, *31* (45), 6549-6552.
33. Schmidt, R. R.; Jung, K. H., Oligosaccharide synthesis with trichloroacetimidates. In *Preparative Carbohydrate Chemistry*, Hanessian, S., Ed. Marcel Dekker, Inc.: New York, 1997; pp 283-312.
34. Matsubara, K.; Mukaiyama, T., *Chem. Lett.* **1993**, *12*, 2145-2148.
35. Fukase, K.; Hasuoka, A.; Kinoshita, I.; Aoki, Y.; Kusumoto, S., *Tetrahedron* **1995**, *51* (17), 4923-4932.
36. Eby, R.; Schuerch, C., *Carbohydr. Res.* **1974**, *34*, 79-90 and references therein.
37. Wulff, G.; Rohle, G., *Angew. Chem., Int. Edit. Engl.* **1974**, *13* (3), 157-170.
38. Demchenko, A.; Stauch, T.; Boons, G. J., *Synlett* **1997**, (7), 818-820.
39. Hashimoto, S.; Hayashi, M.; Noyori, R., *Tetrahedron Lett.* **1984**, *25* (13), 1379-1382.
40. Ishiwata, A.; Munemura, Y.; Ito, Y., *Tetrahedron* **2008**, *64*, 92-102.

41. Adinolfi, M.; Iadonisi, A.; Ravida, A., *Synlett* **2006**, (4), 583-586.
42. Manabe, S.; Ito, Y., *Curr. Bioact. Comp.* **2009**, 4, 258-281.
43. Zhu, X.; Schmidt, R. R., *Angew. Chem. Int. Ed.* **2009**, 48, 1900-1934.
44. Demchenko, A. V., *Handbook of Chemical Glycosylation: Advances in Stereoselectivity and Therapeutic Relevance*. Wiley-VCH: Weinheim, 2008.
45. Michael, A., *Am. Chem. J.* **1879**, 1, 305-312.
46. Fischer, E., *Ber.* **1893**, 26, 2400-2412.
47. Koenigs, W.; Knorr, E., *Ber.* **1901**, 34, 957-981.
48. Fischer, E.; Armstrong, E. F., *Ber.* **1901**, 34, 2885.
49. Igarashi, K., *Adv. Carbohydr. Chem. Biochem.* **1977**, 34, 243-283.
50. Helferich, B.; Bohn, E.; Winkler, S., *Berichte der Deutschen Chemischen Gesellschaft* **1930**, 63, 989.
51. Helferich, B.; Gootz, R., *Berichte der Deutschen Chemischen Gesellschaft* **1931**, 64, 109.
52. Helferich, B.; Wedemeyer, K. F., *Ann.* **1949**, 563, 139-145.
53. Zemplen, G.; Gerecs, A., *Ber.* **1930**, 63B, 2720-2729.
54. Walden, P., *Ber.* **1896**, 29, 133.
55. Streitweiser Jr, A., *Chem. Rev.* **1956**, 56, 571-752.
56. Bochkov, A. F.; Zaikov, G. E., *Chemistry of the O-glycosidic bond: formation and cleavage*. Pergamon Press: 1979.
57. Goodman, L., *Adv. Carbohydr. Chem. Biochem.* **1967**, 22, 109-175.
58. Pigman, W.; Isbell, H., *J. Res. Nat. Bur. Stand.* **1937**, 19, 189-213; and references therein.

59. Isbell, H. S., *Ann. Rev. Biochem.* **1940**, *9*, 65-92.
60. Isbell, H. S.; Frush, H. L., *J. Res. Nat. Bur. Stand.* **1949**, *43*, 161-171.
61. Winstein, S.; Grunwald, E., *J. Am. Chem. Soc.* **1948**, *70*, 828-837.
62. Winstein, S.; Grunwald, E.; Buckles, R. E.; Hanson, C., *J. Am. Chem. Soc.* **1948**, *70*, 816-821.
63. Nukada, T.; Berces, A.; Whitfield, D. M., *Carbohydr. Res.* **2002**, *337*, 765-774.
64. Paulsen, H., Selectivity and reactivity in oligosaccharide synthesis. In *Selectivity - a Goal for Synthetic Efficiency*, Bartmann, W.; Trost, B. M., Eds. Verlag Chemie: Weinheim, 1984; pp 169-190.
65. Uriel, C.; Gomez, A. M.; Lopez, J. C.; Fraser-Reid, B., *Eur. J. Org. Chem.* **2009**, 403-411.
66. Jayaprakash, K. N.; Lu, J.; Fraser-Reid, B., *Angew. Chem. Int. Ed.* **2005**, *44*, 5894-5898.
67. Uriel, C.; Gomez, A. M.; Lopez, J. C.; Fraser-Reid, B., *Synlett* **2003**, 2203-2207.
68. Mach, M.; Schlueter, U.; Mathew, F.; Fraser-Reid, B.; Hazen, K. C., *Tetrahedron* **2002**, *58*, 7345-7354.
69. Fraser-Reid, B.; Lopez, J. C.; Radhakrishnan, K. V.; Nandakumar, M. V.; Gomez, A. M.; Uriel, C., *Chem. Commun.* **2002**, 2104-2105.
70. Spijker, N. M.; van Boeckel, C. A. A., *Angew. Chem. Int. Edit. Engl.* **1991**, *30*, 180-183.
71. Olsson, J. D. M.; Eriksson, L.; Lahmann, M.; Oscarson, S., *J. Org. Chem.* **2008**, *73*, 7181-7188.
72. Pilgrim, W.; Murphy, P., *Org. Lett.* **2009**, *11*, 939-942.

73. Whitfield, D. M., *Adv. Carbohydr. Chem. Biochem.* **2009**, *62*, 83-159.
74. Edward, J. T., *Chem. Ind.* **1955**, 1102-1104.
75. Lemieux, R. U., *Pure Appl. Chem.* **1971**, *25*, 527-548 and references therein.
76. Tvaroska, I.; Bleha, T., *Adv. Carbohydr. Chem. Biochem.* **1989**, *47*, 45-123.
77. Deslongchamps, P., *Stereoelectronic Effects in Organic Chemistry*. Pergamon Press: Oxford, 1983; p 29-40.
78. Deslongchamps, P., *Tetrahedron* **1975**, *31*, 2463-2490.
79. Andrews, C. W.; Fraser-Reid, B.; Bowen, J. P., *J. Am. Chem. Soc.* **1991**, *113*, 8293-8298.
80. Sinnott, M. L., *Adv. Phys. Org. Chem.* **1988**, *24*, 113-204.
81. Lemieux, R. U.; Hendriks, K. B.; Stick, R. V.; James, K., *J. Am. Chem. Soc.* **1975**, *97* (14), 4056-4062 and references therein.
82. Seeman, J. I., *Chem. Rev.* **1983**, *83*, 83-134.

CHAPTER 2

Current Mechanistic Theories

Mydock, L. K.; Demchenko, A. V. “Mechanism of chemical *O*-glycosylation: from early studies to recent discoveries,” *Org. Biomol. Chem.* **2010**, 8, 497–510.

2.1 Current Theories behind Glycosyl Donor Reactivity

When embarking on discussions about the reactivity of the glycosyl donor, we are in effect revealing how energetically favorable the transition from glycosyl donor to its oxacarbenium ion intermediate transition state. While the initial donor-promoter complexation seems to serve as a reflection of the glycosyl donor's reactivity, it is actually the (S_N1) dissociation of the leaving group that is the rate determining step (slow step) (Chapter 1.4.1). Consequently, the reaction rate is largely dependent upon the stability of the oxacarbenium ion formed upon leaving group departure. As such, many of the mechanistic discussions pertaining to the reactivity of the glycosyl donor will be conceptually approached by assessing the stability of the oxacarbenium ion intermediate.

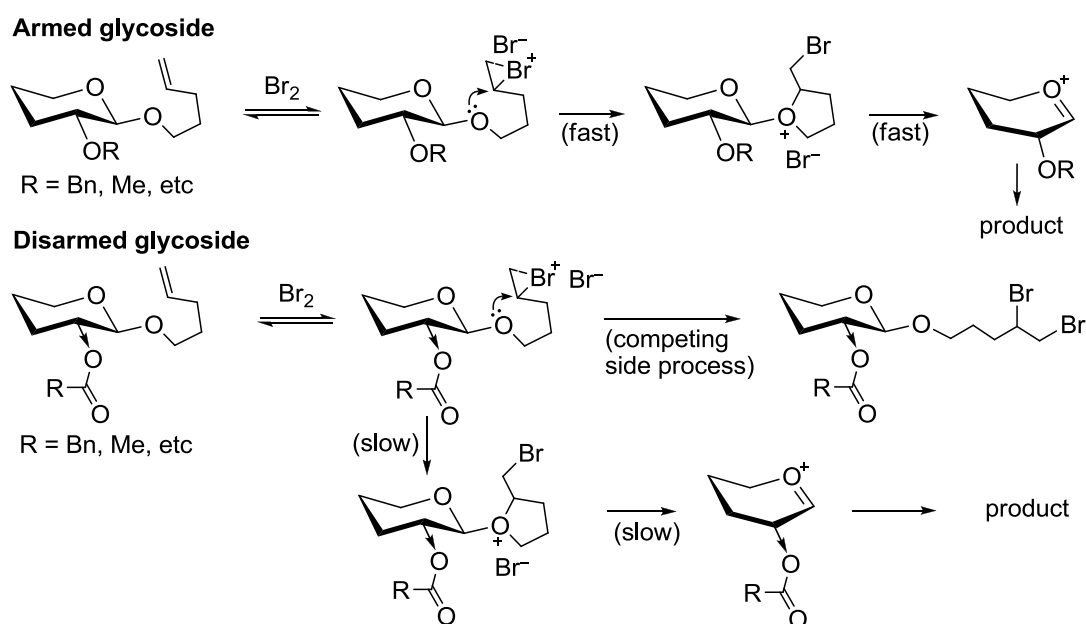
2.1.1 Protecting groups - electronic effects

Protecting groups were initially applied to reduce unwanted side reactions, by masking additional sites of reactivity. However, it soon became evident that the inherent properties of the protecting groups themselves could significantly affect the outcome of the glycosylation; thus, as aptly stated by B. Fraser-Reid, “Protecting groups do more than protect.”¹

Armed-disarmed theory

As previously discussed, one of the more salient effects observed and capitalized upon in carbohydrate synthesis, was that of neighboring group participation. Keeping with this trend, in 1988 Fraser-Reid *et al.* described a new manner by which to exploit the properties of protecting groups. Known as the “armed–disarmed strategy,”² this approach took advantage of the

different electronic effects among the various functional groups (Scheme 2.1). It was noticed that ester-type protecting groups (OAc, OBz, *etc.*) strongly reduced “disarmed” the reactivity of the *n*-pentenyl glycosyl donor, in comparison to the effects of ether-type protecting groups (OBn, OMe, *etc.*). One justification for such an observation, is that the increased electron-withdrawing ability of ester protecting groups decreases the electron density and, hence, the nucleophilicity of the leaving group.



Scheme 2.1 Arming and disarming effects of protecting groups

In the case of *n*-pentenyl glycosides, which are activated at the remote double bond, the arming/disarming effect is noticed in the intramolecular cyclization step. Thus, as seen in scheme 1.2, the less reactive disarmed glycosyl donor yields a vicinal dihalide byproduct that is not observed with the ether-protected armed analog. Another consequence of the decreased electron density at the anomeric center, which is highly relevant to the ensuing mechanistic discussions, is

that upon departure of the leaving group, the resulting oxacarbenium ion is destabilized by the electron withdrawal.

Although this discovery was made using *n*-pentenyl glycosides, this electronic effect ultimately proved to be of a general nature, and can be applied to nearly any class of glycosyl donor. Furthermore, the usefulness of this approach was found in application towards expeditious oligosaccharide synthesis as it circumvents the need for protecting group manipulations at the anomeric center (discussed in Chapter 4).³

Expansions of the armed-disarmed theory

In an attempt to facilitate the armed–disarmed strategy in oligosaccharide synthesis, Ley *et al.* developed a new approach wherein the reactivity of glycosyl donors and acceptors could be “tuned.”⁴ Wong *et al.* further devised a mathematical approach, assigning relative reactivity values (RRVs) to a wide library of over fifty *S*-tolyl donors and acceptors, each containing a different set of protecting groups.⁵ In a further expansion of the basic armed–disarmed theory, Schmidt and Madsen were able to achieve a disarming effect through the strategic placement of a single powerful electron-withdrawing ester group (pentafluorobenzoyl) on the C-6 position of an ether-protected phenyl thioglycoside.⁶ Related studies also revealed that the arming/disarming ability of the protecting groups was highly dependent upon both their location and their core donor structure.^{4, 5} Crich and Vinogradova have also investigated the influence of the electron withdrawal at the C-6 position on the stereoselectivity of the glycosylation. Thus, in exploring a series of 6-deoxy mono-, di-, and trifluoro *S*-phenyl rhamnosyl donors,⁷ they found a clear correlation between the electron withdrawing ability at C-6 and the stability of the glycosyl

triflate reaction intermediate. While common glycosyl triflates undergo rapid decomposition at temperatures above $-60\text{ }^{\circ}\text{C}$, it was shown that their trifluorinated counterparts were stable up to $+10\text{ }^{\circ}\text{C}$.

In addition, this is also the category to which the findings of this doctoral dissertation belong. As will be discussed in detail in the remaining Chapters 3-5, the unusual reactivity of “mixed patterned” glycosyl donors seemingly contradicted the traditional armed-disarmed theory, thus prompting the fundamentals of the theory to be revisited.⁸

2.1.2 Protecting groups - axial vs. equatorial

In 2001, Bols *et al.* began investigating the influence that substituent orientation can have on the reactivity of a molecule.⁹ While these studies were performed using substituted heterocyclic amines, the resultant findings proved to be extremely useful with respect to the reactivity of carbohydrates. Thus, it was found that the pK_a of protonated amines (conjugate acids) could be used to directly measure the electronic effects of various ring substituents. Ultimately, a correlation emerged between the acidity of the molecule and the configuration of the substituent, finding equatorial substituents to be significantly more electron withdrawing (destabilizing) than their axial counterparts (Figure 2.1). This was found to result from the ability of axial substituents to provide stabilization through charge–dipole interactions, as they are spatially oriented closer to the localized charge. The numerical values (substituent constants) shown in Figure 2.1 are given in pH units, and reflect the amount by which the pH decreases with respect to its unsubstituted parent amine (piperidine). As alternative explanations of steric hindrance, resonance, induction, solvation and internal hydrogen bonding have all been ruled out, this

leaves a strong case in favor of the stereoelectronic substituent effects (charge-dipole interactions).¹⁰

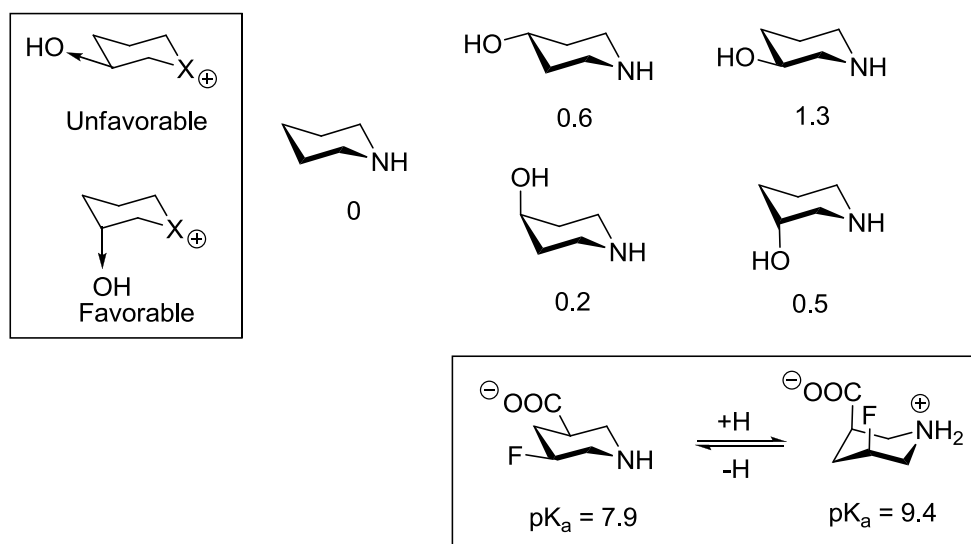


Figure 2.1 Substituent effect and conformational preferences of substituted piperidines

These findings additionally revealed, that a perturbation of the equilibrium conformations also occurred upon protonation of the heterocyclic amine.¹¹ Again, this result is a product of the desire for equatorial substituents to reside axially, wherein they have a greater ability to provide charge stabilization. For example, after protonation of the fluoropiperidine derivative seen in Figure 2.1, it was found to exist solely in the conformation where the electron-withdrawing substituents were axial. Furthermore, in viewing these compounds as analogs for similar cationic structures, they were easily likened to oxacarbenium ion intermediates. This could suggest that positively charged glycosylation intermediates will spontaneously undergo conformational changes in an attempt to maximize the number of axial substituents, which could impact the reactivity and stereoselectivity of the reaction.

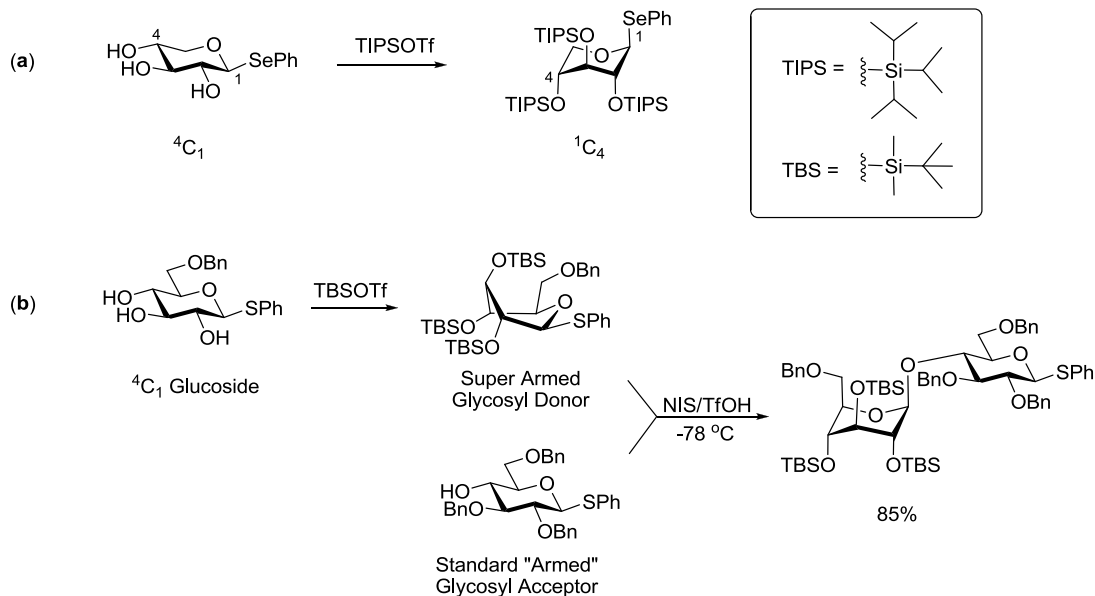
In further application toward carbohydrates, it was subsequently established that a glycosyl donor possessing axial substituents at the C-3 and C-4 position had a more stabilized oxacarbenium ion intermediate, relative to an analogous glycosyl donor with all equatorial substituents. Accordingly, this configurational modification proved to increase the reactivity of the glycosyl donor, and also provided further insight into the reactivity difference between the various sugar derivatives (gluco-, manno-, galacto-, *etc.*), thus bringing to light the profound impact that subtle electronic changes can have on the reactivity of the glycosyl donor. In turn, this led to the concept of conformationally superarming the glycosyl donors, as discussed in the next section.¹²

2.1.3 Pyranose ring conformation (of the glycosyl donor)

It was noticed that the steric bulk accompanying a variety of the groups could have a profound impact on the stereochemical outcome of the reaction.¹³ This was in part due to congestion near the anomeric center, increasing the accessibility of one facial approach over another. However, it was later found that introducing steric congestion at more remote positions (such as the equatorial C-3 and C-4 positions) could cause significant conformational changes in the glycosyl donor.¹⁴

Conformational superarming

This concept was utilized by Matsuda and Shuto *et al.*,¹⁵ wherein bulky triisopropylsilyl (TIPS) protecting groups were installed at the C-3 and C-4 positions, causing xylopyranose derivatives¹⁶ to flip from their typical ⁴C₁ conformation to the less common ¹C₄ conformer (Figure 2.2a).¹⁴



Scheme 2.2 Conformationally modified glycosyl donors (a) 1C_4 chair conformation of TIPS-protected β -D-xylopyranoside (b) application of conformationally superarmed TBS-protected glycosyl donor

However, when this methodology was applied toward glucose analogs, they were found to exist in more of a skew-boat conformation (as shown for the superarmed glycosyl donor in Scheme 2.2b),¹⁷ perhaps due to the added bulk of the substituent at C-5. Nevertheless, this general approach sufficiently induced the conformational change necessary to reconfigure the substituents perpendicular to the sugar ring. As a result, these conformationally armed (ring flipped) glycosyl donors have shown a dramatic increase in reactivity relative to the traditional armed, benzylated derivatives (Scheme 2.2b)¹⁸ This increase in reactivity was further verified through kinetic studies, wherein the conformationally armed donor was found to react 20-fold faster than its armed counterpart, and could be successfully coupled with armed acceptors.¹⁹

Similar observations have been made with glycosyl donors of the manno, rhamno, and galacto series.²⁰

Conformational disarming

In contrast to conformational arming, Fraser-Reid and co-workers discovered that locking the pyranose ring in the 4C_1 chair conformation disarms the glycosyl donor.²¹ This deactivation is attributed to the increased rigidity of the fused ring system, calculating that the oxacarbenium ion intermediate is not able to achieve the requisite planar geometry (about the C-2–C-1–O-5–C-5 atoms) in the half-chair transition state (Figure 2.2a). Additionally, this concept was expanded upon by Ley and co-workers in their exploration of 1,2-diacetal systems.²²

In further mechanistic probing, Bols and co-workers proposed that the source of the disarming effect may not be solely conformational, but may also be partially due to the orientation of the C-6 substituent.²³ Ingeniously, a series of torsionally restricted substrates were designed wherein each one was varied with respect to the orientation of its C-6 substituent (Figure 2.2b, rotamers **b–d**). The reactivities of these analogs were then compared to that of the unrestricted parent compound (**a**). Indeed, it was found that a basic torsional disarming effect *does* exist, as all of the conformationally restricted analogs exhibited a much lower reactivity towards acidic hydrolysis. However, the data suggests that the stereoelectronic effect²⁴ of the substituent configuration *also* plays a significant role in the overall level of disarming. As seen in Figure 2.2b, the torsionally disarmed rotamer (**b**), wherein the methoxy substituent is perpendicular to the ring, is 1.5 times more reactive than rotamer **c**, and 3.5 times more reactive than rotamer **d**, which is the conformation adopted in 4,6-acetal-protected glucosyl donors. Thus, it was concluded that both

conformational restriction and stereoelectronics (charge–dipole interactions) were equally responsible for the observed disarming effect.

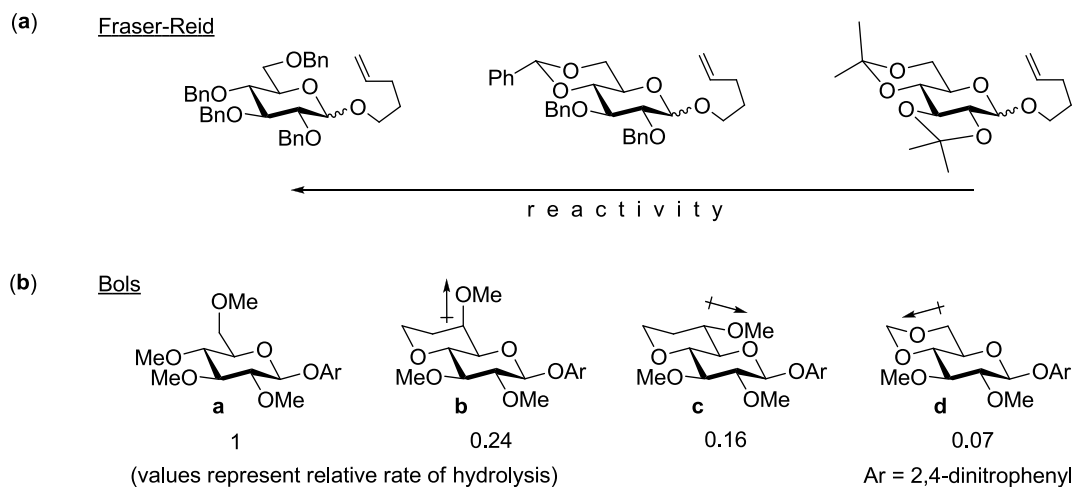


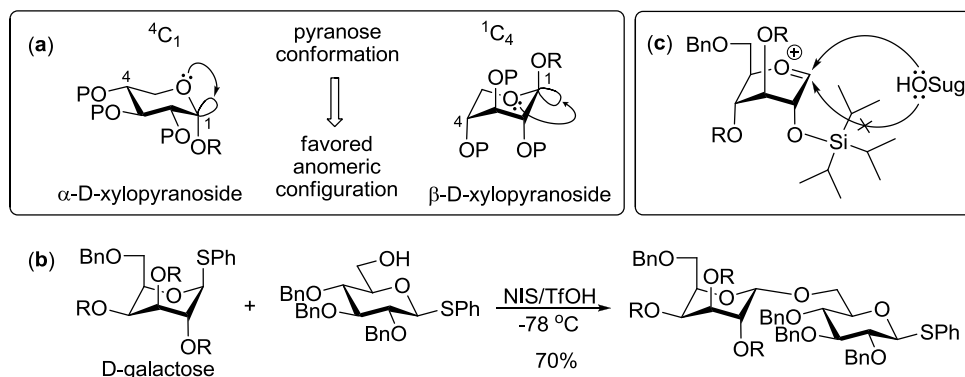
Figure 2.2 (a) Relative reactivities of *O*-pentenyl glycosides (b) electronic effect of the C-6 orientation on glycosyl donor reactivity

2.2 Current Theories behind Glycosylation Stereoselectivity

As previously covered in Chapter 1.4.1, it is thought that the facial preference (α or β) of the approaching nucleophile is largely responsible for the stereoselectivity of the glycosylation reaction. Seeing that both the energy associated with the transition state of the approaching nucleophile and the stability of the formed product can influence the anomeric ratio, the following studies have focused their efforts toward determining (both theoretically and experimentally) the driving force behind the resulting stereoselectivity.

2.2.1 Pyranose ring conformation (of the glycosyl donor) and its influence on the anomeric effect

In 2000, Matsuda and Shuto began investigating various silylated xylopyranosyl donors that existed in the ring-flipped 1C_4 conformation.¹⁵ They found that through this conformational modification, excellent β -stereoselectivity could be achieved, even in the absence of neighboring group participation. This was proposed to be a consequence of the anomeric effect (addressed in Section 1.4.2), wherein formation of the axial anomer is thermodynamically favored (Scheme 2.3a). On this premise, experiments were designed wherein various xylose derivatives were inverted to their 1C_4 conformations, in an attempt to alter the anomeric effect, and thereby reversing their stereoselectivities.¹⁶



Scheme 2.3 Attempts to reverse the anomeric effect with conformationally inverted glycosyl donors. (a) influence of conformation on the anomeric effect, (b) glycosylation using conformationally inverted D-galactosyl donor, (c) steric factors affecting transition state of a ring inverted D-glucosyl donor.

However, a further study by Bols and co-workers revealed that the ring-flipped glycosyl donors of the D-manno-, D-galacto-, and L-rhamno series lead to nearly complete α -stereoselectivity

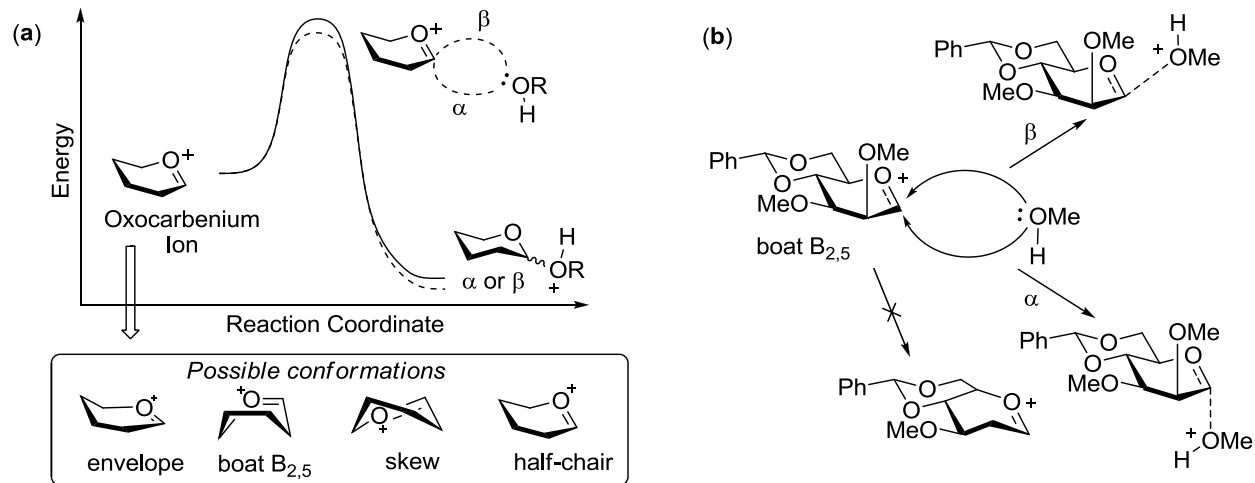
(Scheme 2.3b), a stark contradiction to the anticipated β -influence of the anomeric effect. Interestingly, only the D-glucopyranose analog provided excellent β -stereoselectivity (see Scheme 2.2b).²⁰ Thus, it was subsequently rationalized that steric factors were actually the underlying basis for the selectivity of these reactions. Yamada *et al.*, further reinforced this observation, attributing the β -selectivity in glucose derivatives to the steric environment created by the near 1C_4 (skew-boat) conformation (Scheme 2.3c).¹⁷

2.2.2 Oxacarbenium ion conformation – approach of the acceptor

Whitfield *et al.* also investigated the stereoselectivity with which glycosylation reactions proceed; however, they attributed the glycosylation outcome to the conformational preference of the oxacarbenium ion intermediate.²⁵ As previously touched upon in Chapter 1.4.1, this rationale was based upon the energy differences of the transition states associated with the transformation of the oxacarbenium ion intermediate to the glycoside product (assuming an S_N1 mechanism). Accordingly, each face of attack (α or β) will possess a different transition state energy and therefore, the major glycosylation product will be associated with the lower energy transition state (Scheme 2.4). As various factors can contribute to the energy inequalities in this transition state, theoretical calculations had to consider several effects, including: solvation, hydrogen bonding, bonding interactions between the incoming nucleophile and the oxacarbenium ion, ring strain induced by the incoming nucleophile or by hydrogen bonding, and differential ion pairing.

Before the relative energies of the transition states could be calculated, it followed that the conformation of the oxacarbenium ion intermediate needed to first be established. Previously, it had been proposed that low-energy conformations, such as half-chairs, were the most likely, as

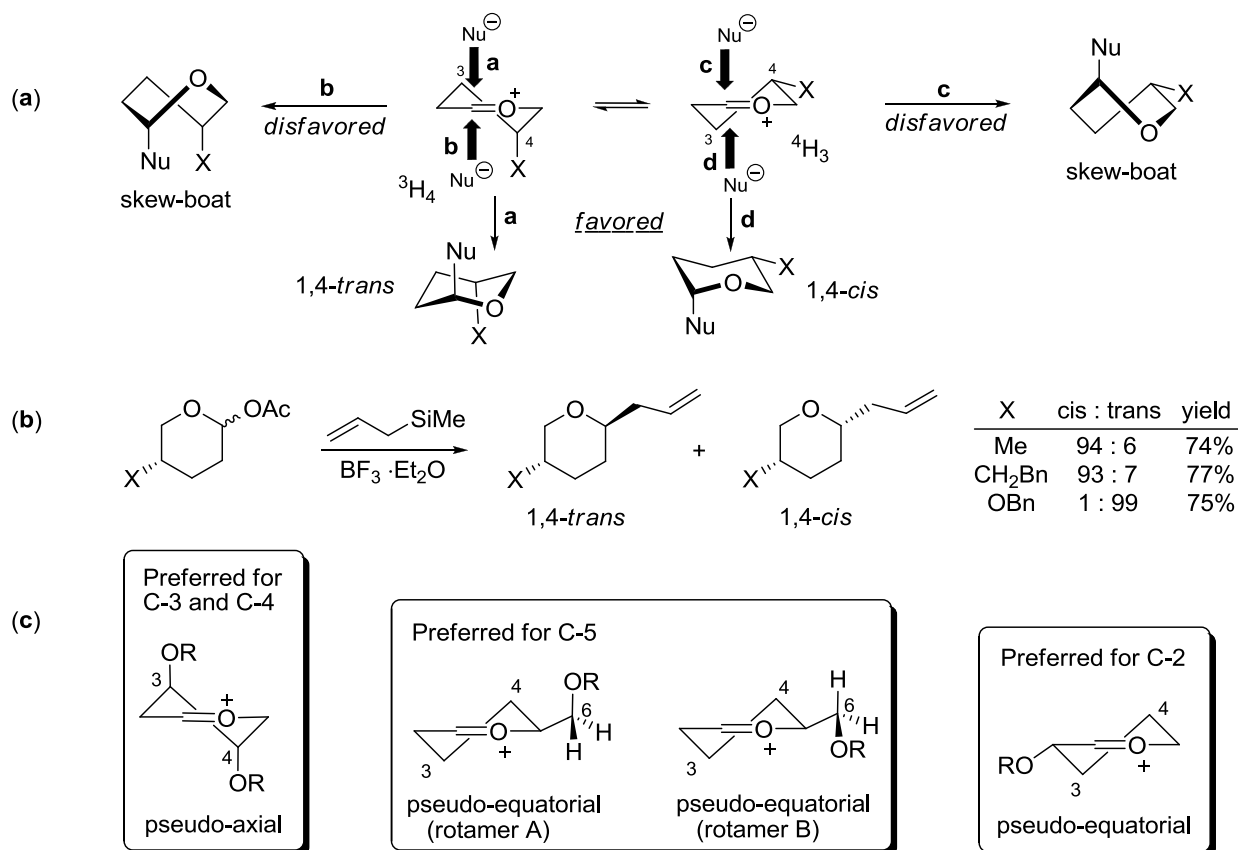
they mimic the flattened sp^2 geometry of the electron deficient anomeric center (C-5–O-5–C-1–C-2).²⁶ However, the ensuing calculations revealed that the flexibility of the pyranose ring actually allowed for a wider variety of intermediates. As such, the boat, skew, and envelope conformations were added to the pool of low-energy intermediate conformations (Scheme 2.4a). This required that the likely oxacarbenium ion conformations, corresponding to each and every glycosyl donor, be individually calculated.²⁷ It was thus found that each glycosyl donor gives rise to two possible series of low-energy oxacarbenium ion conformations,^{25, 28} one series being the ring-flipped version of the other. To simplify the study, one series of conformers was prevented from forming by introducing a rigid 4,6-acetal protecting group to the glycosyl donor. For example, the 4,6-*O*-benzylidene-2,3-di-*O*-methyl-mannopyranosyl cation can only exist in the series corresponding to the B_{2,5} conformation, but not in the family of conformers represented by ring inversion (Scheme 2.4b).²⁵ With this simplification, it was calculated that the transition state formed from the β -attack of the glycosyl acceptor (MeOH) was 38 kJ mol⁻¹ lower in energy than its α -approach, and thus the β -glycoside was predicted to be the major product. While the theoretical calculations of these simplified donor–acceptor systems were in good correlation with the experimental results, it is not to be expected that this method can be used to generally predict the diastereomeric product ratio of any glycosylation. However, it does reinforce the proposed theory that the stereoselectivity arises from the conformational preferences of the oxacarbenium ion intermediate. Furthermore, it implies that the relative energies of the transition states corresponding to α - and β -attack play an important role in defining the final product selectivity. It is thus anticipated that this knowledge can be instrumental in designing future glycosyl donors, wherein conformational restrictions may be implemented to generate a high degree of facial selectivity.



Scheme 2.4 (a) Reaction profile of oxocarbenium ion transition-state, (b) plausible reaction pathways of 4,6-*O*-benzylidene-2,3-di-*O*-methyl-mannopyranosyl cation

2.2.3 Oxocarbenium ion conformation – protecting group influence

Possessing a similar viewpoint, Woerpel and co-workers also reported on the adopted conformations of oxocarbenium ions, and their effect on the facial preferences of incoming nucleophiles. Their approach utilized substituted tetrahydropyrans as model substrates, wherein the steric and electronic effects of the attached substituents could be methodically studied.²⁹ An anomeric acetate was used as the leaving group, and to ensure irreversibility of the glycoside formation, allyltrimethylsilane was employed as the nucleophile. Subsequently, systematic changes were made to the substituted tetrahydropyran glycosyl donor and the resulting *cis/trans* ratios of the *C*-glycoside products were recorded. These ratios were then used to determine how the various protecting group modifications affected the conformation of the ensuing oxocarbenium ion intermediate.



Scheme 2.5 Investigation with C-4 substituted tetrahydropyrans (a) intermediates corresponding to the various trajectories of nucleophilic attack (b) stereoselectivity of C-glycoside formation (c) preferred substituent orientations

As depicted in Scheme 2.5a, Woerpel initially presumed that oxocarbenium ions exist in rapid equilibrium between two diastereomeric half-chair conformations, either 4H_3 or 3H_4 . As dictated by the location and type of substituent(s) attached to the ring, one of these conformers should be generally more preferred. Furthermore, because orbital interactions favor a pseudo-axial attack on the sp^2 carbon, there are only two possible trajectories of attack on each half-chair conformer, each leading to a different product stereoselectivity (α or β).²⁹ However, one of these facial approaches can always be excluded, due to the high energy skew-boat transition state that is

encountered en route to product formation (disfavored pathways **b** or **c**, Scheme 2.5a). Thus, the alternative facial approach, wherein the more stable chair-like transition state occurs (favored pathways **a** or **d**), always predominates.³⁰ As the 4H_3 or 3H_4 half-chairs are diastereomers, the allowed facial attack on one diastereomer will result in an α -glycoside, while the same allowed attack of the other will lead to a β -glycoside. Thus, the major glycoside product will also reveal which oxacarbenium ion conformer predominates.

For example, the experimental results shown in the table in Scheme 2.5b, revealed opposite stereochemical outcomes for an alkyl vs. alkoxy substituent. The product route associated with the 1,4-*cis* formation was traced back to the 4H_3 conformation of the oxacarbenium ion, whereas the 1,4-*trans* product resulted from the 3H_4 conformation.³¹ Using this method, they found that alkoxy substituents at the C-3 and C-4 positions preferred to adopt the half-chair conformation wherein they could exist pseudo-axially, ultimately giving rise to 1,4-*trans* products. Conversely, alkyl substituents preferred conformations wherein they could reside pseudo-equatorially, and thus gave rise to 1,4-*cis* products. These opposing preferences are thought to be a product of electrostatic interactions³¹ similar to those of the charge–dipole effect proposed by Bols (Section 2.1.2 Figure 2.1).⁹ Therefore, in alkyl substituents, wherein there can be no electrostatic stabilization, sterics predominate and so the pseudo-equatorial configuration is preferred. Further revealed, was the preference of the flexible C-5 alkoxyethyl group to reside in a pseudo-equatorial position, and that the orientation (rotamer) of the attached C-6 alkoxy group always pointed back over the ring (Scheme 2.5c, rotamer A).³¹ Lastly, the C-2 alkoxy substituent was found to prefer the pseudo-equatorial orientation, as it is thought to be involved in a stabilizing electronic interaction with the anomeric center (Scheme 2.5c).³¹

Additionally, van der Marel and co-workers have begun studying the influence of the C-5 position on glycosylation stereoselectivity.³²⁻³⁴ It was shown that a carboxylic acid functionality at C-5 (uronic acids) displays an extremely strong axial preference in its oxacarbenium ion transition state, much higher than that of an ether or alkyl protecting group at C-5. Again, the primary motivation for this preference is electrostatic charge stabilization of the oxacarbenium ion. Thus, in the case of mannuronate esters, wherein all substituents occupy their preferred transition state configurations, a completely β -selective glycosylation was achieved.

Armed with this comprehensive knowledge, the preferred half-chair conformation for the model substrates was accurately predicted, however, the established preferences of these simplified systems does not take into account the additional steric (and possibly electronic) factors that are present in actual sugars. Thus, in more complicated systems, the stereoelectronic and steric complexities can compound rather quickly and may alter these established trends.³⁵

This said, both Whitfield and Woerpel ultimately reached the same conclusion, finding the configuration of the oxacarbenium ion intermediate to be highly influential in determining the diastereoselectivity of the glycosylation reaction. As such, the observed product stereoselectivity can ultimately be attributed to a delicate balance between steric and stereoelectronic effects influencing the transition state.

2.3 Exploration of Anomeric Inversion and Participation-Assisted Mechanistic Pathways

In the previous part of this chapter, discussions pertained mainly to oxacarbenium ion intermediates as they were transformed directly into their respective glycoside products, upon nucleophilic attack by the glycosyl acceptor. However, there are often many other reactive species present in the reaction mixture, such as the counter anion of the electrophilic promoter, the leaving group, additives (such as bases), the solvent, or even the intramolecular participation of protecting groups.³⁶ This creates an opportunity for other reactions to occur at the anomeric center prior to the attack of the glycosyl acceptor. As such, the resulting intermediate species can also affect the product stereoselectivity. Therefore, investigating such species can provide further insight into the general mechanistic pathways and preferences of the glycosylation reaction.

Herein, discussions will pertain to a few chosen intermediates, and the pathways and conformational changes undergone en route to product formation. Reaction intermediates of both intermolecular (glycosyl triflate) and intramolecular (neighboring group participation) character will be considered. Often, these intermediate species exert a profound influence upon the stereoselectivity of the glycosylation reaction. Therefore, it is conjectured that these reactions may proceed *via* a concerted nucleophilic displacement.³⁷ However, the probability of an actual S_N2 mechanism occurring at the anomeric center is proposed to be highly unlikely, even in completely stereoselective reactions.³⁸ Such claims have been attributed to the electron–electron repulsions that are encountered upon nucleophile approach,³⁹ as well as the weakness of typical nucleophiles used in glycosylation. Based upon this assumption, an intermediate glycosylation

species that is formed must first transform back into a cationic species before glycosyl acceptor attack occurs. As such, comparisons can be made between the factors that affect the transition of a glycosyl donor directly into a glycoside product and those which affect the transformation of a secondary intermediate into the observed glycoside product.

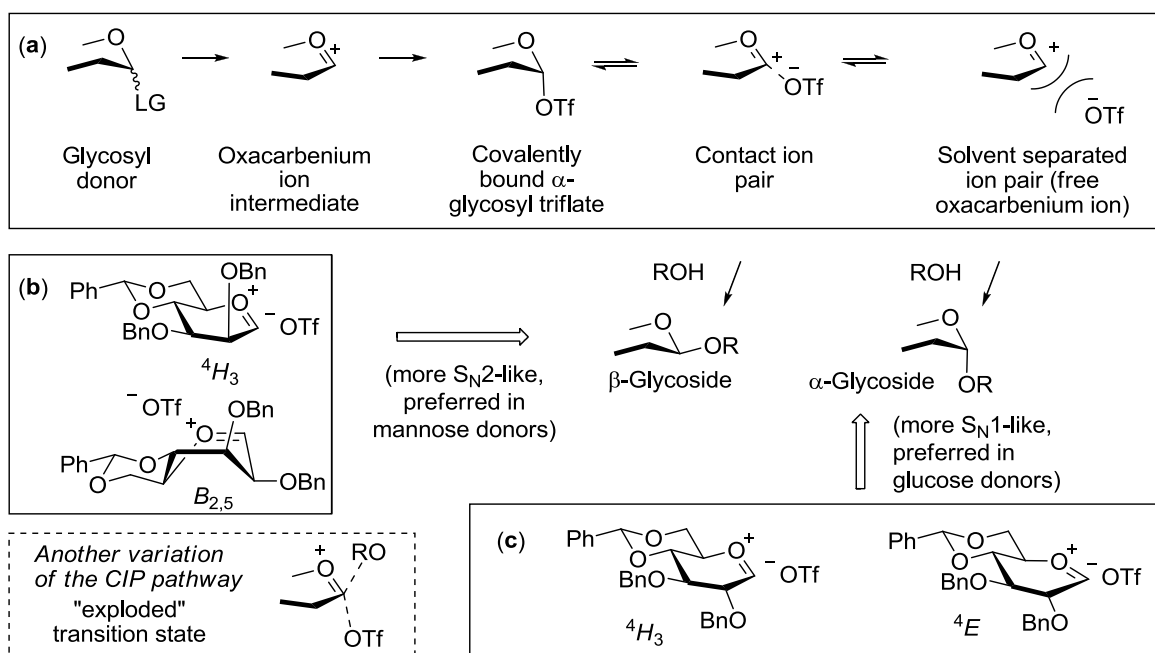
2.3.1 Displacement of counter-anions (glycosyl triflate)

First, we will start by addressing the glycosyl triflate. This species was brought to light when Crich *et al.* found that the stereoselectivity of a glycosidation reaction utilizing glycosyl sulfoxides, triflic anhydride and a pyridine-derived base was completely dependent upon the order of reagent addition.⁴⁰ Through spectroscopic studies, it was determined that when the reagents were added prior to the glycosyl acceptor (“pre-activation” conditions), a covalently bound triflate species would form *in situ*.⁴¹ Furthermore, the characteristics of the glycosidic bond formation reflected that of the intermediate triflate, and were independent of the original leaving group employed.⁴² Probing this mechanism revealed that the stereoselectivity with which the reaction proceeded was strongly dependent upon the core monosaccharide structure and selected protecting groups.^{43, 44} Thus, the pre-activation of a mannosyl donor, possessing the conformationally restrictive 4,6-benzylidene acetal, with Tf₂O and DTBMP (di-*tert*-butyl-4-methylpyridine), yielded a very stable α -triflate. Thereafter, the addition of a nucleophile often resulted in complete β -selectivity. In contrast, mannosyl donors lacking the rigid benzylidene protecting group were much less selective. One could presume that torsional disarming enhances the stability of the α -triflate, which then allows for the inversion product to form *via* concerted bimolecular displacement. Against expectations, however, the use of torsionally disarmed glucosyl donors preferentially led to the formation of α -glucosides.⁴³ Thus, the probability of the

reaction proceeding *via* a true S_N2 mechanism is highly questionable. Additionally perplexing was that the NMR spectra of the 4,6-benzylidene manno- and glucosyl donors revealed that only the α -triflate was present, diminishing the likelihood of an isomerization pathway (akin to Lemieux's halide ion promoted *in situ* anomerization protocol).⁴⁵

In order to discriminate between the possible S_N1 and S_N2 pathways, a kinetic isotope effect study was carried out using the benzylidene-protected α -mannosyl triflate.⁴⁶ By matching the experimentally determined results with already known kinetic isotope effects of simple glycoside hydrolysis, it was ascertained that the results were consistent with that of an S_N1 mechanism. This study led to a mechanistic interpretation wherein the covalently bound triflate first dissociates into a continuum of ionic species prior to nucleophilic attack (Scheme 2.6a). Consequently, the stereoselectivity of these reactions arises from the dominant ionic species through which the product formation occurs. Accordingly, it was concluded that the α -selectivity seen with the 4,6-benzylidene glucosyl donors must have occurred *via* a solvent separated ion pair (*i.e.* free oxocarbenium ion), whereas the β -selectivity seen in 4,6-benzylidene mannosyl donors occurred through a contact ion pair. The rationalization is that the solvent separated ion pair can allow for attack to occur from either face, whereas the contact ion pair will inhibit the bottom face attack. This can either be due to a shielding effect or a remaining loose attachment (*i.e.* “exploded transition state”) as the triflate anion departs from the donor (Scheme 2.6a). In order to bolster this mechanistic interpretation, a study of the various conformations of the corresponding oxocarbenium intermediate species was embarked upon. Therein, it was assumed that the more stable the oxocarbenium ion intermediate was, the more likely its existence. As a consequence, the equilibrium will shift from the covalently bonded α -triflate toward the solvent

separated ion pair, thus decreasing the β -selectivity. Therefore, it was surmised that the energy required for the mannosyl donor to proceed to its cationic intermediate was higher than that of its glucosyl counterpart.



Scheme 2.6 Proposed participation–dissociation pathway in a glycosylation reaction: glycosyl triflates. (a) continuum of ionic species, (b) preferred oxocarbenium ion species for 4,6-*O*-benylidene protected D-mannosyl donor, (c) preferred oxocarbenium ion species for 4,6-*O*-benylidene protected D-glucosyl donor

Seeing as the only structural difference between the two glycosyl donors is the configuration about the C-2 position, the torsional angle about this bond was examined. To begin these studies, a conformational model of the oxocarbenium ion was needed. Taking into consideration the theoretical calculations of prior studies,^{25, 28, 35} plausible conformations were considered to be the

4H_3 half-chair, the $B_{2,5}$ boat, and the 4E envelope (Scheme 2.6b,c). As shown in Table 2.1, there is a greater compression of the O-2-C-2-C-3-O-3 torsional angle upon going from the mannosyl triflate to its proposed oxacarbenium intermediates, as compared to the relaxation of this torsional angle upon transition of the glucosyl species. It was thereby postulated that the rehybridization of the anomeric carbon causes unfavorable changes in the case of the mannosyl donor, whereas this transformation is much more favored in the case of the glucosyl donor.⁴⁷ Therefore, the instability of the mannosyl oxacarbenium ion intermediate, causes the equilibrium to shift toward the covalently bound glycosyl triflate, leading to a more S_N2 -like displacement, and thus higher β -selectivity. The opposite is true for the glucosyl donor, wherein equilibrium will shift toward the free ion pair, resulting in a more S_N1 -like mechanism. In related study by Huang and Whitfield *et al.*,⁴⁸ anomeric triflates equipped with a C-2 participating group were investigated. Therein, it was found that the more electron-deficient the sugar ring was, the more apt the species was to form the covalently bound anomeric triflate. Conversely, the more electron-rich the ring was, the more likely it was to form the positively charged acyloxonium ion, again, reinforcing the notion that the reactivity and selectivity of the reaction was found to be strongly dependent upon the stability of their respective glycosylation intermediates.

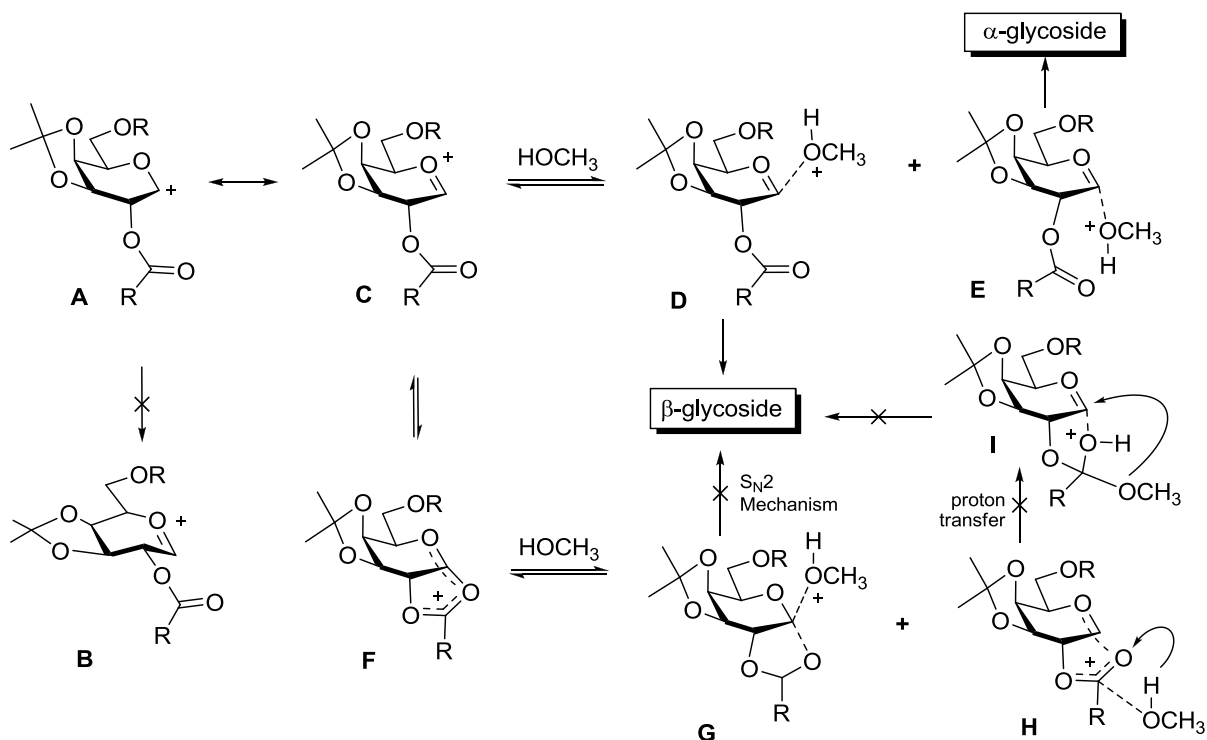
Table 2.1 Torsional angle values (and change) from α -glycosyl triflates to their likely oxacarbenium conformers

Mannosyl	O2-C2-C3-O3	Glucosyl	O2-C2-C3-O3
α -OTf	60°	α -OTf	60°
4H_3	45° (-15°)	4H_3	75° (+15°)
$B_{2,5}$	60° (0°)	4E	90° (+30°)

2.3.2 Intramolecular participation

Whitfield *et al.* further probed the role that auxiliary species may play in the glycosylation reaction. They studied the mechanism by which intramolecular neighboring group participation occurs. These studies uncovered an array of challenges similar to those of the intermolecular glycosyl triflate participation. As aforementioned, the probability of an actual S_N2 mechanism occurring at the anomeric center is highly unlikely, even in highly stereoselective reactions, such as those with the neighboring group participation.³⁸ If true, then the acyloxonium intermediate must first dissociate prior to nucleophilic attack. Consequently, a resulting contact ion pair must be responsible for the observed stereoselectivity. While it is commonly assumed that the bicyclic acyloxonium ion intermediate is solely responsible for the high (and often complete) stereoselectivity achieved with 2-acyl derivatives, Whitfield *et al.* have provided a viable alternative.³⁸ First, they were able to limit the number of possible intermediate conformations to two (oxacarbenium ion **C**, and acyloxonium ion **F**, Scheme 2.7), through the use of conformationally restricted glycosyl donors. Subsequently, low-energy pathways connecting these key intermediates to the other plausible species (*i.e.* **D**, **E**, **G**, **H** and **I**) en route to the anticipated 1,2-*trans* and 1,2-*cis* product, were calculated. It was assumed that acyloxonium ion **F** can form only after the formation of oxacarbenium ion **C**. Although **F** was calculated to be a lower energy intermediate, the C-2 substituent must adopt a pseudo-axial orientation in order to bond with the anomeric center. Therefore, these conformational changes create a small energy barrier that must first be overcome.²⁷ Further still, was the problem that once **F** did form, calculations could not find a reasonable low-energy pathway linking its subsequent intermediates (**G** or **H**) to the observed β -glycoside product.³⁸ While it seems counterintuitive, protonated orthoester **H** was actually calculated to be the preferred intermediate. Hence, if the reaction

mechanism does proceed by this route, it would likely have to involve a proton transfer to form a higher energy intermediate **I**, before formation of the β -linked product could occur.



Scheme 2.7 Plausible mechanism of neighboring group-assisted formation of
1,2-*trans* glycosides

Because this seemed improbable, they presented the possibility that the stereoselectivity may instead emanate from a face-discriminated attack upon the monocyclic oxocarbenium ion **C**.²⁷ To test this hypothesis, the relative energies of adducts **D** and **E** were calculated, wherein the β -methanol adduct **D** was found to be of lower energy.²⁵ The energy disparity in these calculations was shown to be highly influenced by both anomeric and hydrogen bonding preferences. Resultantly, it was reasoned that the pathway involving intermediate **D** could, in fact, be

responsible for the observed β -stereoselectivity; however, the mechanistic possibility of attack occurring *via* the bicyclic species **G** or **H** could not be completely ruled out.

Recently, a variety of alternative neighboring participating groups have also been investigated. For instance, Boons and co-workers have demonstrated that an (*S*)-1-phenyl-2-thiophenylethyl group at the C-2 position of a glycosyl donor is capable of an efficient neighboring group participation *via* a quasi-stable anomeric *trans*-decalin sulfonium ion (Figure 2.3a).^{49, 50} Displacement of the sulfonium ion by a hydroxyl group leads to the stereoselective formation of 1,2-*cis* glycosides. This study was recently reinforced by showing that thioether additives can increase the α -stereoselectivity of the glycosylation reaction by forming an anomeric β -sulfonium ion.⁵¹ The preference for the formation of the β -species was attributed to a minimization of steric interactions, as opposed to the typical stereoelectronic justification of the reverse anomeric effect.

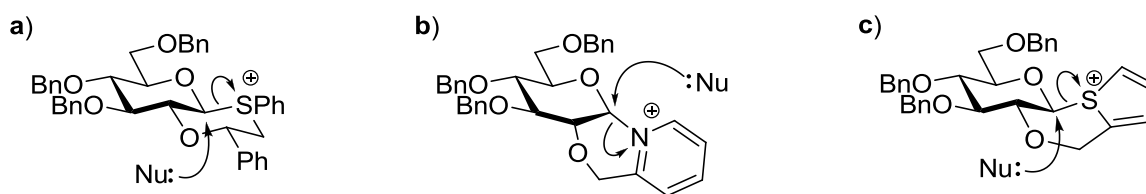
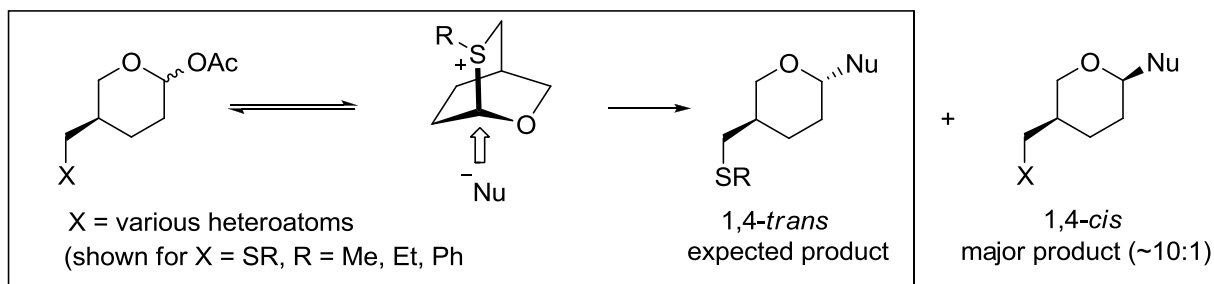


Figure 2.3 Alternative participating groups

Additionally, Demchenko and co-workers studied 2-picolinyl derivatives which provided a stable 1,2-*cis* participation intermediate, leading to a completely stereoselective 1,2-*trans* glycosylation (Figure 2.3b).^{52, 53} NMR experiments were employed to show the presence of the

proposed reaction intermediates shown in Figures 2.3a and 2.3b. Very recently, Fairbanks showed the versatility of 2-(thiophen-2-yl)methyl derivatives capable of stereoselective 1,2-*cis* glycosylation *via* the proposed intermediate shown in Figure 2.3c.⁵⁴

Both α - and β -sulfonium species were recently studied by Yoshida and co-workers, wherein the authors suggest that glycosidation of the sulfonium intermediates may proceed *via* glycosylation (S_N1).⁵⁵ Woerpel *et al*^{56, 57} also proposed that the mechanisms for neighboring group participation may actually proceed through the open cation. Investigations were initially carried out on C-4-sulfur-substituted tetrahydropyrans, wherein it was revealed that the resultant 1,4-*cis* product did not correspond to a pathway involving participation from a sulfonium ion species as expected (Scheme 2.8). Mathematical calculations verified the ring-closed sulfonium ion to be the lowest energy intermediate, and the existence of the sulfonium-ion species resulting from C-4 participation was confirmed by NMR. This phenomenon was further probed by investigating additional C-4-substituted tetrahydropyrans, containing a variety of heteroatoms (selenium, sulfur, oxygen and halogens), yet all analogous species revealed a selectivity preference in favor of the 1,4-*cis* product. External factors such as solvent, promoter and nucleophile were additionally investigated, and unexpectedly, the stereoselectivity got worse as the nucleophilicity was increased. These surprising findings strongly suggest that prudence should be administered when justifying the product formation. Although it is common practice to base reaction outcomes on calculated low-energy intermediates, it does not necessarily mean that these species are involved in the pathway of product formation, an idea reinforced by the Curtin–Hammett kinetic scenario,⁵⁸ which states that product formation does not necessarily have to occur *via* the lowest energy intermediates.



Scheme 2.8 Model study of the neighboring group participation

2.4 Conclusions and Future Implications

As that the studies and examples surveyed herein cannot definitively answer many of the mechanistic questions remaining about the glycosylation reaction, they can at least offer unique perspectives with which problems can be approached. Furthermore, while the topics covered in this chapter seem broad in their ideologies, when coupled with our existing knowledge about the glycosylation reaction, they can only serve to enhance our synthetic capabilities, allowing us to better understand and justify the decisions we make regarding how to control the outcome of the reaction. In turn, this knowledge has aided in the rationalization and understanding of the unusual mechanistic findings discovered within this doctoral dissertation work. As such, the following chapters will intermittently reference many of the aforementioned studies, giving special consideration to discussions of the armed-disarmed theory (Section 2.1.1), displacement of anomeric glycosyl triflates (2.3.1), and the investigations of anomeric sulfonium ions as glycosyl donors (2.3.2).

2.5 References

1. Fraser-Reid, B.; Jayaprakash, K. N.; Cristóbal López, J.; Gómez, A. M.; Uriel, C., Protecting Groups in Carbohydrate Chemistry Profoundly Influence All Selectivities in Glycosyl Couplings. In *Frontiers in Modern Carbohydrate Chemistry*, Demchenko, A. V., Ed. Oxford Univ. Press: 2007; Vol. 960, pp 91-117.
2. Mootoo, D. R.; Konradsson, P.; Udodong, U.; Fraser-Reid, B., *J. Am. Chem. Soc.* **1988**, *110*, 5583-5584.
3. Smoot, J. T.; Demchenko, A. V., *Adv. Carbohydr. Chem. Biochem.* **2009**, *62*, 161-250.
4. Douglas, N. L.; Ley, S. V.; Lucking, U.; Warriner, S. L., *J. Chem. Soc., Perkin Trans. 1* **1998**, 51-65.
5. Zhang, Z.; Ollmann, I. R.; Ye, X. S.; Wischnat, R.; Baasov, T.; Wong, C. H., *J. Am. Chem. Soc.* **1999**, *121*, 734-753.
6. Schmidt, T.; Madsen, R., *Eur. J. Org. Chem.* **2007**, 3935-3941.
7. Crich, D.; Vinogradova, O., *J. Am. Chem. Soc.* **2007**, *129*, 11756-11765.
8. Kamat, M. N.; Demchenko, A. V., *Org. Lett.* **2005**, *7*, 3215-3218.
9. Jensen, H. H.; Lyngbye, L.; Bols, M., *Angew. Chem. Int. Ed.* **2001**, *113* (18), 3555-3557.
10. Jensen, H. H.; Lyngbye, L.; Jensen, A.; Bols, M., *Chem. Eur. J.* **2002**, *8*, 1218-1226.
11. Jensen, H. H.; Bols, M., *Acc. Chem. Res.* **2006**, *39*, 259-265.
12. McDonnell, C.; Lopez, O.; Murphy, P.; Bolanos, J. G. F.; Hazell, R.; Bols, M., *J. Am. Chem. Soc.* **2004**, *126*, 12374-12385.
13. Demchenko, A. V., *Curr. Org. Chem.* **2003**, *7* (1), 35-79.
14. Hosoya, T.; Ohashi, Y.; Matsumoto, T.; Suzuki, K., *Tetrahedron Lett.* **1996**, *37*, 663-666.

15. Shuto, S.; Yahiro, Y.; Ichikawa, S.; Matsuda, A., *J. Org. Chem.* **2000**, *65*, 5547-5557.
16. Abe, H.; Shuto, S.; Matsuda, A., *J. Am. Chem. Soc.* **2001**, *123*, 11870-11882.
17. Okada, Y.; Nagata, O.; Taira, M.; Yamada, H., *Org. Lett.* **2007**, *9*, 2755-2758.
18. Pedersen, C. M.; Nordstrom, L. U.; Bols, M., *J. Am. Chem. Soc.* **2007**, *129*, 9222-9235.
19. Pedersen, C. M.; Marinescu, L. G.; Bols, M., *Chem. Commun.* **2008**, 2465-2467.
20. Jensen, H. H.; Pedersen, C. M.; Bols, M., *Chem. Eur. J.* **2007**, *13*, 7576-7582.
21. Fraser-Reid, B.; Wu, Z.; Andrews, C. W.; Skowronski, E., *J. Am. Chem. Soc.* **1991**, *113*, 1434-1435.
22. Ley, S. V.; Baeschlin, D. K.; Dixon, D. J.; Foster, A. C.; Ince, S. J.; Priepeke, H. W. M.; Reynolds, D. J., *Chem. Rev.* **2001**, *101*, 53-80.
23. Jensen, H. H.; Nordstrom, L. U.; Bols, M., *J. Am. Chem. Soc.* **2004**, *126*, 9205-9213.
24. Kirby, A. J., *Stereoelectronic effects*. Oxford University Press: 1996.
25. Nukada, T.; Berces, A.; Whitfield, D. M., *Carbohydr. Res.* **2002**, *337*, 765-774.
26. Lemieux, R. U., *Chem. Can.* **1964**, *16*, 14-22.
27. Bércecs, A.; Enright, G.; Nukada, T.; Whitfield, D. M., *J. Am. Chem. Soc.* **2001**, *123*, 5460-5464.
28. Nukada, T.; Berces, A.; Wang, L.; Zgierski, M. Z.; Whitfield, D. M., *Carbohydr. Res.* **2005**, *340*, 841-852.
29. Romero, J. A. C.; Tabacco, S. A.; Woerpel, K. A., *J. Am. Chem. Soc.* **2000**, *122* (1), 168-169.
30. Ayala, L.; Lucero, C. G.; Romero, J. A. C.; Tabacco, S. A.; Woerpel, K. A., *J. Am. Chem. Soc.* **2003**, *125*, 15521-15528.
31. Yang, M. T.; Woerpel, K. A., *J. Org. Chem.* **2009**, *74*, 545-553.

32. Walvoort, M. T. C.; Lodder, G.; Mazurek, J.; Overkleeft, H. S.; Codee, J. D. C.; van der Marel, G. A., *J. Am. Chem. Soc.* **2009**, *131*, 12080-12081.
33. Dinkelaar, J.; de Jong, A. R.; van Meer, R.; Somers, M.; Lodder, G.; Overkleeft, H. S.; Codee, J. D. C.; van der Marel, G. A., *J. Org. Chem.* **2009**, *74*, 4982-4991.
34. Codee, J. D. C.; van den Bos, L. J.; de Jong, A.-R.; Dinkelaar, J.; Lodder, G.; Overkleeft, H. S.; van der Marel, G. A., *J. Org. Chem.* **2009**, *74*, 38-47.
35. Lucero, C. G.; Woerpel, K. A., *J. Org. Chem.* **2006**, *71*, 2641-2647.
36. Whitfield, D. M., *Adv. Carbohydr. Chem. Biochem.* **2009**, *62*, 83-159.
37. Whitfield, D. M.; Douglas, S. P., *Glycoconjugate J.* **1996**, *13* (1), 5-17.
38. Nukada, T.; Berces, A.; Zgierski, M. Z.; Whitfield, D. M., *J. Am. Chem. Soc.* **1998**, *120*, 13291-13295.
39. Dewar, M. J. S.; Dougherty, R. C., *The PMO Theory of Organic Chemistry*. Plenum: New York, 1975.
40. Crich, D.; Sun, S., *J. Org. Chem.* **1996**, *61*, 4506-4507.
41. Crich, D.; Sun, S., *J. Am. Chem. Soc.* **1997**, *119*, 11217-11223.
42. Crich, D.; Sun, S., *J. Am. Chem. Soc.* **1998**, *120*, 435-436.
43. Crich, D.; Cai, W., *J. Org. Chem.* **1999**, *64* (13), 4926-4930.
44. Crich, D., *J. Carbohydr. Chem.* **2002**, *21* (7-9), 667-690.
45. Lemieux, R. U.; Hendriks, K. B.; Stick, R. V.; James, K., *J. Am. Chem. Soc.* **1975**, *97* (14), 4056-4062 and references therein.
46. Crich, D.; Chandrasekera, N. S., *Angew Chem., Int. Ed.* **2004**, *43*, 5386-5389 and references therein.
47. Crich, D.; Vinogradova, O., *J. Org. Chem.* **2006**, *71*, 8473-8480.

48. Zeng, Y.; Wang, Z.; Whitfield, D.; Huang, X., *J. Org. Chem.* **2008**, *73*, 7952-7962.
49. Kim, J. H.; Yang, H.; Boons, G. J., *Angew. Chem. Int. Ed.* **2005**, *44*, 947-949.
50. Kim, J. H.; Yang, H.; Park, J.; Boons, G. J., *J. Am. Chem. Soc.* **2005**, *127*, 12090-12097.
51. Park, J.; Kawatkar, S.; Kim, J. H.; Boons, G. J., *Org. Lett.* **2007**, *9*, 1959-1962.
52. Smoot, J. T.; Demchenko, A. V., *J. Org. Chem.* **2008**, *73*, 8838-8850.
53. Smoot, J. T.; Pornsuriyasak, P.; Demchenko, A. V., *Angew. Chem. Int. Ed.* **2005**, *44*, 7123-7126.
54. Cox, D. J.; Fairbanks, A. J., *Tetrahedron: Asymmetry* **2009**, *20*, 773-780.
55. Nokami, T.; Shibuya, A.; Manabe, S.; Ito, Y.; Yoshida, J., *Chem. Eur. J.* **2009**, *15*, 2252-2255.
56. Billings, S. B.; Woerpel, K. A., *J. Org. Chem.* **2006**, *71* (14), 5171-5178.
57. Beaver, M. G.; Billings, S. B.; Woerpel, K. A., *J. Am. Chem. Soc.* **2008**, *130* (6), 2082-2086.
58. Seeman, J. I., *Chem. Rev.* **1983**, *83*, 83-134.

CHAPTER 3

Discovery of a Superarmed *S*-Benzoxazolyl Glycosyl Donor

Mydock, L. K.; Demchenko, A. V. "Super-Arming the *S*-Benzoxazolyl Glycosyl Donors by Simple 2-*O*-Benzoyl-3,4,6-Tri-*O*-Benzyl Protection," *Org. Lett.* **2008**, *10*, 2103–2106.

3.1 Introduction

The use of the thioimidate, 2-mercaptobenzoxazolyl (SBox), as a glycosyl donor leaving group, was first pioneered in our laboratory.¹ To this end, we have put much effort into developing, characterizing, and optimizing SBox glycosides in application to various carbohydrate strategies.²⁻⁵ An important aspect of this process is the incorporation of our SBox donors into current expeditious oligosaccharide methodologies. The utilization of one methodology in particular, the chemoselective activation approach (discussed in detail in Chapter 4), required that we first determine the relative reactivities of various SBox glycosyl donors. As per the premise of Fraser-Reid's armed-disarmed theory, this chemoselective methodology relies on the electronic effects that protecting groups can have on the reactivity of the glycosyl donor.^{6,7}

3.1.1 Armed-disarmed strategy revisited

As discussed in detail in Chapter 2.1.1, it is generally accepted that the reactivity trend in a given class of glycosyl donors, follows the conventional armed-disarmed strategy introduced by Fraser-Reid.⁷ That is, any glycosyl donor bearing all ether-protecting groups (i.e. OBn) will be significantly more reactive than its ester-protected (i.e. OBz) analog,⁸ and are thus referred to as "armed" and "disarmed," respectively (Figure 3.1). Furthermore, it is thought that this effect predominates from the neighboring substituent at C-2,⁹ and in addition, it is presumed that the overall reactivity of the glycosyl donor corresponds to the total number of ether substituents.^{8,10}

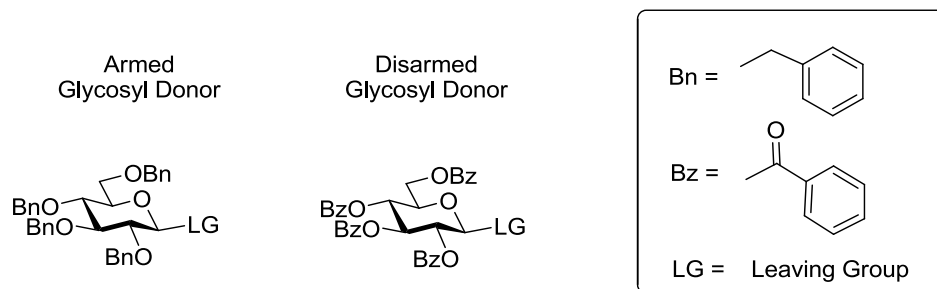


Figure 3.1 Classic armed and disarmed glycosyl donors

As a result, the type of protecting group chosen can generate enough of a reactivity difference between the glycosyl donors that one can be selectively coupled over the other, even though they bear the same type of leaving group. Subsequently, we began to investigate the reactivity of several SBox donors possessing various protecting group arrangements (3.1-3.3, Figure 3.2) in order to evaluate their relative reactivities. Thereupon, it was discovered that “mixed-patterned” SBox glycosyl donors (such as glycosyl donor 3.2) displayed an unexpectedly low reactivity, prompting us to revisit the rationale on which the armed-disarmed theory was built.⁴

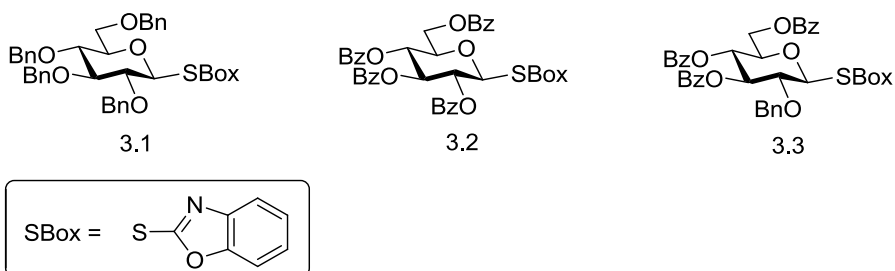


Figure 3.2 SBox glycosyl donors with varying protecting group arrangements

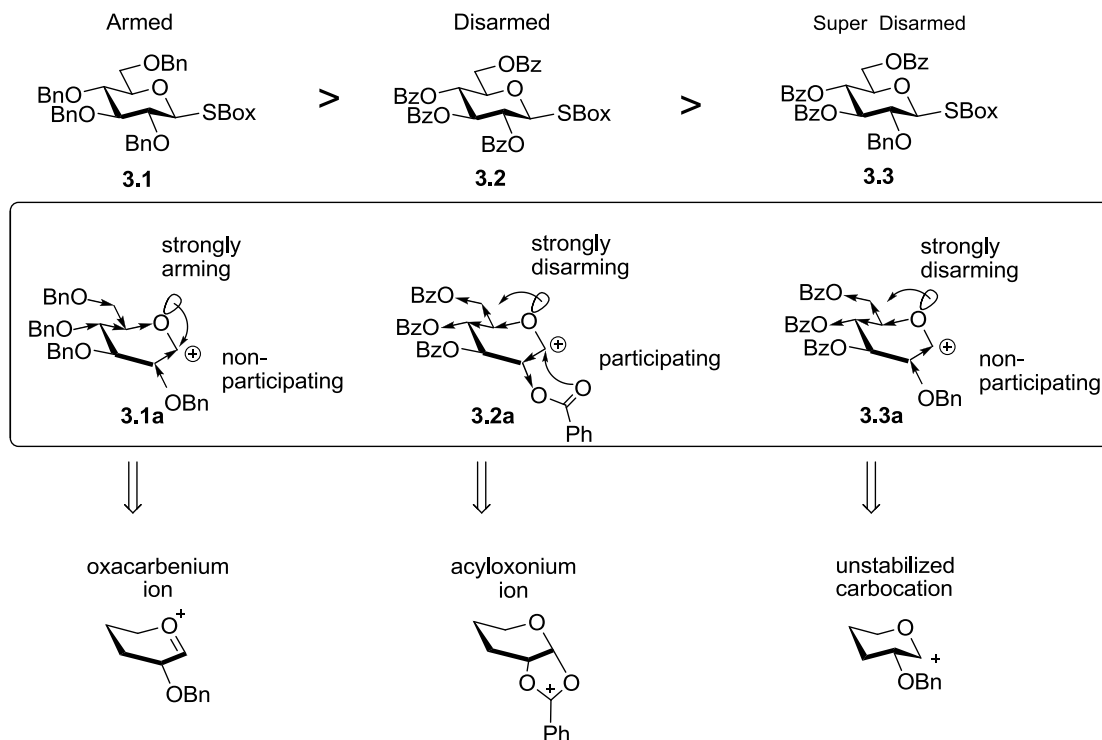
3.1.2 The O-2/O-5 cooperative effect

Although first discovered with *O*-pentenyl glycosides, the armed-disarmed concept has been proven with many other classes of compounds, including thioglycosides,¹¹ selenoglycosides,¹² fluorides,¹³ phosphoramidates,¹⁴ substituted thioformimidates,¹⁵ and glycols.¹⁶ Therefore, when expanded to include the *S*-benzoxazolyl (SBox) and *S*-thiazolanyl (STaz) glycosyl donors developed in our laboratory, these thioimidates were initially found to react accordingly.^{4,17} For example, we confirmed that the armed per-benzylated SBox glycoside **3.1** is significantly more reactive than its disarmed counterpart **3.2**.⁴

The story became intriguing, however, when glycosyl donors containing mixed protecting group patterns, such as 2-*O*-benzyl-3,4,6-tri-*O*-acyl derivative **3.3**, were considered. As per the total number and location of the benzyl substituent(s), it was believed that the reactivity of compound **3.3** would lie in between that of the fully ether-protected, armed donor **3.1** and the fully ester-protected, disarmed donor **3.2**. Unexpectedly, however, glycosyl donor **3.3** was experimentally determined to be less reactive than both the classic armed and disarmed donors, **3.1** and **3.2**, respectively.⁴ This resulted in an unexpected order of relative reactivities for our SBox glycosides (Scheme 3.1).

This was the first indication that there were more effects governing the reactivity of the glycosyl donor than just the electron-withdrawing/donating properties of its protecting groups. Ultimately, this finding gave rise to the theory that we call the “O-2/O-5

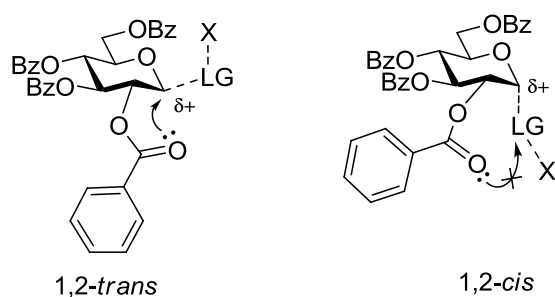
cooperative effect,”⁴ wherein we rationalized that the glycosyl donor reactivity is also dependent upon the stability of the glycosyl cation that is formed upon leaving group departure (Scheme 3.1).



Scheme 3.1 Mechanistic depiction of the O-2/O-5 cooperative effect in SBox glycosyl donors of the D-gluco series; Figures **3.1-3.3** show experimentally determined relative reactivities; Figures **3.1a-3.3a** illustrate the cooperative arming and disarming effects

Thus, as depicted in figure **3.1a**, armed benzylated glycosyl donor **3.1** can be efficiently stabilized through resonance with the “strongly-arming” lone pair electrons of O-5, resulting in the formation of an oxacarbenium ion. Conversely, figure **3.2a** reveals that in the case of disarmed benzoylated derivative **3.2**, this type of stabilization is less likely due to the electron-withdrawing substituents at C-4 and C-6. Instead, however, the

participating acyl substituent at C-2 allows for stabilization via the acyloxonium ion. In combination, these two competing effects result in a decrease in reactivity of glycosyl donor **3.2**, as compared to donor **3.1**. Supplementary to our findings, Crich and Li additionally uncovered the importance of the 1,2-*trans* anomeric configuration (for the SBox glycosyl donors of the D-gluco series), in order for this stabilizing C-2 participation to occur.¹⁸ This implies that the existence of a O-2 lone pair is simply not enough, but that it must also have access to the developing charge upon leaving group departure (Scheme 3.2).

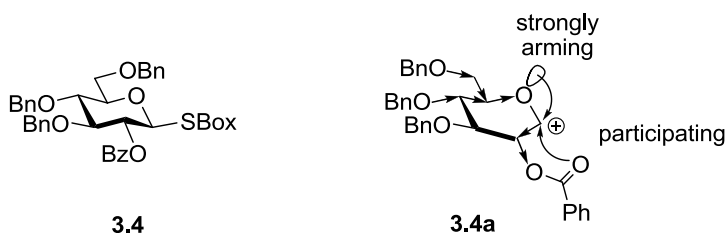


Scheme 3.2 Stabilization from the O-2 position via participation

Finally, the lack of reactivity seen in the case of glycosyl donor **3.3**, can accordingly be rationalized by the effects of its particular mixed protecting group pattern, **3.3a**. Consequently, lack of participation at the O-2 position, is further magnified by the “strongly disarming” lone pair electrons of O-5. Thus, the traditional “arming” benzyl protecting group at O-2 cannot begin to compensate for the unstabilized positive charge at the anomeric center. Therefore, this combination of protecting groups results in an overall super disarming effect for compound **3.3**, as was also observed experimentally.⁴

3.2 Utilization of the O-2/O-5 Cooperative Effect in Superarming Methodology

In utilizing our knowledge of the O-2/O-5 Cooperative effect, we subsequently postulated that “mixed-patterned” glycosyl donors consisting of a protecting group pattern reverse that of compound **3.3**, (such as **3.4**, Figure 3.3), would have exceptionally high reactivity, as it would contain both stabilizing elements, a participating moiety at C-2 and electronically armed lone pair at O-5. If true, in relation to the traditional per-benzylated armed glycosyl donor **3.1**, donor **3.4** could then be considered as “superarmed” (previously the term superarmed was coined by Bols and coworkers in their recent publications dedicated to conformationally modified glycosyl donors).^{19, 20}



Scheme 3.3 Proposed superarming mechanism

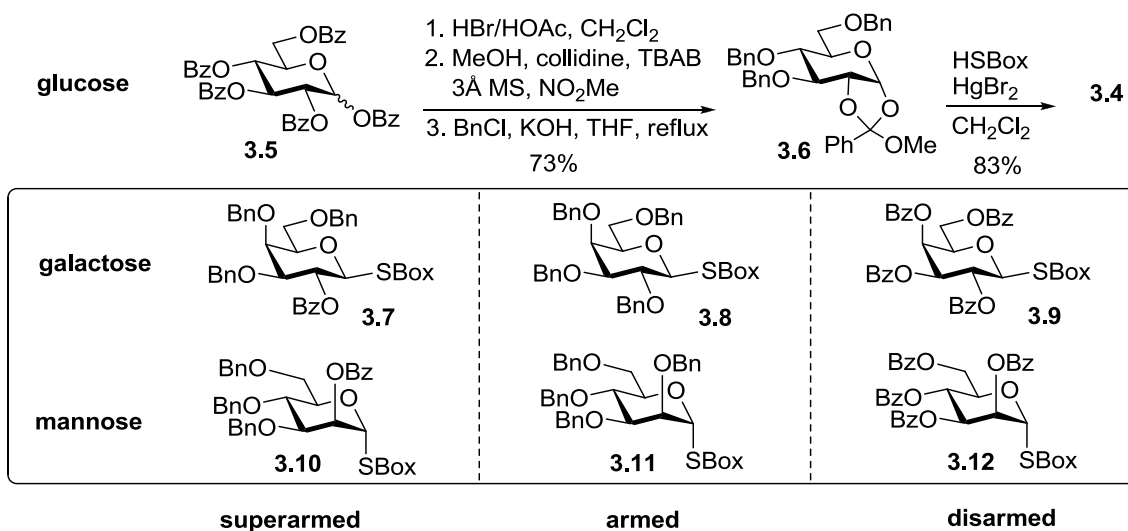
As aforementioned, the armed-disarmed concept gave rise to a commonly accepted belief that benzylated derivatives are always significantly more reactive than their benzoylated counterparts, and as such, the overall glycosyl donor reactivity is also presumed to be in direct correlation with the total number of benzyl substituents.^{8, 10} In this context, the discovery of this superarmed SBox glycoside would seem somewhat surprising, as a

number of glycosyl donors bearing the “superarming” 2-*O*-benzoyl-3,4,6-tri-*O*-benzyl protecting group pattern have previously been investigated, including thioglycosides,²¹⁻²⁶ *O*-pentenyl glycosides,^{27, 28} fluorides,^{25, 28, 29} trichloroacetimidates,³⁰⁻³² hemiacetals,³³ and phosphates^{34, 35} to name a few. Although these building blocks have been probed in various expeditious^{21, 23, 34} and one-pot^{25, 26, 29} approaches for oligosaccharide synthesis, to the best of our knowledge no direct evidence of these glycosyl donors being more reactive than their benzylated counterparts has emerged. As a consequence, numerous glycosyl donors bearing this protecting group pattern have tenuously considered disarmed^{23, 26, 27} or “partially disarmed”.²⁸ Interestingly, in a few occasions their reactivity has even been quantified and determined to be lower than that of the corresponding benzylated derivatives.^{27, 36} It should be noted, however, that this protecting group pattern is predominantly used due its relatively simple synthesis via common orthoesters or glycals, as well as for its flexibility in selectively liberating 2-OH, and is not typically used in chemoselective oligosaccharide strategies. Application to glycosyl donors of the D-manno series in the synthesis of (branched) polymannans is arguably their most representative use.²²

3.2.1 Synthesis of superarmed *S*-benzoxazolyl glycosyl donors

To explore the viability of concept, we obtained benzoxazolyl 2-*O*-benzoyl-3,4,6-tri-*O*-benzyl- β -D-glucopyranoside **3.4**, as shown in Scheme 3.4. In addition, we generated a series of glycosyl donors of the D-galacto and D-manno series that would further allow us to investigate comparative superarming (**3.7** and **3.10**), arming (**3.8** and **3.11**^{2, 5}), and disarming effects (**3.9**^{2, 5} and **3.12**^{2, 5} Scheme 2). These relatively simple building blocks

were generated from known advanced precursors³⁷⁻⁴⁵ by known or slightly modified experimental procedures.^{17, 45-49}



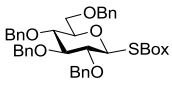
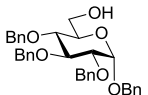
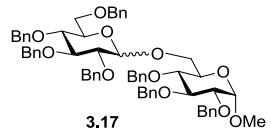
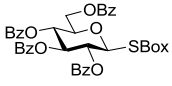
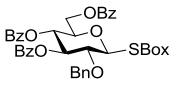
Scheme 3.4 Synthesis of the SBox glycoside **3.4** and its analogues

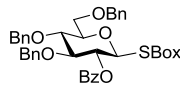
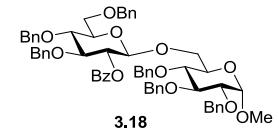
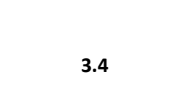
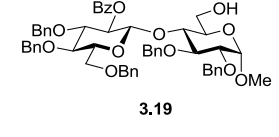
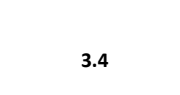
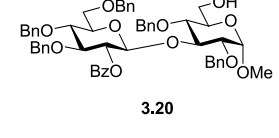
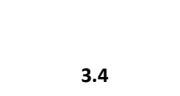
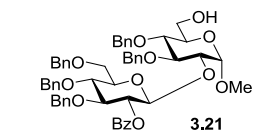
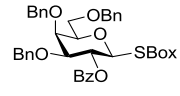
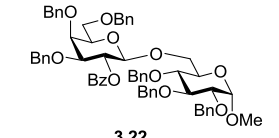
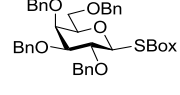
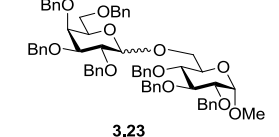
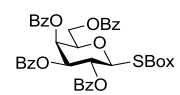
3.2.2 Glycosylation results

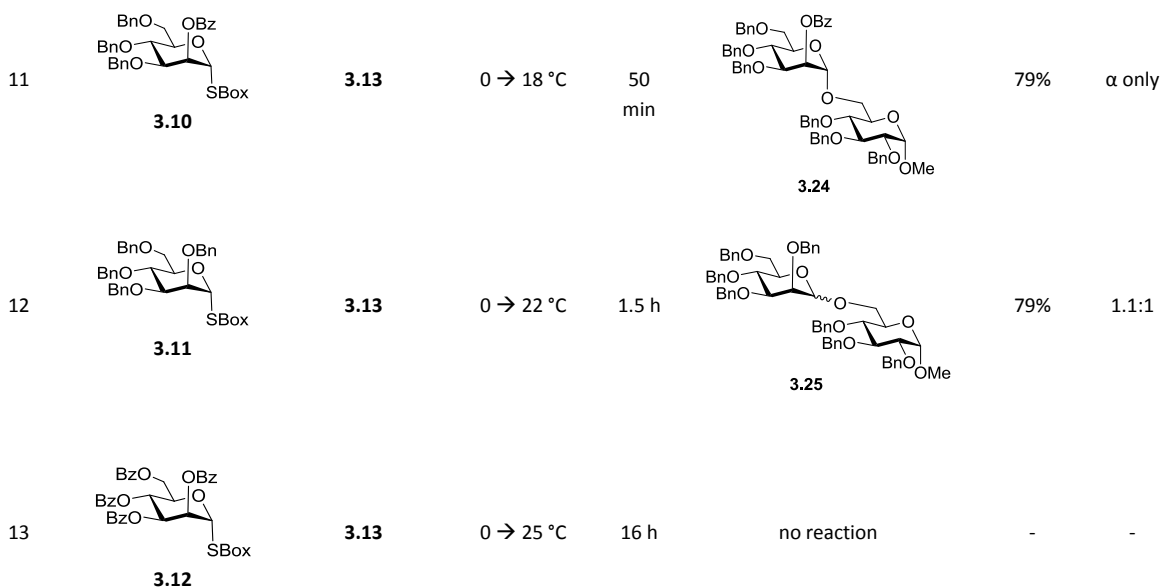
Having synthesized a variety of glycosyl donors, we then turned our attention toward evaluating their relative reactivities through comparative glycosidations. It is important to note, that in order to easily differentiate among the reactivity levels of the various armed and disarmed substrates, the choice of activator (promoter) is key. Thus upon investigating a range of activators (including the mildly electrophilic copper(II) triflate, iodonium(di- γ -collidine) perchlorate (IDCP), and methyl triflate), we found dimethyl(methylthio)sulfonium triflate (DMTST)⁵⁰ to be the most suitable promoter. As such, the results of the DMTST (3 equiv) mediated glycosylations in 1,2-dichloroethane are summarized in Table 3.1.

Glycosidation of the benzylated SBox donor **3.1** with glycosyl acceptor **3.13**⁵¹ proceeded smoothly and was completed in 2 h affording the corresponding disaccharide **3.17**³³ in 91% yield (entry 1, Table 3.1). However, when reactions of the disarmed and super-disarmed glycosyl donors (**3.2** and **3.3**, respectively) with glycosyl acceptor **3.13** were set up under essentially the same reaction conditions, no formation of the corresponding coupling products was detected (entries 2 and 3). Encouragingly, the anticipated superarmed glycosyl donor **3.4** reacted nearly instantaneously, under the same reaction conditions, to provide disaccharide **3.18**³³ in 90% yield (entry 4).

Table 3.1 Comparative glycosidations of glycosyl donors **3.1-3.4** and **3.7-3.12** in the presence of DMTST

entry	donor	acceptor	temperature ^a	time	product	yield	$\alpha:\beta$ ratio
1	 3.1	 3.13	0 \rightarrow 25 °C	2 h	 3.17	91%	1.2:1
2	 3.2	3.13	0 \rightarrow 25 °C	16 h	no reaction	-	-
3	 3.3	3.13	0 \rightarrow 25 °C	16 h	no reaction	-	-

4	 <p>3.4</p>	3.13	0 °C	< 5 min	 <p>3.18</p>	90%	β only
5	 <p>3.4</p>	3.14	0 °C	< 5 min	 <p>3.19</p>	92%	β only
6	 <p>3.4</p>	3.15	0 °C	< 5 min	 <p>3.20</p>	97%	β only
7	 <p>3.4</p>	3.16	0 °C	< 5 min	 <p>3.21</p>	88%	β only
8	 <p>3.4</p>	3.13	0 °C	< 5 min	 <p>3.22</p>	92%	β only
9	 <p>3.4</p>	3.13	0 → 13 °C	40 min	 <p>3.23</p>	85%	2:1
10	 <p>3.9</p>	3.13	0 → 25 °C	16 h	no reaction	-	-



^a – all glycosylations were started at 0 °C and then the temperature was allowed to gradually increase

As such, the reactivity of the superarmed glycosyl donor **3.4** was then tested in reactions with less reactive secondary glycosyl acceptors **3.14**, **3.15**, and **3.16**.⁵²⁻⁵⁴ These couplings were also efficient, resulting in the formation of their respective disaccharides **3.19**,³³ **3.20**,⁵⁵ and **3.21** in high yields (88-97%, entries 5-7, Table 1).

We then refocused our investigation to superarmed galactosyl donor **3.7**. Similar to our previous observations, compound **3.7** was found to be significantly more reactive than its armed perbenzylated derivative **3.8**. Thus, disaccharides **3.22**⁵⁵ and **3.23**³³ were formed in 5 min (92%) and 40 min (85%), respectively (entries 8 and 9). As in the previous case, no reaction took place with the disarmed per-benzoylated galactoside **3.9** (entry 10). Similar observations were also made with mannosides **3.10-3.12**, wherein disaccharides **3.24**³⁵ and **3.25**⁵⁶ were formed in 50 min (79%) and 90 min (79%), respectively (entries 11 and 12), and no glycosidation of the disarmed donor took place (entry 13). To this end, we

determined that *not only* did the 2-*O*-benzoyl-3,4,6-tri-*O*-benzyl donors **3.4**, **3.7**, and **3.10** readily react, while disarmed glycosyl donors (**3.2**, **3.3**, **3.9**, **3.12**) did not, but as postulated, they *also* proved to be more reactive than their armed counterparts (**3.1**, **3.8**, **3.11**).

3.3 Conclusions

In conclusion, we have devised a novel method for “superarming” glycosyl donors, through the strategic placement of common protecting groups. Furthermore, these superarmed glycosyl donors are easily obtained, through either an orthoester (glucosyl and mannosyl donors) or a glycal (galactosyl donor) route. Complementary to the anomeric mixture often obtained with the classic armed per-benzylated analogues, the superarmed glycosyl donor offers an entirely 1,2-*trans* stereoselective glycosidation, which can be achieved at ambient or slightly reduced temperatures. Although not covered by the scope of these preliminary studies, it is expected that these super-reactive glycosyl donors will be useful in cases of difficult glycosylations, wherein classic per-acylated glycosyl donors fail. The further expansion and application of this concept to chemoselective oligosaccharide synthesis will be discussed in the following chapter.

3.4 Experimental

General remarks. Column chromatography was performed on silica gel 60 (EM Science, 70-230 mesh), reactions were monitored by TLC on Kieselgel 60 F₂₅₄ (EM Science). The compounds were detected by examination under UV light and by charring with 10% sulfuric acid in methanol. Solvents were removed under reduced pressure at < 40 °C. CH₂Cl₂ and ClCH₂CH₂Cl were distilled from CaH₂ directly prior to application. Anhydrous DMF (EM Science) was used as is. Methanol was dried by refluxing with magnesium methoxide, distilled and stored under argon. Pyridine was dried by refluxing with CaH₂ and then distilled and stored over molecular sieves (3 Å). Molecular sieves (3 Å or 4 Å), used for reactions, were crushed and activated *in vacuo* at 390 °C during 8 h in the first instance and then for 2-3 h at 390 °C directly prior to application. AgOTf (Acros) was co-evaporated with toluene (3 x 10 mL) and dried *in vacuo* for 2-3 h directly prior to application. DMTST was prepared in accordance to previously reported methods. Optical rotations were measured at 'Jasco P-1020' polarimeter. ¹H-n.m.r. spectra were recorded in CDCl₃ at 300 MHz, ¹³C-NMR spectra were recorded in CDCl₃ at 75 MHz (Bruker Avance) unless otherwise noted. HR FAB-MS determinations were made with the use of JEOL MStation (JMS-700) Mass Spectrometer, matrix *m*-nitrobenzyl alcohol, with NaI as necessary.

The synthesis of armed glycosyl donors 3.8, 3.11, and disarmed glycosyl donor 3.12

Benzoxazolyl 2,3,4,6-tetra-O-benzyl-1-thio- β -D-galactopyranoside (3.8). The solution of ethyl 2,3,4,6-tetra-O-benzyl-1-thio- β -D-galactopyranoside⁴² (2.73 g, 4.68 mmol) and activated molecular sieves (3 Å, 2.34 g) in CH₂Cl₂ (70 mL) was stirred under argon for 1 h. A Freshly prepared solution of Br₂ in CH₂Cl₂ (44 mL, 1/165, v/v) was then added and the reaction mixture was kept for 5 min at rt. After that, the solid was filtered-off and the filtrate was concentrated *in vacuo* at rt. Crude residue was then treated with KSBox (11.68 mmol) and 18-crown-6 (0.47 mmol) in dry acetone (10 mL) under argon for 16 h at rt. Upon completion, the mixture was diluted with dichloromethane, the solid was filtered-off and the residue was washed with dichloromethane. The combined filtrate (200 mL) was washed with 1% aq. NaOH (50 mL) and water (3 x 50 mL). The organic layer was separated, dried with MgSO₄, and concentrated *in vacuo*. The residue was purified by silica gel column chromatography (ethyl acetate-toluene gradient elution) to afford compound **3.8** (2.25 g, 71 %). $R_f = 0.52$ (ethyl acetate - hexanes, 3/7, v/v); $[\alpha]_D^{25} +0.29$ ($c = 1.0$, CHCl₃); ¹H-n.m.r.: δ , 3.53-3.55 (m, 2H, H-6a, 6b), 3.64 (dd, 1H, $J_{3,4} = 9.2$ Hz, H-3), 3.73 (dd, 1H, H-5), 3.95-4.02 (m, 2H, H-2, 4), 4.28-4.40 (m, 2H, CH₂Ph), 4.54-4.91 (m, 6H, 3CH₂Ph), 5.03 (d, 1H, $J_{1,2} = 9.9$ Hz, H-1), 7.14-7.28 (m, 23H, aromatic), 7.52 (d, 1H, aromatic) ppm, ¹³C-n.m.r.: δ , 68.4, 72.8, 73.6, 73.7, 74.8, 75.9, 77.7, 78.0, 84.1, 85.5, 110.1, 119.0, 124.2, 124.4, 127.7 (x2), 127.9 (x2), 128.0 (x2), 128.1 (x2), 128.3 (x2), 128.4 (x6) 128.5 (x2), 128.6 (x2), 137.9 (x2), 138.2, 138.7, 142.0, 151.9, 162.3 ppm; HR-FAB MS $[M+Na]^+$ calcd for C₄₁H₃₉NO₆SN⁺ 696.2396, found 696.2374. (See Appendix; Figure A-7, A-8, A-9)

Benzoxazolyl 2,3,4,6-tetra-*O*-benzyl-1-thio- α -D-mannopyranoside (3.11) A mixture of ethyl 2,3,4,6-tetra-*O*-benzyl-1-thio- α -D-mannopyranoside³⁹ (2.73 g, 4.68 mmol) and activated molecular sieves (3 Å, 2.34 g) in CH₂Cl₂ (70 mL) was stirred under argon for 1h. Freshly prepared solution of Br₂ in CH₂Cl₂ (44 mL, 1/165, v/v) was then added and the reaction mixture was kept for 5 min at rt. After that, the solid was filtered-off and the filtrate was concentrated *in vacuo* at rt. Crude residue was then treated with KSBox (2.2 g, 11.68 mmol) and 18-crown-6 (164 mg, 0.47 mmol) in dry acetone (10 mL) under argon for 16 h at rt. Upon completion, the mixture was diluted with CH₂Cl₂ (150 mL), the solid was filtered-off and washed with CH₂Cl₂ (2 x 25 mL). The combined filtrate was then washed with 1% aq. NaOH (50 mL) and water (3 x 50 mL). The organic layer was separated, dried over MgSO₄, and concentrated *in vacuo*. The residue was purified by column chromatography on silica gel (ethyl acetate - toluene gradient elution) to afford **3.11** as a colorless syrup in 75% yield. $R_f = 0.60$ (ethyl acetate - toluene, 1/9, v/v); $[\alpha]_D^{22} -12.8^\circ$ (c = 1.0, CHCl₃); ¹H-n.m.r.: δ , 3.63-3.77 (m, 4H, H-3, 5, 6a, 6b), 4.00 (dd, 1H, $J_{4,5} = 9.3$ Hz, H-4), 4.13 (br d, 1H, H-2), 4.42 (d, 1H, $\frac{1}{2}CH_2Ph$), 4.53 (dd, 2H, CH_2Ph), 4.70-4.83 (m, 4H, 2 x CH_2Ph), 5.02 (d, 1H, $\frac{1}{2}CH_2Ph$), 5.74 (d, 1H, $J_{1,2} = 1.1$ Hz, H-1), 7.11-7.53 (m, 24H, aromatic) ppm; ¹³C-n.m.r.: δ 69.1, 72.9, 73.4, 74.4, 75.0, 75.0, 76.8, 80.5, 83.7, 84.7, 110.0, 118.6, 124.1, 124.4, 127.4, 127.6 (x2), 127.7, 127.8, 127.9 (x3), 127.9 (x2), 128.2 (x2), 128.2 (x2), 128.3 (x2), 128.3 (x2), 128.5 (x2), 137.9, 138.0, 138.2, 138.3, 141.7, 151.8, 163.2 ppm; HR-FAB MS $[M+H]^+$ calcd for C₄₁H₃₉NO₆SH⁺ 674.2576, found 674.2574. (See Appendix; Figure A-13, A-14, A-15)

Benzoxazolyl 2,3,4,6-tetra-O-benzoyl-1-thio- α/β -D-mannopyranoside (3.12) was obtained from 2,3,4,6-tetra-O-benzoyl- α -D-mannopyranosyl bromide³⁷ as a white foam in 92%, as described in the synthesis of compound **3.11** ($\alpha/\beta = 1/1$). Selected data for α -**3.12**: $R_f = 0.53$ (ethyl acetate - toluene, 1/9, v/v); ¹Hn.m.r.: δ , 4.45 (dd, 1H, $J_{5,6b} = 4.8$ Hz, 6b), 4.56 (dd, 1H, $J_{6a,6b} = 12.4$ Hz, $J_{5,6a} = 2.5$ Hz, H-6a), 4.73 (m, 1H, H-5), 5.73 (dd, $J_{2,3} = 3.2$ Hz, $J_{3,4} = 10.1$ Hz, H-3), 6.0 (dd, 1H, H-2), 6.15 (dd, 1H, $J_{4,5} = 10.1$ Hz, H-4), 6.67 (d, 1H, $J_{1,2} = 1.4$ Hz, H-1), 7.09-8.03 (m, 24H, aromatic) ppm; ¹³C-n.m.r.: δ , 62.5, 66.5, 70.4, 71.2, 71.7, 83.7, 110.3, 119.3, 124.7, 124.8, 128.4 (x2), 128.4 (x2), 128.5 (x2), 128.7, 128.7(x2), 128.9, 129.0, 129.6 (x2), 129.6, 129.8 (x2), 129.8 (x2), 130.0 (x2), 133.0, 133.5, 133.7, 133.8, 141.6, 152.0, 159.6, 165.1, 165.3, 165.5, 165.9 ppm; HR-FAB MS $[M+H]^+$ calcd for $C_{41}H_{31}NO_{10}SH^+$ 730.1747, found 730.1740. (See Appendix; Figure A-16, A-17, A-18)

The synthesis of super armed glycosyl donor 3.4 and precursor 3.6

3,4,6-tri-O-benzyl-1,2-O-(1-methoxybenzylidene)- α -D-glucopyranose (3.6). To a stirred solution of a glycosyl pentabenzoylate **3.5** (3.10 g, 4.4 mmol) in dry CH_2Cl_2 (10 mL) was added dropwise 33% HBr soln. in acetic acid (3.18 mL, 53.1 mmol). The reaction mixture was stirred under argon for 16 h at rt, and then diluted with CH_2Cl_2 (20 mL), and washed with water (10 mL), saturated aq. $NaHCO_3$ (2 x 10 mL), and water (3 x 10 mL). The organic phase was separated, dried over $MgSO_4$, and concentrated *in vacuo*. The following transformation was performed in a fashion similar to that previously reported.⁴⁷ The resulting residue was then dissolved in nitromethane (25 mL), to which

molecular sieves (3Å, 416 mg) were added and the resulting mixture was stirred under argon for 1 h. The flask was then covered with foil, and added sequentially was γ -collidine (0.75 mL, 5.68 mmol), dry methanol (0.153 mL, 3.79 mmol), and tert-butylammonium bromide (2.5 mmol, 0.81g). After stirring for 16 h, triethyl amine (0.2 mL) was added, the solid was filtered off and the filtrate was washed with saturated aq. NaHCO₃ (20 mL). The organic layer was separated, and the remaining aqueous layer was extracted with CH₂Cl₂ (2 x 10 mL). The organic fractions were combined and washed with water (20 mL), then dried over MgSO₄, and concentrated *in vacuo*. The crude mixture was then simultaneously debenzoylated and benzylated by a previously reported procedure.⁴⁶ The compound was purified by column chromatography on silica gel (ethyl acetate – hexane gradient elution) to afford known compound **3.6**³⁸ in 73% yield.

Benzoxazolyl 2-O-benzoyl-3,4,6-tri-O-benzyl-1-thio- β -D-glucopyranoside (3.4) was obtained from the orthoester **3.6**³⁸ in a procedure similar to that previously reported.^{17, 45, 49} Orthoester **3.6** (1.2 g, 2.11 mmol) was mixed with molecular sieves (3Å, 500 mg), dry acetonitrile (5 mL), and the resulting mixture was stirred under argon for 1 h. 2-Mercaptobenzoxazole (3.19 g, 21.3 mmol) and mercuric(II) bromide (0.076 g, 0.211 mmol) were added, and the mixture was refluxed for 2.5 h. After that, the solid was filtered off and the filtrate was concentrated *in vacuo*. The residue was diluted with CH₂Cl₂ (20 mL) and washed successively with 1% aq. NaOH (10 mL), water (3 x 10 mL), dried over MgSO₄, and concentrated *in vacuo*. The residue was purified by column chromatography on silica gel (ethyl acetate – hexane gradient elution) to afford the requisite super-armed glycosyl donor as colorless crystals in 83% yield. Analytical data

for **3.4**: $R_f = 0.48$ (ethyl acetate-hexane, 3/7, v/v); $[\alpha]_D^{24} = +106.7^\circ$ ($c = 1$, CHCl_3); m.p. +96-97 °C (hexane – diethyl ether); $^1\text{H-n.m.r.}$: δ , 3.68-3.76 (m, 3H, H-5, 6a, 6b), 3.80-3.93 (m, 2H, H-3, 4), 4.40-4.78 (m, 6H, 3 x CH_2Ph), 5.43 (dd, 1H, $J_{2,3} = 8.7$ Hz, H-2), 5.70 (d, 1H, $J_{1,2} = 10.3$ Hz, H-1), 7.13-7.90 (m, 24H, aromatic) ppm; $^{13}\text{C-n.m.r.}$: δ , 68.6, 72.5, 73.7, 75.3, 75.6, 77.7, 80.2, 84.0, 84.1, 110.3, 118.9, 124.4, 124.6, 127.8, 127.9, 128.0 (x3), 128.1 (x2), 128.2 (x2), 128.5 (x2), 128.5 (x2), 128.6 (x2), 128.6 (x2), 129.4, 130.0 (x2), 133.5, 137.8, 138.1 (x2), 141.8, 152.0, 162.1, 165.5 ppm; HR-FAB MS $[\text{M}+\text{Na}]^+$ calcd for $\text{C}_{41}\text{H}_{37}\text{NO}_7\text{SNa}^+$ 710.2189, found 710.2169. (See Appendix; Figure A-1, A-2, A-3)

The synthesis of super armed glycosyl donor 3.7

Benzoxazolyl 2-O-benzoyl-3,4,6-tri-O-benzyl-1-thio- β -D-galactopyranoside (3.7).

To a stirring solution of 1,2-anhydro-3,4,6-tri-O-benzyl- β -D-galactopyranose⁴¹ in dry CH_2Cl_2 (12 mL) at 0 °C, was added 2-mercaptobenzoxazolyl (1.18 g, 2.74 mmol) and ZnCl_2 (0.019 g, 0.137 mmol). The reaction was allowed to stir under argon for 45 min upon which the reaction mixture was diluted with CH_2Cl_2 (40 mL) and washed successively with water (20 mL), saturated aq. NaHCO_3 (20 mL), water (3 x 20 mL), dried over MgSO_4 , and concentrated *in vacuo*. The residue was then dissolved in dry pyridine (5 mL) and cooled to 0°C. Benzoyl chloride (0.37 g, 3.22 mmol) was then added dropwise and the reaction was stirred under argon for 30 minutes. The reaction was then allowed to warm to rt and stir for 2 hours, upon which the reaction was cooled to 0°C, and quenched with dry MeOH (0.15 mL), and concentrated in vacuo. The residue

was then diluted with CH₂Cl₂ (50 mL) and washed successively with water (20 mL), 1 N aq. HCl (20 mL), water (3 x 20 mL), dried over MgSO₄, and concentrated *in vacuo*. The residue was purified by column chromatography on silica gel (ethyl acetate – hexane gradient elution) to afford compound purified by column chromatography on silica gel (ethyl acetate – hexane gradient elution) yielding both compound **3.7** in 56%, and the unreactive N-linked isomer of **3.7** in 24%, in a combined total of 80% yield. Analytical data for **3.7**: R_f = 0.38 (ethyl acetate-hexane, 3/7, v/v); [α]_D²⁴ = +106.8° (c = 1, CHCl₃); ¹H-n.m.r.: δ, 3.60 (m, 2H, H-6a, 6b), 3.76 (dd, 1H, J_{3,4} = 2.7 Hz, H-3), 3.83 (m, 1H, H-5), 4.05 (d, 1H, H-4), 4.31-4.62 (m, 5H, 2.5 x CH₂Ph), 4.93 (d, 1H, ½ CH₂Ph), 5.69 (d, 1H, J_{1,2} = 10.2 Hz, H-1), 5.80 (dd, 1H, J_{2,3} = 9.7 Hz, H-2) 7.12-8.15 (m, 24H, aromatic) ppm; ¹³C-n.m.r.: δ, 68.4, 70.3, 72.2, 73.0, 73.8, 74.9, 78.5, 80.9, 84.5, 110.3, 118.8, 124.4, 124.5, 127.9, 128.0 (x2), 128.0 (x2), 128.2 (x2), 128.5 (x2), 128.5 (x4), 128.6 (x2), 128.6 (x2), 129.6, 130.1 (x2), 133.4, 137.6, 137.9, 138.5, 141.8, 152.0, 162.5, 165.6 ppm; HR-FAB MS [M+Na]⁺ calcd for C₄₁H₃₇NO₇SN⁺ 710.2189, found 710.2213. (See Appendix; Figure A-4, A-5, A-6)

The synthesis of super armed glycosyl donor 3.10

Benzoxazolyl 2-O-benzoyl-3,4,6-tri-O-benzyl-1-thio-α-D-mannopyranoside (3.10).

To a stirring solution of known compound benzoxazolyl 3,4,6-tri-O-benzyl-1-thio-α-D-mannopyranoside,⁴⁵ (1.5 g, 2.57 mmol) in dry pyridine (10 mL) at 0 °C, was added dropwise benzoyl chloride (0.59 mL, 5.15 mmol). The reaction was stirred under argon for 30 minutes, upon which it was allowed to warm to rt and continue stirring for 1h. The

reaction was then cooled to 0 °C, quenched with dry MeOH (0.15 mL), and concentrated *in vacuo*. The residue was then diluted with CH₂Cl₂ (50 mL) and washed successively with water (20 mL), 1 N aq. HCl (20 mL), water (3 x 20 mL), dried over MgSO₄, and concentrated *in vacuo*. The residue was purified by column chromatography on silica gel (ethyl acetate – hexane gradient elution) to afford compound **3.10** in 99% yield. Analytical data for **3.10**: $R_f = 0.62$ (ethyl acetate-hexane, 3/7, v/v); $[\alpha]_D^{24} = +126.0^\circ$ (c = 1, CHCl₃); ¹H-n.m.r.: δ , 3.67 (dd, 1H, $J_{6b,6a} = 11.7$ Hz, H-6b), 3.84-3.93 (m, 2H, $J_{3,4} = 10.3$ Hz, H-3, 6a), 4.07 (m, 1H, H-5), 4.18 (dd, 1H, $J_{4,5} = 10.3$ Hz, H-4), 4.39-4.84 (m, 6H, CH₂Ph), 5.84 (dd, 1H, $J_{2,3} = 2.4$ Hz, H-2), 6.54 (d, 1H, $J_{1,2} = 1.8$ Hz, H-1), 7.13-8.03 (m, 24H, aromatic) ppm; ¹³C-n.m.r.: δ , 68.8, 70.4, 72.1, 73.6, 74.1, 75.1, 75.7, 78.5, 84.6, 110.4, 119.3, 124.7 (x2), 127.7 (x3), 128.0, 128.1, 128.2 (x2), 128.4 (x2), 128.5 (x2), 128.6 (x2), 128.6 (x2), 128.7 (x2), 129.7, 130.3 (x2), 133.6, 137.5, 138.3, 138.5, 141.9, 152.2, 160.8, 165.5 ppm; HR-FAB MS $[M+H]^+$ calcd for C₄₁H₃₇NO₇SH⁺ 688.2370, found 688.2359. (See Appendix; Figure A-10, A-11, A-12)

Synthesis of disaccharides.

General DMTST-promoted glycosylation procedure. A mixture of glycosyl donor (0.030 mmol), glycosyl acceptor (0.027 mmol), and freshly activated molecular sieves (4Å, 70 mg), in 1,2-dichloroethane (0.5 mL) was stirred under argon for 1h. The reaction mixture was cooled to 0 °C (or as indicated in Tables 1 and 2), DMTST (0.082 mmol) was added, and the reaction mixture was monitored by TLC. Upon completion (see Tables), the reaction mixture was quenched with triethyl amine (1 drop), the solid was filtered off, the

filtrate was diluted with CH₂Cl₂ (15 mL), washed with 1% NaOH (5 mL) and water (3 x 5 mL). The organic layer was separated, dried with MgSO₄, filtered and concentrated *in vacuo*. The residue was purified by column chromatography on silica gel (ethyl acetate – toluene gradient elution) to obtain the corresponding disaccharide.

Methyl 6-O-(2,3,4,6-tetra-O-benzyl- α/β -D-glucopyranosyl)-2,3,4-tri-O-benzyl- α -D-glucopyranoside (3.17) was obtained from **3.1** and **3.13** as a clear foam in 91% yield. Analytical data for **3.17** is the same as reported previously.³³

Methyl 6-O-(2-O-benzoyl-3,4,6-tri-O-benzyl- β -D-glucopyranosyl)-2,3,4-tri-O-benzyl- α -D-glucopyranoside (3.18) was obtained from **3.4** and **3.13** as a clear film in 90% yield. Analytical data for **3.18** is the same as reported previously.³³

Methyl 4-O-(2-O-benzoyl-3,4,6-tri-O-benzyl- β -D-glucopyranosyl)-2,3,6-tri-O-benzyl- α -D-glucopyranoside (3.19) was obtained from **3.4** and **3.14** as a clear film in 92% yield. Analytical data for **3.19** is the same as reported previously.³³

Methyl 3-O-(2-O-benzoyl-3,4,6-tri-O-benzyl- β -D-glucopyranosyl)-2,4,6-tri-O-benzyl- α -D-glucopyranoside (3.20) was obtained from **3.4** and **3.15** as a colorless foam in 97% yield. Analytical data for **3.20** is the same as reported previously.⁵⁵

Methyl 2-O-(2-O-benzoyl-3,4,6-tri-O-benzyl- β -D-glucopyranosyl)-3,4,6-tri-O-benzyl- α -D-glucopyranoside (3.21) was obtained from **3.4** and **3.16** as a clear film in 88% yield. Analytical data for **3.21**: $R_f = 0.44$ (ethyl acetate-hexanes, 3/7, v/v); $[\alpha]_D^{27} = +48.1^\circ$ (c = 1, CHCl_3); $^1\text{H-n.m.r.}$: δ , 3.28 (s, 3H, OCH_3), 3.48-3.85 (m, 11H, H-2, 3, 4, 5, 6a, 6b, 3', 4', 5', 6a', 6b'), 4.26 (d, 1H, $\frac{1}{2} \text{CH}_2\text{Ph}$), 4.35-4.73 (m, 11H, 5.5 CH_2Ph), 4.78 (d, 1H, $J_{1,2'} = 10.0$ Hz, H-1'), 4.95 (d, 1H, $J_{1,2} = 3.4$ Hz, H-1), 5.35 (dd, 1H, H-2'), 6.86-7.35 (m, 33H, aromatic), 7.76 (d, 2H, aromatic) ppm; $^{13}\text{C-n.m.r.}$: δ , 55.5, 68.8, 69.1, 70.0, 73.7, 73.8, 73.8, 75.1, 75.2, 75.3 (x3), 78.0, 78.1, 81.2, 81.4, 83.3, 99.8, 102.5, 127.2, 127.3 (x2), 127.7, 127.8, 127.9, 127.9, 128.0 (x2), 128.0 (x2), 128.1 (x3), 128.2 (x4), 128.2 (x2), 128.4 (x2), 128.4 (x2), 128.5 (x2), 128.6 (x2), 128.6 (x4), 129.9, 129.9 (x2), 133.0, 137.9, 138.1, 138.2, 138.2, 138.4, 139.0, 165.2 ppm; HR-FAB MS $[\text{M}+\text{Na}]^+$ calcd for $\text{C}_{62}\text{H}_{64}\text{O}_{12}\text{Na}^+$ 1023.4295, found 1023.4284.

Methyl 6-O-(2-O-benzoyl-3,4,6-tri-O-benzyl- β -D-galactopyranosyl)-2,3,4-tri-O-benzyl- α -D-glucopyranoside (3.22) was obtained from **3.7** and **3.13** as a clear film in 92% yield. Analytical data for **3.22** is the same as reported previously.⁵⁵

Methyl 6-O-(2,3,4,6-tetra-O-benzyl- α/β -D-galactopyranosyl)-2,3,4-tri-O-benzyl- α -D-glucopyranoside (3.23) was obtained from **3.8** and **3.13** as a clear film in 85% yield. Analytical data for **3.23** is the same as reported previously.³³

Methyl 6-O-(2-O-benzoyl-3,4,6-tri-O-benzyl- α -D-mannopyranosyl)-2,3,4-tri-O-benzyl- α -D-glucopyranoside (3.24) was obtained from **3.10** and **3.13** as a clear film in 79% yield. Analytical data for **3.24** is the same as reported previously.³⁵

Methyl 6-O-(2,3,4,6-tetra-O-benzyl- α/β -D-mannopyranosyl)-2,3,4-tri-O-benzyl- α -D-glucopyranoside (3.25) was obtained from **3.11** and **3.13** as a clear film in 79% yield. Analytical data for **3.25** is the same as reported previously.⁵⁶

3.5 References

1. Demchenko, A. V.; Malysheva, N. N.; De Meo, C., *Org. Lett.* **2003**, *5*, 455-458.
2. Kamat, M. N.; De Meo, C.; Demchenko, A. V., *J. Org. Chem.* **2007**, *72*, 6947-6955.
3. Bongat, A. F. G.; Kamat, M. N.; Demchenko, A. V., *J. Org. Chem.* **2007**, *72*, 1480-1483.
4. Kamat, M. N.; Demchenko, A. V., *Org. Lett.* **2005**, *7*, 3215-3218.
5. Kamat, M. N.; Rath, N. P.; Demchenko, A. V., *J. Org. Chem.* **2007**, *72*, 6938-6946.
6. Fraser-Reid, B.; Udodong, U. E.; Wu, Z. F.; Ottosson, H.; Merritt, J. R.; Rao, C. S.; Roberts, C.; Madsen, R., *Synlett* **1992**, (12), 927-942 and references therein.
7. Mootoo, D. R.; Konradsson, P.; Udodong, U.; Fraser-Reid, B., *J. Am. Chem. Soc.* **1988**, *110*, 5583-5584.

8. Paulsen, H., *Angew. Chem. Int. Edit. Engl.* **1982**, *21* (3), 155-173.
9. Lemieux, R. U., *Adv. Carbohydr. Chem. Biochem.* **1954**, *9*, 1-57 and references therein.
10. Green, L. G.; Ley, S. V., Protecting groups: effects on reactivity, glycosylation specificity and coupling efficiency. In *Carbohydrates in Chemistry and Biology*, Ernst, B.; Hart, G. W.; Sinay, P., Eds. Wiley-VCH: Weinheim, New York, 2000; Vol. 1, pp 427-448.
11. Veeneman, G. H.; van Boom, J. H., *Tetrahedron Lett.* **1990**, *31* (2), 275-278.
12. Baeschlin, D. K.; Chaperon, A. R.; Charbonneau, V.; Green, L. G.; Ley, S. V.; Lucking, U.; Walther, E., *Angew. Chem. Int. Edit.* **1998**, *37* (24), 3423-3428.
13. Barrena, M. I.; Echarri, R.; Castillon, S., *Synlett* **1996**, 675-676.
14. Hashimoto, S. I.; Sakamoto, H.; Honda, T.; Abe, H.; Nakamura, S. I.; Ikegami, S., *Tetrahedron Lett.* **1997**, *38* (52), 8969-8972.
15. Chiba, H.; Funasaka, S.; Kiyota, K.; Mukaiyama, T., *Chem. Lett.* **2002**, 746-747.
16. Friesen, R. W.; Danishefsky, S. J., *J. Am. Chem. Soc.* **1989**, *111*, 6656-6660.
17. Smoot, J. T.; Pornsuriyasak, P.; Demchenko, A. V., *Angew. Chem. Int. Ed.* **2005**, *44*, 7123-7126.
18. Crich, D.; Li, M., *Org. Lett.* **2007**, *9*, 4115-4118.
19. Jensen, H. H.; Pedersen, C. M.; Bols, M., *Chem. Eur. J.* **2007**, *13*, 7576-7582.
20. Pedersen, C. M.; Nordstrom, L. U.; Bols, M., *J. Am. Chem. Soc.* **2007**, *129*, 9222-9235.
21. Geurtsen, R.; Cote, F.; Hahn, M. G.; Boons, G. J., *J. Org. Chem.* **1999**, *64*, 7828-7835.

22. Geng, X.; Dudkin, V. Y.; Mandal, M.; Danishefsky, S. J., *Angew. Chem. Int. Ed.* **2004**, *43*, 2562-2565.
23. Hederos, M.; Konradsson, P., *J. Org. Chem.* **2005**, *70* (18), 7196-7207.
24. Sato, K.; Akai, K. S.; Kojima, M.; Murakami, H.; Idoji, T., *Tetrahedron Lett.* **2005**, *46*, 7411-7414.
25. Tanaka, H.; Adachi, M.; Takahashi, T., *Chem. Eur. J* **2005**, *11*, 849-862.
26. Wang, C.; Wang, H.; Huang, X.; Zhang, L. H.; Ye, X. S., *Synlett* **2006**, (17), 2846-2850.
27. Fraser-Reid, B.; Lopez, J. C.; Radhakrishnan, K. V.; Nandakumar, M. V.; Gomez, A. M.; Uriel, C., *Chem. Commun.* **2002**, 2104-2105.
28. Lopez, J. C.; Uriel, C.; Guillamon-Martin, A.; Valverde, S.; Gomez, A. M., *Org. Lett.* **2007**, *9*, 2759-2762.
29. Hashihayata, T.; Ikegai, K.; Takeuchi, K.; Jona, H.; Mukaiyama, T., *Bull. Chem. Soc. Jpn.* **2003**, *76*, 1829-1848.
30. Okada, Y.; Nagata, O.; Taira, M.; Yamada, H., *Org. Lett.* **2007**, *9*, 2755-2758.
31. Jayaprakash, K. N.; Chaudhuri, S. R.; Murty, C. V. S. R.; Fraser-Reid, B., *J. Org. Chem.* **2007**, *72*, 5534-5545.
32. Rising, T. W. D. F.; Heidecke, C. D.; Fairbanks, A. J., *Synlett* **2007**, (9), 1421-1425.
33. Nguyen, H. M.; Chen, Y. N.; Duron, S. G.; Gin, D. Y., *J. Am. Chem. Soc.* **2001**, *123*, 8766-8772.
34. Plante, O. J.; Palmacci, E. R.; Andrade, R. B.; Seeberger, P. H., *J. Am. Chem. Soc.* **2001**, *123*, 9545-9554.

35. Ravidà, A.; Liu, X.; Kovacs, L.; Seeberger, P. H., *Org. Lett.* **2006**, *8*, 1815 - 1818.
36. Wilson, B. G.; Fraser-Reid, B., *J. Org. Chem.* **1995**, *60*, 317-320.
37. Lemieux, R. U., Acylglycosyl halides. Tetra-O-acetyl- α -D-glucopyranosyl bromide. In *Methods in carbohydrate chemistry*, Whistler, R. L.; Wolfrom, M. L., Eds. Academic Press Inc.: New York and London, 1963; Vol. 2, pp 226-228.
38. Ekborg, G.; Glaudemans, C. P. J., *Carbohydr. Res.* **1984**, *129*, 287-292.
39. Dasgupta, F.; Garegg, P. J., *Acta Chem. Scand.* **1989**, *43*, 471-475.
40. Ottosson, H., *Carbohydr. Res.* **1990**, *197*, 101-107.
41. Kong, F.; Du, J.; Shang, H., *Carbohydr. Res.* **1987**, *162*, 217-225.
42. Kihlberg, J. O.; Leigh, D. A.; Bundle, D. R., *J. Org. Chem.* **1990**, *55*, 2860-2863.
43. Houdier, S.; Vottero, P. J. A., *Carbohydr. Res.* **1993**, *248*, 377-384.
44. Ruda, K.; Lindberg, J.; Garegg, P. J.; Oscarson, S.; Konradsson, P., *J. Am. Chem. Soc.* **2000**, *122*, 11067-11072.
45. Abdel-Rahman, A. A. H.; El Ashry, E. S. H.; Schmidt, R. R., *Carbohydr. Res.* **2002**, *337*, 195-206.
46. Franks, N. E.; Montgomery, R., *Carbohydr. Res.* **1968**, *6*, 286-298.
47. Kochetkov, N. K.; Backinowsky, L. V.; Tsvetkov, Y. E., *Tetrahedron Lett.* **1977**, *41*, 3681-3684.
48. Halcomb, R. L.; Danishefsky, S. J., *J. Am. Chem. Soc.* **1989**, *111*, 6661-6666.
49. Beignet, J.; Tiernan, J.; Woo, C. H.; Benson, M. K.; Cox, L. R., *J. Org. Chem.* **2004**, *69*, 6341-6356.
50. Ravenscroft, M.; Roberts, R. M. G.; Tillett, J. G., *J. Chem. Soc. Perkin Trans. 2* **1982**, 1569-1972.

51. Kuester, J. M.; Dyong, I., *Justus Liebigs Ann. Chem.* **1975**, (12), 2179-2189.
52. Garegg, P. J.; Hultberg, H., *Carbohydr. Res.* **1981**, 93 (1), C10-C11.
53. Koto, S.; Takebe, Y.; Zen, S., *Bull. Chem. Soc. J.* **1972**, 45, 291-293.
54. Pearce, A. J.; Sinay, P., *Angew. Chem. Int. Ed.* **2000**, 39 (20), 3610-3612.
55. Mukaiyama, T.; Takeuchi, K.; Jona, H.; Maeshima, H.; Saitoh, T., *Helv. Chim. Acta* **2000**, 83, 1901-1918.
56. Hotha, S.; Kashyap, S., *J. Am. Chem. Soc.* **2006**, 128, 9620-9621.

CHAPTER 4

Application of the Superarmed Glycosyl Donor to Chemoselective Oligosaccharide Synthesis

Mydock, L. K.; Demchenko, A. V. “Application of the Superarmed Glycosyl Donor to Chemoselective Oligosaccharide Synthesis,” *Org. Lett.* **2008**, *10*, 2103–2106.

4.1 Introduction

In the expansion of our studies on the reactivity of *S*-benzoxazolyl (SBox) glycosides, we discovered that the strategic placement of common protecting groups has allowed for a new method of “super-arming” glycosyl donors.¹ Conceptualized from our studies on the O-2/O-5 Cooperative Effect,² it was determined that *S*-benzoxazolyl (SBox) glycosides possessing both a participating moiety at O-2 (benzoyl) and remote benzyl substituents that electronically arm the lone pair at O-5 (e.g., glycosyl donors **4.1-4.3**, Figure 4.1) are exceptionally reactive.¹ As, they have proven to be even more reactive than the traditional per-benzylated (armed) glycosyl donors, they have been appropriately titled as “superarmed.” (first coined by Bols)^{3, 4} Furthermore, these building blocks possess the desirable quality of being both arming and participating glycosyl donors, traits not commonly found in other systems.⁵

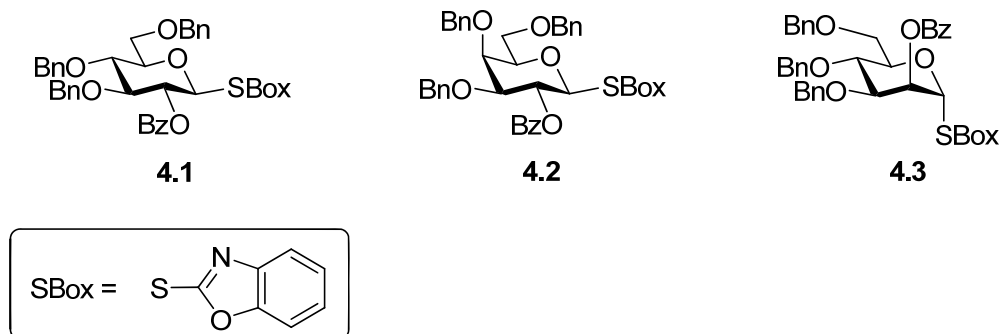


Figure 4.1 Superarmed glycosyl donors

As the previous chapter was centered upon the development of this superarming methodology, this chapter focuses on the optimization of this concept for use in

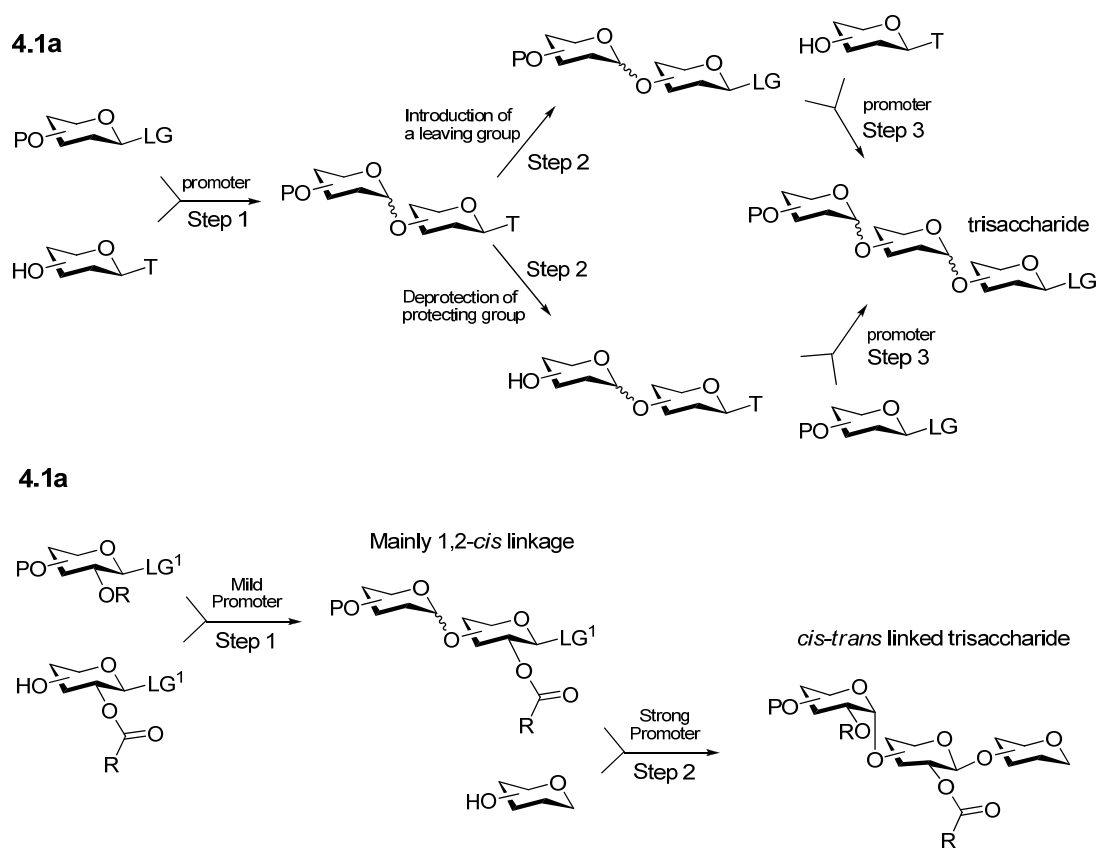
oligosaccharide synthesis. Herein, the successful application of the superarmed SBox donors (4.1-4.3) to both chemoselective and competitive glycosylations conditions is detailed, as the superarmed glycosyl donor was able to be successfully activated over both the traditional “armed” and disarmed glycosyl acceptors. Ultimate proof of this concept is further exemplified in a chemoselective one-pot trisaccharide synthesis.

4.1.1 Chemoselective oligosaccharide synthesis strategy

With the availability of pure natural carbohydrate isolates still far from being satisfactory, the chemical and enzymatic synthesis of these natural products has become increasingly important. This has led to the development of many excellent new methods for glycoside synthesis,⁶ from which a variety of expeditious strategies for oligosaccharide assembly have emerged.⁷⁻⁹ While older (linear) methodologies suffer from both extensive yield loss due to excessive protecting group manipulations, and a significant decrease in reactivity resulting from an increased chain length (scheme 4.1), newer methods rely on more efficient strategies that minimize the number of synthetic steps while maximizing the length of the oligosaccharide.⁸

Among these strategies, three major concepts could be identified: the chemoselective (protecting group based),^{10, 11} the selective (leaving group based),¹²⁻²¹ and the preactivation-based approaches.^{22, 23} While all three of these approaches serve to expedite oligosaccharide synthesis, only chemoselective activation employs the use of only one type of leaving group, making it a very attractive strategy. This approach is theoretically based upon the principles governing the armed-disarmed strategy (Chapter 2.1.1) strategy,

and as such, the reactivities of the building blocks involved are differentiated by the electronic characteristics of the protecting groups.^{10, 11} Therefore, while both the armed glycosyl donor and disarmed glycosyl acceptor bear the same leaving group, the activation of the donor over the acceptor can still be achieved in the presence of a mildly activating promoter. A subsequent glycosylation can then follow, wherein the newly formed disarmed disaccharide can then be activated through the use of a stronger promoter (Scheme 4.1b).



Scheme 4.1 Oligosaccharide synthesis strategies; **a)** linear approach,

b) chemoselective activation approach

As seen in scheme 3.2, the traditional armed-disarmed strategy allows for the convenient synthesis of a *cis-trans* patterned oligosaccharide sequence; less conveniently, a *cis-cis* sequence can be achieved if deprotection and reprotection (OBz → OBn) is carried out after the disaccharide step).⁸ However, we have now been able to broaden the scope of possible linkages obtained in chemoselective activation strategies, through the use of our “mixed-patterned” donors, allowing for the efficient installation of any and all linkage sequences, *cis-trans*, *cis-cis*, *trans-cis*, and *trans-trans*.^{2,24}

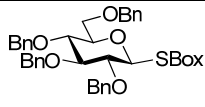
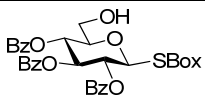
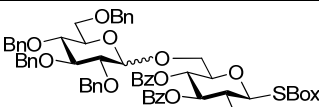
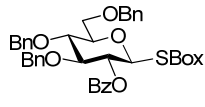
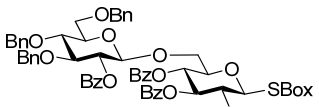
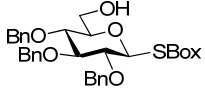
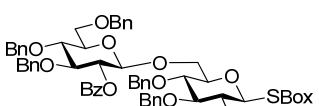
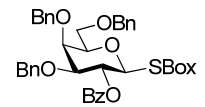
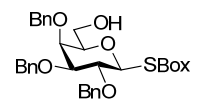
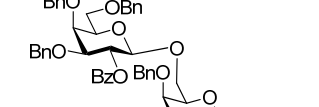
4.2 Application of the Superarmed Glycosyl Donor in Chemoselective Glycosylation

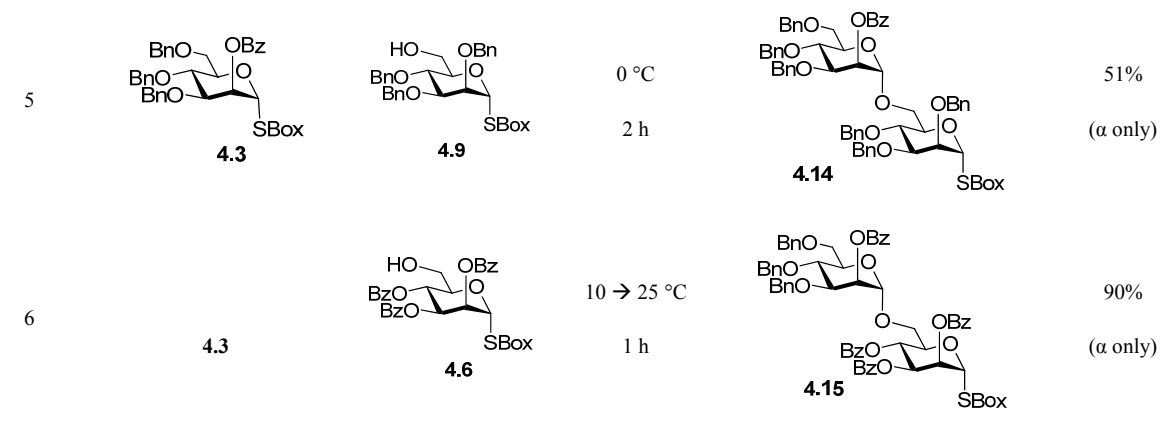
4.2.1 Chemoselective activation

Thus, we proceeded to investigate whether the enhanced reactivity of our superarmed donors **4.1-4.3** was sufficient to allow for direct chemoselective couplings. For the purpose of this study, we chose disarmed glycosyl acceptors **4.5** and **4.6**, as well as armed benzylated building blocks **4.7-4.9**, all bearing the same leaving group (SBox). The key results of these preliminary studies are summarized in Table 4.1. We already demonstrated that armed glycosyl donor **4.4** can be activated over disarmed glycosyl acceptor **4.5** to afford disaccharide **4.10** in 65% yield (entry 1, Table 4.1).² Expectedly, the superarmed glycosyl donor **4.1** also smoothly reacted with acceptor **4.5** to afford the corresponding disaccharide **11** in 72% yield (entry 2). Ultimately, the superarmed concept was validated by the direct coupling of the superarmed glycosyl donor **4.1** and

benzylated (“armed”) acceptor **4.7**. As in the previous coupling, no self-condensation products were detected, and disaccharide **4.12** was isolated in 70% yield (entry 3). The superarmed galactosyl donor **4.2** corroborated the previous result: its coupling with benzylated galactosyl acceptor **4.8** afforded the corresponding disaccharide **4.13** in 80% yield (entry 4). To ensure successful coupling, the reaction temperature was lowered to -20 °C, so as to minimize the competing side reaction of the isomerization of galactosyl donor **4.2** into its corresponding unreactive N-linked (NBox) counterpart.²

Table 4.1 Chemoselective activation of superarmed donors **4.1-4.3** over glycosyl acceptors **4.4-4.8**.²⁵⁻²⁷

entry	donor	acceptor	temp/ time	product	yield (α : β ratio)
1 ²	 4.4	 4.5		 4.10	65% (3/1)
2	 4.1	4.5	0 °C 15 min	 4.11	72% (β only)
3	4.1	 4.7	0 °C 12 min	 4.12	70% (β only)
4	 4.2	 4.8	-20 °C 45 min	 4.13	80% (β only)

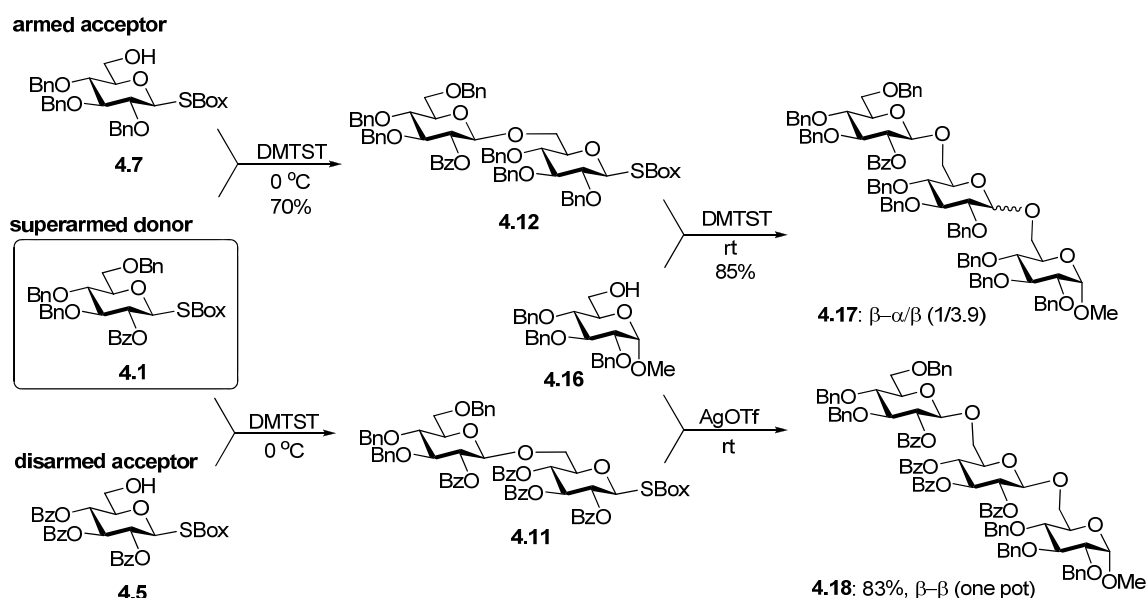


Coupling between the superarmed mannosyl donor **4.3** and benzylated mannosyl acceptor **4.9** was somewhat less efficient. Although no self-condensation products were observed, the disaccharide **4.14** could only be isolated in 51% yield (entry 5). Furthermore, the only additional compound recovered after 2 h was the unreacted glycosyl acceptor **4.9** (30%). We believe that this complication derives from the less significant difference of the reactivity between mannosyl donor **4.3** and its per-benzylated counterpart¹ In lieu of this result, the additional glycosylation of the disarmed mannosyl acceptor **4.6** with the superarmed mannosyl donor **4.3** was performed. As anticipated, this reaction was straightforward and afforded the anticipated disaccharide **4.15** in 90% yield.

4.2.2 One-pot trisaccharide synthesis

Additionally, sequential trisaccharide syntheses were carried out with the use of the superarmed glycosyl donor **4.1**, thus allowing us to introduce a 1,2-*trans* linkage prior to other linkages. This is not possible in the classic armed-disarmed approach. In the first sequence, we performed a stepwise coupling of building blocks **4.1** and **4.7**, and the isolated disaccharide **4.12** was reacted with glycosyl acceptor **4.16**²⁸ at room temperature,

to afford trisaccharide **4.17** in 60% overall yield (Scheme 4.2). The same sequencing could also be performed in a one-pot fashion without isolating the intermediate. In this case, trisaccharide **4.17** was isolated in a 74% yield. Similarly, a one-pot synthesis of the *trans-trans*-linked trisaccharide **4.18**, from building blocks **4.1**, **4.5**, and **4.16**, was accomplished in 83% overall yield.

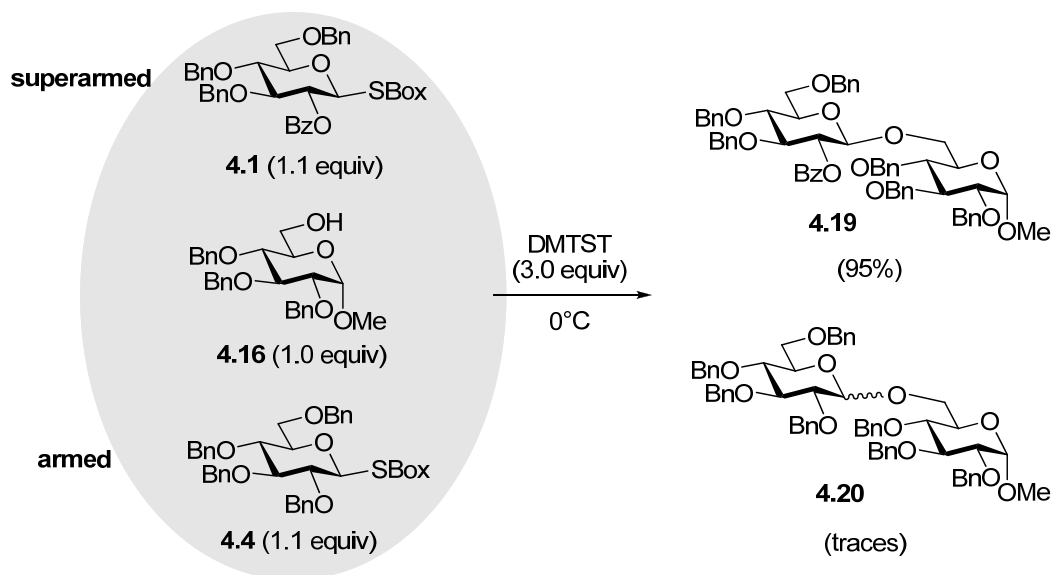


Scheme 4.2 Chemoselective sequential synthesis of trisaccharides **4.17** and **4.18**

4.2.3 Competitive Glycosylations

As a verification of these results, we also deemed it necessary to carry out a series of competitive glycosylations, wherein both the armed and superarmed donor (**4.4** and **4.1**, respectively), would be placed in the same reaction vessel with the glycosyl acceptor **4.16**. Upon addition of the promoter (DMTST), the two glycosyl donors would then compete to react with the one equivalent glycosyl acceptor **4.16**. As depicted in Scheme 4.3, the superarmed glycosyl donor **4.1** was clearly significantly more reactive than its per-benzylated analogue **4.4** and led to the formation of the corresponding disaccharide

4.19 which contained only trace (<5%) amounts of disaccharide **4.20** for a combined yield of 95%. In addition, the unreacted glycosyl donor **4.4** was recovered in 87% yield.



Scheme 4.3 Competitive glycosidations of glycosyl donors **4.1** and **4.4** with glycosyl acceptor **4.16** in the presence of DMTST

4.3 Conclusions

In conclusion, we have discovered a new concept for superarming glycosyl donors through the use of common protecting groups which allows for the expansion of the classic armed-disarmed strategy. These easily accessible superarmed glycosyl donors offer an entirely 1,2-*trans* stereoselective glycosidation. Consequently, the novelty of having *both* an armed *and* a 1,2-*trans* directing glycosyl donor makes this approach a very useful concept in many practical applications. Although not covered by the scope of these preliminary studies, it is expected that these super-reactive glycosyl donors can be

extremely useful in cases of difficult glycosylations, wherein classic per-acylated glycosyl donors fail. In combination with our previous studies on the O-2/O-5 cooperative effect, this superarmed glycosyl donor offers further significance, as it has allowed for the development of a versatile “tool kit,” consisting of both 1,2-*cis* and 1,2-*trans* directing armed glycosyl donors, as well as both 1,2-*cis* and 1,2-*trans* directing disarmed glycosyl donors, respectively. Additional studies on the superarmed glycosyl donor concept remain ongoing in our laboratory, wherein the concept has also been successful in application to other classes of glycosyl donor.²⁹

4.4 Experimental

General remarks. Column chromatography was performed on silica gel 60 (EM Science, 70-230 mesh), reactions were monitored by TLC on Kieselgel 60 F₂₅₄ (EM Science). The compounds were detected by examination under UV light and by charring with 10% sulfuric acid in methanol. Solvents were removed under reduced pressure at < 40 °C. CH₂Cl₂ and ClCH₂CH₂Cl were distilled from CaH₂ directly prior to application. Anhydrous DMF (EM Science) was used as is. Methanol was dried by refluxing with magnesium methoxide, distilled and stored under argon. Pyridine was dried by refluxing with CaH₂ and then distilled and stored over molecular sieves (3 Å). Molecular sieves (3 Å or 4 Å), used for reactions, were crushed and activated *in vacuo* at 390 °C during 8 h in the first instance and then for 2-3 h at 390 °C directly prior to application. AgOTf (Acros) was co-evaporated with toluene (3 x 10 mL) and dried *in vacuo* for 2-3 h directly prior to application. DMTST was prepared in accordance to previously reported methods. Optical

rotations were measured at 'Jasco P-1020' polarimeter. ^1H -n.m.r. spectra were recorded in CDCl_3 at 300 MHz, ^{13}C -NMR spectra were recorded in CDCl_3 at 75 MHz (Bruker Avance) unless otherwise noted. HR FAB-MS determinations were made with the use of JEOL MStation (JMS-700) Mass Spectrometer, matrix *m*-nitrobenzyl alcohol, with NaI as necessary.

General procedure for the synthesis of glycosyl acceptors 4.6-4.9 and precursor 4.21.

Ethyl 2,3,4-tri-O-benzyl(or benzoyl)-6-O-triphenylmethyl-1-thio- β -D-glycopyranoside (1.0 mmol) and freshly activated molecular sieves (3Å, 0.5 g) were dissolved in dry dichloromethane and the mixture was stirred under argon for 1 h. A freshly prepared solution of Br_2 in CH_2Cl_2 (9.5 mL, 1/165, v/v) was added and the reaction mixture was kept for 5 min at rt. After that, the solid was filtered-off and the filtrate was concentrated *in vacuo*. The crude residue was mixed with KSBBox (2.0 mmol), 18-crown-6 (0.2 mmol) and dry acetone (10 mL) and the reaction mixture was stirred under argon for 16 h at rt. After that, the reaction mixture was diluted with dichloromethane, the solid was filtered-off and the filtrate was concentrated *in vacuo*. The residue was diluted with dichloromethane (50 mL) and washed with 1% aq. NaOH (10 mL) and water (3 x 10 mL). The organic layer was separated, dried with MgSO_4 , filtered, and concentrated *in vacuo*. The residue was then dissolved in dichloromethane (25 mL) cooled to 0 °C and a solution of trifluoroacetic acid in dichloromethane (7.5 mL, 1/92, v/v) was added dropwise followed by 1 drop of water (~18 μL). The reaction mixture was stirred for 1 h, then diluted with dichloromethane, washed with saturated NaHCO_3 (15 mL) and water (3 x 15 mL). The organic layer was separated, dried with MgSO_4 , filtered, and concentrated

in vacuo. The residue was purified by column chromatography on silica gel (ethyl acetate – hexane gradient elution) to obtain the corresponding acceptor.

Benzoxazolyl 2,3,4-tri-O-benzyl-1-thio-β-D-glucopyranoside (4.7) was obtained from ethyl 2,3,4-tri-O-benzyl-1-thio-6-O-triphenylmethyl-β-D-glucopyranoside²⁶ as a white solid in 59% over-all yield. Analytical data for **4.7**: $R_f = 0.58$ (ethyl acetate-hexanes, 1/1, v/v); $[\alpha]_D^{27} = -1.08^\circ$ (c = 1, CHCl₃); ¹H-n.m.r: δ, 3.46-3.89 (m, 6H, H-2, 3, 4, 5, 6a, 6b), 4.70 (d, 1H, ½ CH₂Ph), 4.85-4.94 (m, 5H, 2.5 CH₂Ph), 5.46 (d, 1H, J_{1,2} = 9.8 Hz, H-1), 7.26-7.67 (m, 19H, aromatic) ppm; ¹³C-n.m.r.: δ, 62.0, 75.4, 75.8, 76.1, 77.5, 80.2, 80.8, 84.7, 86.7, 110.3, 119.3, 124.7, 124.7, 128.0 (x3), 128.1, 128.2 (x3), 128.4 (x2), 128.6 (x2), 128.7 (x2), 128.8 (x2), 137.6, 138.0, 138.4, 141.9, 151.9, 161.6 ppm; HR-FAB MS [M+H]⁺ calcd for C₃₄H₃₃NO₆SH⁺ 584.2107, found 584.2120. (See Appendix; Figure A-19, A-20, A-21)

Benzoxazolyl 2,3,4-tri-O-benzyl-1-thio-β-D-galactopyranoside (4.8) was obtained from ethyl 2,3,4-tri-O-benzyl-1-thio-6-O-triphenylmethyl-β-D-galctopyranoside²⁷ as a white solid in 48% yield. Analytical data for **4.8**: $R_f = 0.24$ (ethyl acetate-hexanes, 1/1, v/v); $[\alpha]_D^{24} = -12.1^\circ$ (c = 1, CHCl₃); ¹H-n.m.r: δ, 3.40 (m, 1H, H-5), 3.60 (dd, 1H, H-6b), 3.66 (dd, 1H, J_{3,4} = 2.8 Hz, H-3), 3.74 (dd, 1H, J_{6a,6b} = 11.1 Hz, H-6a), 3.83 (d, 1H J_{4,5} = 2.2 Hz H-4), 4.00 (dd, 1H, J_{2,3} = 9.5 Hz, H-2), 5.44 (d, 1H, J_{1,2} = 9.9 Hz, H-1), 4.58-4.92 (m, 6H, 3 CH₂Ph) 7.16-7.55 (m, 19H, aromatic) ppm; ¹³C-n.m.r.: δ, 62.2, 73.2, 73.4, 74.5, 76.0, 77.8, 79.8, 84.2, 85.3, 110.2, 119.0, 124.4, 124.6, 127.9 (x2), 128.0, 128.1, 128.2, 128.4 (x2), 128.5 (x2), 128.5 (x2), 128.7 (x2), 128.7 (x2), 137.8, 138.1, 138.2,

141.8, 151.9, 162.5 ppm; HR-FAB MS $[M+Na]^+$ calcd for $C_{34}H_{33}NO_6SNa^+$ 606.1926, found 606.1943. (See Appendix; Figure A-22, A-23, A-24)

Benzoxazolyl 2,3,4-tri-O-benzyl-1-thio- α -D-mannopyranoside (4.9) was obtained from ethyl 2,3,4-tri-O-benzyl-1-thio-6-O-triphenylmethyl- α -D-mannopyranoside²⁵ as a clear syrup in 47% overall yield. Analytical data for **4.9**: R_f = 0.55 (ethyl acetate-hexanes, 1/1, v/v); $[\alpha]_D^{24} = -12.7^\circ$ ($c = 1$, $CHCl_3$); 1H -n.m.r: δ , 3.51 (m, 1H, H-5), 3.63-3.85 (m, 3H, $J_{3,4} = 9.4$ Hz, H-3, 6a, 6b), 3.96 (dd, 1H, $J_{4,5} = 9.4$ Hz, H-4), 4.11 (m, 1H, H-2), 4.61-5.04 (m, 6H, 3 CH_2Ph), 5.72 (d, 1H, H-1), 7.15-7.58 (m, 19H, aromatic) ppm; ^{13}C -n.m.r.: δ , 62.3, 73.3, 74.5, 75.4, 75.5, 77.2, 80.7, 83.8, 85.0, 110.2, 118.9, 124.4, 124.6, 127.8 (x2), 128.1, 128.1 (x2), 128.3 (x2), 128.5 (x2), 128.6 (x2), 128.7 (x2), 128.7 (x2), 137.8, 138.0, 138.2, 141.8, 152.0, 163.1 ppm; HR-FAB MS $[M+Na]^+$ calcd for $C_{34}H_{33}NO_6SNa^+$ 606.1926, found 606.1924. (See Appendix; Figure A-25, A-26, A-27)

Ethyl 2,3,4-tri-O-benzoyl-6-O-triphenylmethyl-1-thio- α -D-mannopyranoside (4.21).

To a stirring solution of ethyl 1-thio-6-O-triphenylmethyl- α -D-mannopyranoside²⁵ (1.0g, 2.14 mmol) in pyridine (5 mL) was cooled to 0°C benzoyl chloride (1.11 mL, 9.65 mmol) was added. The reaction was monitored by TLC, and upon completion (6 h), the reaction was cooled to 0 °C and MeOH (0.25 mL) was added. The reaction mixture was then concentrated, the residue was diluted with dichloromethane (20 mL), and washed successively with water (5 mL), 1M HCl (5 mL), water (5 mL), saturated $NaHCO_3$ (5 mL), and water (3 x 5 mL). The organic layer was separated, dried with $MgSO_4$, filtered, and concentrated *in vacuo*. The residue was purified by column chromatography on

silica gel (ethyl acetate – hexane gradient elution) to obtain compound **4.21** as a white foam in 88% yield. Analytical data for **4.21**: Rf = 0.53 (ethyl acetate-hexanes, 3/7, v/v); $[\alpha]_D^{27} = -69.7^\circ$ (c = 1, CHCl₃); ¹H-n.m.r.: δ , 1.31 (t, 3H, CH₂CH₃), 2.65-2.75 (m, 2H, CH₂CH₃), 3.20-3.25 (dd, 1H, H-6a), 3.30-3.34 (dd, 1H, H-6b), 4.50-4.54 (m, 1H, H-5), 5.55 (d, 1H, J_{1,2} = 1.4, H-1), 5.63-5.67 (dd, 1H, J_{3,4} = 10.1 Hz, H-3), 5.71-5.73 (dd, 1H, J_{2,3} = 3.3 Hz, H-2), 6.00 (dd, 1H, J_{4,5} = 10.11 Hz, H-4), 7.00-7.55 (m, 24H, aromatic), 7.70 (d, 2H, aromatic), 7.75 (d, 2H, aromatic), 8.08 (d, 2H, aromatic) ppm; ¹³C-n.m.r.: δ 15.0, 25.6, 62.4, 67.4, 71.1, 71.2, 72.6, 82.3, 86.8, 127.0 (x3), 127.9 (x6), 128.4 (x2), 128.5 (x2), 128.8 (x6), 128.9 (x2), 129.3, 129.5, 129.8, 129.9 (x2), 130.0 (x2), 130.2 (x2), 133.2, 133.3, 133.6, 143.9 (x3), 165.3, 165.7, 165.8 ppm; HR-FAB MS [M+Na]⁺ calcd for C₄₈H₄₂O₈SNa⁺ 801.2498, found 801.2482 (See Appendix, Figure A-71, A-72, A-73)

Benzoxazolyl 2,3,4-tri-O-benzoyl-1-thio- α -D-mannopyranoside (4.6) was obtained from compound **4.21** as a clear syrup in 52% yield. Analytical data for **4.6**: Rf = 0.42 (ethyl acetate-hexanes, 1/2, v/v); $[\alpha]_D^{27} = +20.5^\circ$ (c = 1, CHCl₃); ¹H-n.m.r.: δ , 3.71-3.76 (m, 2H, H-6a, 6b), 4.34-4.39 (m, 1H, H-5), 5.75-5.81 (dd, 1H, H-3), 5.88-5.96 (m, 2H, H-2, 4), 6.62 (d, 1H, J_{1,2} = 2.0 Hz, H-1), 7.19-7.46 (m, 13H, aromatic), 7.78 (d, 2H, aromatic), 7.93 (d, 2H, aromatic), 8.03 (d, 2H, aromatic) ppm; ¹³C-n.m.r.: δ , 61.6, 67.0, 70.1, 71.3, 74.5, 83.6, 110.5, 119.4, 124.9, 125.1, 128.5, 128.7 (x2), 128.8 (x2), 128.9 (x2), 129.1, 130.0 (x2), 130.2 (x2), 130.2 (x2), 130.3, 133.7, 134.0 (x2), 141.7, 152.2, 160.2, 165.4, 165.6, 166.3 ppm; HR-FAB MS [M+Na]⁺ calcd for C₃₄H₂₇NO₉SNa⁺ 648.1304, found 648.1313. (See Appendix; Figure A-28, A-29, A-30)

Synthesis of disaccharides.

General DMTST-promoted glycosylation procedure. A mixture of glycosyl donor (0.030 mmol), glycosyl acceptor (0.027 mmol), and freshly activated molecular sieves (4Å, 70 mg), in 1,2-dichloroethane (0.5 mL) was stirred under argon for 1 h. The reaction mixture was cooled to 0 °C (or as indicated in Tables 1 and 2), DMTST (0.082 mmol) was added, and the reaction mixture was monitored by TLC. Upon completion (see Tables), the reaction mixture was quenched with triethyl amine (1 drop), the solid was filtered off, the filtrate was diluted with CH₂Cl₂ (15 mL), washed with 1% NaOH (5 mL) and water (3 x 5 mL). The organic layer was separated, dried with MgSO₄, filtered and concentrated *in vacuo*. The residue was purified by column chromatography on silica gel (ethyl acetate – toluene gradient elution) to obtain the corresponding disaccharide.

Benzoxazolyl 2,3,4-tri-O-benzoyl-6-O-(2-O-benzoyl-3,4,6-tri-O-benzyl-β-D-glucopyranosyl)-1-thio-β-D-glucopyranoside (4.11) was obtained from **4.1** and **4.5** as a clear film in 72% yield. Analytical data for **4.11**: R_f = 0.33 (ethyl acetate-hexane, 3/7, v/v); [α]_D²⁴ = +73.6° (c = 1, CHCl₃); ¹H-n.m.r: δ, 3.30 (m, 1H, H-5') 3.52 (dd, 1H, H-3'), 3.57-3.65 (m, 3H, H-4', 6a', 6b') 3.78 (m, 1H, H-6b), 3.93 (dd, 1H, H-6a), 4.13 (m, 1H, H-5) 4.38-4.68 (m, 7H, J_{1,2'} = 8.8 Hz, H-1', 3 x CH₂Ph), 5.14 (dd, 1H, J_{2',3'} = 8.5 Hz, H-2') 5.40 (dd, 1H, J_{4,5} = 9.8 Hz, H-4) 5.55 (dd, 1H, J_{2,3} = 9.8 Hz, H-2) 5.75-5.89 (m, 2H, J_{1,2} = 9.8 Hz, J_{3,4} = 9.8 Hz, H-1, 3), 7.00-7.95 (m, 39H, aromatic) ppm; ¹³C-n.m.r.: δ, 67.6, 68.7, 69.4, 71.0, 73.7, 73.9, 74.1, 75.0, 75.2, 75.4, 77.9, 79.3, 83.1, 83.7, 101.0, 110.5, 119.2, 124.6, 124.7, 127.8 (x2), 127.9, 128.0 (x2), 128.1 (x3), 128.4 (x2), 128.5 (x2), 128.5 (x3), 128.6 (x3), 128.6 (x2), 128.8, 128.9 (x2), 130.0 (x3), 130.0 (x2), 130.1 (x4),

130.1 (x2), 130.3, 133.1, 133.4, 133.6, 133.6, 138.1, 138.3, 138.4, 141.7, 152.1, 161.2, 165.3, 165.4, 165.4, 165.8 ppm; HR-FAB MS $[M+Na]^+$ calcd for $C_{68}H_{59}NO_{15}SNa^+$ 1184.3503, found 1184.3518. (See Appendix; A-31, A-32, A-33)

Benzoxazolyl 6-O-(2-O-benzoyl-3,4,6-tri-O-benzyl- β -D-glucopyranosyl)-2,3,4-tri-O-benzyl-1-thio- β -D-glucopyranoside (4.12) was obtained from **4.1** and **4.7** as a clear film in 70% yield. Analytical data for **4.12**: Rf = 0.35 (ethyl acetate-hexane, 3/7, v/v); $[\alpha]_D^{24} = +14.5^\circ$ (c = 1, $CHCl_3$); 1H -n.m.r.: δ , 3.50-3.75 (m, 10H, H-6b, 4, 3, 5, 2, 5', 6a', 6b', 3', 4'), 4.02 (d, 1H, H-6a), 4.34-4.74 (m, 13H, $J_{1',2'}=8.4$ Hz, H-1', 6 CH_2Ph) 5.22 (dd, 1H, $J_{2',3'}=8.4$ Hz, H-2'), 5.34 (d, 1H, $J_{1,2} = 9.5$ Hz, H-1) 6.95-7.95 (m, 39H aromatic) ppm; ^{13}C -n.m.r.: δ , 67.6, 68.9, 73.6, 74.0, 75.0, 75.1, 75.2, 75.5, 75.7, 77.3, 77.4, 78.1, 79.6, 80.9, 83.1, 85.0, 86.6, 101.0, 110.4, 119.2, 124.4, 124.6, 127.7, 127.8, 127.8 (x2), 127.9 (x2), 127.9 (x2), 128.0, 128.1 (x2), 128.1 (x2), 128.2, 128.2, 128.3 (x2), 128.4 (x2), 128.5 (x9), 128.6 (x2), 128.7, 128.7, 130.0 (x2), 130.1, 133.2, 137.7, 138.1 (x2), 138.2, 138.4, 138.5, 142.0, 152.0, 162.1, 165.3 ppm; HR-FAB MS $[M+Na]^+$ calcd for $C_{68}H_{65}NO_{12}SNa^+$ 1142.4125, found 1142.4160. (See Appendix; A-34, A-35, A-36)

Benzoxazolyl 6-O-(2-O-benzoyl-3,4,6-tri-O-benzyl- β -D-galactopyranosyl)-2,3,4-tri-O-benzyl-1-thio- β -D-galactopyranoside (4.13) was obtained from **4.2** and **4.8** as a clear film in 80% yield. Analytical data for **4.13**: Rf = 0.33 (ethyl acetate-hexane, 3/7, v/v); $[\alpha]_D^{24} = +23.7^\circ$ (c = 1, $CHCl_3$); 1H -n.m.r.: δ , 3.35-3.65 (m, 7H, H-3, 3', 6a, 6a', 6b, 6b', 5'), 3.82-3.91 (m, 4H, H-2, 5, 4, 4') 4.23-4.91 (m, 13H, $J_{1',2'}=7.9$ Hz, H-1', 6 CH_2Ph), 5.31 (d, 1H, $J_{1,2}=9.9$ Hz, H-1), 5.54 (dd, 1H, $J_{2',3'}=7.9$ Hz, H-2'), 7.06-8.00 (m, 39H,

aromatic) ppm; ^{13}C -n.m.r.: δ , 66.9, 68.6, 72.1, 72.5, 72.6, 72.8, 73.3, 73.9, 74.0, 75.0, 75.1, 76.1, 77.6, 77.7, 80.3, 84.3, 85.7, 101.6, 110.5, 119.2, 124.5, 124.7, 127.8, 127.9 (x2), 127.9 (x2), 128.0, 128.0, 128.1, 128.1, 128.3, 128.4 (x2), 128.5 (x2), 128.6 (x2), 128.6 (x8), 128.7 (x2), 128.8 (x2), 128.9 (x2), 128.9 (x2), 130.2 (x2), 130.5, 133.5, 138.1, 138.1 (x2), 138.4, 138.9, 139.0, 142.2, 152.2, 162.7, 165.7 ppm; HR-FAB MS $[\text{M}+\text{Na}]^+$ calcd for $\text{C}_{68}\text{H}_{65}\text{NO}_{12}\text{SNa}^+$ 1142.4125, found 1142.4138. (See Appendix; A-37, A-38, A-39)

Benzoxazolyl 6-O-(2-O-benzoyl-3,4,6-tri-O-benzyl- α -D-mannopyranosyl)-2,3,4-tri-O-benzyl-1-thio- α -D-mannopyranoside (4.14) was obtained from **4.3** and **4.9** as a clear film in 51% yield. Analytical data for **4.14**: Rf = 0.38 (ethyl acetate-hexane, 3/7, v/v); $[\alpha]_{\text{D}}^{27} = -6.62^{\circ}$ (c = 1, CHCl_3); ^1H -n.m.r.: δ , 3.50 (m, 10H, H-3, 3', 4, 4', 5, 5', 6a, 6a', 6b, 6b'), 4.14 (m, 1H, H-2), 4.22-5.04 (m, 13 H, $J_{1,2'} = 1.7$ Hz, H-1', 6 CH_2Ph), 5.59 (dd, 1H, $J_{2,3'} = 2.2$ Hz, H-2'), 5.73 (d, 1H, $J_{1,2} = 1.1$ Hz, H-1), 6.97-7.51 (m, 39H, aromatic) ppm; ^{13}C -n.m.r.: δ , 67.0, 68.9, 69.1, 71.4, 71.8, 73.2, 73.5, 74.3, 74.6, 75.1, 75.2 (x2), 77.44, 78.1, 79.3, 83.9, 84.8, 98.2, 110.3, 118.8, 124.2, 124.5, 127.6, 127.7 (x3), 127.9, 127.9 (x2), 128.0 (x2), 128.0 (x2), 128.2, 128.3 (x2), 128.4 (x5), 128.4 (x4), 128.5 (x4), 128.6 (x2), 128.8 (x2), 130.2 (x2), 130.2, 133.2, 138.0 (x2), 138.2, 138.3, 138.8, 138.9, 141.9, 152.1, 163.5, 165.7 ppm; HR-FAB MS $[\text{M}+\text{Na}]^+$ calcd for $\text{C}_{68}\text{H}_{65}\text{NO}_{12}\text{SNa}^+$ 1142.4125, found 1142.4087. (See Appendix; A-40, A-41, A-42)

Benzoxazolyl 2,3,4-tri-O-benzoyl-6-O-(2-O-benzoyl-3,4,6-tri-O-benzyl- α -D-mannopyranosyl)-1-thio- α -D-mannopyranoside (4.15) was obtained from **4.3** and **4.6**

as a clear film in 90% yield. Analytical data for **4.15**: Rf = 0.45 (ethyl acetate-hexane, 3/7, v/v); $[\alpha]_D^{27} = +41.8^\circ$ (c = 1, CHCl₃); ¹H-n.m.r.: δ, 3.46 (d, 1H, H-6a'), 3.60-3.69 (m, 3H, H-5', 4', 6a), 3.87-3.95 (m, 3H, H-3', 6b', 6b), 4.08 (d, 1H, ½ CH₂Ph), 4.28 (d, 1H, ½ CH₂Ph), 4.36-4.41 (m, 2H, CH₂Ph), 4.47-4.54 (m, 2H, H-5, ½ CH₂Ph), 4.72 (d, 1H, ½ CH₂Ph), 4.90 (s, 1H, H-1'), 5.48 (s, 1H, H-2'), 5.70 (dd, 1H, H-3), 5.98 (br s, 1H, H-2), 6.08 (dd, 1H, H-4), 6.64 (s, 1H, H-1), 7.09-7.48 (m, 31H, aromatic), 7.79 (d, 2H, aromatic) 7.91-7.95 (dd, 4H aromatic), 8.06 (d, 2H, aromatic) ppm; ¹³C-n.m.r.: δ, 66.6, 67.1, 68.9 (x2), 70.6, 71.5, 71.7, 72.0, 72.6, 73.5, 74.3, 75.3, 78.8, 84.1, 98.4, 110.5, 119.6, 124.8, 124.9, 127.6, 127.6 (x2), 127.7, 128.2 (x2), 128.2 (x2), 128.4 (x3), 128.5 (x2), 128.5 (x2), 128.6 (x2), 128.7 (x2), 129.0 (x2), 129.1, 129.2, 130.0 (x2), 130.1, 130.1 (x2), 130.2 (x7), 133.2, 133.6, 133.7, 134.0, 138.3, 138.6, 138.9, 141.8, 152.3, 160.0, 165.4, 165.4, 165.6, 165.7 ppm; HR-FAB MS [M+Na]⁺ calcd for C₆₈H₅₉NO₁₅SNa⁺ 1184.3503, found 1184.3478. (See Appendix; A-43, A-44, A-45)

Methyl O-(2-O-benzoyl-3,4,6-tri-O-benzyl-β-D-glucopyranosyl)-(1→6)-O-(2,3,4-tri-O-benzyl-D-glucopyranosyl)-(1→6)-2,3,4-tri-O-benzyl-α-D-glucopyranoside (4.17)

was obtained from **4.12** and **4.16** as a clear film in 85% yield (α/β = 1/3.9). Analytical data for β-**4.17**: Rf = 0.56 (acetone-hexanes-toluene, 1/2/4, v/v/v); ¹H-n.m.r.: δ, 3.19 (s, 3H, OCH₃), 3.24-3.35 (m, 3H), 3.38-3.49 (m, 4H), 3.52-3.78 (m, 7H), 3.85-3.89 (m, 2H), 4.25 (d, 1H), 4.11 (d, 1H, J_{1',2'}=9.8 Hz, H-1'), 4.28-4.38 (m, 2H, CH₂Ph), 4.44-4.74 (m, 16H, H-1, 1'', 7 CH₂Ph), 4.82-4.88 (m, 2H, CH₂Ph), 5.23 (dd, 1H, 2''), 7.03-7.26 (m, 48H, aromatic), 7.85 (d, 2H, aromatic) ppm; ¹³C-n.m.r.: δ, 55.6, 68.0, 68.9, 69.9, 73.5, 73.8, 74.0, 74.9, 75.0, 74.9, 75.0, 75.1, 75.1, 75.2 (x2), 75.5, 75.7, 75.8, 77.8 (x2), 77.9,

78.2, 79.9, 82.1, 82.2, 83.0, 84.9, 98.3, 101.3, 103.6, 127.5, 127.7, 127.7, 127.8 (x3), 127.8, 127.9, 127.9 (x3), 128.0 (x4), 128.0, 128.2 (x4), 128.2, 128.3 (x3), 128.5 (x4), 128.5 (x5), 128.6 (x4), 128.6 (x3), 128.7 (x3), 129.8 (x2), 130.1, 133.2, 138.0, 138.2, 138.2, 138.4 (x2), 138.5, 138.7, 139.1, 165.1 ppm; HR-FAB MS $[M+Na]^+$ calcd for $C_{89}H_{92}O_{17}Na^+$ 1455.6232, found 1455.6204.

One-pot synthesis of Methyl O-(2-O-benzoyl-3,4,6-tri-O-benzyl- β -D-glucopyranosyl)-(1 \rightarrow 6)-O-(2,3,4-tri-O-benzoyl- β -D-glucopyranosyl)-(1 \rightarrow 6)-2,3,4-tri-O-benzyl- α -D-glucopyranoside (4.18). A mixture of glycosyl donor **4.1** (0.030 mmol), glycosyl acceptor **4.5** (0.027 mmol), and freshly activated molecular sieves (4Å, 0.070 g), in dichloroethane (0.5 mL) was stirred under argon for 1h. The reaction mixture was cooled to 0 °C, DMTST (0.082 mmol), was added and the reaction mixture stirred for 20 min. Upon formation of the intermediate disaccharide **4.11**, the reaction mixture was warmed to rt, and acceptor **4.16** (0.030 mmol) and AgOTf (0.082 mmol) were added. The reaction mixture was stirred for 30 min, and then quenched with triethyl amine (1 drop). The solid was filtered off and washed with dichloromethane, the combined filtrate (30 mL) was washed with 1% NaOH (10 mL) and water (3 x 10 mL). The organic phase was separated, dried with MgSO₄, filtered, and concentrated *in vacuo*. The residue was purified by column chromatography on silica gel (acetone-toluene/hexanes gradient elution) to obtain the corresponding trisaccharide **4.18** as a clear film in 83%. Analytical data for **4.18**: Rf = 0.46 (acetone-hexane-toluene, 1/2/4, v/v/v); $[\alpha]_D^{24} = +13.8^\circ$ (c = 1, CHCl₃); ¹H-n.m.r: δ , 3.15 (s, 3H, OCH₃), 3.20-3.43 (m, 5H, H-2, 4, 6a', 6b', 5''), 3.60-3.89 (m, 9H, H-5, 5', 3'', 3, 4'', 6b, 6a, 6b'', 6a''), 4.08 (d, 1H, $\frac{1}{2}$ CH₂Ph), 4.29-4.81 (m,

14H, H-1, 1', 1'', 5.5 CH₂Ph), 5.14-5.24 (m, 2H, H-2'', 4'), 5.35 (dd, 1H, J_{3',4'}=7.8 Hz, H-3'), 5.61 (dd, 1H, J_{2,3'}=9.6 Hz H-2'), 6.87-8.14 (m, 50H, aromatic) ppm; ¹³C-n.m.r.: δ, 55.5, 67.5, 68.2, 68.6, 69.6, 69.8, 72.0, 73.1, 73.6, 73.7, 74.1, 74.6, 74.7, 75.2, 75.4, 75.6, 76.3, 77.4, 78.0, 79.9, 82.0, 82.9, 98.3, 100.8, 101.4, 127.5 (x3), 127.6, 127.7, 127.8, 127.9, 128.0 (x6), 128.1 (x3), 128.1 (x3), 128.3 (x3), 128.4 (x3), 128.5 (x3), 128.6 (x4), 128.6 (x4), 128.6 (x3), 129.0, 129.0, 129.4, 129.8 (x2), 129.9 (x3), 130.0 (x2), 130.2, 133.3, 133.4 (x2), 133.7, 137.9, 138.1, 138.2, 138.4, 138.6, 139.1, 165.0, 165.2, 165.6, 165.9 ppm; HR-FAB MS [M+Na]⁺ calcd for C₈₉H₈₆O₂₀Na⁺ 1497.5610, found 1497.5642.

Competitive glycosylation procedure.

Methyl 6-O-(2-O-benzoyl-3,4,6-tri-O-benzyl-β-D-glucopyranosyl)-2,3,4-tri-O-benzyl-α-D-glucopyranoside (4.19). A mixture of glycosyl donor **4.1** (0.020 g, 0.029 mmol), glycosyl donor **4.4** (0.0196g, 0.029 mmol), and glycosyl acceptor **4.16** (0.0123 g, 0.026 mmol), and freshly activated molecular sieves (4Å, 139 mg), in 1,2-dichloroethane (0.75 mL) was stirred under argon for 1h. The reaction mixture was cooled to 0 °C, DMTST (0.021 g, 0.079 mmol) was added, and the reaction mixture was monitored by TLC. Upon disappearance of the glycosyl acceptor, the reaction mixture was quenched with triethyl amine (1 drop), the solid was filtered off, the filtrate was diluted with CH₂Cl₂ (15 mL), washed with sat. NaHCO₃ (5 mL) and water (3 x 5 mL). The organic layer was separated, dried with MgSO₄, filtered and concentrated *in vacuo*. The residue was purified by column chromatography on silica gel (ethyl acetate – hexanes gradient

elution) to obtain disaccharide **4.19** as a clear film in 95% yield, and recover unreacted glycosyl donor **4.4** in 87% yield. Analytical data and spectra for compound **4.19** is the same as previously reported.¹

4.5 References

1. Mydock, L. K.; Demchenko, A. V., *Org. Lett.* **2008**, *10*, 2103-2106.
2. Kamat, M. N.; Demchenko, A. V., *Org. Lett.* **2005**, *7*, 3215-3218.
3. Pedersen, C. M.; Nordstrom, L. U.; Bols, M., *J. Am. Chem. Soc.* **2007**, *129*, 9222-9235.
4. Jensen, H. H.; Pedersen, C. M.; Bols, M., *Chem. Eur. J.* **2007**, *13*, 7576-7582.
5. Smoot, J. T.; Pornsuriyasak, P.; Demchenko, A. V., *Angew. Chem. Int. Ed.* **2005**, *44*, 7123-7126.
6. Demchenko, A. V., *Handbook of Chemical Glycosylation: Advances in Stereoselectivity and Therapeutic Relevance*. Wiley-VCH: Weinheim, 2008.
7. Boons, G. J., *Tetrahedron* **1996**, *52* (4), 1095-1121.
8. Demchenko, A. V., *Lett. Org. Chem.* **2005**, *2*, 580-589.
9. Codee, J. D. C.; Litjens, R. E. J. N.; van den Bos, L. J.; Overkleeft, H. S.; van der Marel, G. A., *Chem. Soc. Rev.* **2005**, *34*, 769-782.
10. Mootoo, D. R.; Konradsson, P.; Udodong, U.; Fraser-Reid, B., *J. Am. Chem. Soc.* **1988**, *110*, 5583-5584.
11. Fraser-Reid, B.; Udodong, U. E.; Wu, Z. F.; Ottosson, H.; Merritt, J. R.; Rao, C. S.; Roberts, C.; Madsen, R., *Synlett* **1992**, (12), 927-942 and references therein.

12. Koto, S.; Uchida, T.; Zen, S., *Bull. Chem. Soc. Jpn.* **1973**, *46*, 2520-2523.
13. Nicolaou, K. C.; Dolle, R. E.; Papahatjis, D. P.; Randall, J. L., *J. Am. Chem. Soc.* **1984**, *106*, 4189-4192.
14. Randall, J. L.; Nicolaou, K. C., *ACS Symp. Ser.* **1988**, *374*, 13-28.
15. Kanie, O.; Ito, Y.; Ogawa, T., *J. Am. Chem. Soc.* **1994**, *116*, 12073-12074.
16. Kanie, O., Orthogonal strategy in oligosaccharide synthesis. In *Carbohydrates in Chemistry and Biology*, Ernst, B.; Hart, G. W.; Sinay, P., Eds. Wiley-VCH: Weinheim, New York, 2000; Vol. 1, pp 407-426.
17. Baeschlin, D. K.; Chaperon, A. R.; Charbonneau, V.; Green, L. G.; Ley, S. V.; Lucking, U.; Walther, E., *Angew. Chem. Int. Edit.* **1998**, *37* (24), 3423-3428.
18. Demchenko, A. V.; De Meo, C., *Tetrahedron Lett.* **2002**, *43* (49), 8819-8822.
19. Tanaka, H.; Adachi, M.; Tsukamoto, H.; Ikeda, T.; Yamada, H.; Takahashi, T., *Org. Lett.* **2002**, *4* (24), 4213-4216.
20. Demchenko, A. V.; Kamat, M. N.; De Meo, C., *Synlett* **2003**, 1287-1290.
21. Pornsuriyasak, P.; Demchenko, A. V., *Tetrahedron: Asymmetry* **2005**, *16*, 433-439.
22. Codee, J. D. C.; Litjens, R. E. J. N.; Heeten, R.; Overkleeft, H. S.; van Boom, J. H.; van der Marel, G. A., *Org. Lett.* **2003**, *5* (9), 1519-1522.
23. Huang, X.; Huang, L.; Wang, H.; Ye, X. S., *Angew Chem., Int. Ed.* **2004**, *43*, 5221-5224.
24. Mydock, L. K.; Demchenko, A. V., *Org. Lett.* **2008**, *10*, 2107-2110.
25. Ottosson, H., *Carbohydr. Res.* **1990**, *197*, 101-107.
26. Houdier, S.; Vottero, P. J. A., *Carbohydr. Res.* **1993**, *248*, 377-384.

27. Ruda, K.; Lindberg, J.; Garegg, P. J.; Oscarson, S.; Konradsson, P., *J. Am. Chem. Soc.* **2000**, *122*, 11067-11072.
28. Kuester, J. M.; Dyong, I., *Justus Liebigs Ann. Chem.* **1975**, (12), 2179-2189.
29. Premathilake, H.; Mydock, L. K.; Demchenko, A. V., *Journal of Organic Chemistry* **2010**, (75), 1095-1100.

CHAPTER 5

The Investigation of Sulfonium Species as Key Intermediates in Chemical Glycosylation

5.1 Introduction

While the prior two chapters have focused on a superarming methodology for glycosyl donors that was founded upon the electronic nature of the O-2/O-5 Cooperative Effect, this chapter explores the consequences of reversing the protecting groups to produce the opposite effect. As aforementioned (Chapter 3.1.2), the O-2/O-5 Cooperative Effect was initially brought to light by the discovery of a very unreactive SBox glycosyl donor bearing a “mixed” 2-*O*-benzyl-3,4,6-tri-*O*-benzoyl protecting group pattern (Figure 5.1, superdisarmed).¹ This finding in turn, led to the discovery of the superarming methodology, wherein SBox glycosyl donors bearing the reverse “mixed” pattern, 2-*O*-benzyl-3,4,6-tri-*O*-benzoyl, were exploited for their super-reactive character (Figure 5.1, superarmed). Subsequently, this superarming strategy was applied to chemoselective oligosaccharide strategies.^{2,3}

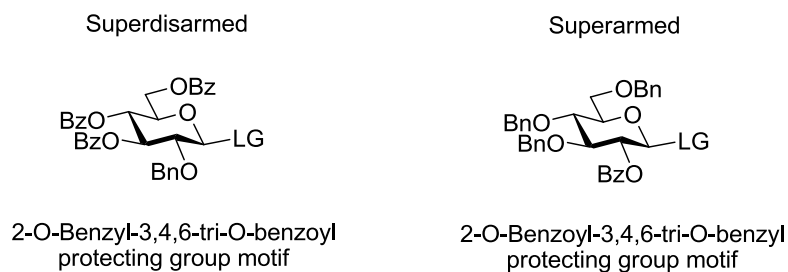


Figure 5.1 Mixed patterned glycosides

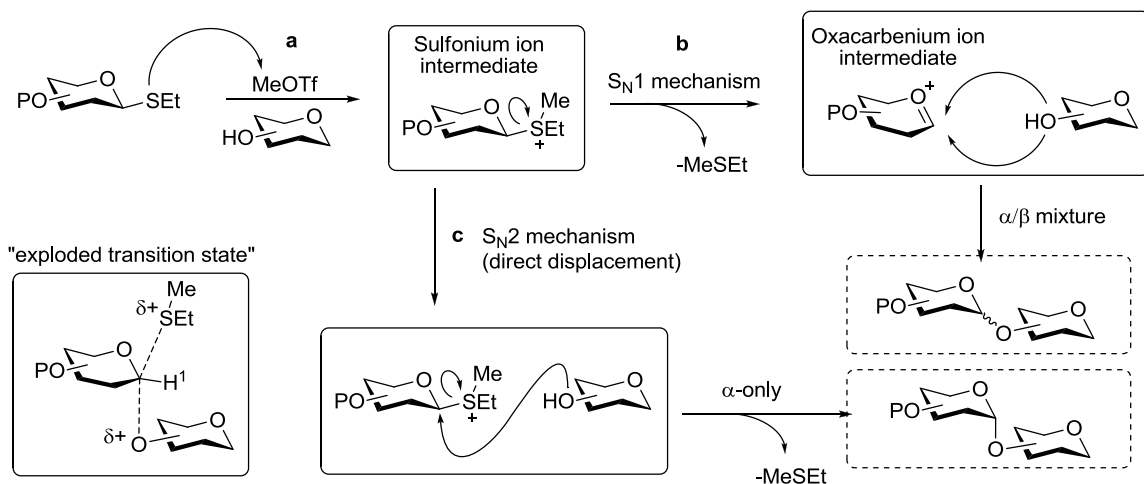
With these unusual reactivities well established in SBox glycosides, we wanted to generalize our findings by expanding our methodology to encompass other classes of glycosyl donors. Accordingly, in an attempt to further explore the implications of the O-

2/O-5 Cooperative Effect we first chose to investigate commonly utilized ethyl-thioglycosides (*S*-ethyl). It was during the investigation of this class of glycosyl donors, that an unexpectedly stable glycosylation intermediate was discovered.

As highlighted in Scheme 5.1a, methyl triflate (MeOTf) is a commonly utilized activator (promoter) for *S*-ethyl donors, whereby activation occurs through methylation of the sulfur atom (pathway a). The activated leaving group (MeSEt) then typically departs in an S_N1 fashion (pathway b), which often results in a lack of stereoselectivity during product formation (discussed in detail in Chapter 1.2). Although this S_N1 leaving group departure is generally considered to be the rate determining (slow) step of the glycosylation reaction, the formation and departure of anomeric sulfonium species (such as MeSEt) often occurs at a rate wherein it cannot be observed (although there are a few cases where anomeric sulfonium species are detectable at lowered temperatures using modern spectroscopic methods).^{4, 5 6}

However, through the course of our investigations, specific conditions were found wherein we were able to detect this activated leaving group at room temperature, via thin layer chromatography (TLC). Thought to be yet another a consequence of the O-2/O-5 Cooperative Effect, this unusually stable intermediate also presented itself as an ideal species to undergo an S_N2 glycosylation, as it could be considered to be in a “pre-activated” state. Thus, one could expect this cationic leaving group to be labile enough to be displaced in an S_N2 fashion upon exposure to a nucleophile (pathway c). Although the viability of a true S_N2 reaction is still in question an alternative mechanistic pathway⁷

offers the same stereoselectivity by first dissociating into a more loosely attached “exploded” transition state (Scheme 5.1), in which both the incoming nucleophile and departing leaving group are loosely attached to the anomeric center (as addressed in Chapter 2.3.1).



Scheme 5.1 Plausible *S*-ethyl glycosylation mechanism

As such, we became interested in this sulfonium species for its potential application toward the stereoselective formation of glycosidic linkages. Furthermore, many recent examples have shown that the generation of these anomeric “onium” (positively charged) species can increase the α -selectivity of the glycosylation reaction,^{4, 6, 8, 9} as they generally prefer to reside in the β -configuration (which can be attributed to the reverse anomeric effect^{10,11}).

5.2 Discovery of an Anomeric β -Sulfonium Glycoside

5.2.1 Initial observation

Investigation into the reactivity of ethyl thioglycosides began in a similar fashion to that of our studies with SBox glycosides, wherein a series of glycosyl donors bearing different protecting group patterns were first synthesized (Figure 5.2). As these were known compounds, we easily synthesized the classic armed (**5.1**)¹² and disarmed (**5.2**)^{13, 14} thioglycosides, along with the “mixed” patterned thioglycoside displaying the superarming (**5.3**)¹⁵ motif. As seen in Scheme 5.2, superdisarmed thioglycoside (**5.4**) was easily synthesized from benzylidene protected thioglycoside **5.5**, (which can be simply obtained in 3 steps from commercially available glucose pentaacetate). Subsequently, building block **5.5** was selectively benzylated under phase transfer conditions, to achieve compound **5.6** in 58% yield. This was followed by benzylidene removal with TFA, and benzoyl protection, to yield compound **5.4** in 97% yield.

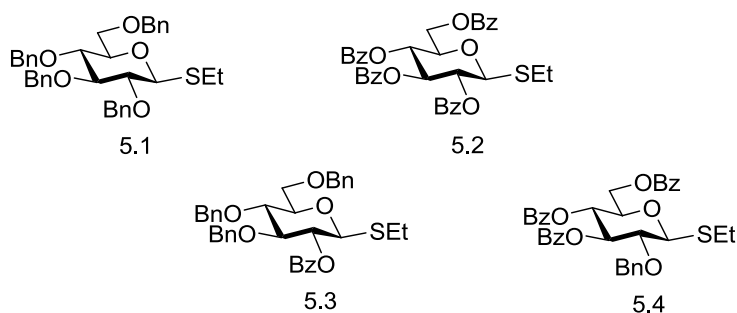
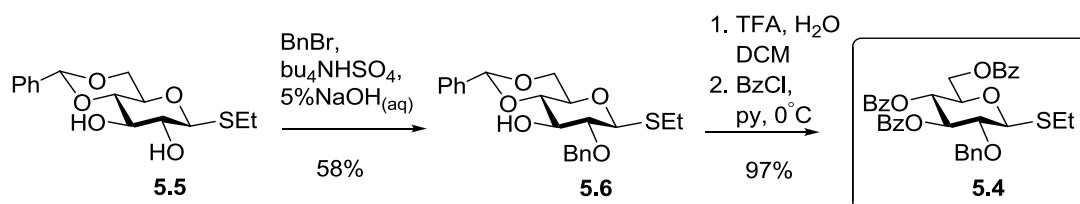


Figure 5.2 Ethyl thioglycosyl donors with varying protecting group arrangements

With the desired thioglycosyl donors in hand, it was now possible to investigate their relative reactivities through comparative glycosylation. As per the premise of the armed-disarmed theory^{16, 17} (Chapter 2.1.1 and 3.1.1) and chemoselective activation strategy (Chapter 4.1.1), it is essential to employ mild activation conditions in order to easily differentiate among the reactivity levels of the various glycosyl donors. Therefore, we initially selected methyl triflate (MeOTf) as our activator of choice (promoter **a**). Accordingly, the results of the MeOTf (3 equiv) mediated glycosylations in 1,2-dichloroethane are summarized in Table 5.1.



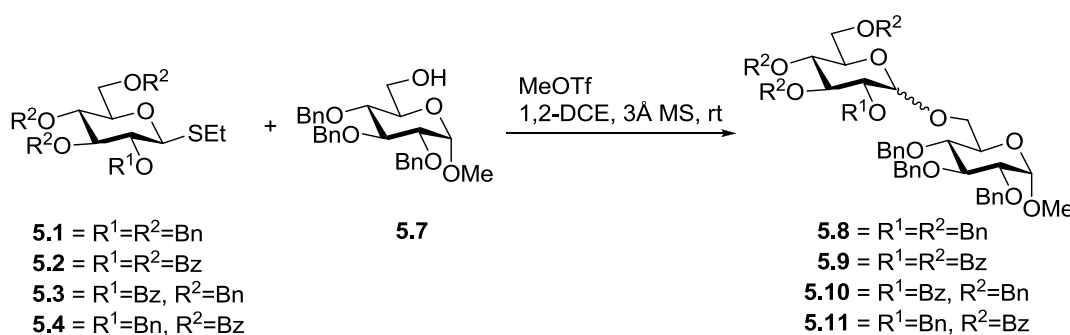
Scheme 5.2 Synthesis of the superdisarmed ethyl thioglycoside **5.4**

As expected, the armed per-benzylated glycosyl donor **5.1** reacted smoothly and efficiently with glycosyl acceptor **5.7**,¹⁸ to yield the corresponding disaccharide **5.8** in 80% yield (Entry 1). Disarmed per-benzylated glycosyl donor **5.2** was also found to react relatively quickly under these conditions, taking only 4 hours until completion, yielding disaccharide **5.9** in 84% yield (Entry 2).

With the glycosylation results from the classic armed and disarmed donors established, we next looked to glycosidate our mixed pattern donors. In the case of thioglycosyl donor **5.3**, bearing the superarmed protecting group motif, the reaction proceeded efficiently to

give disaccharide **5.10** in 80% yield (Entry 3). Unfortunately, these conditions proved to be inadequate for resolving the relative reactivities between donor **5.3**, and its armed analog **5.1**, as they proceeded at approximately the same rate; although since, significantly milder reaction conditions (I_2) have shown **5.3** to be more reactive.¹⁹

Table 5.1 Comparative glycosidations of glycosyl donors **5.1-5.4** with acceptor **5.7** in the presence of (a) MeOTf (3 equiv) at rt



entry	donor	time	product	yield
1	5.1	2h	5.8	80%
2	5.2	4h	5.9	84%
3	5.3	2h	5.10	80%
4	5.4	4h*	5.11	53%

* time at which the incomplete reaction was quenched

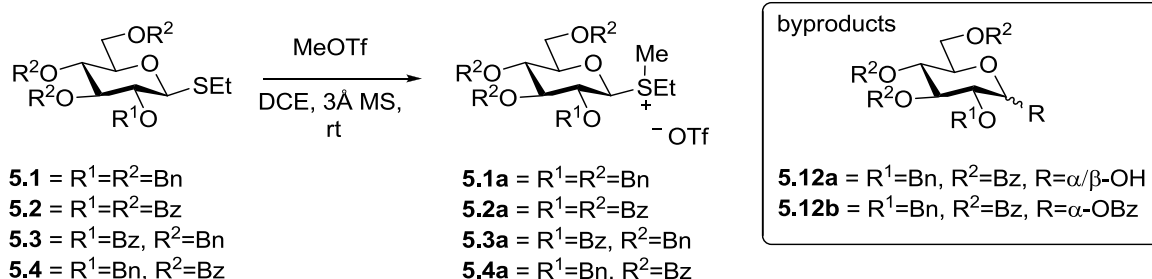
Upon first glance, it seemed that the glycosidation of superdisarmed patterned glycosyl donor **5.4** with glycosyl acceptor **5.7** (Entry 4) was typical, proceeding at a rate comparable to that of its disarmed thioglycosyl counterpart **5.2**. However, as the glycosyl donor was completely consumed within 4 hours, a large amount of glycosyl acceptor still

remained (as visualized by thin layer chromatography, TLC), while there was only partial formation of the anticipated disaccharide product **5.11**. Further inspection of the TLC plate revealed that a new unknown compound had formed as an intense spot at the baseline (ethyl acetate-toluene 1/9, v/v). For comparison, in the same system donor **5.4** has $R_f = 0.55$. In addition, when investigated in a more polar TLC system (methanol- CH_2Cl_2 1/9, v/v), this compound was visualized as an elongated spot at $R_f = 0.5$, which was heavily concentrated at the top and became more diffuse toward the bottom, eventually fading away. At this point, the reaction was subjected to aqueous work up, whereupon it was found that the remaining “baseline species” was decomposed, resulting in mainly hemiacetal **5.12a** and a benzoyl transfer product **5.12b** (Scheme 5.3), and therefore, the formed disaccharide was isolated in only 53%. Upon repeating this reaction (as discussed below in the description of Table 5.4), the reaction required an additional 2 hours in order for this baseline spot to completely disappear/react.

In lieu of this finding, a closer look at the previous glycosylation reactions also revealed that a weak spot, corresponding to a trace amount of a similar unknown compound, was present in the glycosylation reaction with the disarmed glycosyl donor **5.2**. Although, in later investigations, it was found that this faint baseline spot was no longer detectable after 4 hours in the reaction vessel. Seeing as the observed intermediates were more polar than the other reaction components (including hemiacetal **5.12a**), it was subsequently proposed that they may correspond to “stable” anomeric sulfonium species, formed upon methylation of the thioethyl leaving group (Scheme 5.3).

5.2.2 Isolation and characterization

With this knowledge, we wanted to re-investigate glycosyl donors **5.1-5.4**, however this time in the absence of a glycosyl acceptor, as it was hoped that these conditions would provide an environment wherein the proposed sulfonium ions **5.1a-5.3a** could form, in addition to the previously observed **5.4a** (Scheme 5.3). Thus, glycosyl donors **5.1-5.4** were each treated with 3 equivalents of MeOTf in the presence of molecular sieves in 1,2-dichloroethane (DCE) at room temperature. Consistent with earlier observations, neither the superarmed (**5.3**) nor the armed (**5.1**) glycosyl donors yielded a sulfonium salt, and again the less reactive disarmed glycosyl donor (**5.2**) showed only nominal signs of “salt” formation. While efforts were made to isolate sulfonium salt **5.2a**, the high lability of this species, rendered all attempts unsuccessful. Finally, as expected, the salt **5.4a** corresponding to glycosyl donor **5.4** was again formed, in approximately 1 hour, at which point the reaction mixture was worked up and attempts were made to purify and characterize the unknown polar compound.



Scheme 5.3 Sulfonium salt formation in the absence of a glycosyl acceptor

Anticipating the lability of this compound, attempts to purify this compound from the reaction mixture were approached with care. As it was assumed that it may not survive column chromatography, compound **5.4a** was purified by preparative TLC, using anhydrous solvents. This separation was immediately followed by spectral analysis, whereupon $^1\text{H-NMR}$ spectral data confirmed the existence of a new compound.

As can be seen from the $^1\text{H-NMR}$ spectra (Figure 5.3a vs 5.3b) a number of signals have shifted downfield, however, the most significant shifts were those of the H-1 and *S*-ethyl protons. Thus, the H-1 peak was shifted from 4.72 ppm to 5.31 ppm, while retaining its β -configuration ($J_{1,2} = 9.8$ Hz), and the methylene hydrogens (H-7a,b, Figure 5.3a) were both shifted and split due to the chiral environment created by the addition of a methyl group. Importantly, the appearance of a singlet at 2.44 ppm, integrating to 3 protons, was evidence of the newly acquired methyl group (Me). In addition, a follow-up spectrum taken after 16 hours revealed that the compound had hydrolyzed and consisted of only hemiacetal **5.12a** (Figure 5.3c) and liberated ethylmethylsulfide, as confirmed through comparison with authentic samples. Furthermore, the $^{13}\text{C-NMR}$ spectra also reinforced these findings, as various carbon shifts were observed. This includes the anomeric carbon (C-1), which was found to shift only slightly from the original anomeric signal at 85.5 ppm to 82.3 ppm, and the ethyl carbons were found to diverge, C-7 moving downfield by 10.6 ppm and C-8 moving upfield by 6.1 ppm. In addition, a new methyl peak appeared at 16.3 ppm. Mass spectral data was also consistent with the anticipated compound **5.4a**, exhibiting an ion peak at m/z equal to 641.2219 (calculated for $\text{C}_{37}\text{H}_{37}\text{O}_8\text{S}^+$, 641.2209)

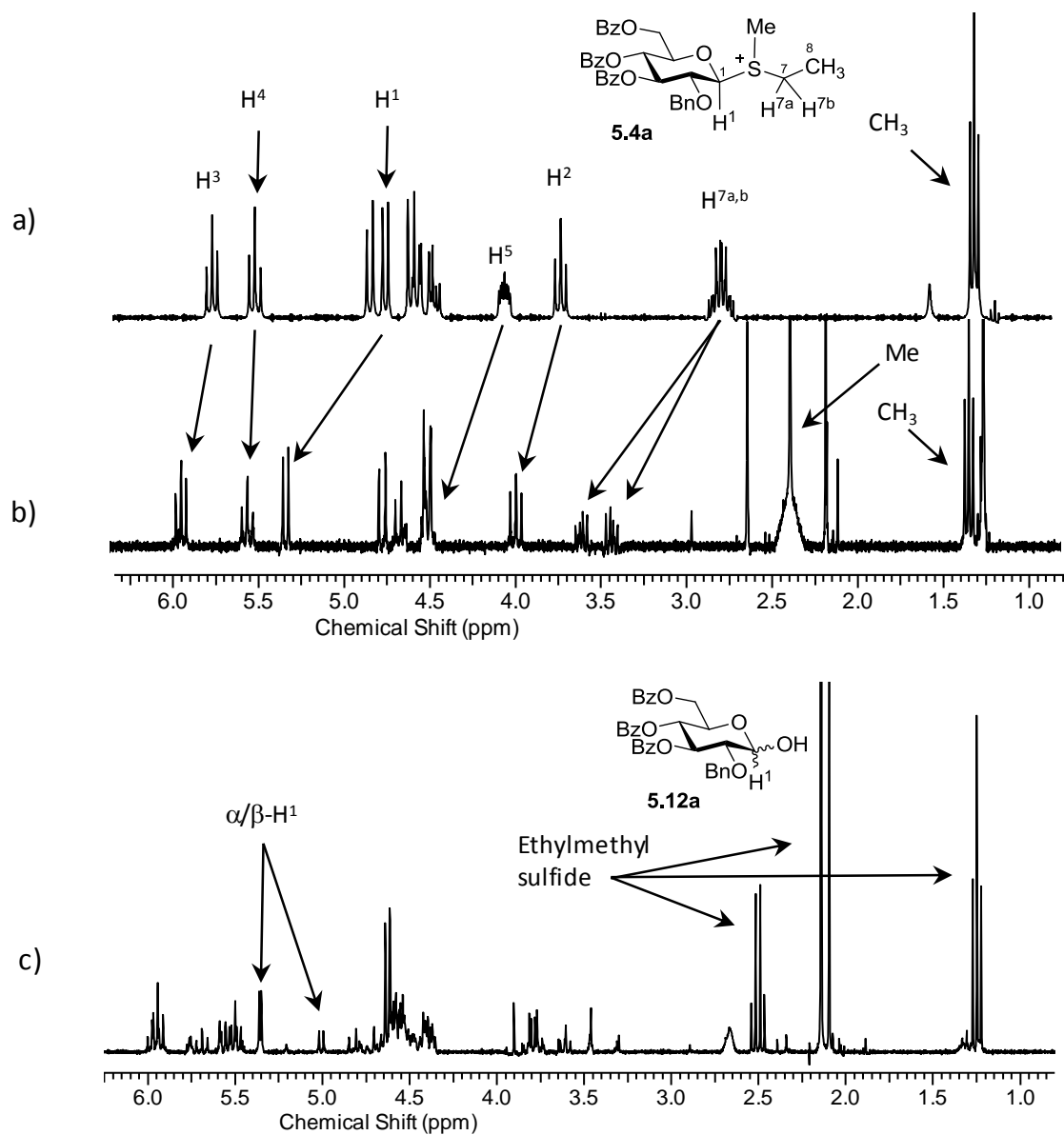


Figure 5.3 ^1H NMR of (a) starting material **5.4**, (b) β -sulfonium ion **5.4a**, (c) hydrolysis product **5.12a**

5.2.3 Mechanistic rationalization via the O-2/O-5 cooperative effect

It can be inferred that the “stability” of this intermediate is a product of the O-2/O-5 Cooperative Effect. As discussed in detail in Chapter 3.1.1, the electronic consequences of the superdisarmed protecting group pattern cause the glycosyl donor to be very

unreactive, presumably due to the instability of the intermediate carbocation formed upon leaving group departure. Applying this rationale, it would then follow that the thioethyl leaving group of donor **5.4** would be less likely to depart, as the instability of the resulting carbocation greatly increases the energy of activation (E_A). However, it can also be presumed that because a strong methylating reagent (such as MeOTf) was used, it can still be attacked by the lone pair on the sulfur atom.

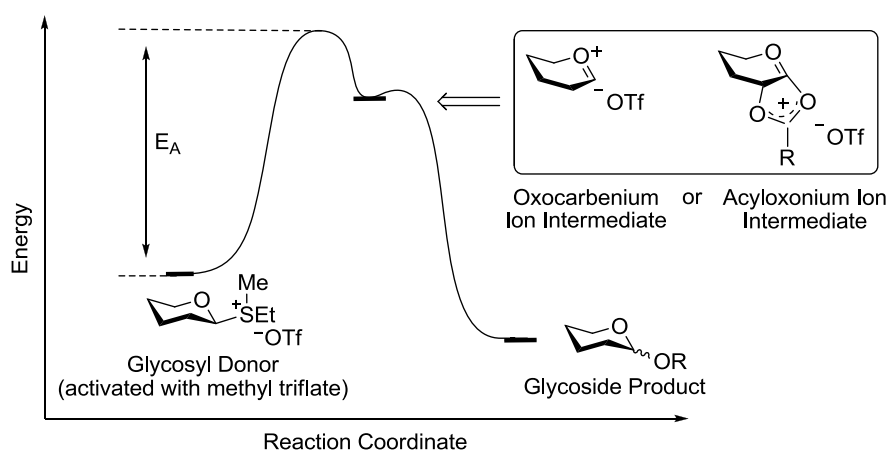
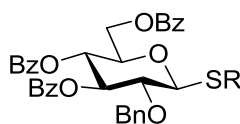


Figure 5.4 Simplified energy diagram of a glycosylation reaction

At this point the superarmed, armed and disarmed glycosyl donors (**5.3**, **5.1**, and **5.2** respectively), readily transition into their respective oxocarbenium/acyloxonium ions and then on to product formation (Figure 5.4). However, the superdisarmed glycosyl donor **5.4** cannot overcome its high energy of activation (E_A), and so remains as a sulfonium salt **5.4a**. Interestingly, two examples of anomeric sulfonium ions have recently been reported, wherein the compounds also displayed the “superdisarming” protecting group motif (bearing a nonparticipating azide group at C-2 and electron withdrawing acyl groups at the remaining positions).^{4,5}

5.2.4 Investigating other classes of thioglycosides

At this point, other superdisarmed glycosyl donors equipped with sulfur-based leaving groups were also investigated for their potential ability to form sulfonium ions (Figure 5.5). Interestingly, no trace of salt formation was observed with any of these glycosyl donors. As they were all able to undergo glycosylations with methyl triflate, it is believed that the intermediate sulfonium species are just too reactive to be detected/isolated (vide TLC) at room temperature. Accordingly, no salt was observed, even at lowered reaction temperatures.



R = phenyl, tolyl, benzoxazolyl

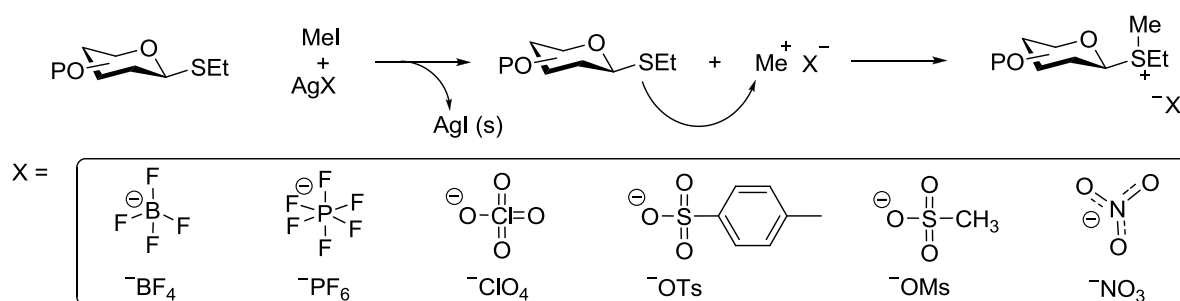
Figure 5.5 Additionally investigated superdisarmed thioglycoside donors

5.3 Investigation of the Counter-anion

5.3.1 Methodology for β -sulfonium ion generation

We next investigated both the stability and reactivity of the ethylmethylsulfonium ion **5.4a**. First, in an attempt to enhance the stability of the cationic donor, we decided to investigate the role that the (often overlooked) counter-anion could be playing. To accomplish this task, we opted to take an approach wherein we could generate a variety of “methylating promoters” *in situ*. Seeing as methyl iodide (MeI) is not a strong enough methylating reagent to promote *S*-ethyl glycosylations, we chose it as the source of

methyl cation (Me^+). Conversely, commercially available silver salts (AgX) were chosen as the source of counter-anion, as these reagents alone also do not promote thioglycoside glycosylations. Exploiting the known affinity of silver compounds to readily undergo anion exchange with an alkyl halides (such as MeI), we were then able to generate a series of new “methylating promoters” *in situ* (MeX), from which a range of sulfonium salts (each containing a different counter-anion) could be generated, while precipitating out an insoluble silver iodide (AgI) byproduct. It should be noted that assuming the independent existence of such new MeX species is not entirely correct, as it is more likely that the methylation of the leaving group would occur concomitantly with counter-anion exchange through a more complex transition state. Herein, however, it is referred to as such for the purpose of simplification. As seen in Scheme 5.4, six different silver salts were selected as potential precursors; silver tetrafluoroborate (AgBF_4); silver hexafluorophosphate (AgPF_6); silver perchlorate (AgClO_4); silver tosylate (AgOTs); silver mesylate (AgOMs) and silver nitrate (AgNO_3).

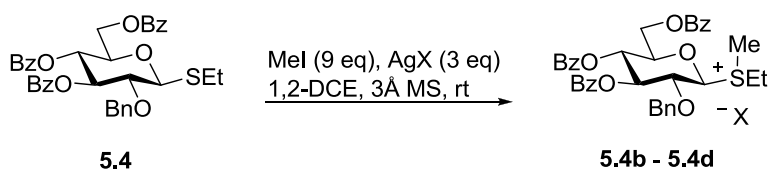


Scheme 5.4 *In situ* promoter formation and glycosyl donor activation

To verify that no reaction took place prior to the generation of the active promoter *in situ*, two glycosylations were attempted in the presence of MeI and separately in the presence

of the silver salt (AgX), wherein no reactions were observed (vide TLC). Furthermore, ^1H NMR was found to be in agreement. It should be noted, however, that a few proton shifts did occur in the NMR spectra upon the addition of any silver salt. Furthermore, these shifts were also seen to be dependent upon the amount of silver reagent added and the length of exposure. As such, the changes in chemical shifts were more pronounced after the glycosyl donor and the silver salt were allowed to remain in solution for 16 hours. We assume that such shifts are due to the complexation of the silver atom with negatively charged atoms on the glycosyl donor, including the sulfur leaving group.

Table 5.2 β -Sulfonium ion formation using *in situ* generated methylating promoters



entry	AgX	<i>in situ</i> promoters		time to salt formation ^a	β -sulfonium ion
		b	MeBF ₄		
1	AgBF ₄	b	MeBF ₄	0.5 h	5.4b
2	AgPF ₆	c	MePF ₆	0.5 h	5.4c
3	AgClO ₄	d	MeClO ₄	0.5 h	5.4d
4	AgOTs	e	MeOTs	--	none
5	AgOMs	f	MeOMs	--	none
6	AgNO ₃	g	MeNO ₃	--	none

^atime at which significant amount of salt formation was detected

To test the ability of these promoters to produce a β -sulfonium ion, our experiments were setup similar to that of our previous “preactivation” investigation utilizing MeOTf, promoter **a** (Scheme 5.3). Thus, in the absence of a glycosyl acceptor, thioglycoside **5.4** was stirred for 30 min with a large excess of MeI (9 equiv), followed by the addition of the desired silver salt (Table 5.2) to generate promoters **b-g**. As the various sulfonium salts began to form, the precipitation of yellow AgI was noticed among the reactions. As such, the reactions between MeI and AgBF₄, AgPF₆ and AgClO₄ yielded sulfonium salts **5.4b-d** (Entries 1-4). However, in the reactions between MeI and AgOTs, AgOMs and AgNO₃, little-to-no AgI precipitate was observed, even after an extended period of time (entries 5-7). It then followed that in these cases no sulfonium salt was detected, as anion exchange did not occur.

5.3.2 Characterization of the silver catalyzed β -sulfonium salts

At this point, sulfonium salts **5.4b-d** were purified by preparative layer chromatography (PLC) and subsequent NMR spectra were recorded. Interestingly, unlike the solitary H-1 signal seen at 5.31 ppm in the previous spectrum of figure **5.4a** (Figure 5.3b), the ¹H NMR spectra of these sulfonium salts **5.4b-d** revealed the presence of two new downfield H-1 signals. As exemplified in the reaction between **5.4** and promoter **d** (Scheme 5.5), the NMR spectrum (Figure 5.7) showed the new H-1 signals to be at 5.30 ppm and 5.17 ppm (although slightly different for each counter-anion), and to each have a coupling constant consistent with that of a β -glycoside (9.7 Hz and 9.8 Hz, respectively). Additionally, these H-1 shifts could each be linked (through integration) to a different set of *S*-ethyl protons, and to a new singlet indicative of an acquired methyl group.

Furthermore, while there was splitting seen amongst the H-1 protons and the leaving group protons, the rest of the signals remained overlapping. This led us to believe that these were diastereomeric β -sulfonium ions, as this occurrence has been documented previously.⁴

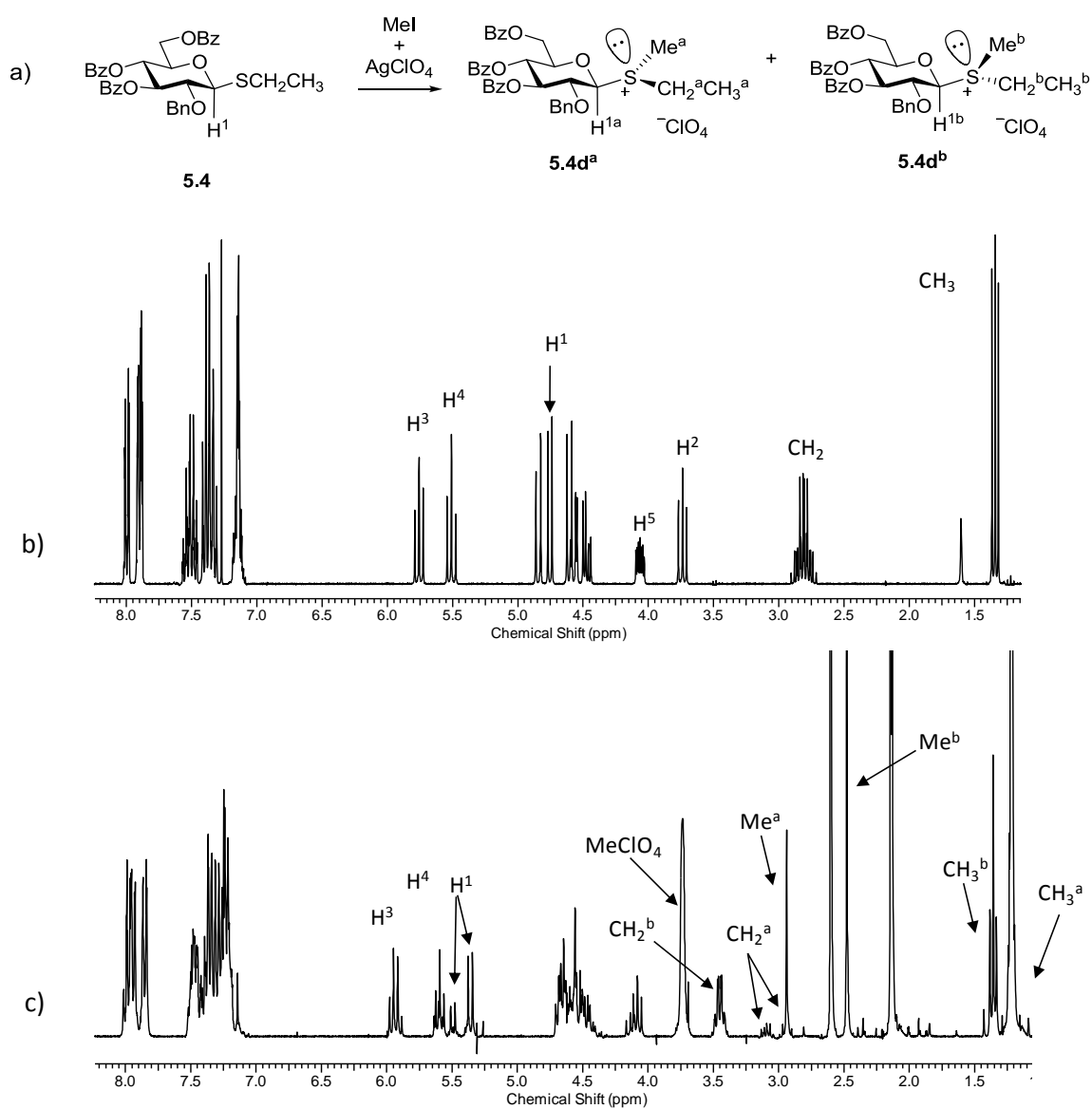


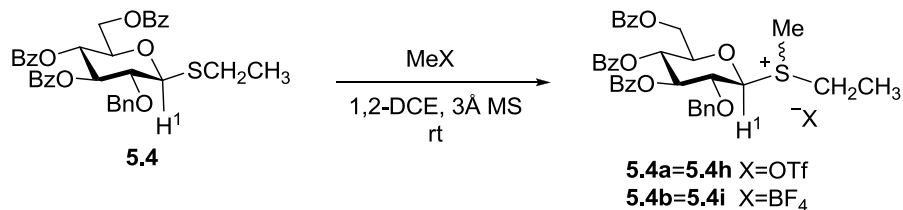
Figure 5.7 (a) Reaction of glycosyl donor **5.4** with MeI/AgClO₄, (b) ¹H NMR spectrum of glycosyl donor **5.4**; (c) ¹H NMR spectrum of resulting diastereomeric β -sulfonium ions **5.4d^a** and **5.4d^b**

5.3.3 Diastereomer investigation

As previously mentioned, we had observed that the silver salts (AgX) were found to coordinate with the sulfur atom of thioglycosyl donors. This led us to wonder whether the silver coordination was causing a diastereomeric pair to be generated (Scheme 5.5), or whether it was only acting as a shift reagent; revealing previously unseen overlapping H-1 signals (as only one diastereomer was observed with **5.4a**, Figure 5.3b).

To resolve this uncertainty, we decided to investigate the ^1H NMR spectrum generated from *in situ* generated MeOTf, allowing us to directly compare the results with our purchased, reagent grade MeOTf (**a**). As seen in Table 5.3, we used our prior methodology, mixing MeI and AgOTf to yield promoter **h**. As previously seen with promoter **a**, the reaction using promoter **h** yielded only one observable H-1 signal in the ^1H NMR spectra of both the crude and purified reaction mixtures (Entry 1). These findings imply that this is a characteristic of the triflate counter-anion, and not of the silver reagent.

Similarly, we also investigated another set of methylating promoters, both containing a tetrafluoroborate counter-anions, but only one promoter containing silver (Table 5.3, Entries 3 and 4). Results from the powerful methylating promoter, trimethyloxonium tetrafluoroborate (Me_3OBF_4 , promoter **i**) were compared to those of the silver generated promoter **b**. As expected, there was no difference in the ^1H NMR spectra of sulfonium salts **5.4b** and **5.4i**. Thus, in both the purified and crude ^1H NMR two diastereomeric H-1 signals were clearly observed.

Table 5.3 Diastereomer investigation

entry	reagent A	sulfonium salt	time	H ¹ : methyl signals (crude) ^a	H ¹ : methyl signals (PLC) ^b
1	a MeOTf	5.4a	1 h	1 : 2	1 : 1 ^c
2	h MeI + AgOTf	5.4h	1 h	1 : 2	1 : 1 ^c
3	i Me ₃ OBF ₄	5.4i	3 h	2 : 2	2 : 2
4	b MeI + AgBF ₄	5.4b	0.5 h	2 : 2	2 : 2

^acrude NMR taken immediately following salt formation, ^bafter preparative layer chromatography; ^conly trace amounts of second diastereomer were detected

Interestingly however, having just previously identified the diastereomeric *S*-methyl (Me^{a,b}) and *S*-ethyl (CH₂^{a,b} and CH₃^{a,b}) signals in β -sulfonium salts **5.4b-d**, we also found that these signals were present in the crude NMRs of **5.4a** and **5.4h**. This implies that, *in fact*, two diastereomers are being generated even though only one H-1 signal is discernable. Formerly, these diastereomeric leaving group peaks had not been recognized, as it was unclear that they were related to a second stereoisomer. In the crude NMR spectrum, residual starting material and various byproducts often present, which obscure proper integration of the related ring-proton signals. Conversely, after PLC purification proof of the second diastereomer was even more difficult to detect, as the only remaining evidence was a hint of the methyl (Me^a) singlet around 2.9 ppm (as can be seen in Figure 5.3b). As this peak, and its associated *S*-CH₂CH₃ signals, were much

more prominent in the NMR spectra of the crude reaction mixture, it can be assumed that this second diastereomer is more labile than the other; as it is less able to survive purification.

Upon further investigation, this lability was found to be the case with all sulfonium salt species. Moreover, in the case of harsher workup conditions, whereupon the salt was washed with cold water before preparative TLC, there was even further degradation of this second diastereomer. At this point, it was also observed that in general, both the tetrafluoroborate (**5.4b**, **5.4i**) and hexafluorophosphate (**5.4c**) salts seemed to be more stable than those containing the perchlorate (**5.4d**) and then triflate (**5.4a**, **5.4h**) counter-anions. This is presumably due to the more nucleophilic nature of the perchlorate and triflate anions, as they have the ability to covalently attach to the anomeric carbon, effectively disassembling the salt. Previously, these counter-anions have been documented to participate in reactions at the anomeric center, and in this case they could actually be engendering the leaving group departure.

Furthermore, the same distinct β -diastereomer tends to be generated in excess of the other, which corresponds to the more shielded H-1 signal. Conversely, the β -diastereomer corresponding to the more deshielded H-1 signal forms more sluggishly, and is found to be more labile, as it is found in lesser amount subsequent to purification. Figure 5.8 illustrates this phenomenon, following the formation of diastereomeric β -sulfonium ions **5.4d^a** and **5.4d^b** in real time via NMR. It can easily be seen that the more deshielded H-1, is much slower to form.

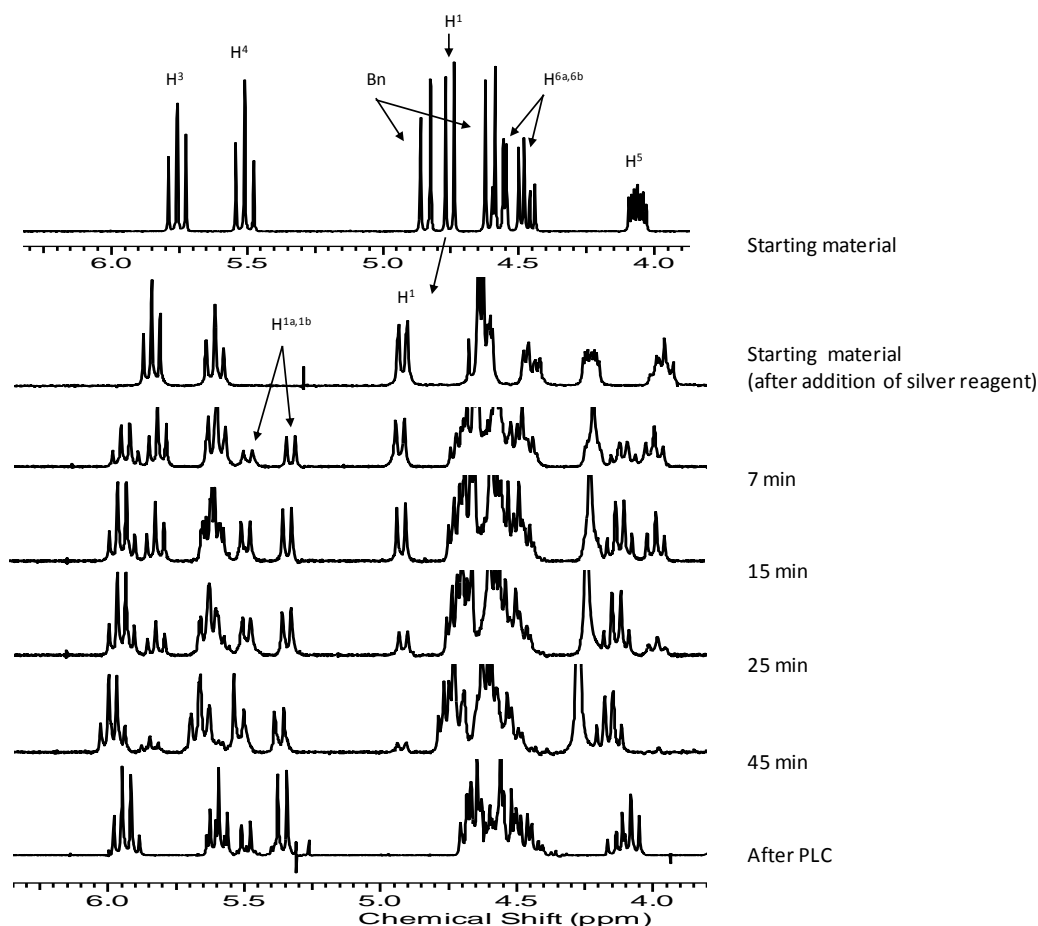


Figure 5.8 Formation of diastereomeric β -sulfonium ions **5.4d^a** and **5.4d^b**

Resulting from this difference in rate of formation, it should be noted that the ratio of β -diastereomers seen in any given NMR spectrum generally differs, as it is found to be a product of both the amount of time in the reaction vessel, and the work up and/or purification conditions. Furthermore, although the silver was not found to be a part of the mechanism of diastereomer formation, there have been cases wherein unusual H-1 shifts have been documented. Figure 5.9 is comprised of three different ^1H NMR spectra, each

corresponding to an experiment wherein β -sulfonium salt **5.4c** was obtained from MeI and AgPF₆, under similar reaction conditions.

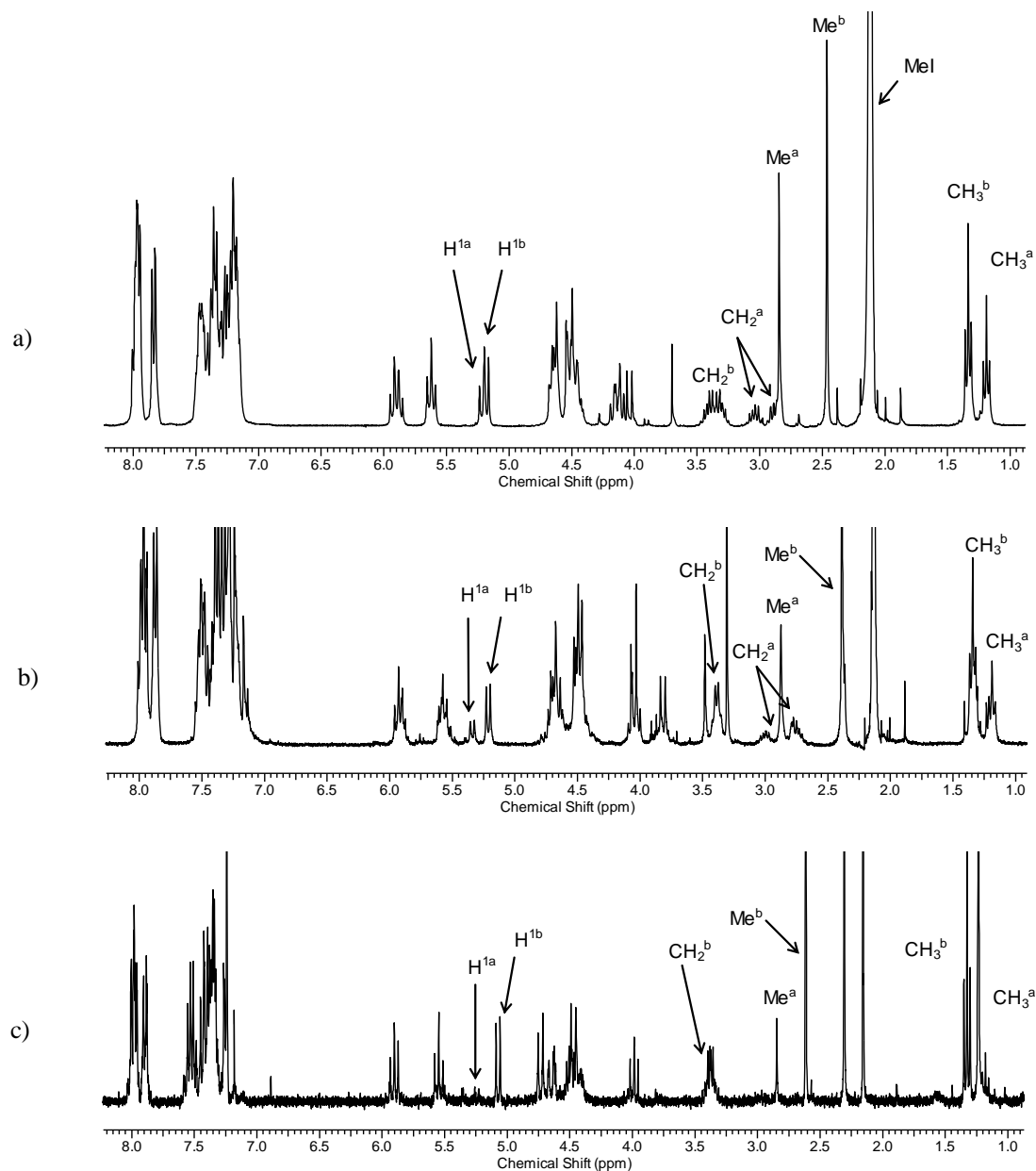


Figure 5.9 Spectra of β -sulfonium salt **5.4c**; (a) 20 min, crude; (b) 1 h, after PLC;
(c) 3 h, after workup followed by PLC

As can be seen, in Figure 5.9a, while both diastereomers are both present in substantial amounts (1:1.6), there is little separation between the two H-1 signals. This reaction was done on a slightly larger scale, wherein salt formation occurred more quickly than normal. Resultantly, there was not a great difference in the chemical shifts of the diastereomeric H-1 signals. In the case of Figure 5.9b, the salt formation was allowed to remain in the reaction vessel for 1 hour, whereupon it was loaded directly on to PLC, and immediately following a ^1H NMR spectra was obtained. Lastly, Figure 5.9c depicts salt **5.4c**, after 3 hours in the reaction vessel, and exposure to both an aqueous workup and PLC. As seen, the amount of diastereomer corresponding to H-1a has decreased significantly.

From the differing characteristics of the β -diastereomers, it can be inferred that one of the diastereotopic lone pairs (Figure 5.10, a and b) on the sulfur atom is more likely to be methylated, and is more stable upon methylation than the other (pathway a vs. b). Looking to explain this, density functional theory (DFT) calculations have been pursued, wherein we hope to find the most likely rotamer of compound **5.4** (Figure 5.10, **5.4^x**, **5.4^y**, **5.4^z**). Preliminary calculations have pinned rotamer **5.4^x** as the likely configuration. This rotamer (**5.4^x**) is also supported experimentally through crystal structure data, and theoretically pointed to by the exo-anomeric effect.²⁰ From these calculations, we then hope to gain some insight into why methylation of the sulfur atom prefers to proceed through one of the diastereotopic lone pair vs. the other (Figure 5.10, pathway a vs. b).

Furthermore, a preferred low energy rotamer is expected for each of the diastereomeric sulfonium ions (**5.4a^a** and **5.4a^b**) along with their predicted H-1 shifts in ¹H NMR. Seeing as we have experimentally determined the more shielded H-1 to be formed more quickly and to be more robust, we expect the theoretical data will reinforce this observation.

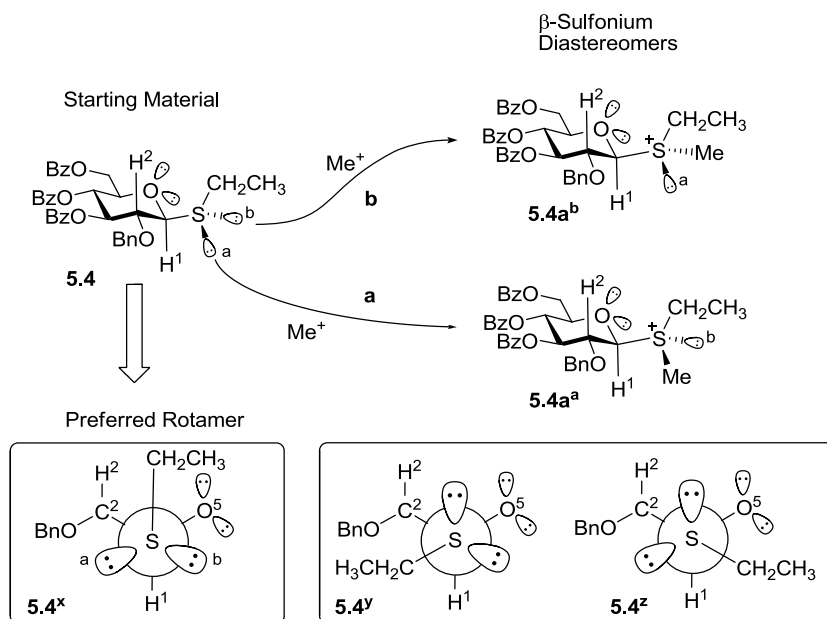


Figure 5.10 Possible preferred rotamers (**5.4^x**, **5.4^y**, **5.4^z**) of glycosyl donor **5.4**, and methylated β -sulfonium diastereomers **5.4a^a** and **5.4a^b**

5.4 Glycosylation Results

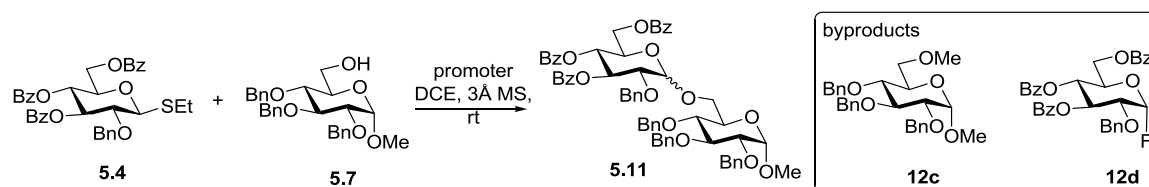
As aforementioned in Section 5.1.1, the interest in these β -sulfonium glycosyl donors, lies in achieving a stereoselective glycosylation. Thus, promoters capable of generating a sulfonium salt (**b-d**, **h**, as well as the purchased MeOTf (**a**), and Me₃OBF₄ (**i**)), were next utilized in glycosylation.

Throughout these investigations, it was found that the α/β -ratios were similar for the both the “preactivation” conditions (donor and promoter mixed first, prior to the addition of the acceptor) and the standard conditions (donor and acceptor mixed first, followed by addition of the promoter). As found previously, sulfonium ion **5.4a** was observed whether or not the acceptor was present (as seen in Table 5.1), indicating that it is a reactive intermediate through which the reaction must proceed. As a consequence, the activation conditions (preactivation vs standard) do not affect the diastereoselectivity of the reaction. Therefore, in order to minimize reaction side-products and maximize disaccharide yield, glycosylations were typically carried out under standard activation conditions (unless otherwise specified).

As seen from Table 5.4, neither the yields nor the stereoselectivity proved to be encouraging. Furthermore, there seemed to be no real correlation between the stability/speed of salt formation and the stereoselectivity with which the glycosylation reaction proceeds. Unlike the previous reaction that was stopped after 4 hours (Table 5.1, Entry 1), this reaction with MeOTf (promoter **a**) was kept until completion (Table 5.5, Entry 1). While the yield improved, the resulting stereoselectivity remained poor. Reactions with promoters **b** and **c**, fared no better. In fact, although these promoters gave rise to the two most stable β -sulfonium salts (**5.4b** and **5.4c**, respectively), they were actually found to perform the worst in glycosylation. A nominal amount of the hexafluorophosphate salt **5.4c** did undergo glycosidation with acceptor **5.7** to give the highest stereoselectivity among the group, however, the disaccharide yield was

inadequate, as the salt remained even after 96 hours (Entry 3). Similarly, glycosylations with the tetrafluoroborate salt **5.4b** were also unsatisfactory, yielding disaccharide **5.11** in only 17% (Entry 2), as the salt slowly reacted to give various byproducts, including **5.12a** and **5.12b**. Furthermore, a competing side-reaction was the methylation of acceptor **5.7**, which began concomitantly with the salt formation. Therefore, upon workup the unreacted glycosyl acceptor (**5.7**) was recovered in 50% yield.

Table 5.4 Glycosidation of thioglycoside donor **5.4** and acceptor **5.7** using various methylating promoters



entry	promoter	time ^a	disaccharide 5.11	$\alpha:\beta$ ratio	identified byproducts
1	a	6 h	77%	2.4 : 1	---
2	b	78 h ^b	10%	2.4 : 1	12c, 12d
3	c	78 h ^b	51%	4.7 : 1	---
4	d	16 h	78%	3.8 : 1	---
5	h	6 h	86 %	2.8 : 1	---
6	i	78 h ^b	8 %	3.5 : 1	12d

^a complete salt disappearance, ^b time at which the incomplete reaction was stopped

Reactions utilizing promoters **d** and **h** proved to be more promising, although stereoselectivity was still poor (Entries 4 and 5). However, this increase in reactivity did

reinforce the idea that the counter-anion was actively participating in the dissociation of the leaving group from the sugar. Hence, it could be the reason for the lack of stereoselectivity seen (discussed in Section 5.6). Finally, promoter **i**, proved too reactive, as the major product was methylation of the acceptor (50% based on acceptor **5.7**) and donor hydrolysis (70% based on donor **5.4**), the expected disaccharide formed in only a meager 15% yield. However, as seen with promoter **b** (same tetrafluoroborate counter-anion), there was still evidence of the salt at the time the reaction was worked up.

Table 5.5 Glycosidation of thioglycoside donor **5.4** with low weight alcohol acceptors under preactivation conditions.



entry	R	equivalents	glycoside	yield	$\alpha:\beta$
1	Me	10	5.13	88%	2.2 : 1
2	iPr	10	5.14	78%	2.6 : 1
3	Cp	10	5.15	87%	2.7 : 1
4 ^a	Me	solvent	5.13	83%	20 : 1
5 ^a	iPr	solvent	5.14	61%	3 : 1
6 ^a	Cp	solvent	5.15	75%	3.7 : 1

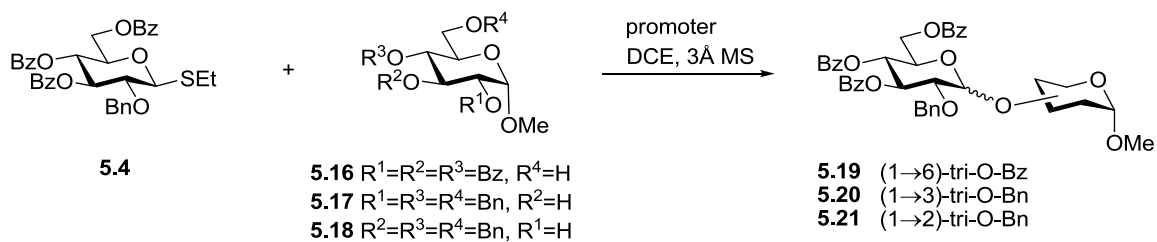
^a salt formation was carried out in 1-2DCE, whereupon the solvent was evaporated and replaced with the selected acceptor/solvent

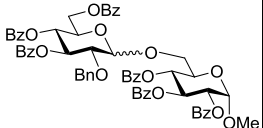
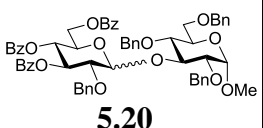
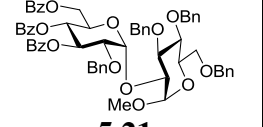
In lieu of these results, we thought it might be practical to start with a smaller, more reactive acceptor, as it should be more likely to proceed via an S_N2 pathway. Thus, methanol (MeOH), isopropanol (iPrOH) and cyclopentanol (CpOH) were chosen as suitable glycosyl acceptors. Subsequent glycosylation reactions were carried out utilizing only the most promising candidate among the generated promoters, MeI/AgClO₄ (**d**). Unfortunately, as seen in Table 5.5 (Entries 1-3), when the alcohol acceptors (10 equiv) were glycosylated with donor **5.4**, the α/β -ratios of the resulting glycosides (**5.13**, **5.14** and **5.15**) showed little anomeric selectivity.

Furthermore, for the reactions in which the alcohol acceptor functioned as both the acceptor and the reaction solvent (Entries 4-6), the α/β -ratio only improved in the case of methanol (Entry 4), wherein near-complete α -selectivity of methyl glycoside **5.13** was obtained. However, it was found that this high stereoselectivity could be achieved regardless of the type of promoter employed. Such a phenomenon has been previously documented, and can be attributed to the increase in acceptor concentration causing an increase in the “rate of trapping” as the leaving group departs.²¹

Table 5.6 shows additional glycosylation reactions using a variety of less reactive sugar acceptors, both primary and secondary (**5.16-5.18**).²²⁻²⁵ Interestingly, we found that among these glycosylations, the stereoselectivities showed more promise. However, when repeated with other classes of promoters (including NIS/Cu(OTf)₂), similar results were achieved. Thus, the stereoselectivity was found to be inherent to the match between the donor and acceptor pair, and not the “stable” sulfonium intermediate.

Table 5.6 Comparative glycosidation of thioglycoside donor **5.4** with various acceptors under varied promoter conditions



entry	promoter	acceptor	temp ^o C	time	disaccharide	yield	$\alpha:\beta$
1	MeOTf	5.16	rt	16 h	 5.19	81%	7.4 : 1
2		5.17	rt	16 h	 5.20	87%	6.2 : 1
3		5.18	rt	16 h	 5.21	90%	α -only
4	MeI / AgClO ₄	5.16	rt	16 h	5.19	75%	14.9 : 1
5		5.17	rt	16 h	5.20	83%	13 : 1
6		5.18	rt	16 h	5.21	67%	α -only
7	NIS/ CuOTf ₂	5.16	0°	0.3 h	5.19	65%	5.5 : 1
8		5.17	0° → rt	1 h	5.20	53%	10 : 1
9		5.18	0° → rt	1 h	5.21	65%	α -only

5.5 Expanding Upon the Methodology

5.5.1 Dimethyl(thiomethyl)sulfonium triflate (DMTST) generated sulfonium ion

In order to further investigate the willingness of donor **5.4** to form a “stable” cationic species, we also searched for other common thioglycoside promoters that could potentially give rise to a β -sulfonium ion. As a result, it was found that when donor **5.4** was preactivated with DMTST (dimethyl(methylthio)sulfonium triflate), it also gave rise to the baseline spot on TLC, indicative of a polar sulfonium species. When attempts were made to isolate this proposed thiomethylated glycosyl donor (**5.4j**, Figure 5.11a), this species was found to be less stable than its methylated analog (**5.4a**). The ^1H NMR of purified compound **5.4j**, contained a significant amount of hemiacetal **5.12a** (see Appendix, Figures A-66 and A-67; compare with ^1H NMR of **5.12a**, Figure 5.3c). Therefore, a crude NMR of **5.4j** was taken, wherein a new H-1 peak could easily be identified (Figure 5.11c) at 6.45 ppm.

Interestingly, unlike the H-1 signal seen in the NMR spectrum of methylated glycosyl donor **5.4a**, the H-1 signal of donor **5.4j** was much more deshielded and displayed a significantly smaller coupling constant ($J_{1,2} = 4.5$ Hz). Upon first glance, it was thought that the thiomethylated leaving group had anomerized into the α -configuration, possibly forming a glycosyl triflate (Figure 5.12). Soon after however, other peculiarities were also noticed, such as the unusually small coupling constants of H-3 ($J_{3,4} = 5.3$ Hz, $J_{2,3} = 5.3$ Hz) and the 0.88 ppm downfield shift of H-2 (For comparison, data from sulfonium ion **5.4a**; H-3 ($J_{3,4} = 9.1$ Hz, $J_{2,3} = 9.4$ Hz), H-2 shifted downfield by 0.31 ppm). This led

us to believe that the pyranose ring was no longer residing in a 4C_1 chair conformation, but may have undergone a conformational change, as the NMR data was more indicative of a half chair conformation (Figure 5.12). Furthermore, the signals from the leaving group were difficult to detect, complicating the elucidation of the proposed salt structure.

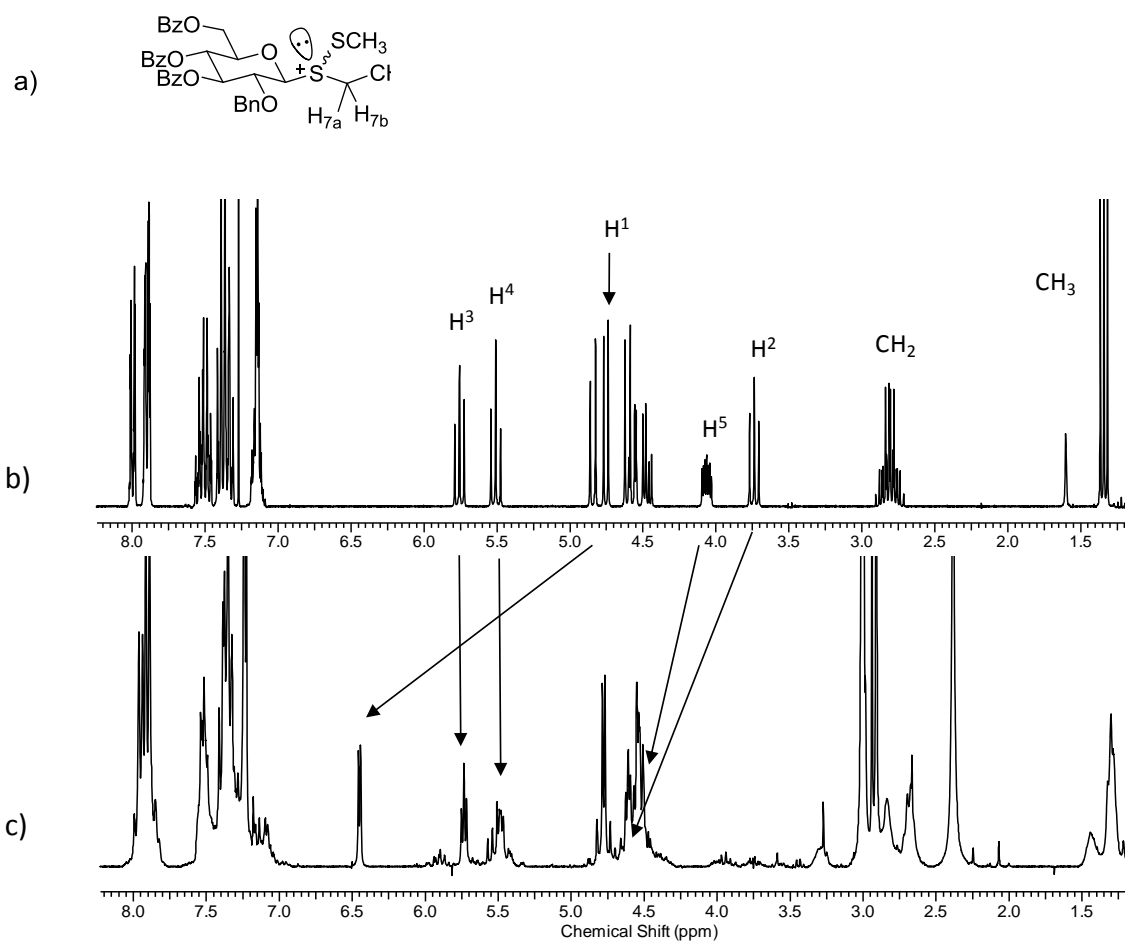


Figure 5.11 (a) proposed thiomethylated β -sulfonium ion **5.4j**, (b) starting material **5.4**, (c) *in situ* NMR of **5.4j**

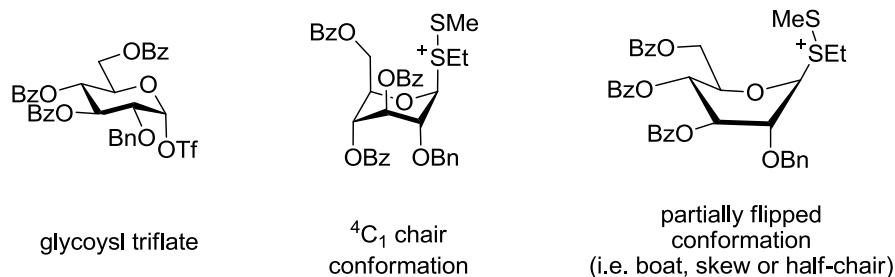


Figure 5.12 Possible structures and conformations of **5.4j**

In an effort to gain further insight into the exact salt structure, we attempted to break the labile disulfide bond of the proposed salt **5.4j**, hoping to recover our initial β -starting material **5.4**. We first attempted to add triphenyl phosphine, however this reagent did not liberate the starting material, but instead reacted to form a more complex salt species. Therefore, we next thought to add a large excess of bulky *p*-toluenethiol (HSTol) hoping that sterics would make the thiomethyl transfer more favorable than glycosylation. However, glycosylation did occur, unexpectedly proceeding with complete stereoselectivity to yield an α -tolyl thioglycoside.

We subsequently turned our attention toward the application of the thiomethyl salt (**5.4j**) in glycosylation, hopeful that completely α -stereochemistry could consistently be achieved. As seen in Table 5.7, results proved to be similar to those seen with the methylating promoters (Table 5.6, Entries 1-8), yielding significant alpha/beta ratios only in the case of the secondary glycosyl acceptors (Entries 5 and 6). Interestingly, in the case of methanol as both an acceptor and solvent (Entry 2), the β -methyl glycoside began forming almost exclusively, unlike the previous MeI/AgClO₄ promoted glycosylation wherein near complete α -selectivity was achieved (Table 5.5, Entry 4). It was only as the

reaction progressed, that the α -methyl glycoside (**5.13**) began to form in any substantial amount, and upon reaction completion the final α : β ratio was 1:3.6. Although the structure of **5.4j** is not yet verified, this result may imply that the starting anomeric configuration is in fact α , as a β inversion product would be expected; and not just a skewed ring conformation, which would be more likely to yield the α -glycoside.

Table 5.7 DMTST-promoted glycosylations



entry	acceptor	equiv	time	product	yield	α : β ratio
1	MeOH	3	3 h	5.13	84 %	1.9 : 1
2 ^{a,b}	MeOH	solvent	3 h	5.13	98%	1 : 3.6
3	5.7	1	3.5 h	5.11	98%	1.1 : 1
4	5.16	1	3.5 h	5.19	98%	3.0 : 1
5	5.17	1	3.5 h	5.20	76%	4.8 : 1
6	5.18	1	10 h	5.21	75%	25 : 1

^a reaction was run under preactivation conditions, ^b methanol was used as both the glycosyl acceptor and the reaction solvent

5.5.2 Investigation of superdisarmed α -S-ethyl glycosyl donor

As a result of our findings with β -SEt donor **5.4**, we also decided to synthesize its α -epimer (**5.22**, Figure 5.13) in order to compare the resultant glycosylation data. Immediately, it became apparent that the reactivity of this analog was much greater than

previously seen with the β -glycosyl donor **5.4**. Accordingly, only small amounts of the α -sulfonium salt were detected upon TLC analysis, and only when utilizing the *in situ* generated promoters **b** and **c**. What's more, there was absolutely no observable salt when using the MeOTf reagent that had initially revealed the existence of the β -sulfonium salt **5.4a**.

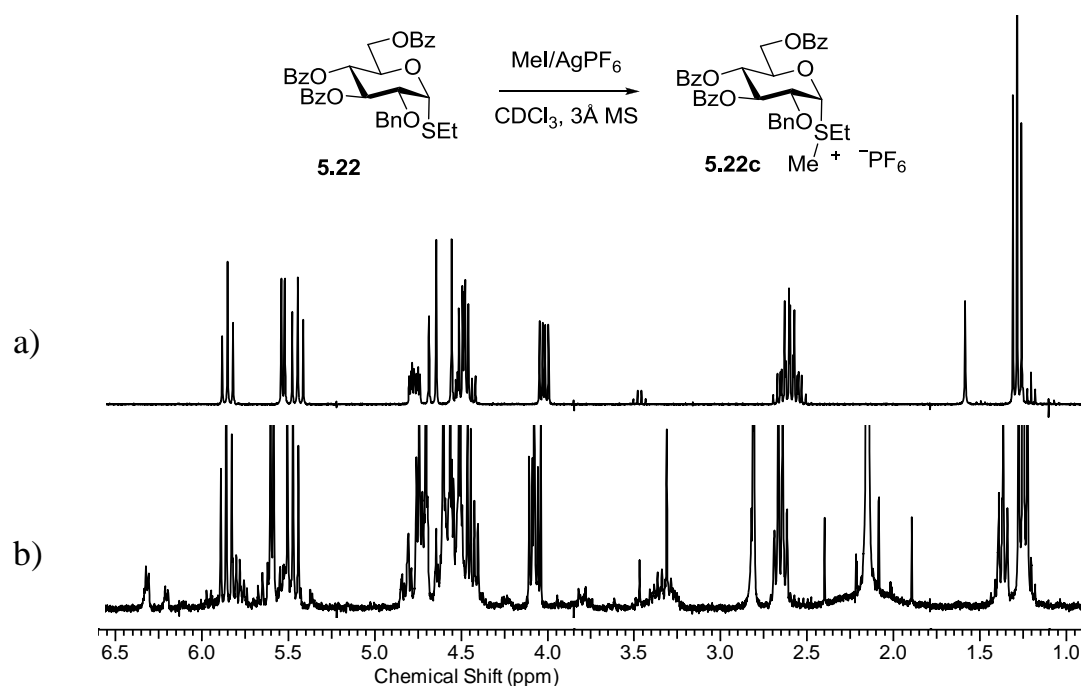


Figure 5.13 α -SEt **5.22** and sulfonium salt **5.22c** (a) ¹H NMR of α -SEt starting material **5.22** (b) ¹H NMR of diastereomeric salt formation **5.22c**

Spectral data reinforced these findings. Thus, while the crude ¹H NMR spectra of the reaction between promoter **b** and **5.22** did hint at the presence of two new α -anomeric signals at around 6.21 and 6.31 ppm, there was little else that seemed to indicate that a new “stable” sulfonium species was present (Figure 5.13). Accordingly, the spectrum was comprised of mostly starting material and/or other unwanted byproducts. Reinforcing

these findings are the similar results found by both Yoshida and Boons, wherein β -sulfonium species were found to be more stable than their α -counterparts.^{4,5}

Table 5.8 α -SEt glycosylations



entry	acceptor	time	product	yield	α : β ratio
1	5.7	0.5 h	5.11	75%	2.4 : 1
2	5.16	0.5 h	5.19	92%	5.9 : 1
3	5.18	0.5 h	5.21	82%	α -only
4 ^a	MeOH	16 h	 5.13	60%	1 : 17.5

^a methanol was used as both the glycosyl acceptor and the reaction solvent

Upon glycosidation of α -sulfonium salt **5.22** with various glycosyl acceptors, the α / β -ratios of the resulting glycosides were found to be no more or less selective than those of the β -sulfonium salts (Table 5.8). The near identical stereoselectivities resulting from the α - and β -glycosyl donors (**5.22** and **5.4**, respectively), only serves to reinforce the S_N1 mechanism by which their intermediate sulfonium salts react. Again, in the case of methanol as an acceptor and solvent, inversion of stereochemistry occurred, to yield predominately the β -methyl glycoside **5.13** (Entry 4).

5.6 Rationalization

Overall, the results of this investigation suggest that while the discovered β -sulfonium glycosyl donor should be easily displaced by an incoming nucleophile, it still prefers to react via the typical S_N1 glycosylation mechanism. Not only did the glycosylations proceed with poor α -selectivity, but the similarities in stereoselectivity between the epimeric α and β -SEt donors implies that nucleophilic attack is occurring indiscriminately upon a flattened, sp^2 hybridized anomeric carbon, and not through the pentacoordinate geometry necessitated by an S_N2 transition state (Figure 5.14).

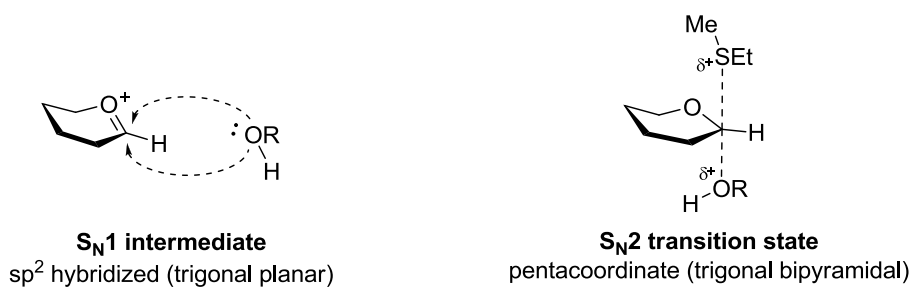
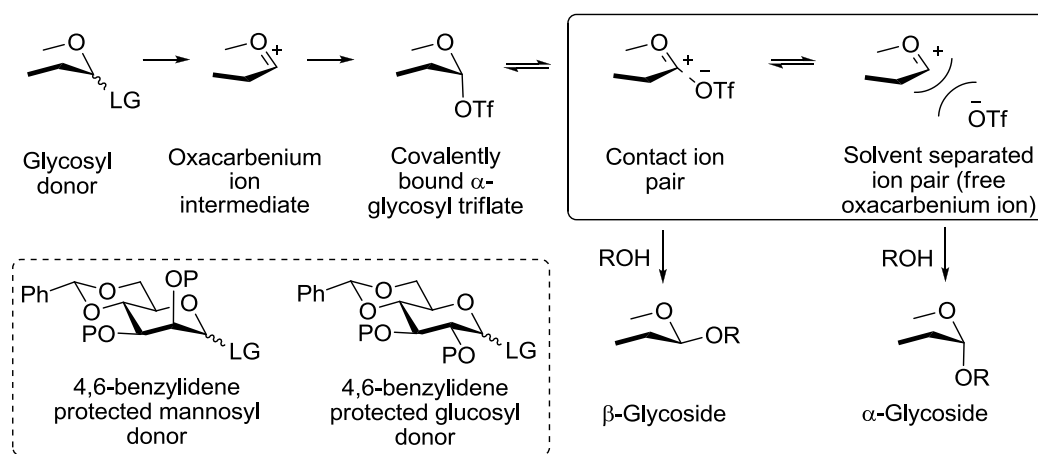


Figure 5.14 Geometry of S_N1 intermediate vs. S_N2 transition state

Unable to achieve the desired stereoselectivity outcome, we turned to the literature in attempt to help us explain this result. As touched upon previously in Chapter 2.3, there is accumulating evidence that implies that an actual S_N2 reaction is not possible at the anomeric center. Such claims have been based upon the electron–electron repulsions that are encountered upon nucleophile approach²⁶ and the weakness of the nucleophiles typically employed as glycosyl acceptors.

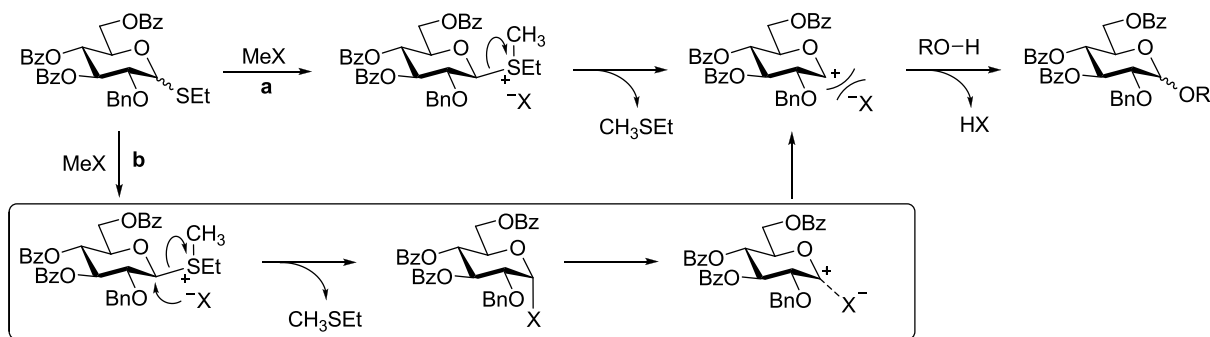
To this end, several groups have also encountered similar unexpected anomeric selectivities when dealing with glycosyl intermediates.^{5, 27-32} Of particular interest to the findings herein, are the studies undertaken by Crich *et al*, who they investigated the mechanistic pathway followed upon the reaction of intermediate α -glycosyl triflates with glycosyl acceptors (discussed in Section 2.3.1).^{31, 32}



Scheme 5.5 Continuum of ionic species upon dissociation of anomeric triflate

It was discovered that the stereochemical outcome of these reactions was based upon the core donor structure (glucose vs. mannose), and not the configuration of the initial glycosyl donor, nor the α -configuration adopted by the triflate (OTf) intermediate. Thus, while rigid, 4,6-benzylidene protected mannosyl donors gave complete β -stereoselectivity, 4,6-benzylidene protected glucosyl donors yielded quite the opposite, giving predominately α -selectivity. Kinetic studies revealed, that even in the cases of complete inversion of configuration (mannosyl donors), the reactions were still proceeding via an S_N1 mechanism.⁷ Product stereoselectivity was found, instead, to result

from the attack of the glycosyl acceptor upon a particular “dissociation species,” which is found to be favored based upon the glycosyl donor structure (Scheme 5.5).



Scheme 5.6 Possible reaction pathways of β -sulfonium salt dissociation

If this rationale is applied to any of our β -sulfonium donors (**5.4a-d, h-j**), this would result in a mechanistic pathway in which the leaving group would first depart as a neutral species, leaving the glycosyl cation and counter-anion to exist as an ion pair (Scheme 5.6, pathway a). At this point, nucleophilic attack could occur upon the solvent separated ion pair (preferred in glycosyl donors lacking the 4,6-benzylidene rigidity), hampering any prospect of stereoselectivity. Furthermore, this type of mechanism would also explain why the various β -sulfonium salts displayed different stabilities. If the reaction must first dissociate into an ion pair, then the perchlorate and triflate counter-anions would be more reactive, as the oxygen atom could displace the leaving group from the anomeric center (pathway b); the fluoride atoms of the hexafluorophosphate and tetrafluoroborate anions do not have that ability. This inability to participate in stabilizing the freed oxocarbenium ion, may also explain the fluoride transfer byproduct obtained in the case of the tetrafluoroborate counter-anion (cf. Table 5.4)

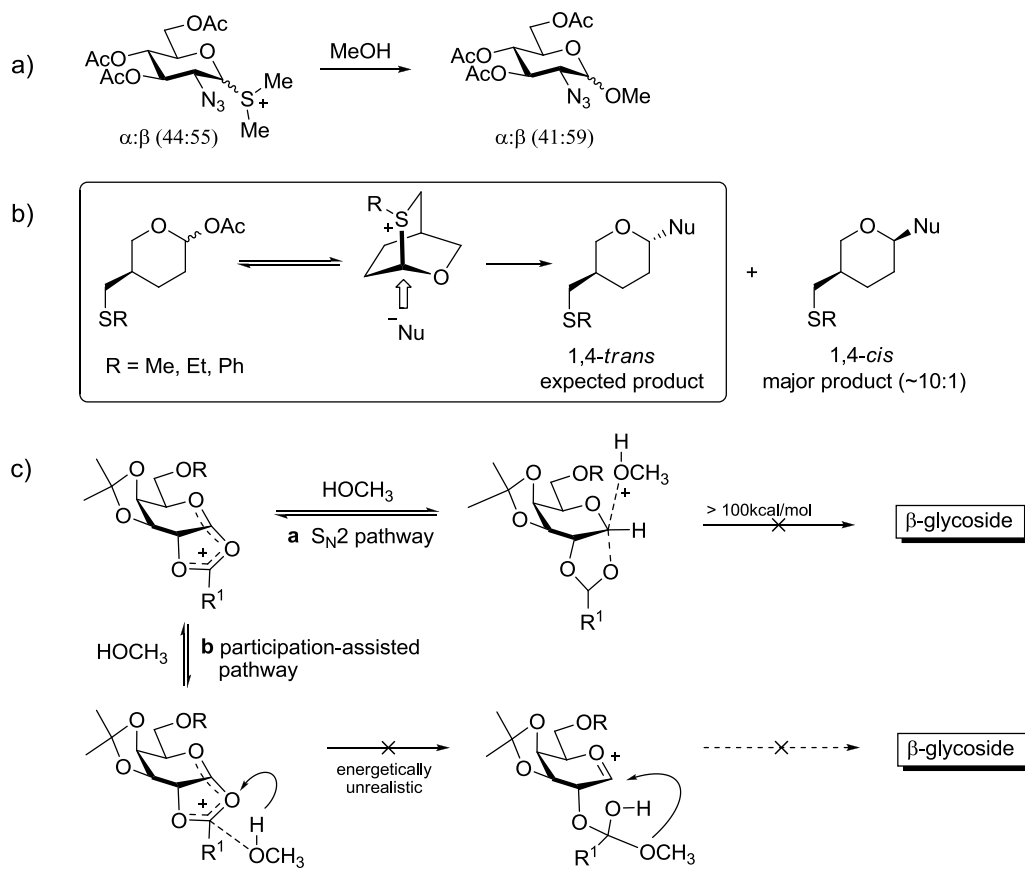


Figure 5.15 Examples of reactions not occurring through their expected inversion pathways, (a) anomeric dimethyl sulfonium species, Yoshida *et al.*, (b) intramolecular glycosyl sulfonium species, Woerpel *et al.*, (c) possible reaction pathways of acyloxonium ion intermediates, Whitfield *et al.*

Additional studies by Whitfield,^{27, 28} Woerpel,^{29, 30} and Yoshida⁵ all further support the findings herein (previously discussed in Section 2.3.2). For instance, Yoshida *et al.* have reported a similar anomeric dimethyl sulfonium species to exist at low temperatures in a 2-azido-2-deoxy glycosyl donor. Furthermore, it was found to exist as a mixture of both the α - and β -sulfonium ion. Nonetheless, subsequent glycosylation reactions failed to yield the stereoselectivity expected had both the α - and β -sulfonium species undergone

S_N2 inversion (Scheme 5.15a). Likewise, Woerpel *et al.*^{29, 30} also found an intramolecular glycosyl sulfonium species to exist (through both NMR and theoretical calculation) as the lowest energy intermediate in glycosylation (Scheme 5.15b). However, while this intermediate species should yield an inverted 1,4-*trans* product, this was not the case. In fact, the stereoselectivity was quite the opposite. Therefore, here again is another case wherein the glycosylation mechanism displays a preference for the open cation (S_N1) pathway over the concerted (S_N2) displacement. In a similar vein, Whitfield *et al.*^{27, 28} have repeatedly been unable to find low energy, concerted, pathways connecting acyloxonium ion intermediates with their resulting β -glycoside products (Figure 5.15c). This implies that an alternative mechanism (other than that of the presumed concerted nucleophilic attack on the anomeric center), may be behind the selectivity that results from intramolecular participation.

In conjunction with the results obtained from studying β -sulfonium salts, these findings strongly suggest that caution should be applied when justifying the product formation. As restated from Chapter 2, “Although it is common practice to base reaction outcomes on calculated low-energy intermediates, it does not necessarily mean that these species are involved in the pathway of product formation, an idea reinforced by the Curtin–Hammett kinetic scenario,³³ which states that product formation does not necessarily have to occur *via* the lowest energy intermediates.”

5.7 Experimental

General remarks. Column chromatography was performed on silica gel 60 (EM Science, 70-230 mesh), reactions were monitored by TLC on Kieselgel 60 F₂₅₄ (EM Science). Preparative layer chromatography was performed on PLC silica gel 60 glass plates, Kieselgel 60 F₂₅₄, 1 mm (Merck). The compounds were detected by examination under UV light and by charring with 10% sulfuric acid in methanol. Solvents were removed under reduced pressure at < 40 °C. CH₂Cl₂ and ClCH₂CH₂Cl were distilled from CaH₂ directly prior to application. Pyridine was dried by refluxing with CaH₂ and then distilled and stored over molecular sieves (3 Å). Molecular sieves (3 Å or 4 Å), used for reactions, were crushed and activated *in vacuo* at 390 °C during 8 h in the first instance and then for 2-3 h at 390 °C directly prior to application. AgOTf (Acros) was co-evaporated with toluene (3 x 10 mL) and dried *in vacuo* for 2-3 h directly prior to application. DMTST was prepared in accordance to previously reported methods.³⁴ Optical rotations were measured at 'Jasco P-1020' polarimeter. ¹H-n.m.r. spectra were recorded in CDCl₃ at 300 MHz, ¹³C-NMR spectra were recorded in CDCl₃ at 75 MHz (Bruker Avance) unless otherwise noted. HR FAB-MS determinations were made with the use of JEOL MStation (JMS-700) Mass Spectrometer, matrix *m*-nitrobenzyl alcohol, with NaI as necessary.

Synthesis of Glycosyl Donors 5.4 and 5.22 and precursor 5.6

Ethyl 2-O-benzyl-4,6-O-benzylidene-1-thio-β-D-glucopyranoside (5.6). Similar to a previously reported synthesis,³⁵ a stirred solution of **5.5**³⁶ (1.00 g, 3.21 mmol) in CH₂Cl₂ (100 mL), was added sequentially tetrabutylammonium hydrogen sulfate (0.54 g, 1.60

mmol, benzyl bromide (0.42 mL, 3.53 mmol), and 5% aq. NaOH (8.33mL). The reaction mixture was heated to 45 °C and allowed to reflux for 16 h, whereupon the reaction was brought to room temperature. The organic and aqueous phases were then separated and the aqueous phase was extracted with CH₂Cl₂ (2 x 5 mL). The organic fractions were then combined and washed with saturated aq. NaHCO₃ (20 mL), brine (20 mL), dried over MgSO₄, and concentrated *in vacuo*. The residue was purified by column chromatography on silica gel (ethyl acetate – toluene gradient elution) to afford compound **5.6** as the major regioisomer in 59% yield. Analytical data for **5.6** is the same as previously reported³⁵

Ethyl 2-O-benzyl-3,4,6-tri-O-benzoyl-1-thio-β-D-glucopyranoside (5.4). To compound **5.6** (1.57 g, 3.91 mmol) stirring in wet CH₂Cl₂ (25 mL) was added dropwise a solution of trifluoroacetic acid in CH₂Cl₂, (5 mL; 1/20, v/v). Upon reaction completion (2h), the reaction was neutralized with triethylamine, and concentrated *in vacuo*. The residue was purified by column chromatography on silica gel (methanol – dichloromethane gradient elution) to afford ethyl 2-O-benzyl-1-thio-β-D-glucopyranoside in 98% yield. Ethyl 2-O-benzyl-1-thio-β-D-glucopyranoside (1.53g, 4.88 mmol) was dissolved in anhydrous pyridine (25 mL) under argon at 0°C, whereupon benzoyl chloride (2.55 mL, 21.93 mmol) was added dropwise. After 15 min, the reaction mixture was brought to room temperature, and allowed to stir for 16h. The reaction was then cooled to 0 °C, quenched with dry MeOH (0.5 mL), and concentrated *in vacuo*. The residue was then diluted with CH₂Cl₂ (50 mL) and washed successively with H₂O (10 mL), saturated aq. NaHCO₃ (2 x 10 mL), H₂O (10 mL), dried over MgSO₄, and

concentrated *in vacuo*. The residue was purified by column chromatography on silica gel (ethyl acetate – hexane gradient elution) to afford compound **5.4** as colorless crystals in quantitative yield. Analytical data for **5.4**: $R_f = 0.55$ (ethyl acetate-toluene, 1/9, v/v); $[\alpha]_D^{23.9} = -19.81^\circ$ ($c = 1$, CHCl_3); m.p. +124-126 °C (hexanes – diethyl ether); ^1H NMR (CDCl_3): δ , 1.31 (t, 3H, SCH_2CH_3), 2.75-2.81 (m, 2H, SCH_2CH_3), 3.70 (dd, 1H, $J_{2,3} = 9.3$ Hz, H-2), 4.00-4.07 (m, 1H, H-5), 4.40-4.47 (dd, 1H, $J = 6.0$ Hz, $J = 12.1$ Hz, H-6a), 4.51-4.59 (m, 2H, H-6b, $J = 10.9$ Hz, phCH_2^a), 4.72 (d, 1H, $J_{1,2} = 9.7$ Hz, H-1), 4.81 (d, 1H, $J = 10.8$ Hz, phCH_2^b), 5.47 (dd, 1H, $J_{4,5} = 9.8$ Hz, H-4) 5.72 (dd, 1H, $J_{3,4} = 9.4$ Hz, H-3), 7.06-7.15 (m, 5H, aromatic), 7.28-7.38 (m, 6H, aromatic), 7.43-7.54 (m, 3H, aromatic), 7.85-7.89 (m, 4H, aromatic), 7.94-7.98 (m, 2H, aromatic) ppm; ^{13}C NMR (CDCl_3): δ , 15.3, 25.5, 63.9, 70.1, 75.3, 75.9, 76.1, 79.3, 85.5, 128.0, 128.4, 128.5, 128.5, 128.6, 129.0, 129.6, 129.9, 129.9, 130.0, 133.2, 133.3, 133.5, 137.3, 165.6, 165.8, 166.3 ppm. (See Appendix, Figure A-46, A-47, A-48)

Ethyl 2-O-benzyl-3,4,6-tri-O-benzoyl-1-thio- α -D-glucopyranoside (5.22) was obtained as colorless crystals from ethyl 4,6-O-benzylidene-1-thio- α -D-glucopyranoside,³⁷ as described for the synthesis of **5.4**. Analytical data for **5.22**: $R_f = 0.59$ (ethyl acetate-toluene, 1/9, v/v); m.p. +110-113 °C (hexanes – diethyl ether); ^1H NMR (CDCl_3): δ , 1.27 (t, 3H, SCH_2CH_3), 2.54-2.64 (m, 2H, SCH_2CH_3), 4.02 (dd, 1H, $J_{2,3} = 9.8$ Hz, H-2), 4.41-4.55 (m, 3H, H-6a, H-6b, phCH_2^a), 4.66 (d, 1H, $J = 12.5$ Hz, phCH_2^b), 4.73-4.80 (m, 1H, H-5), 5.44 (dd, 1H, $J_{4,5} = 10.0$ Hz, H-4), 5.53 (d, 1H, $J_{1,2} = 5.6$ Hz, H-1), 5.85 (dd, 1H, $J = 9.6$ Hz, H-3) 7.13-7.25 (m, 5H, aromatic), 7.29-7.41 (m, 6H, aromatic), 7.42-7.57 (m, 3H, aromatic), 7.89-7.92 (m, 4H, aromatic), 7.98-8.00 (m,

2H, aromatic) ppm; ^{13}C NMR (CDCl_3): δ , 14.7, 23.8, 63.4, 68.2, 70.0, 72, 2, 72.6, 76.3, 82.9, 128.1, 128.1, 128.4, 128.5, 128.5, 129.1, 129.7, 129.8, 129.9, 130.1, 133.2, 133.2, 133.5, 137.3, 165.6, 165.7, 166.3 ppm. (See Appendix, Figure A-68, A-69, A-70)

General Glycosylation Procedures

Method A: Typical MeOTf-promoted glycosylation procedure: A mixture containing the glycosyl donor (0.048 mmol), glycosyl acceptor (0.044 mmol), and freshly activated molecular sieves (3Å, 105 mg) in DCE (0.5 mL) was stirred under argon for 1 h. MeOTf (0.131 mmol) was added and the reaction mixture was stirred for time specified in paper (Tables 5.1, 5.4, and 5.6). The mixture was then diluted with CH_2Cl_2 , the solid was filtered-off and the combined filtrate (15 mL) was washed with sat. NaHCO_3 (5 mL) and H_2O (5 mL). The organic phase was separated, dried and concentrated *in vacuo*. The residue was purified by column chromatography on silica gel (ethyl acetate-toluene gradient elution).

Method B: Typical NIS/Cu(OTf) $_2$ -promoted glycosylation procedure: A mixture containing the glycosyl donor (0.048 mmol), glycosyl acceptor (0.044 mmol), and freshly activated molecular sieves (3Å, 105 mg) in DCE (0.5 mL) was stirred under argon for 1 h. The reaction mixture was cooled to 0°C, whereupon NIS (0.096 mmol) and $\text{Cu}(\text{OTf})_2$ (0.005 mmol) were added, and the reaction was allowed to slowly warm to rt, or until time of reaction completion (Table 5.6). Upon completion, the mixture was diluted with CH_2Cl_2 , the solid was filtered-off and the residue was rinsed successively with CH_2Cl_2 . The combined filtrate (15 mL) was washed with 10% $\text{Na}_2\text{S}_2\text{O}_3$ (5 mL) and water (5 mL).

The organic phase was separated, dried and concentrated *in vacuo*. The residue was purified by column chromatography on silica gel (ethyl acetate-toluene gradient elution).

Method C: Typical DMTST-promoted glycosylation procedure: A mixture containing the glycosyl donor (0.048 mmol), glycosyl acceptor (0.044 mmol), and freshly activated molecular sieves (3Å, 150 mg) in 1,2-dichloroethane (DCE, 0.5 mL) was stirred under argon for 1 h. DMTST³⁴ (0.088 mmol) was then added, and the reaction mixture was stirred for 3– 10 h (see Table 5.7). Upon completion, the mixture was diluted with CH₂Cl₂, the solid was filtered-off and rinsed successively with CH₂Cl₂. The combined filtrate (15 mL) was washed with sat. NaHCO₃ (5 mL) and water (5 mL). The organic phase was separated, dried and concentrated *in vacuo*. The residue was purified by column chromatography on silica gel (ethyl acetate-hexane gradient elution).

Method D: Typical MeI/AgX-promoted glycosylation procedure: A mixture containing the glycosyl donor (0.048 mmol), glycosyl acceptor (0.044 mmol), and freshly activated molecular sieves (3Å, 105 mg) in DCE (0.5 mL) was stirred under argon for 1 h. MeI (0.392 mmol) was added and the reaction mixture was stirred for an additional 30 min, at which point the specified silver salt was added (0.131 mmol). The reaction mixture was allowed to stir for 6-78 h (see Tables 5.4-5.6 and 5.8). The mixture was then diluted with CH₂Cl₂, the solid was filtered-off and the combined filtrate (15 mL) was washed with sat. NaHCO₃ (5 mL) and H₂O (5 mL). The organic phase was separated, dried and concentrated *in vacuo*. The residue was purified by column chromatography on silica gel (ethyl acetate-toluene gradient elution).

Method E: Preactivation conditions for low weight alcohols as solvent and acceptor: A mixture containing the glycosyl donor (0.048 mmol), and freshly activated molecular sieves (3Å, 105 mg) in DCE (0.5 mL) was stirred under argon for 1 h. Specified promoter (either MeOTf, 0.144 mmol; or MeI/AgClO₄, 0.431/0.144 mmol) was added and the reaction mixture was monitored for donor disappearance. The reaction mixture was then concentrated *in vacuo*, whereupon the chosen acceptor/reaction solvent was added (0.5 mL) and the reaction mixture was stirred for 3-16 h (see Table 5.5 and 5.7). The mixture was then diluted with CH₂Cl₂, the solid was filtered-off and the combined filtrate (15 mL) was washed with sat. NaHCO₃ (5 mL) and water (5 mL). The organic phase was separated, dried and concentrated *in vacuo*. The residue was purified by column chromatography on silica gel (ethyl acetate-toluene gradient elution).

Methyl 6-O-(2,3,4,6-tetra-O-benzyl- α/β -D-glucopyranosyl)-2,3,4-tri-O-benzyl- α -D-glucopyranoside (5.8) was obtained by *method A* from **5.1** and **5.7** as a clear foam in 80% yield. Analytical data for **5.8** is the same as reported previously.³⁸

Methyl 6-O-(2,3,4,6-tetra-O-benzoyl- β -D-glucopyranosyl)-2,3,4-tri-O-benzyl- α -D-glucopyranoside (5.9) was obtained by *method A* from **5.2** and **5.7** as a clear foam in 84% yield. Analytical data for **5.9** is the same as reported previously.³⁹

Methyl 6-O-(2-O-benzoyl-3,4,6-tri-O-benzyl- β -D-glucopyranosyl)-2,3,4-tri-O-benzyl- α -D-glucopyranoside (5.10) was obtained by *method A* from **5.3** and **5.7** as a clear film in 80% yield. Analytical data for **5.10** is the same as reported previously.³⁸

Methyl 2,3,4-tri-O-benzyl-6-O-(2-O-benzyl-3,4,6-tri-O-benzoyl- α/β -D-glucopyranosyl)- α -D-glucopyranoside (5.11) was obtained by *methods A and B and D*, using glycosyl donor **5.4** or **5.22** and glycosyl acceptor **5.7**, in a variety of yields, ranging from 8-98% (See Tables 1,4,7 and 8). Selected analytical data for α -**5.11**: ^1H NMR (CDCl_3): δ , 3.43 (s, 3H, OCH_3), 5.06 (d, 1H, $J_{1,2} = 3.5$ Hz, H-1'), 5.41 (dd, 1H, $J_{4,5} = 9.7$ Hz, H-4'), 5.94 (dd, 1H, $J_{3,4} = 9.7$ Hz, H-3') ppm; ^{13}C NMR (CDCl_3): δ , 55.4 (OCH_3), 63.4, 66.3, 67.9, 70.0, 70.6, 72.0, 72.3, 73.5, 75.2, 75.9, 78.0, 80.0, 82.3, 96.8 (C-1'), 98.1 (C-1), 127.7, 127.9, 127.9, 128.0, 128.1, 128.5, 128.6, 128.6, 129.2, 129.9, 130.0, 130.0, 133.2, 133.2, 133.5, 137.8, 138.3, 138.6, 139.0, 165.7, 165.9, 166.3 ppm. Selected analytical data for β -**5.11**: ^1H NMR (CDCl_3): δ , 3.34 (s, 3H, OCH_3), 5.47 (dd, 1H, H-4'), 5.66 (dd, 1H, $J_{3,4} = 9.4$ Hz, H-3') ppm.

Methyl 2-O-benzyl-3,4,6-tri-O-benzoyl- α/β -D-glucopyranoside (5.13) was obtained by *methods D and E*, from glycosyl donor **5.4** or **5.22** and methanol as a clear film in 60 to 98% yield. Analytical data for α -**5.13**: ^1H NMR (CDCl_3): δ , 3.46 (s, 3H, OCH_3), 3.76 (dd, 1H, $J_{2,3} = 9.9$ Hz, H-2), 4.27-4.33 (m, 1H, H-5), 4.37-4.43 (dd, 1H, H-6a), 4.48-4.53 (dd, 1H, H-6b), 4.55-4.65 (m, 2H, phCH_2), 4.79 (d, 1H, $J_{1,2} = 3.5$ Hz, H-1), 5.45 (dd, 1H, $J_{4,5} = 9.8$ Hz, H-4), 5.96 (dd, 1H, $J_{3,4} = 9.8$ Hz, H-3), 7.20-7.52 (m, 14 H, aromatic), 7.87-8.00 (m, 6H, aromatic) ppm; Analytical data for β -**5.13**: ^1H NMR (CDCl_3): δ , 3.58-3.64 (m, 2H, H-2, OCH_3), 3.98-4.04 (m, 1H, H-5), 4.41-4.47 (dd, 1H, H-6a), 4.54-4.64 (m, 3H, H-6b, H-1, phCH_2^a), 4.80 (d, 1H, $J = 11.8$ Hz, phCH_2^b), 5.46 (dd, 1H, $J_{4,5} = 9.8$ Hz, H-4), 5.67 (dd, 1H, $J_{3,4} = 9.6$ Hz, H-3), 7.03-7.54 (m, 14 H, aromatic), 7.83-8.00 (m, 6H, aromatic) ppm.

Isopropyl 2-O-benzyl-3,4,6-tri-O-benzoyl- α/β -D-glucopyranoside (5.14) was obtained by *methods D and E*, from glycosyl donor **5.4** and isopropanol as a clear film in 61 to 78% yield. Selected analytical data for α -**5.14**: $^1\text{H NMR}$ (CDCl_3): δ , 1.22 (d, 6H, $\text{OCH}(\text{CH}_3)_2$), 3.74 (dd, 1H, $J_{2,3} = 9.4$ Hz, H-2), 3.87-3.96 (m, 1H, $\text{OCH}(\text{CH}_3)_2$), 5.00 (d, 1H, $J_{1,2} = 3.7$ Hz, H-1), 5.44 (dd, 1H, $J_{4,5} = 9.5$ Hz, H-4), 5.95 (dd, 1H, $J_{3,4} = 9.8$ Hz, H-3) ppm; Selected analytical data for β -**5.14**: $^1\text{H NMR}$ (CDCl_3): δ , 3.61 (dd, 1H, $J_{2,3} = 9.6$ Hz, H-2), 3.96-4.06 (m, 1H, $\text{OCH}(\text{CH}_3)_2$), 4.73 (d, 1H, $J_{1,2} = 7.7$ Hz, H-1), 5.66 (dd, 1H, $J_{3,4} = 9.6$ Hz, H-3) ppm.

Cyclopentyl 2-O-benzyl-3,4,6-tri-O-benzoyl- α/β -D-glucopyranoside (5.15) was obtained by *methods D and E*, from glycosyl donor **5.4** and cyclopentanol as a clear film in 80 to 87% yield. Selected analytical data for α -**5.15**: $^1\text{H NMR}$ (CDCl_3): δ , 3.71 (dd, 1H, $J_{2,3} = 10.0$ Hz, H-2), 4.96 (d, 1H, $J_{1,2} = 3.6$ Hz, H-1), 5.44 (dd, 1H, $J_{4,5} = 9.7$ Hz, H-4), 5.93 (dd, 1H, $J_{3,4} = 9.8$ Hz, H-3) ppm; Selected analytical data for β -**5.15**: $^1\text{H NMR}$ (CDCl_3): δ , 3.60 (dd, 1H, $J_{2,3} = 9.5$ Hz, H-2), 3.97-4.03 (m, 1H, H-5), 4.70 (d, 1H, H-1, $J_{1,2} = 7.7$ Hz), 5.44 (dd, 1H, $J_{4,5} = 9.7$ Hz, H-4), 5.66 (dd, 1H, $J_{3,4} = 9.6$ Hz, H-3) ppm.

Methyl 6-O-(2-O-benzyl-3,4,6-tri-O-benzoyl- α/β -D-glucopyranosyl)-2,3,4-tri-O-benzoyl- α -D-glucopyranoside (5.19) was obtained by *methods A, B, C or D*, using glycosyl donor **5.4** or **5.22** and glycosyl acceptor **5.16**, and was obtained in a variety of yields, ranging from 65-98%. Selected analytical data for α -**5.19**: $^1\text{H NMR}$ (CDCl_3): δ , 3.63 (s, 3H, OCH_3), 3.79 (dd, 1H, $J_{2,3} = 10.0$ Hz, H-2'), 4.88 (d, 1H, $J_{1,2} = 3.4$ Hz, H-1'), 6.02 (dd, 1H, $J_{3,4} = 9.7$ Hz, H-3'), 6.15 (dd, 1H, $J_{3,4} = 9.8$ Hz, H-3) ppm; Selected

analytical data for β -**5.19**: ^1H NMR (CDCl_3): δ , 3.45 (s, 3H, OCH_3), 4.81 (d, 1H, $J_{1,2} = 7.5$ Hz, H-1'), 5.69 (dd, 1H, $J_{3,4} = 9.6$ Hz, H-3') ppm.

Methyl 3-0-(2-O-benzyl-3,4,6-tri-O-benzoyl- α/β -D-glucopyranosyl)-2,4,6-tri-O-benzyl- α -D-glucopyranoside (5.20) was obtained by *methods A, B, C or D*, using glycosyl donor **5.4** and glycosyl acceptor **5.17**, and was obtained in a variety of yields, ranging from 53-87%. Selected analytical data for α -**5.20**: ^1H NMR (CDCl_3): δ , 3.34 (s, 3H, OCH_3), 4.01 (dd, 1H, $J_{2,3} = 12.3$ Hz, H-2'), 5.45 (dd, 1H, $J_{4,5} = 9.8$ Hz, H-4'), 5.71 (d, 1H, $J_{1,2} = 3.5$ Hz, H-1'), 6.10 (dd, 1H, $J_{3,4} = 9.8$ Hz, H-3') ppm; Selected analytical data for β -**5.20**: ^1H NMR (CDCl_3): δ , 3.30 (s, 3H, OCH_3), 5.36 (d, 1H, $J_{1,2} = 7.9$ Hz, H-1') ppm.

Methyl 2-0-(2-O-benzyl-3,4,6-tri-O-benzoyl- α/β -D-glucopyranosyl)-3,4,6-tri-O-benzyl- α/β -D-glucopyranoside (5.21) was obtained by *methods A, B, C or D*, using glycosyl donor **5.4** or **5.22** and glycosyl acceptor **5.18**, and was obtained in a variety of yields, ranging from 65-90% (stereoselectivities ranging from 25:1 to α -only). Analytical data for α -**5.21**: ^1H NMR (CDCl_3): δ , 3.44 (s, 3H, OCH_3), 3.61-3.82 (m, 5H, H-2', H-5, H-6a, H-6b, H-4), 3.95 (dd, 1H, $J_{2,3} = 9.9$ Hz, H-2), 4.05-4.17 (m, 2H, H-3, H-6a'), 4.34 (dd, 1H, $J_{6a,b} = 12.3$, $J_{5,6a} = 2.4$ Hz, H-6a), 4.46-4.79 (m, 7H, H-5', 3 x phCH_2), 4.94-4.99 (m, 2H, H-1, phCH_2^a), 5.08-5.16 (m, 2H, H-1', phCH_2^b), 5.40 (dd, 1H, $J_{4,5} = 9.9$ Hz, H-4'), 6.01 (dd, 1H, $J_{3,4} = 9.8$ Hz, H-3'), 7.08-7.49 (m, 29H, aromatic), 7.67-7.70 (m, 2H, aromatic), 7.88-7.92 (m, 2H, aromatic), 8.00-8.03 (m, 2H, aromatic) ppm.

Synthesis of Sulfonium Salts 5.4a-d, h-j

The typical procedure for sulfonium salt formation is similar to preactivation *method D*; a mixture containing the glycosyl donor (0.048 mmol), and freshly activated molecular sieves (3Å, 105 mg) in DCE (0.5 mL) was stirred under argon for 1 h. The specified amount of promoter was added and the reaction mixture was monitored for donor disappearance and concomitant salt formation. *MeOTf promoter a*: 0.144 mmol, reaction was stirred for 1 h; *MeI/AgX promoters b-h*: MeI (0.431 mmol) was added, after 0.5 h AgX (0.144 mmol) was added, and the reaction was allowed to stir for time specified in Tables 5.2 and 5.3; *Me₃OBF₄ promoter i*: 0.144 mmol, reaction was stirred for 3 h; *DMTST promoter j*: 0.096 mmol, reaction was stirred for 0.5 h. Upon formation of the sulfonium salt, the reaction mixture was then diluted with anhydrous DCE (5 mL), filtered and worked up following one of three procedures: (1) the crude residue was concentrated *in vacuo*, whereupon was dissolved in CDCl₃ and subsequent NMR spectral data was obtained; (2) the crude residue was purified by PLC (acetone:DCM, 3.5/6.5, v/v); or (3) the crude residue was washed with cold water (5 mL), and the organic phase was separated, dried and concentrated *in vacuo* before purifying by PLC (acetone:DCM, 3.5/6.5, v/v);

Analytical data given for compound 5.4a (purified via procedure 3): ¹H NMR (CDCl₃): δ, 1.32 (t, 3H, SCH₂CH₃), 2.36 (s, 3H, SCH₃), 3.37-3.47 (m, 1H, SCH₂^aCH₃), 3.53-3.63 (m, 1H, SCH₂^bCH₃), 3.97 (dd, 1H, J_{2,3} = 9.8 Hz, H-2), 4.47-4.51 (m, 3H, H-5, H-6a, phCH₂^a), 4.66 (dd, 1H, H-6b), 4.75 (d, 1H, ²J = 11.5 Hz, phCH₂^b), 5.31 (d, 1H, J_{1,2} = 9.8 Hz, H-1), 5.54 (dd, 1H, J_{4,5} = 9.6 Hz, H-4), 5.93 (dd, 1H, J_{3,4} = 9.4 Hz, H-3), 7.24-7.60 (m, 14H,

aromatic), 7.88-8.01 (m, 6H, aromatic) ppm; Selected data for ^{13}C NMR (CDCl_3): δ , 9.3 (CH_3), 16.3 (SCH_3), 36.1 (SCH_2), 82.3 (C-1), 133.7, 134.0, 135.5, 165.3, 165.4, 166.2 ppm; HR-FAB MS calcd. for $\text{C}_{37}\text{H}_{37}\text{O}_8\text{S}^+$ 641.2209, found 641.2219. (See Appendix, Figure A-49, A-50, A-51)

Analytical data given for diastereomeric compounds **5.4c^a** and **5.4c^b** (crude sample, procedure 1): Data for compound **5.4c^a**: ^1H NMR (CDCl_3): δ , 1.18 (t, 3H, SCH_2CH_3), 2.83-2.92 (s, m, 4H, SCH_3 , $\text{SCH}_2^{\text{a}}\text{CH}_3$), 2.97-3.09 (m, 1H, $\text{SCH}_2^{\text{b}}\text{CH}_3$), 4.13 (dd, 1H, H-2), 4.42-4.67 (m, 5H, H-5, H-6a, H-6b, phCH_2), 5.21 (d, 1H, $J_{1,2} = 9.8$ Hz, H-1), 5.61 (dd, 1H, H-4), 5.88 (dd, 1H, H-3), 7.14-7.46 (m, 14H, aromatic), 7.82-7.85 (dd, 2H, aromatic), 7.94-8.00 (m, 4H, aromatic) ppm; Selected data for ^{13}C NMR (CDCl_3): δ , 8.9 (CH_3), 20.5 (SCH_3), 31.8 (SCH_2), 62.0, 68.0, 74.5, 74.6, 75.8, 85.3 (C-1) ppm; Data for compound **5.4c^b**: ^1H NMR (CDCl_3): δ , 1.32 (t, 3H, SCH_2CH_3), 2.44, (s, 3H, SCH_3), 3.26-3.46 (m, 2H, SCH_2CH_3), 4.09 (dd, 1H, $J_{2,3} = 9.4$ Hz, H-2), 4.42-4.67 (m, 5H, H-5, H-6a, H-6b, phCH_2), 5.17 (d, 1H, $J_{1,2} = 9.8$ Hz, H-1), 5.61 (dd, 1H, H-4), 5.91 (dd, 1H, H-3), 7.14-7.46 (m, 14H, aromatic), 7.82-7.85 (dd, 2H, aromatic), 7.94-8.00 (m, 4H, aromatic) ppm; Selected data for ^{13}C NMR (CDCl_3): δ , 9.0 (CH_3), 15.8 (SCH_3), 35.7 (SCH_2), 73.6, 74.8, 75.7, 82.4 (C-1), 133.5, 133.8, 135.4, 165.1, 165.3, 166.1 ppm. (See Appendix, Figure A-54, A-55, A-56)

See Appendix for additional spectral data of sulfonium salts:

5.4b (Figure A-52, A-53); **5.4d** (Figure A-57, A-58, A-59); **5.4h** (Figure A-60, A-61); **5.4i** (Figure A-62, A-63); **5.4j** (crude, Figure A-64, A-65; purified, Figure A-66, A-67)

5.8 References

1. Kamat, M. N.; Demchenko, A. V., *Org. Lett.* **2005**, *7*, 3215-3218.
2. Mydock, L. K.; Demchenko, A. V., *Org. Lett.* **2008**, *10*, 2103-2106.
3. Mydock, L. K.; Demchenko, A. V., *Org. Lett.* **2008**, *10*, 2107-2110.
4. Park, J.; Kawatkar, S.; Kim, J. H.; Boons, G. J., *Org. Lett.* **2007**, *9*, 1959-1962.
5. Nokami, T.; Shibuya, A.; Manabe, S.; Ito, Y.; Yoshida, J., *Chem. Eur. J.* **2009**, *15*, 2252-2255.
6. Kim, J. H.; Yang, H.; Park, J.; Boons, G. J., *J. Am. Chem. Soc.* **2005**, *127*, 12090-12097.
7. Crich, D.; Chandrasekera, N. S., *Angew Chem., Int. Ed.* **2004**, *43*, 5386-5389 and references therein.
8. Dauben, W. G.; Kohler, P., *Carbohydrate Research* **1990**, *203*, 47-56.
9. West, A. C.; Schuerch, C., *J. Am. Chem. Soc.* **1973**, *95*, 1333-1335.
10. Lemieux, R. U.; Morgan, A. R., *Canadian Journal of Chemistry* **1965**, *43*, 2205-2213.
11. Perrin, C. L., *Tetrahedron* **1995**, *51* (44), 11901-11935.
12. Andersson, F.; Fugedi, P.; Garegg, P. J.; Nashed, M., *Tetrahedron Lett.* **1986**, *27* (33), 3919-3922.
13. Jamois, F.; Goffic, F. L.; Yvin, J. C.; Plusquellec, D.; Ferrières, V., *Open Glycoscience* **2008**, *1*, 19-24.
14. Valerio, S., *Journal of Organic Chemistry* **2007**, *72* (16), 6097.
15. Ekelof, K.; Oscarson, S., *J. Org. Chem.* **1996**, *61*, 7711-7718.

16. Mootoo, D. R.; Konradsson, P.; Udodong, U.; Fraser-Reid, B., *J. Am. Chem. Soc.* **1988**, *110*, 5583-5584.
17. Fraser-Reid, B.; Udodong, U. E.; Wu, Z. F.; Ottosson, H.; Merritt, J. R.; Rao, C. S.; Roberts, C.; Madsen, R., *Synlett* **1992**, (12), 927-942 and references therein.
18. Kuester, J. M.; Dyong, I., *Justus Liebigs Ann. Chem.* **1975**, (12), 2179-2189.
19. Premathilake, H.; Mydock, L. K.; Demchenko, A. V., *Journal of Organic Chemistry* **2010**, (75), 1095-1100.
20. Tvaroska, I.; Bleha, T., *Advances in Carbohydrate Chemistry and Biochemistry* **1989**, *47*, 45-123.
21. Wallace, J. E.; Schroeder, L. R., *Journal of the Chemical Society, Perkin Transactions 2* **1976**.
22. Byramova, N. E.; Ovchinnikov, M. V.; Backinowsky, L. V.; Kochetkov, N. K., *Carbohydr. Res.* **1983**, *124* (1), C8-C11.
23. Garegg, P. J.; Hultberg, H., *Carbohydr. Res.* **1981**, *93* (1), C10-C11.
24. Koto, S.; Takebe, Y.; Zen, S., *Bull. Chem. Soc. J.* **1972**, *45*, 291-293.
25. Pearce, A. J.; Sinay, P., *Angew. Chem. Int. Ed.* **2000**, *39* (20), 3610-3612.
26. Dewar, M. J. S.; Dougherty, R. C., *The PMO Theory of Organic Chemistry*. Plenum: New York, 1975.
27. Nukada, T.; Berces, A.; Whitfield, D. M., *Carbohydr. Res.* **2002**, *337*, 765-774.
28. Zeng, Y.; Wang, Z.; Whitfield, D.; Huang, X., *J. Org. Chem.* **2008**, *73*, 7952-7962.
29. Billings, S. B.; Woerpel, K. A., *J. Org. Chem.* **2006**, *71* (14), 5171-5178.

30. Beaver, M. G.; Billings, S. B.; Woerpel, K. A., *J. Am. Chem. Soc.* **2008**, *130* (6), 2082-2086.
31. Crich, D.; Cai, W., *J. Org. Chem.* **1999**, *64* (13), 4926-4930.
32. Crich, D., *J. Carbohydr. Chem.* **2002**, *21* (7-9), 667-690.
33. Seeman, J. I., *Chem. Rev.* **1983**, *83*, 83-134.
34. Ravenscroft, M.; Roberts, R. M. G.; Tillett, J. G., *J. Chem. Soc. Perkin Trans. 2* **1982**, 1569-1972.
35. Matsuo, I.; Wada, M.; Manabe, S.; Yamaguchi, Y.; Otake, K.; Kato, K.; Ito, Y., *J. Am. Chem. Soc.* **2003**, *125* (12), 3402-3403.
36. Garegg, P. J.; Kvarnstrom, I.; Niklasson, A.; Niklasson, G.; Svensson, S. C. T., *J. Carbohydr. Chem.* **1993**, *12* (7), 933-953.
37. Takeo, K.; Maki, K.; Wada, Y.; Kitamura, S., *Carbohydrate Research* **1993**, *245*, 81-96.
38. Nguyen, H. M.; Chen, Y. N.; Duron, S. G.; Gin, D. Y., *J. Am. Chem. Soc.* **2001**, *123*, 8766-8772.
39. Huang, K. T.; Winssinger, N., *Eur. J. Org. Chem.* **2007**, 1887-1890.

CHAPTER 6

Appendix

Selected NMR spectral data

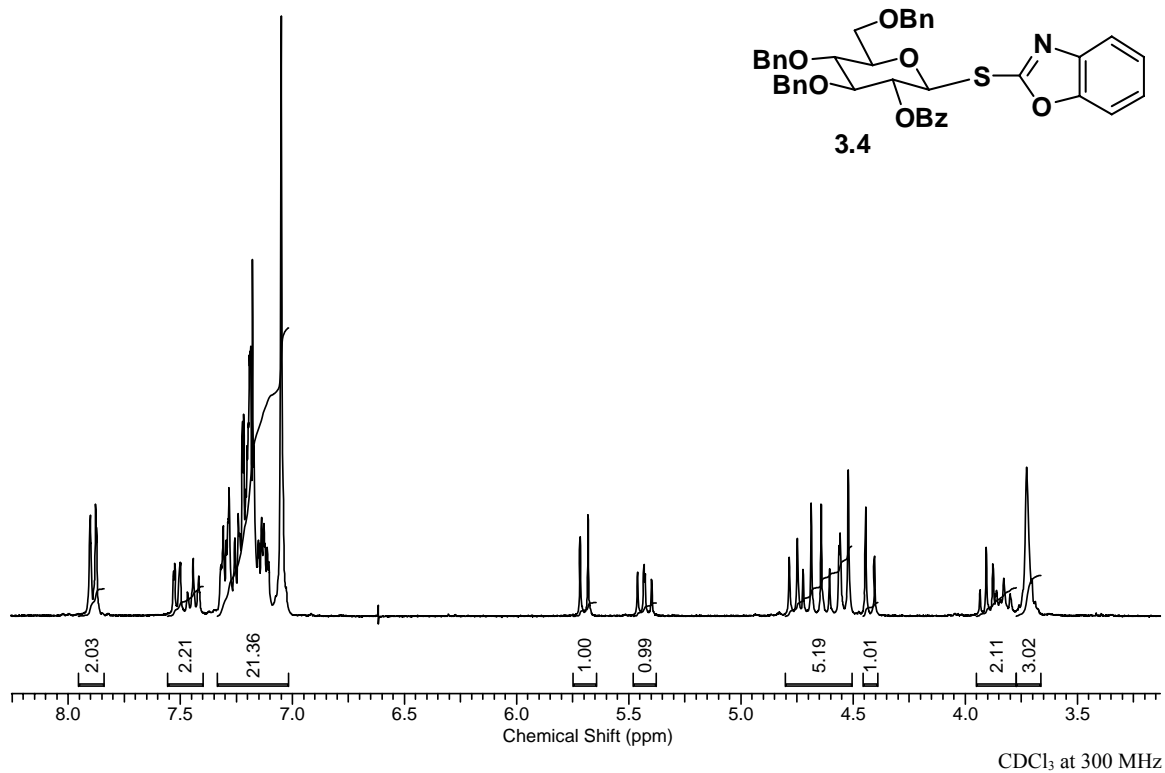


Figure A-1: ^1H NMR spectrum of Benzoxazolyl 2-O-benzoyl-3,4,6-tri-O-benzyl-1-thio-β-D-glucopyranoside (**3.4**)

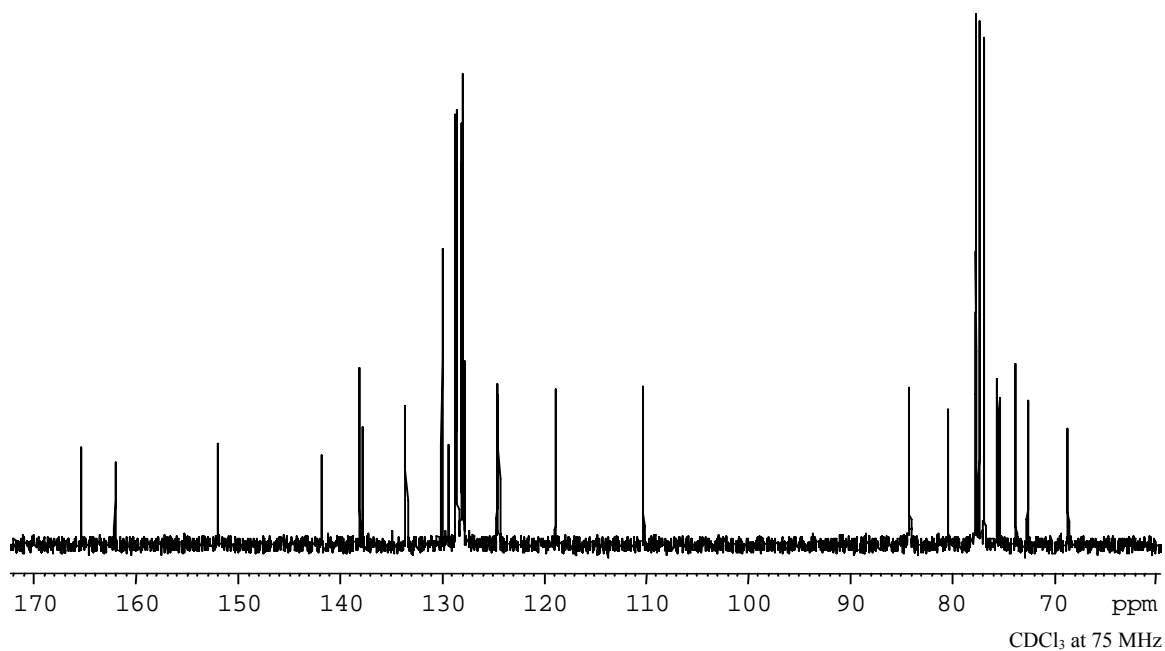


Figure A-2: ^{13}C NMR spectrum of Benzoxazolyl 2-O-benzoyl-3,4,6-tri-O-benzyl-1-thio-β-D-glucopyranoside (**3.4**)

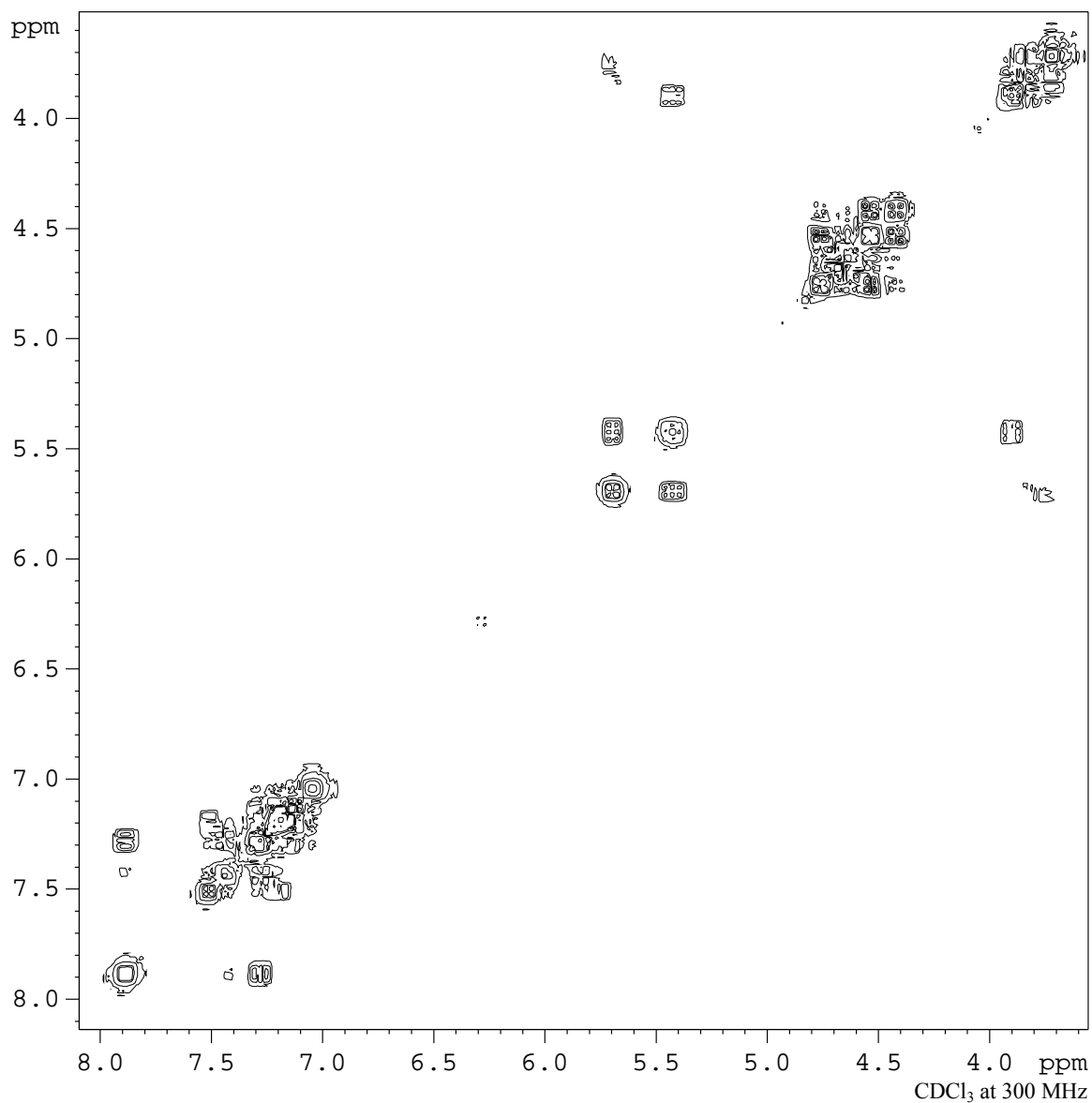
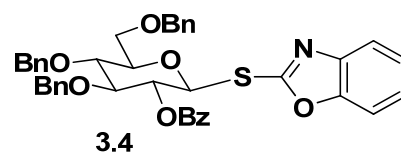


Figure A-3: 2-D NMR COSY spectrum of Benzoxazolyl 2-O-benzoyl-3,4,6-tri-O-benzyl-1-thio- β -D-glucopyranoside (**3.4**)

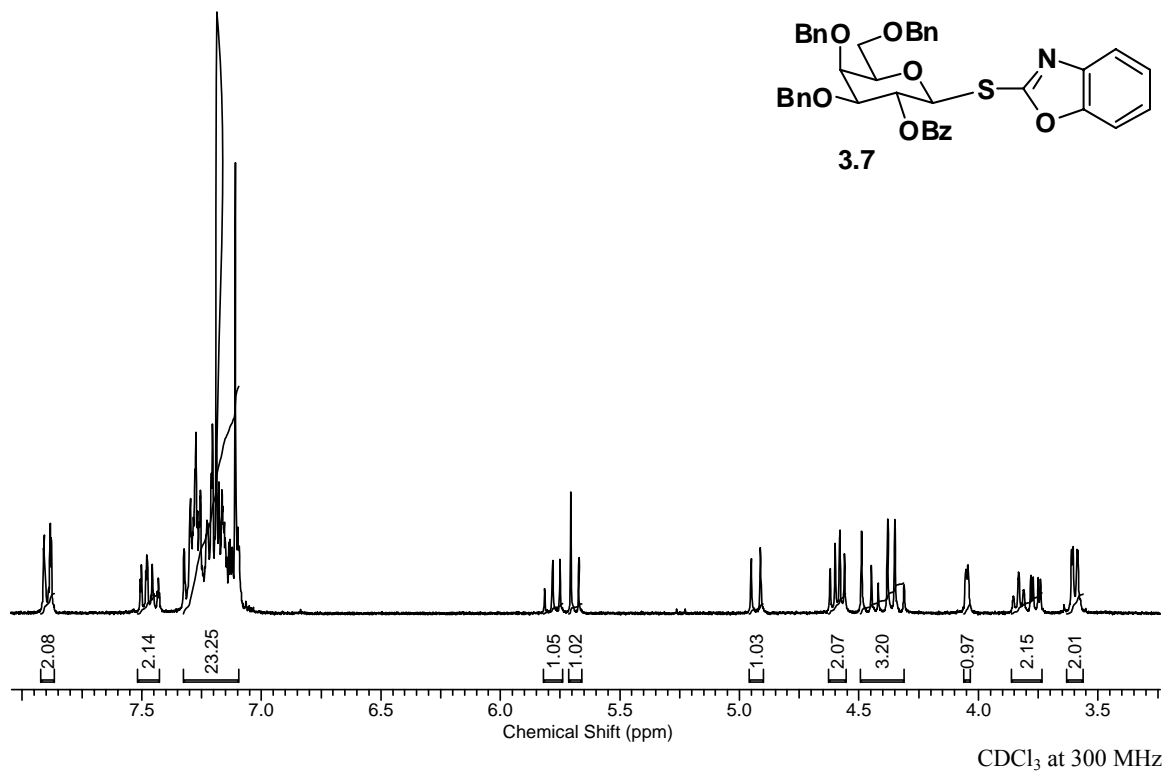


Figure A-4: ¹H NMR spectrum Benzoxazolyl 2-O-benzoyl-3,4,6-tri-O-benzyl-1-thio-β-D-galactopyranoside (**3.7**)

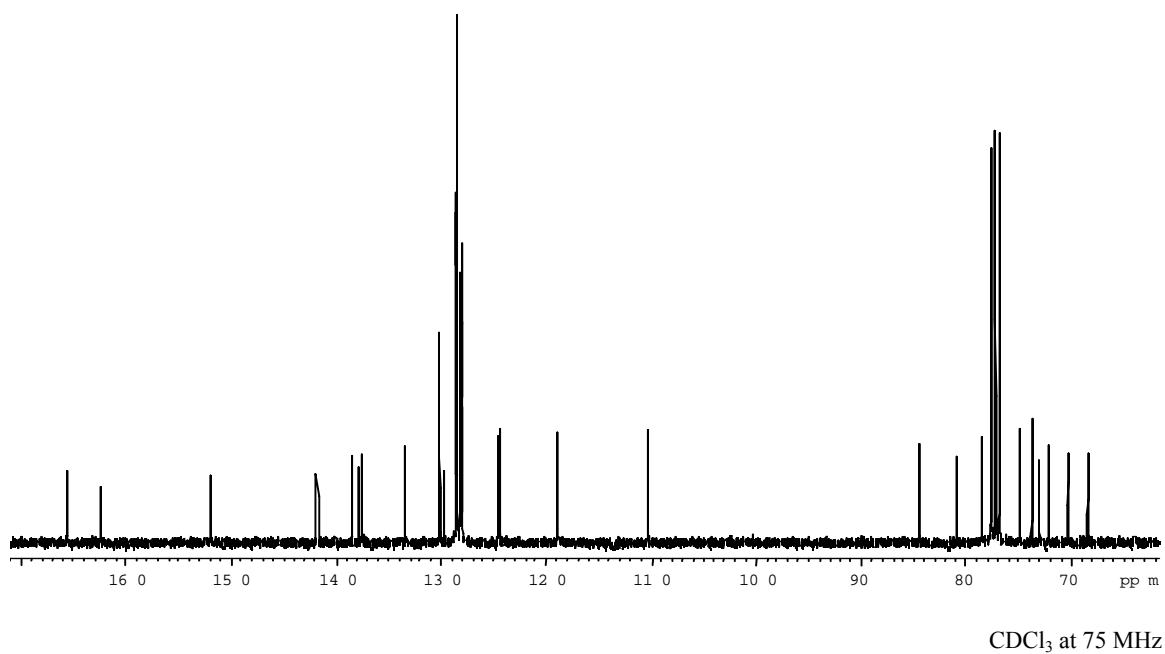


Figure A-5: ¹³C NMR spectrum of Benzoxazolyl 2-O-benzoyl-3,4,6-tri-O-benzyl-1-thio-β-D-galactopyranoside (**3.7**)

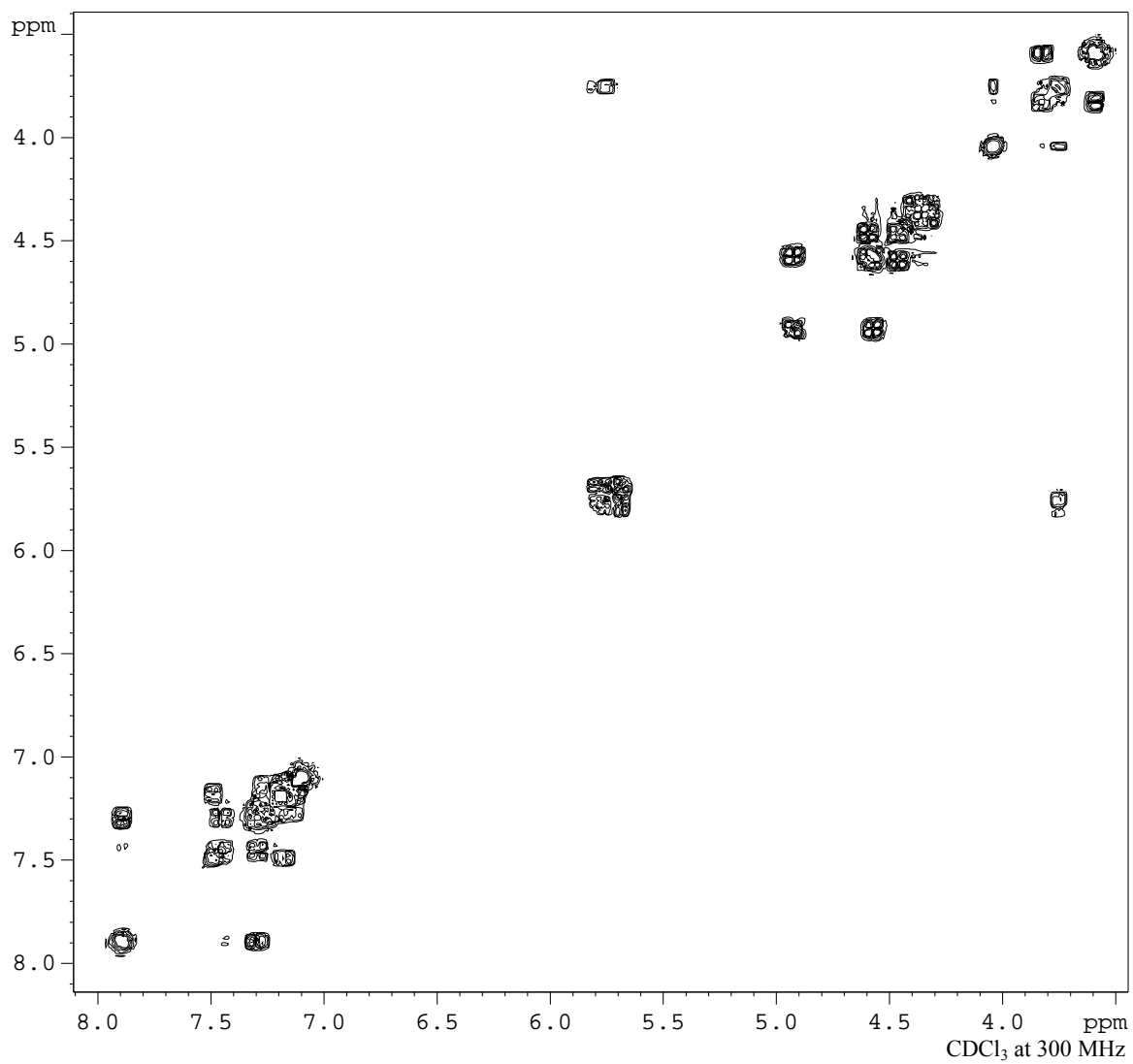
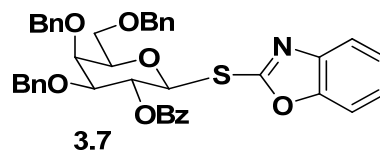


Figure A-6: 2-D NMR COSY spectrum of Benzoxazolyl 2-O-benzoyl-3,4,6-tri-O-benzyl-1-thio- β -D-galactopyranoside (**3.7**)

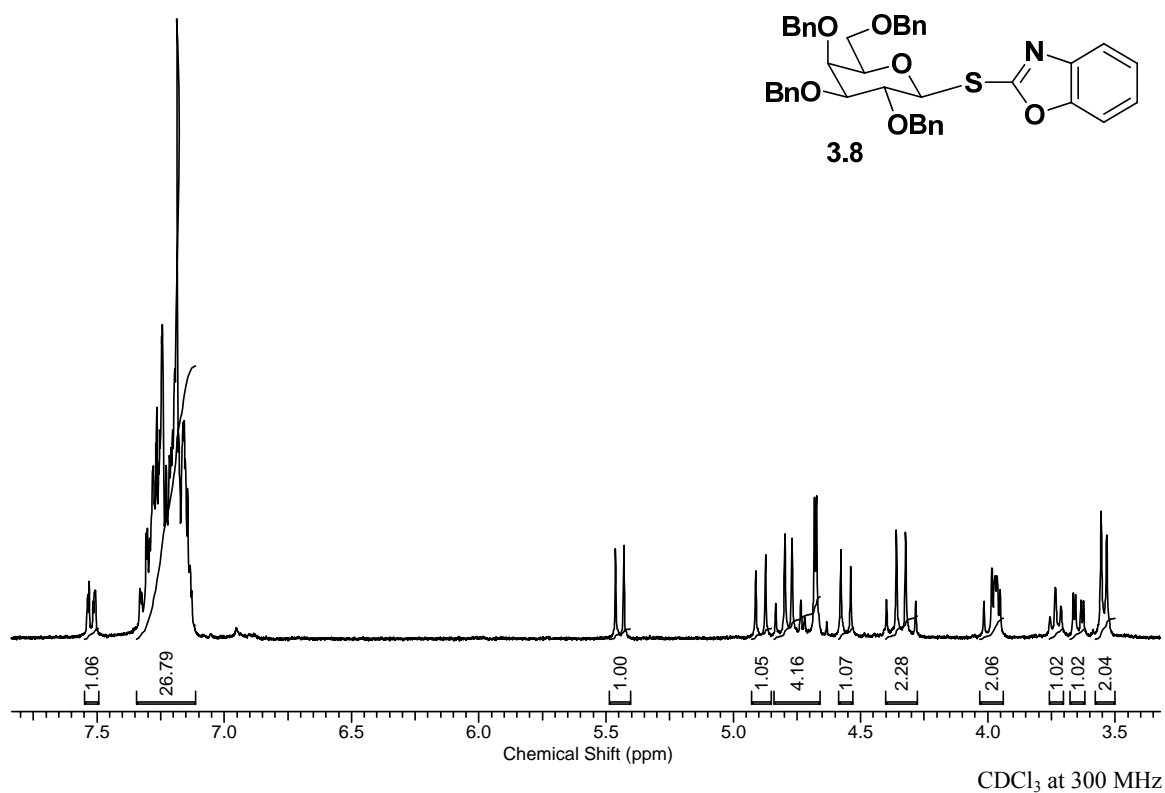


Figure A-7: ¹H NMR spectrum of Benzoxazolyl 2,3,4,6-tetra-O-benzyl-1-thio-β-D-galactopyranoside (**3.8**)

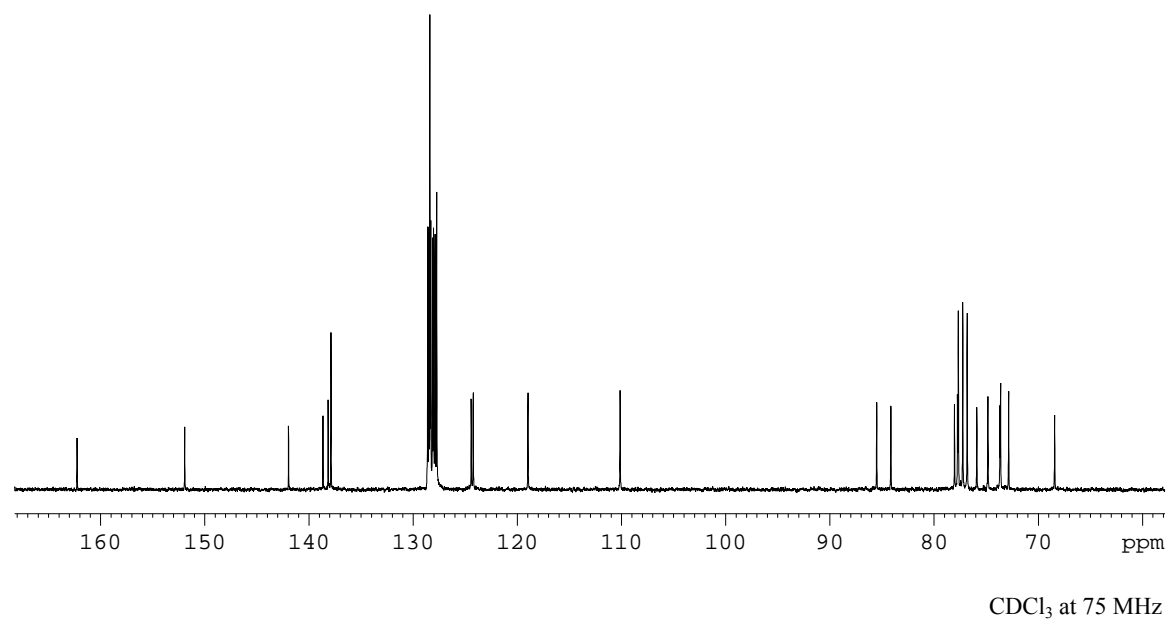


Figure A-8: ¹³C NMR spectrum of Benzoxazolyl 2,3,4,6-tetra-O-benzyl-1-thio-β-D-galactopyranoside (**3.8**)

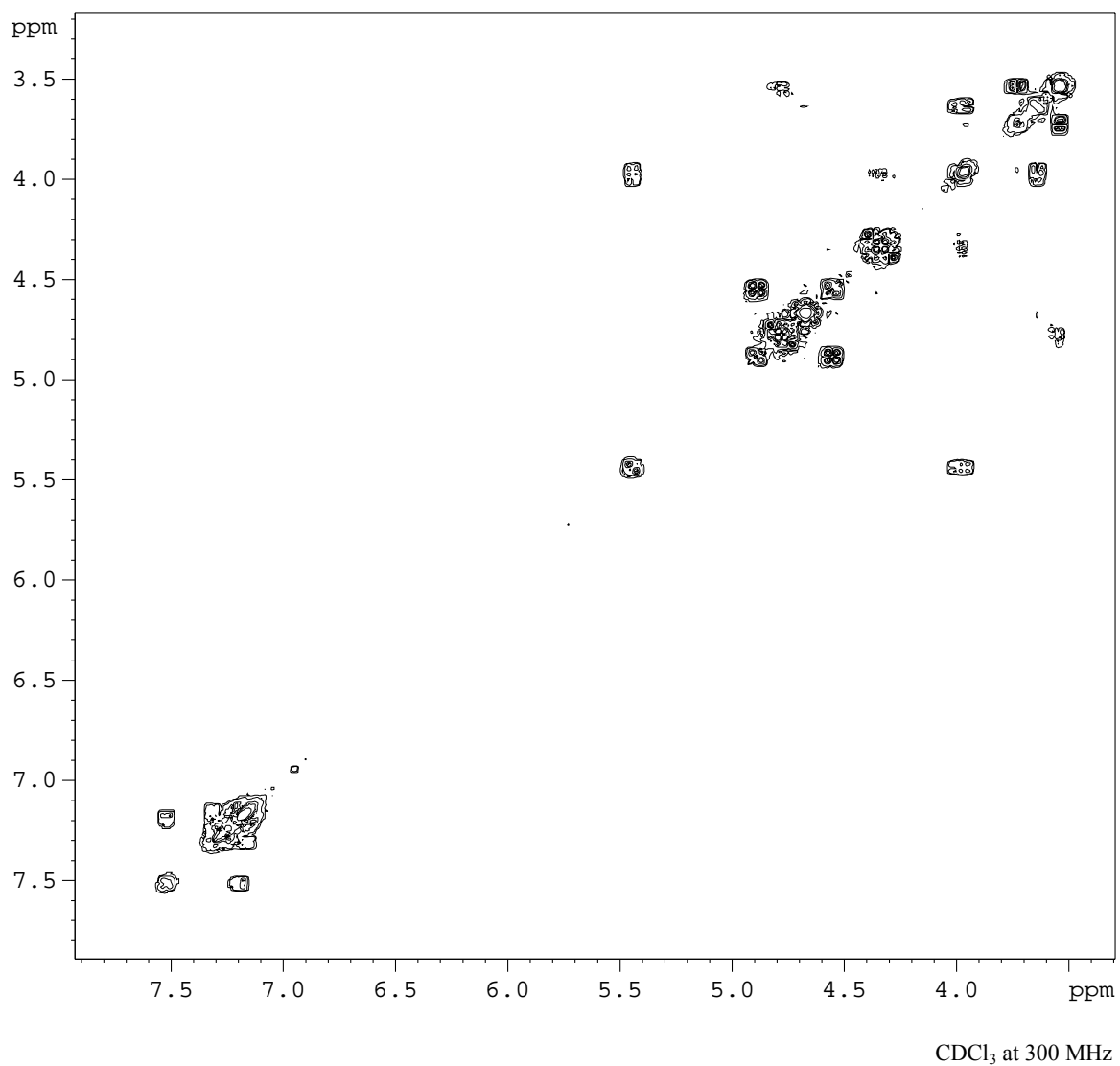
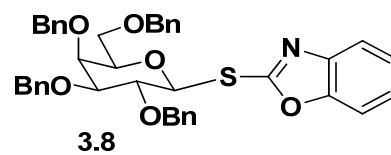


Figure A-9: 2-D NMR COSY spectrum of Benzoxazolyl 2,3,4,6-tetra-O-benzyl-1-thio- β -D-galactopyranoside (**3.8**)

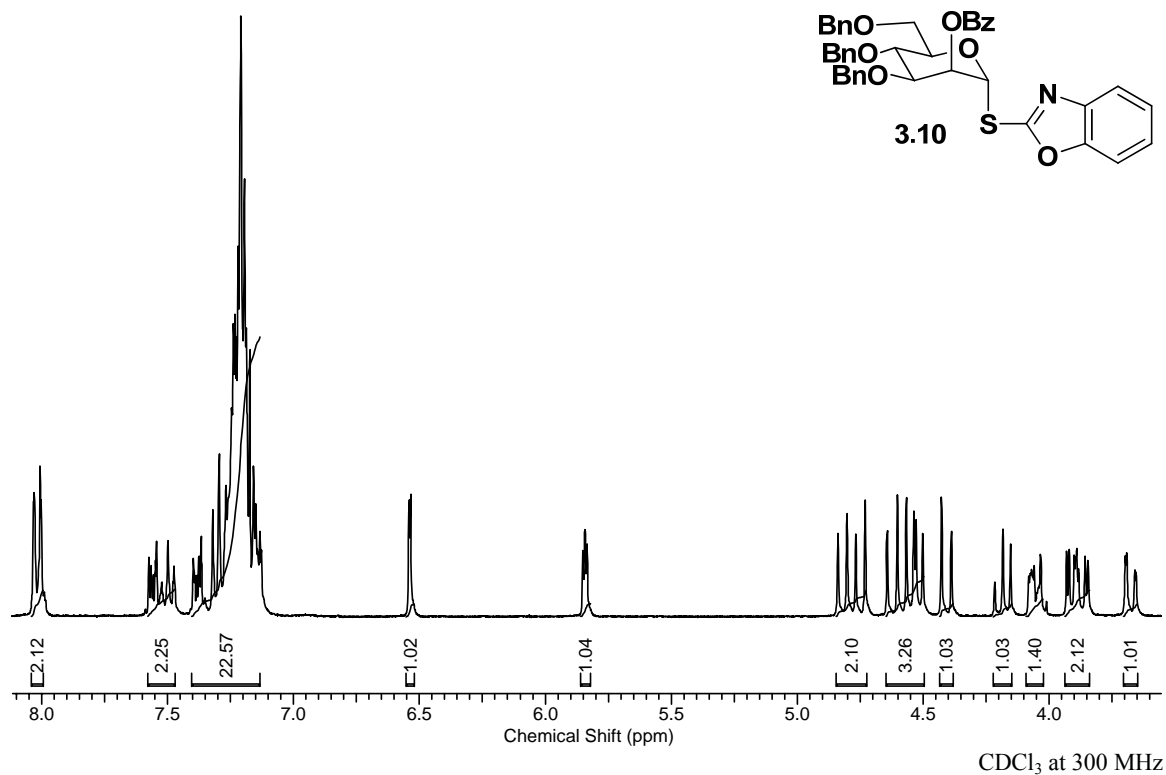


Figure A-10: ¹H NMR spectrum of Benzoxazolyl 2-O-benzoyl-3,4,6-tri-O-benzyl-1-thio- α -D-mannopyranoside (**3.10**)

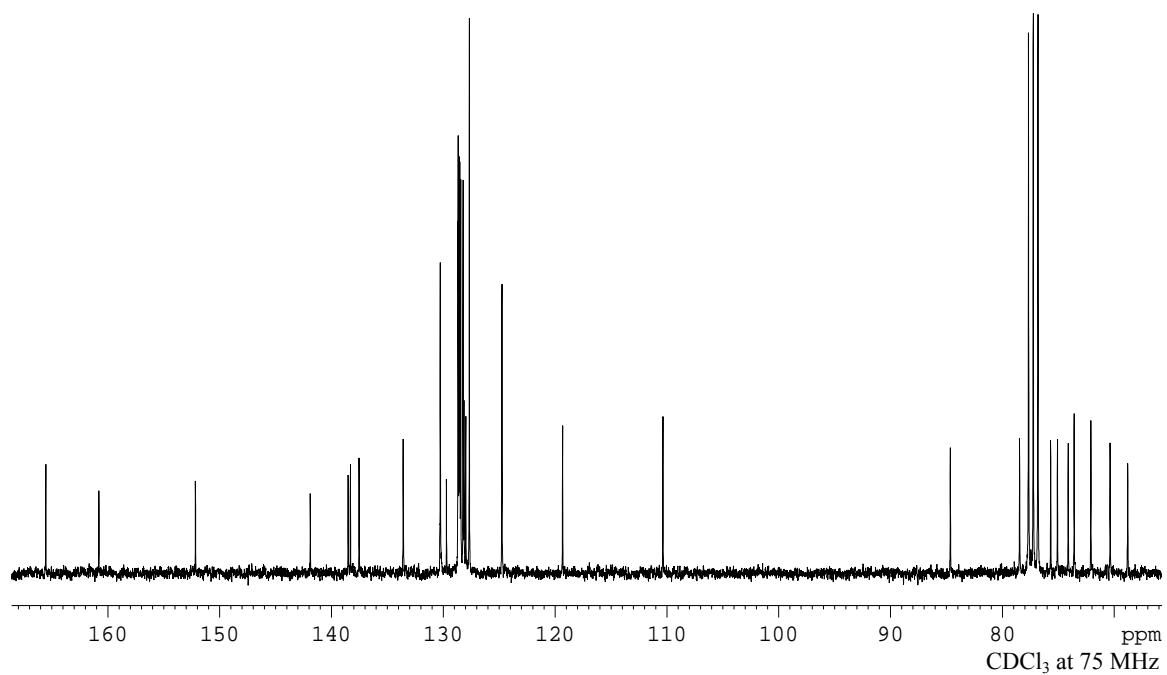


Figure A-11: ¹³C NMR spectrum of Benzoxazolyl 2-O-benzoyl-3,4,6-tri-O-benzyl-1-thio- α -D-mannopyranoside (**3.10**)

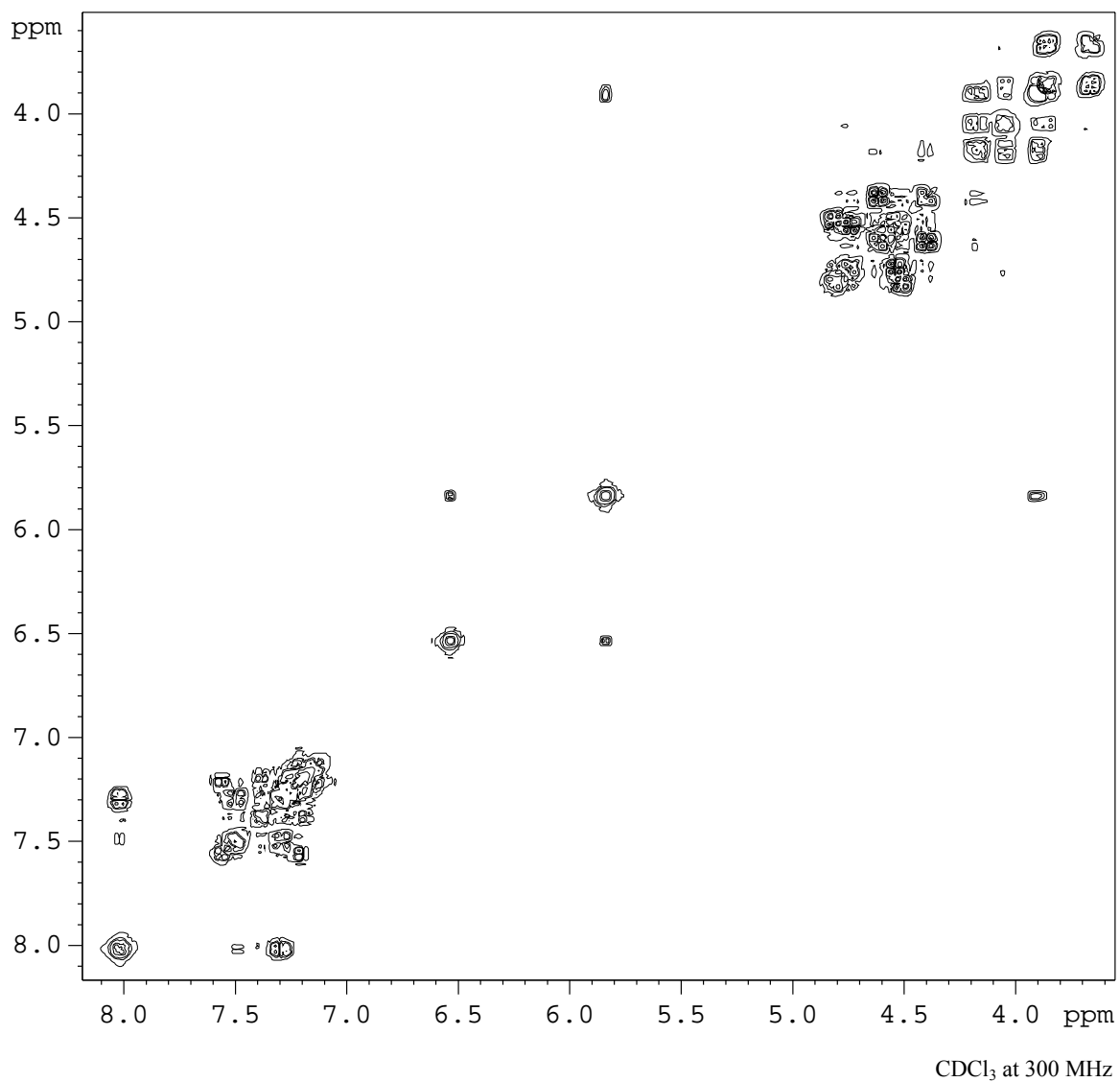
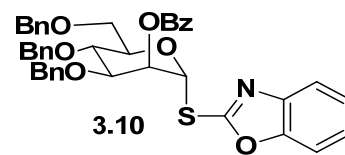


Figure A-12: 2-D NMR COSY spectrum of Benzoxazolyl 2-O-benzoyl-3,4,6-tri-O-benzyl-1-thio- α -D-mannopyranoside (**3.10**)

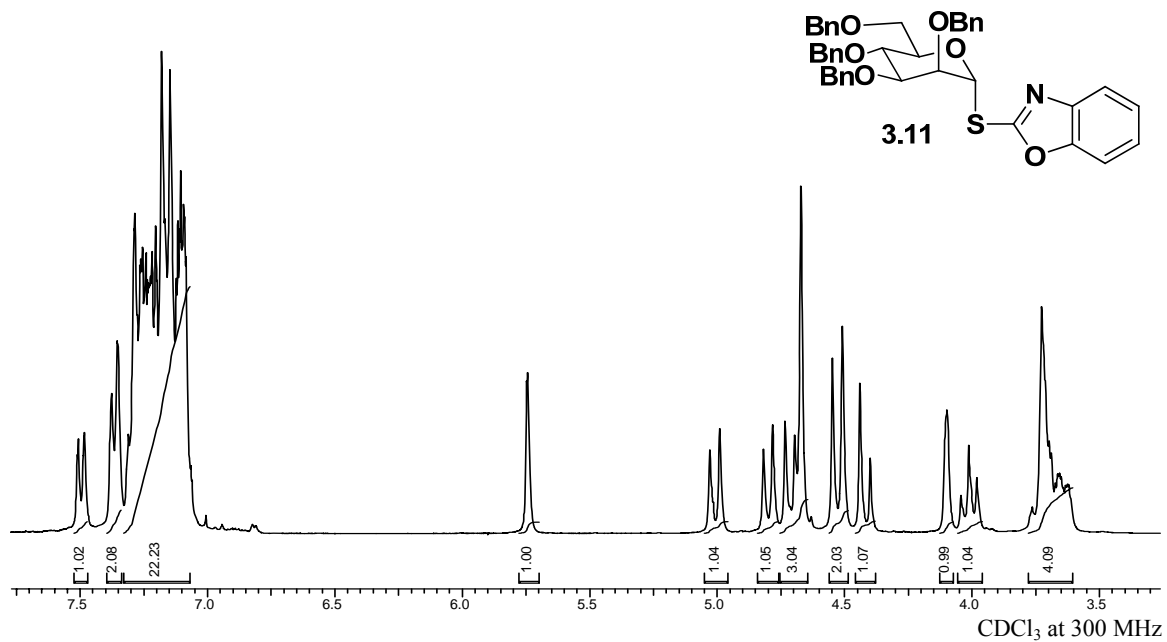


Figure A-13: ^1H NMR spectrum of Benzoxazolyl 2,3,4,6-tetra-*O*-benzyl-1-thio- α -D-mannopyranoside (**3.11**)

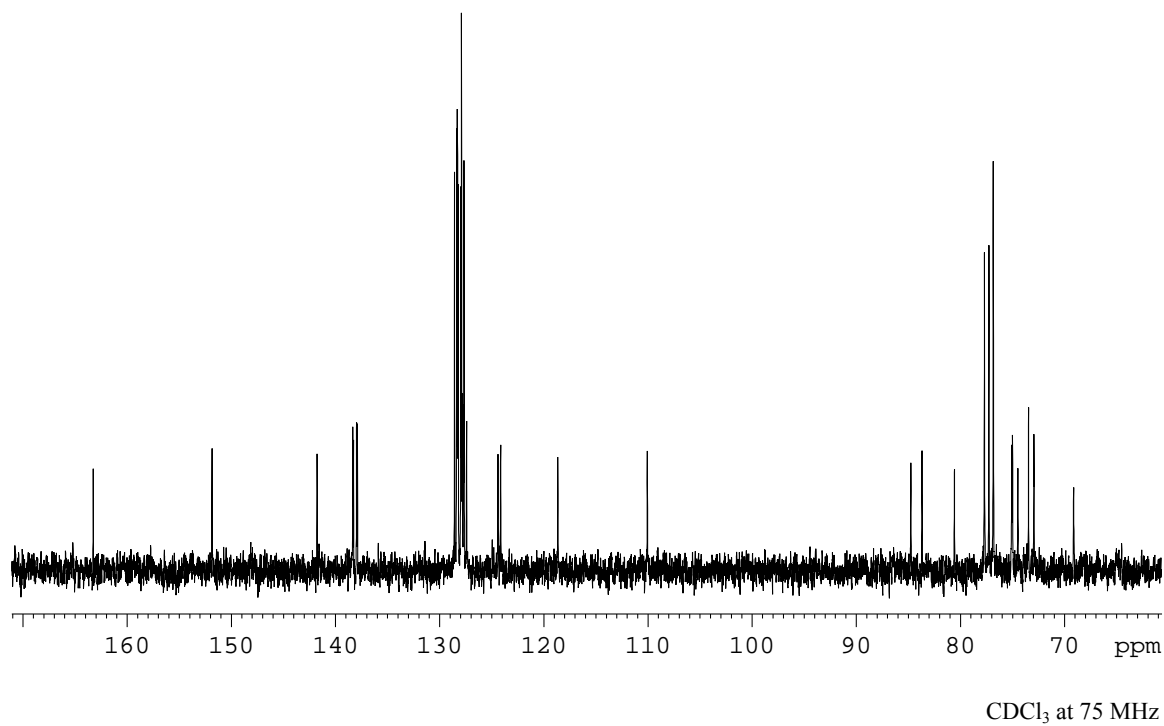


Figure A-14: ^{13}C NMR spectrum of Benzoxazolyl 2,3,4,6-tetra-*O*-benzyl-1-thio- α -D-mannopyranoside (**3.11**)

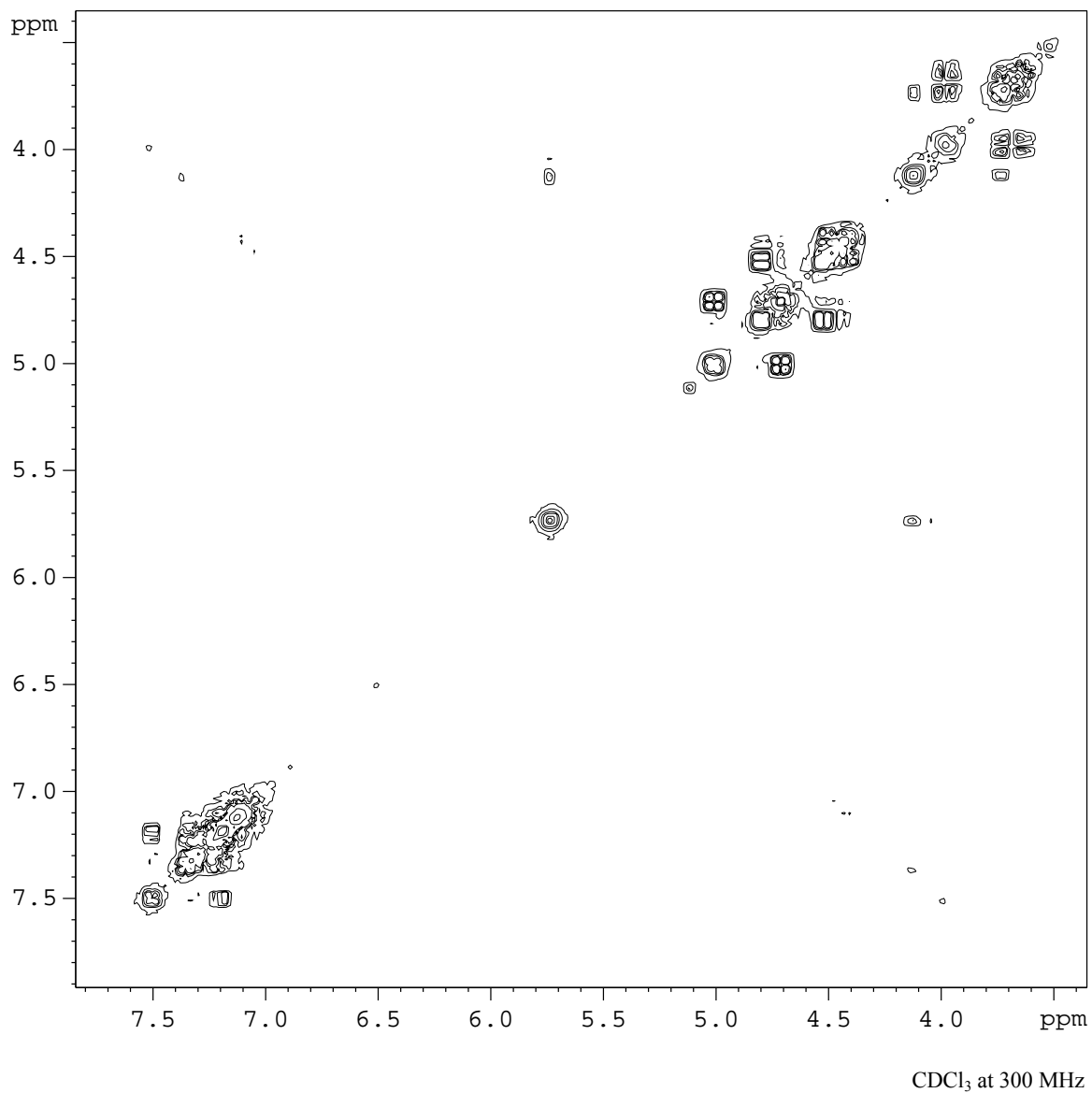
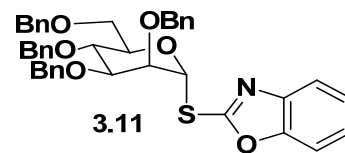


Figure A-15: 2-D NMR COSY spectrum of Benzoxazolyl 2,3,4,6-tetra-*O*-benzyl-1-thio- α -D-mannopyranoside (**3.11**)

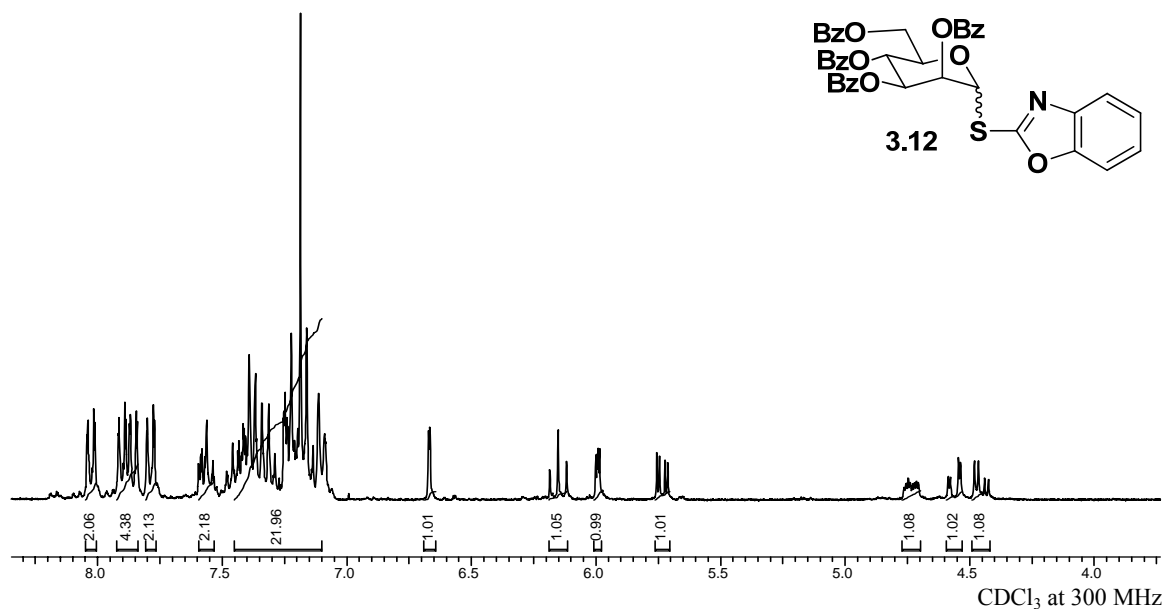


Figure A-16: ¹H NMR spectrum of Benzoxazolyl 2,3,4,6-tetra-*O*-benzoyl-1-thio- α/β -D-mannopyranoside (**3.12**)

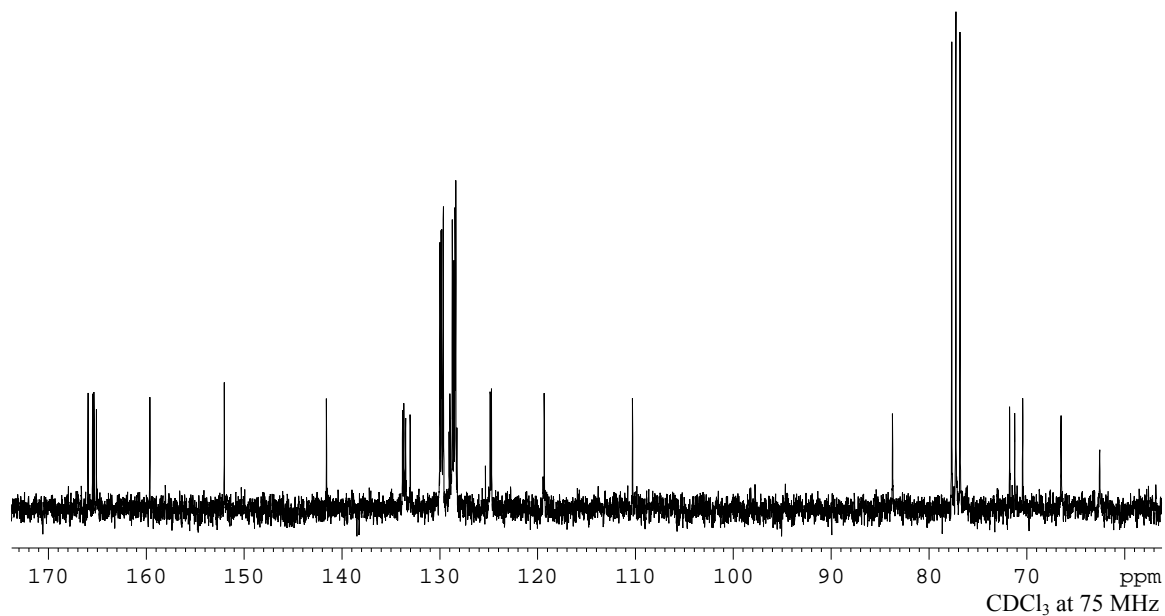


Figure A-17: ¹³C NMR spectrum of Benzoxazolyl 2,3,4,6-tetra-*O*-benzoyl-1-thio- α/β -D-mannopyranoside (**3.12**)

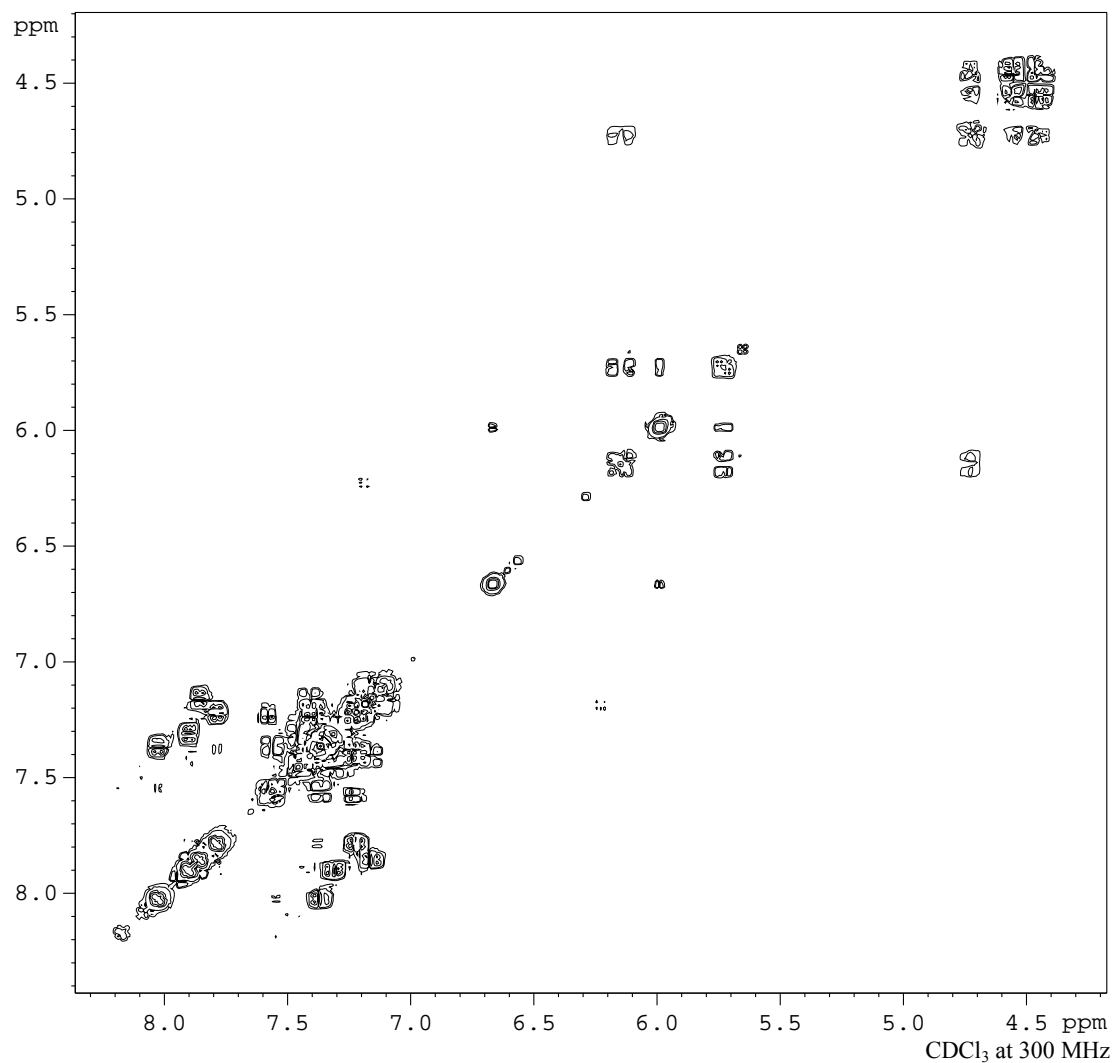
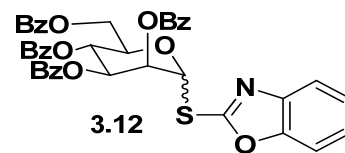


Figure A-18: 2-D NMR COSY spectrum of Benzoxazolyl 2,3,4,6-tetra-*O*-benzoyl-1-thio- α/β -D-mannopyranoside (**3.12**)

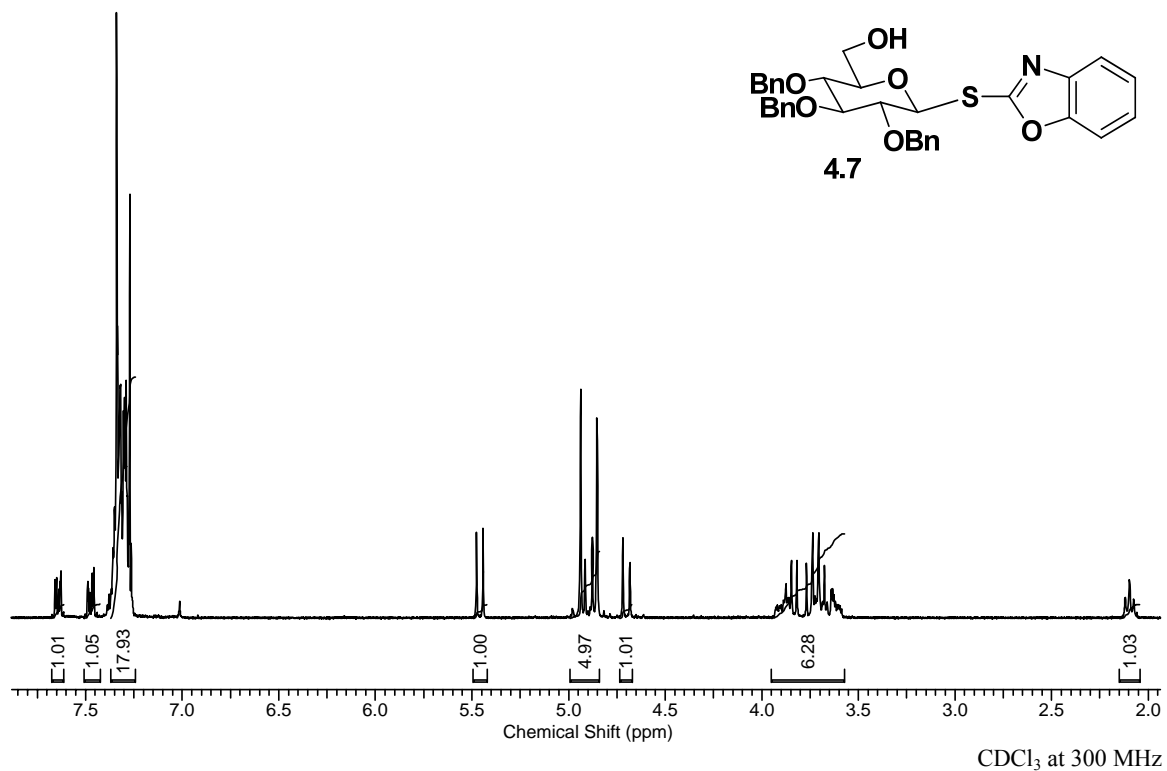


Figure A-19: ¹H NMR spectrum of Benzoxazolyl 2,3,4-tri-O-benzyl-1-thio-β-D-glucopyranoside (4.7)

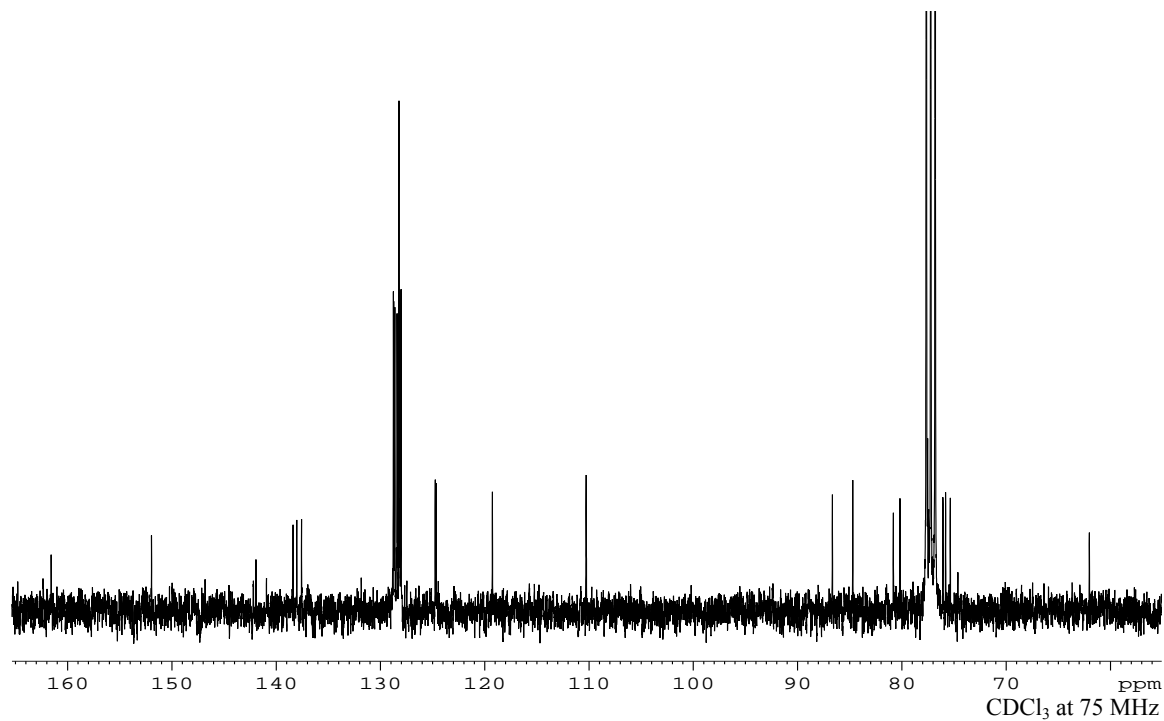


Figure A-20: ¹³C NMR spectrum of Benzoxazolyl 2,3,4-tri-O-benzyl-1-thio-β-D-glucopyranoside (4.7)

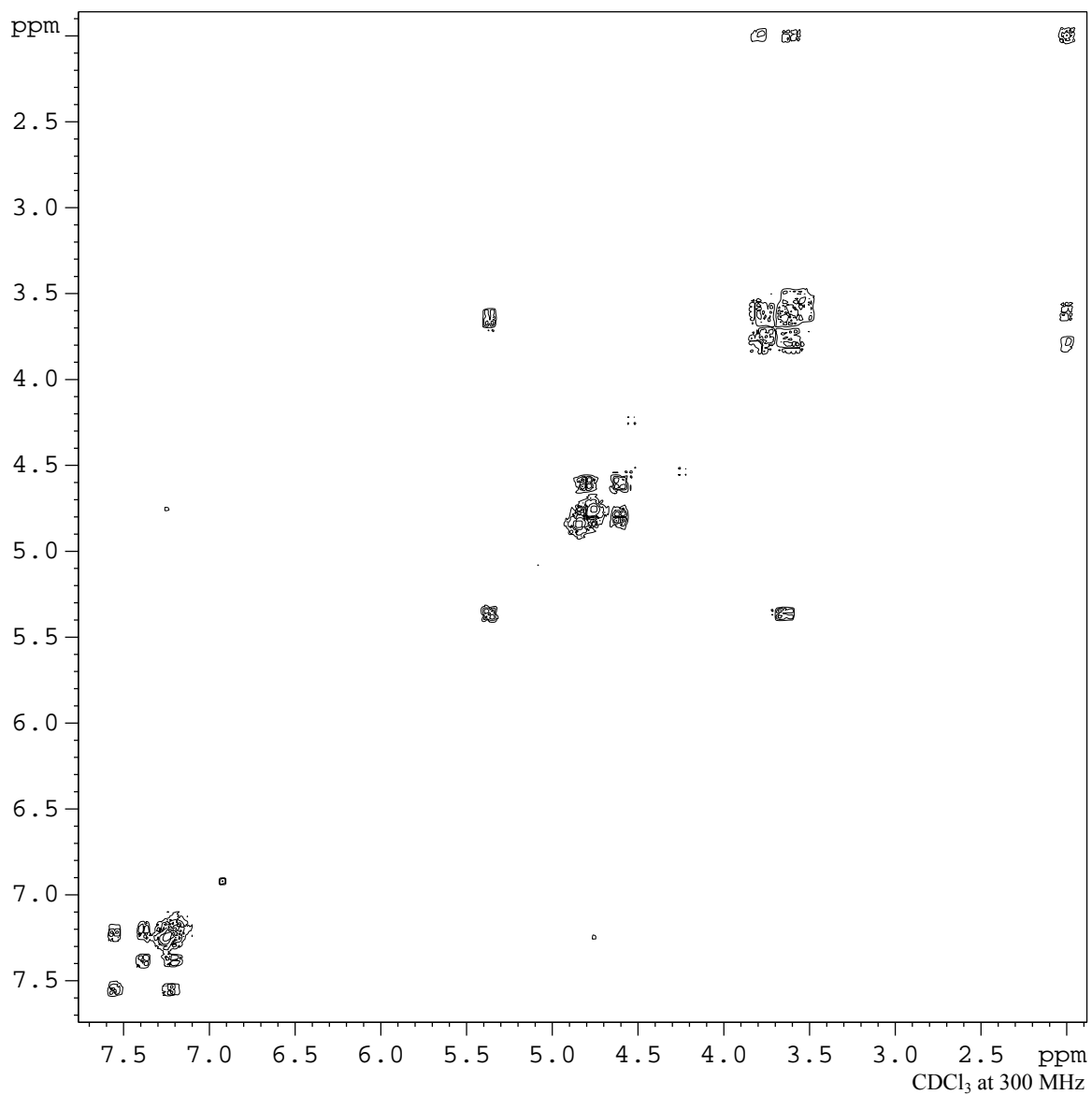
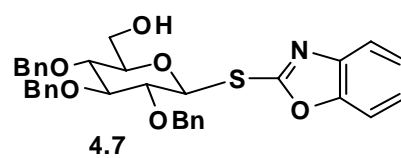


Figure A-21: 2-D NMR COSY spectrum of Benzoxazolyl 2,3,4-tri-O-benzyl-1-thio- β -D-glucopyranoside (**4.7**)

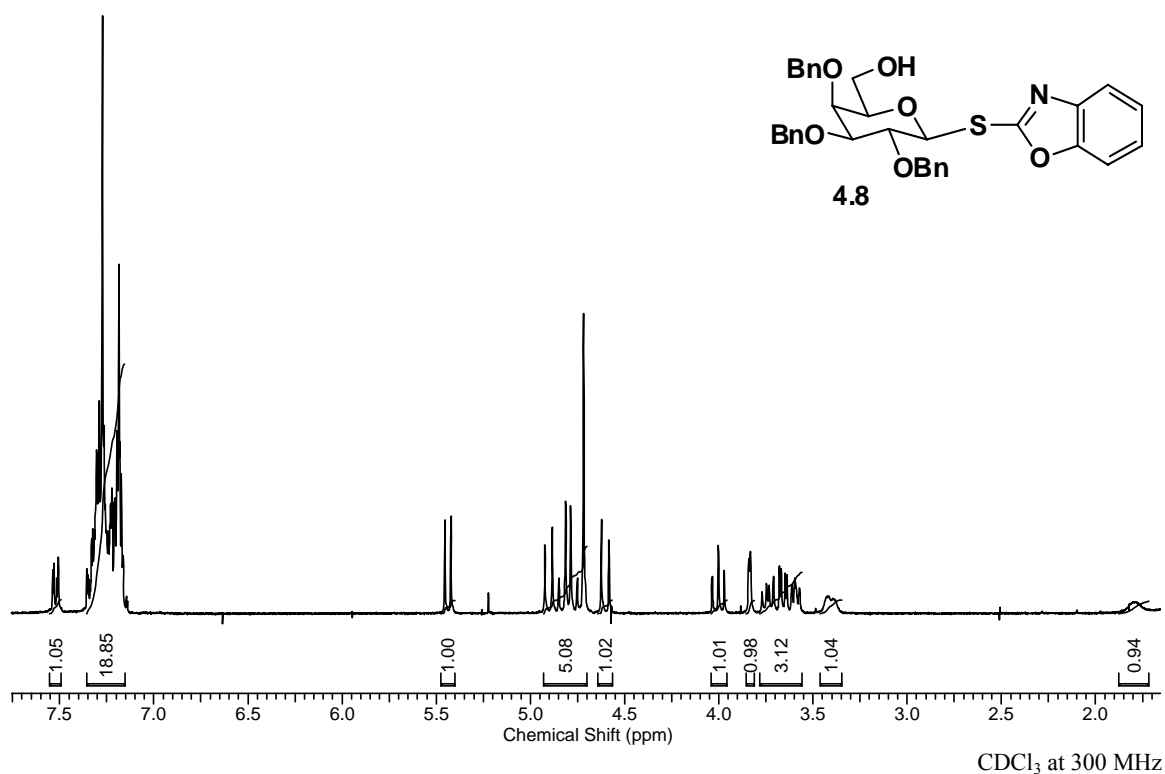


Figure A-22: ¹H NMR spectrum of Benzoxazolyl 2,3,4-tri-O-benzyl-1-thio-β-D-galactopyranoside (**4.8**)

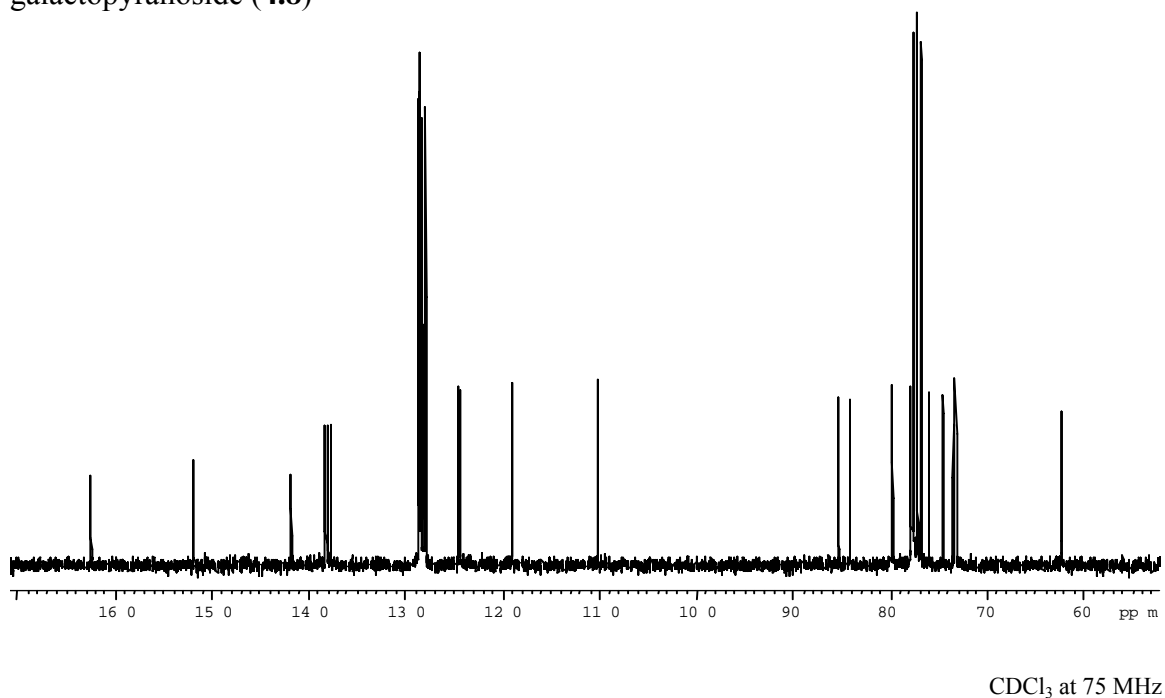


Figure A-23: ¹³C NMR spectrum of Benzoxazolyl 2,3,4-tri-O-benzyl-1-thio-β-D-galactopyranoside (**4.8**)

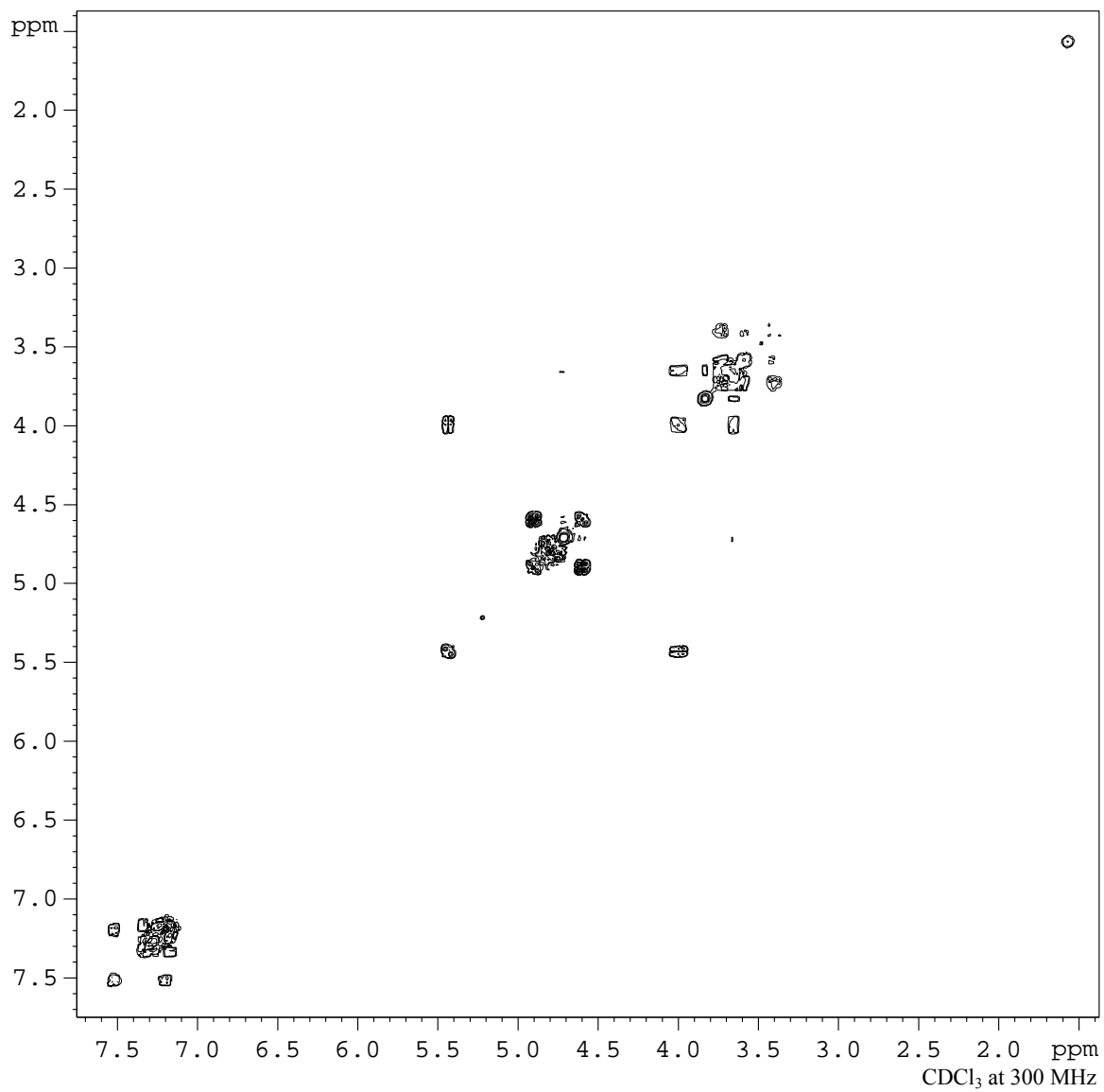
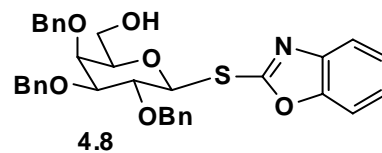


Figure A-24: 2-D NMR COSY spectrum of Benzoxazolyl 2,3,4-tri-O-benzyl-1-thio- β -D-galactopyranoside (**4.8**)

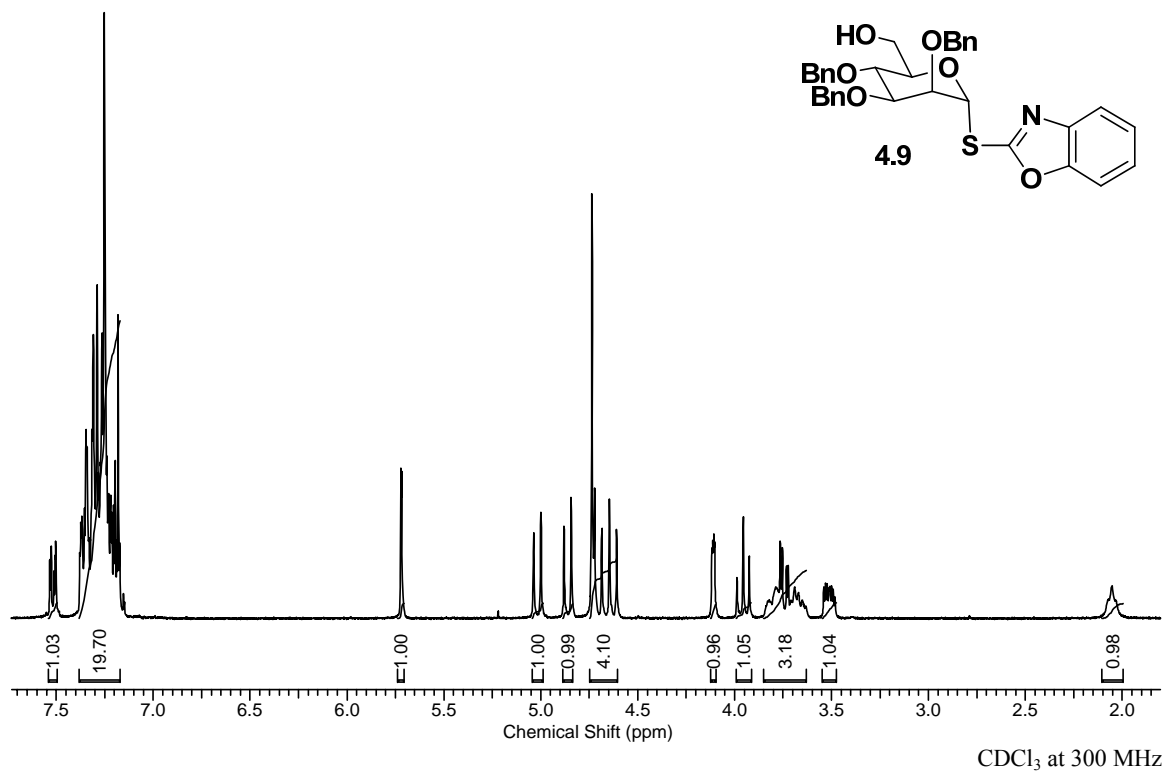


Figure A-25: ¹H NMR spectrum of Benzoxazolyl 2,3,4-tri-O-benzyl-1-thio- α -D-mannopyranoside (**4.9**)

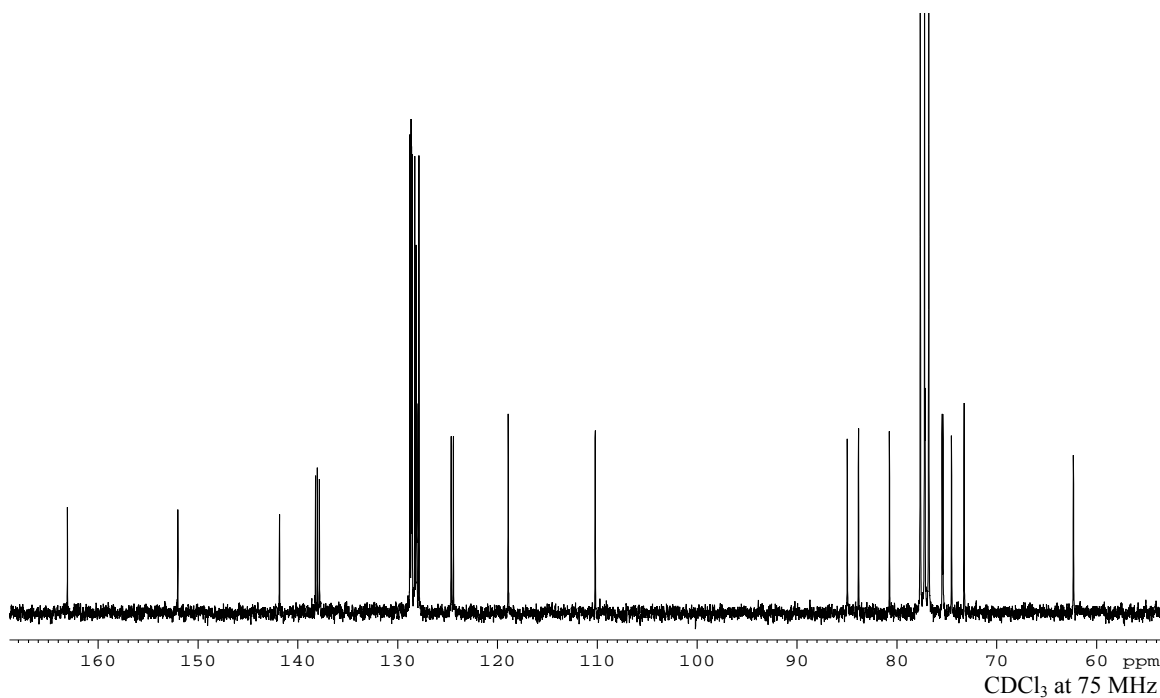


Figure A-26: ¹³C NMR spectrum of Benzoxazolyl 2,3,4-tri-O-benzyl-1-thio- α -D-mannopyranoside (**4.9**)

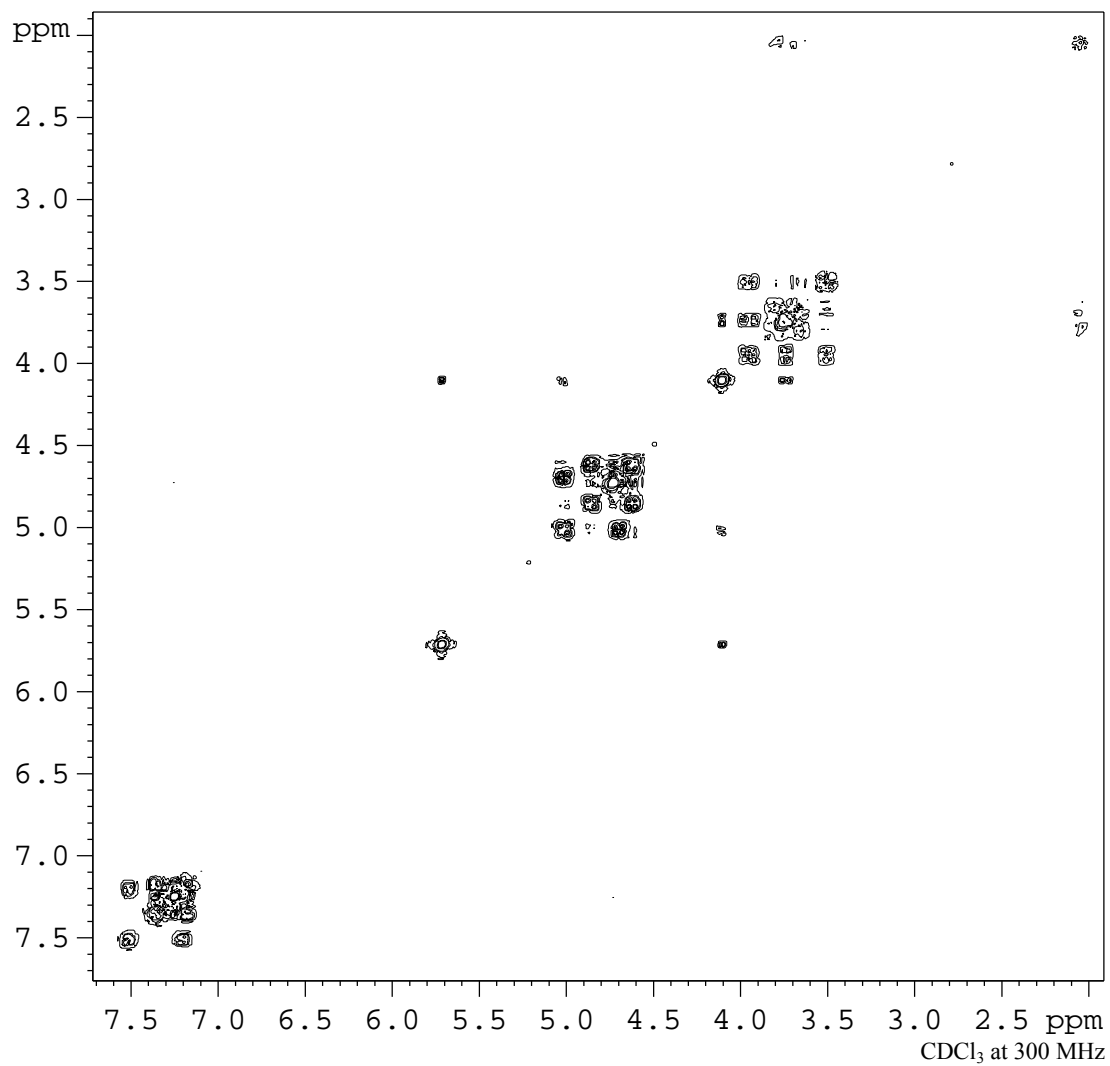
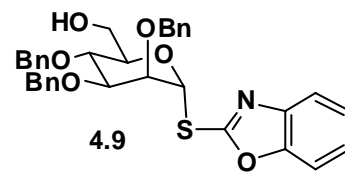


Figure A-27: 2-D NMR COSY spectrum of Benzoxazolyl 2,3,4-tri-O-benzyl-1-thio- α -D-mannopyranoside (**4.9**)

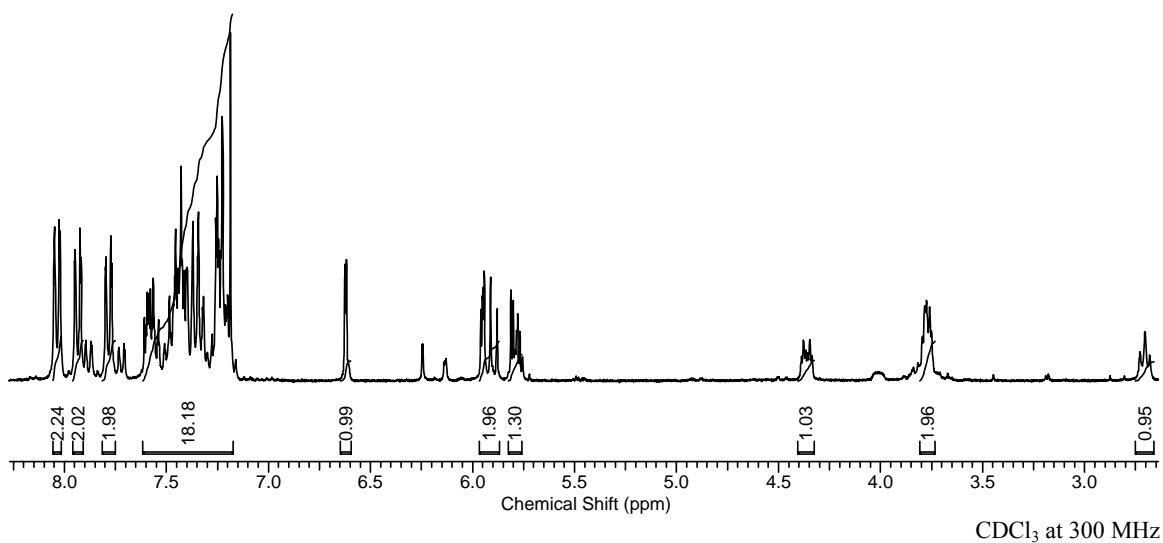
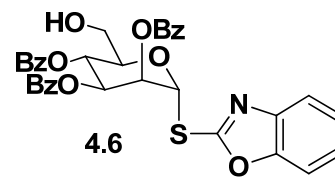


Figure A-28: ^1H NMR spectrum of Benzoxazolyl 2,3,4-tri-O-benzoyl-1-thio- α -D-mannopyranoside (**4.6**)

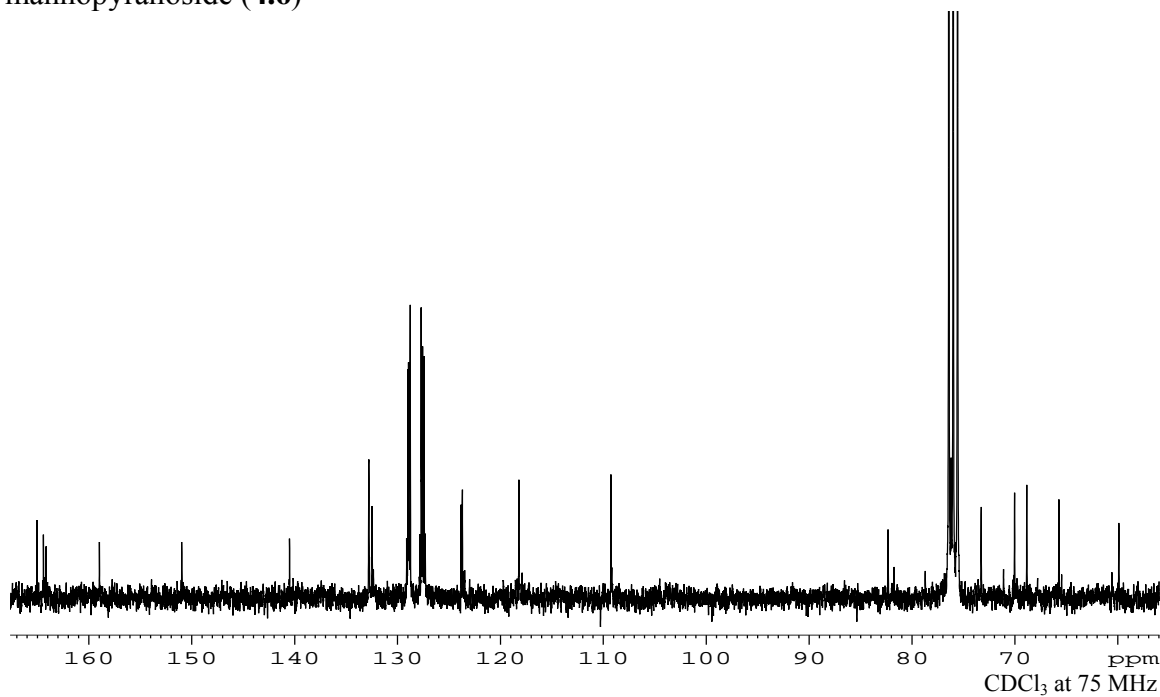


Figure A-29: ^{13}C NMR spectrum of Benzoxazolyl 2,3,4-tri-O-benzoyl-1-thio- α -D-mannopyranoside (**4.6**)

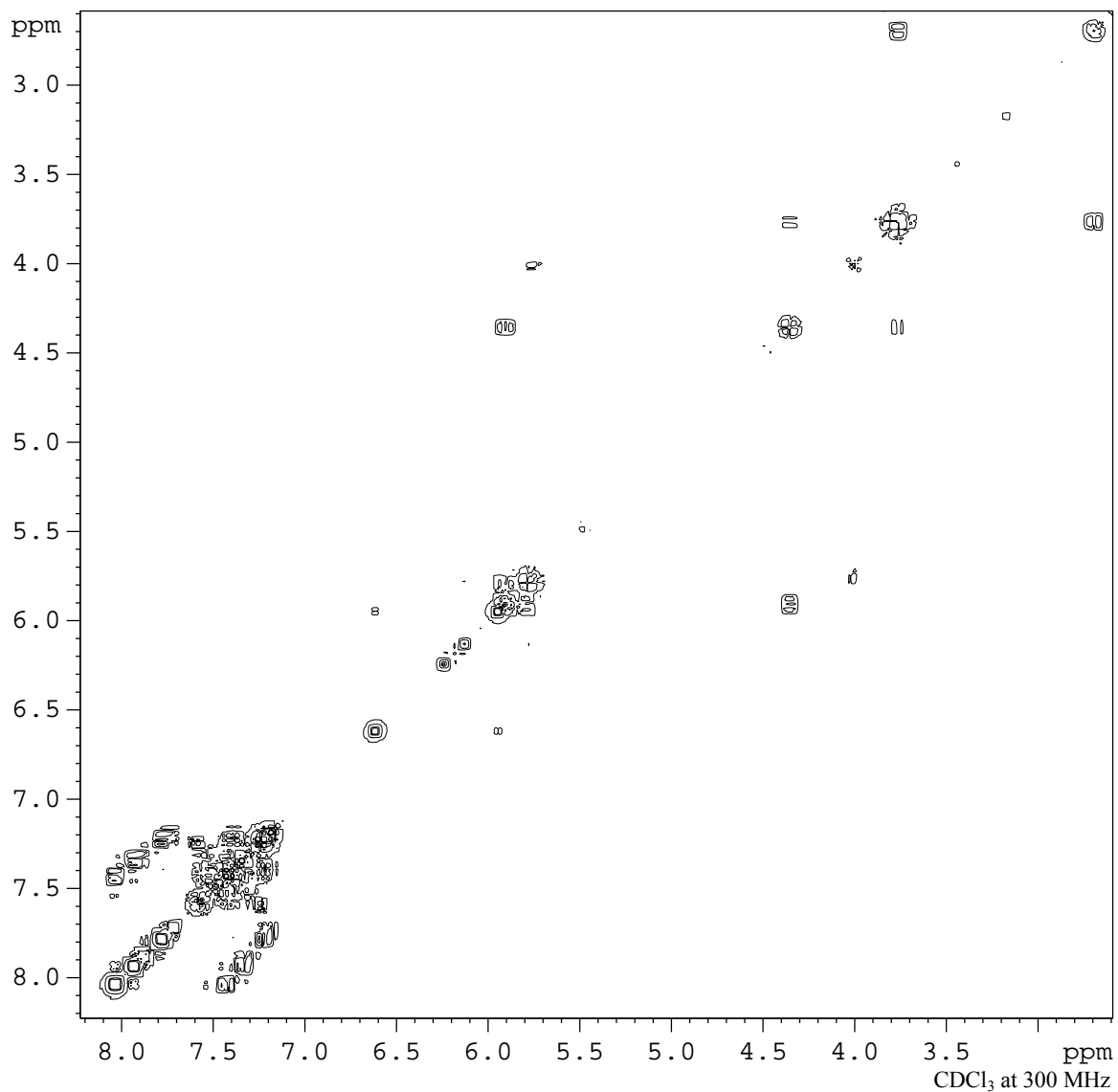
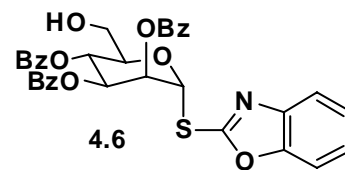


Figure A-30: 2-D NMR COSY spectrum of Benzoxazolyl 2,3,4-tri-O-benzoyl-1-thio- α -D-mannopyranoside (**4.6**)

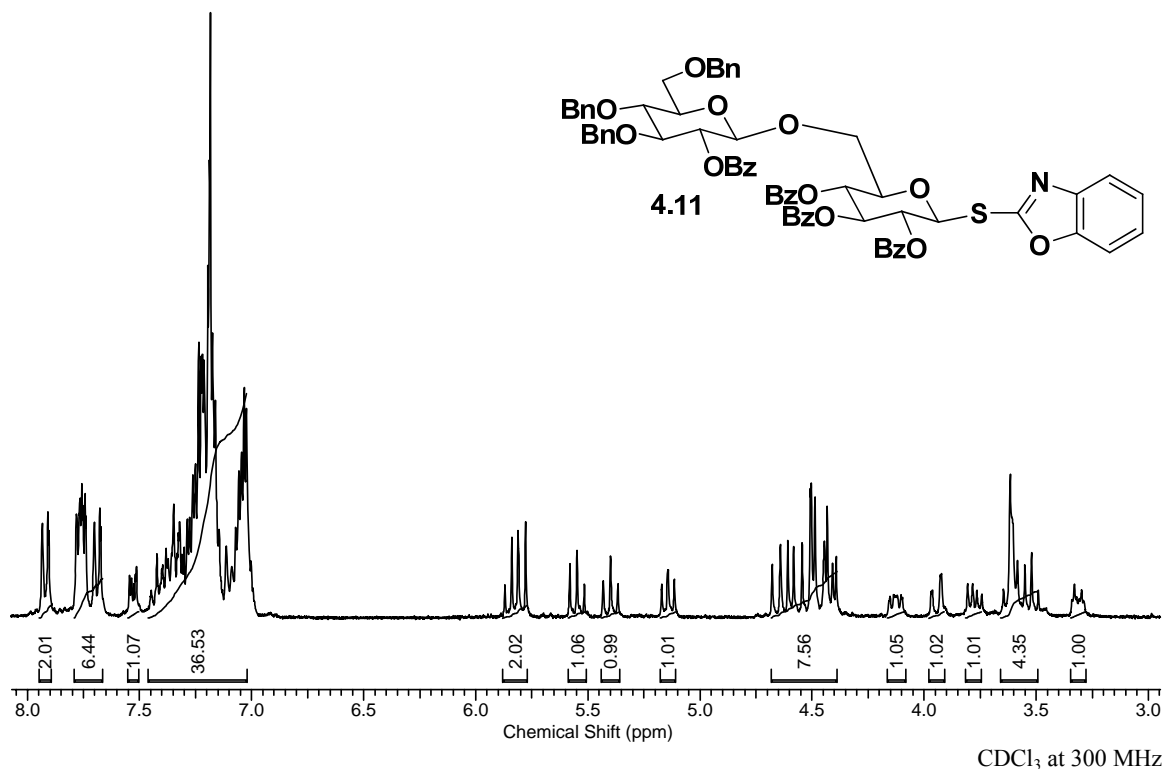


Figure A-31: ¹H NMR spectrum of Benzoxazolyl 2,3,4-tri-O-benzoyl-6-O-(2-O-benzoyl-3,4,6-tri-O-benzyl-β-D-glucopyranosyl)-1-thio-β-D-glucopyranoside (**4.11**)

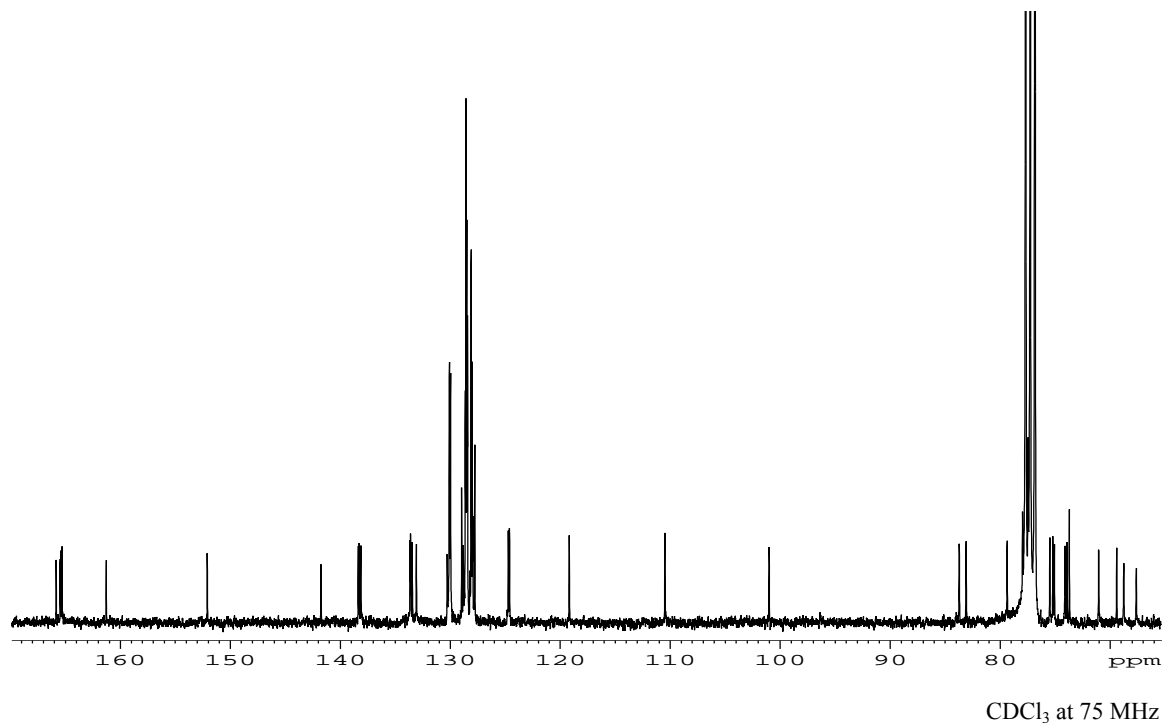


Figure A-32: ¹³C NMR spectrum of Benzoxazolyl 2,3,4-tri-O-benzoyl-6-O-(2-O-benzoyl-3,4,6-tri-O-benzyl-β-D-glucopyranosyl)-1-thio-β-D-glucopyranoside (**4.11**)

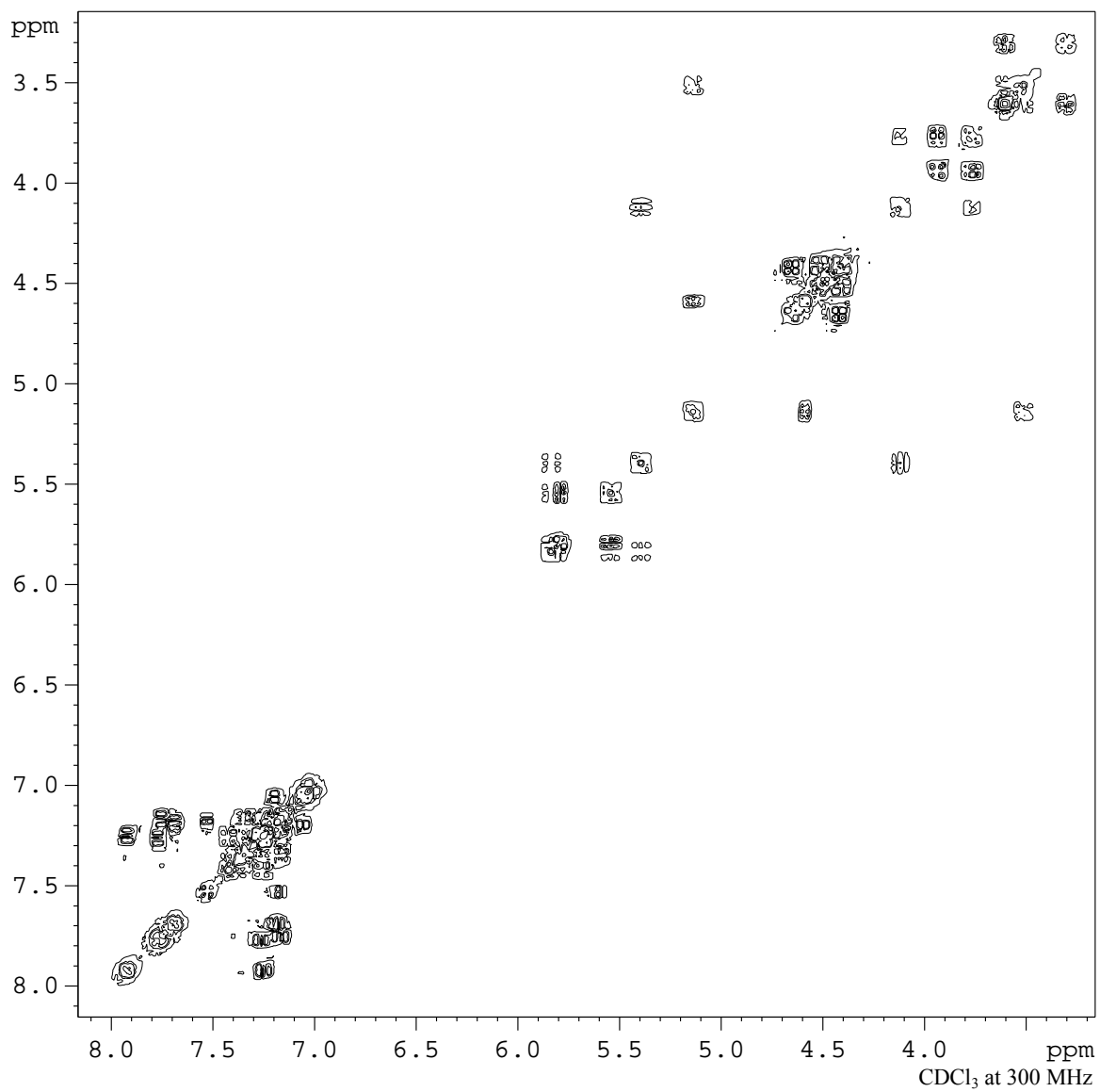
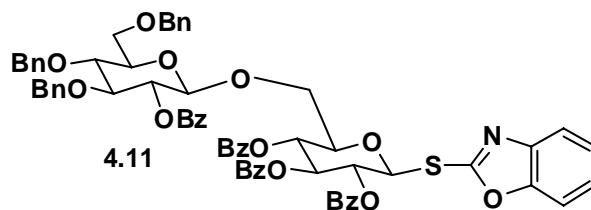


Figure A-33: 2-D NMR COSY spectrum of Benzoxazolyl 2,3,4-tri-O-benzoyl-6-O-(2-O-benzoyl-3,4,6-tri-O-benzyl- β -D-glucopyranosyl)-1-thio- β -D-glucopyranoside (**4.11**)

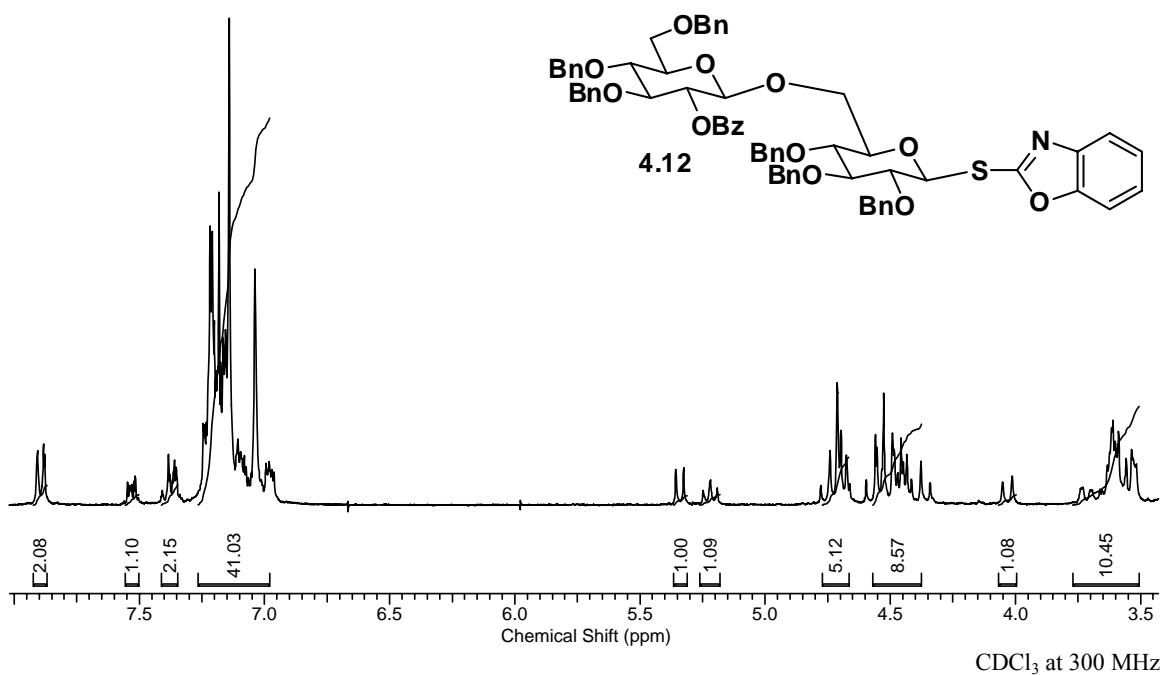


Figure A-34: ¹H NMR spectrum of Benzoxazolyl 6-O-(2-O-benzoyl-3,4,6-tri-O-benzyl- β -D-glucopyranosyl)-2,3,4-tri-O-benzyl-1-thio- β -D-glucopyranoside (**4.12**)

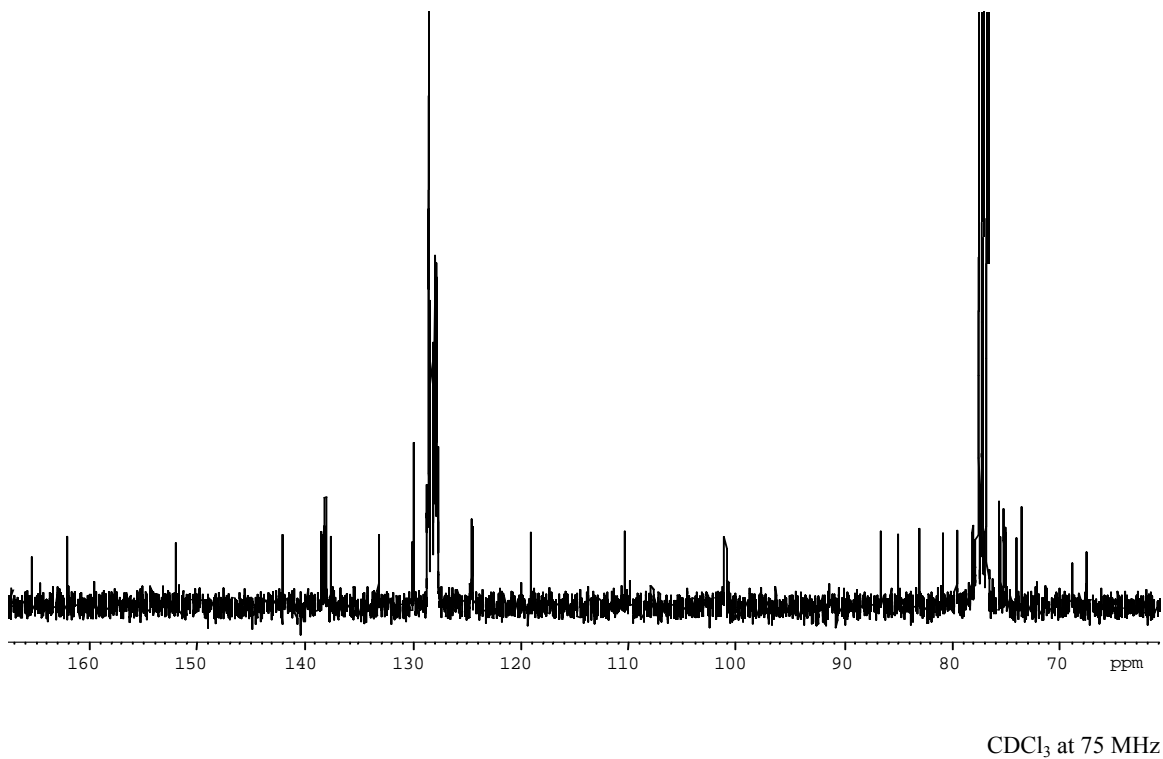


Figure A-35: ^{13}C NMR spectrum of Benzoxazolyl 6-O-(2-O-benzoyl-3,4,6-tri-O-benzyl- β -D-glucopyranosyl)-2,3,4-tri-O-benzyl-1-thio- β -D-glucopyranoside (**4.12**)

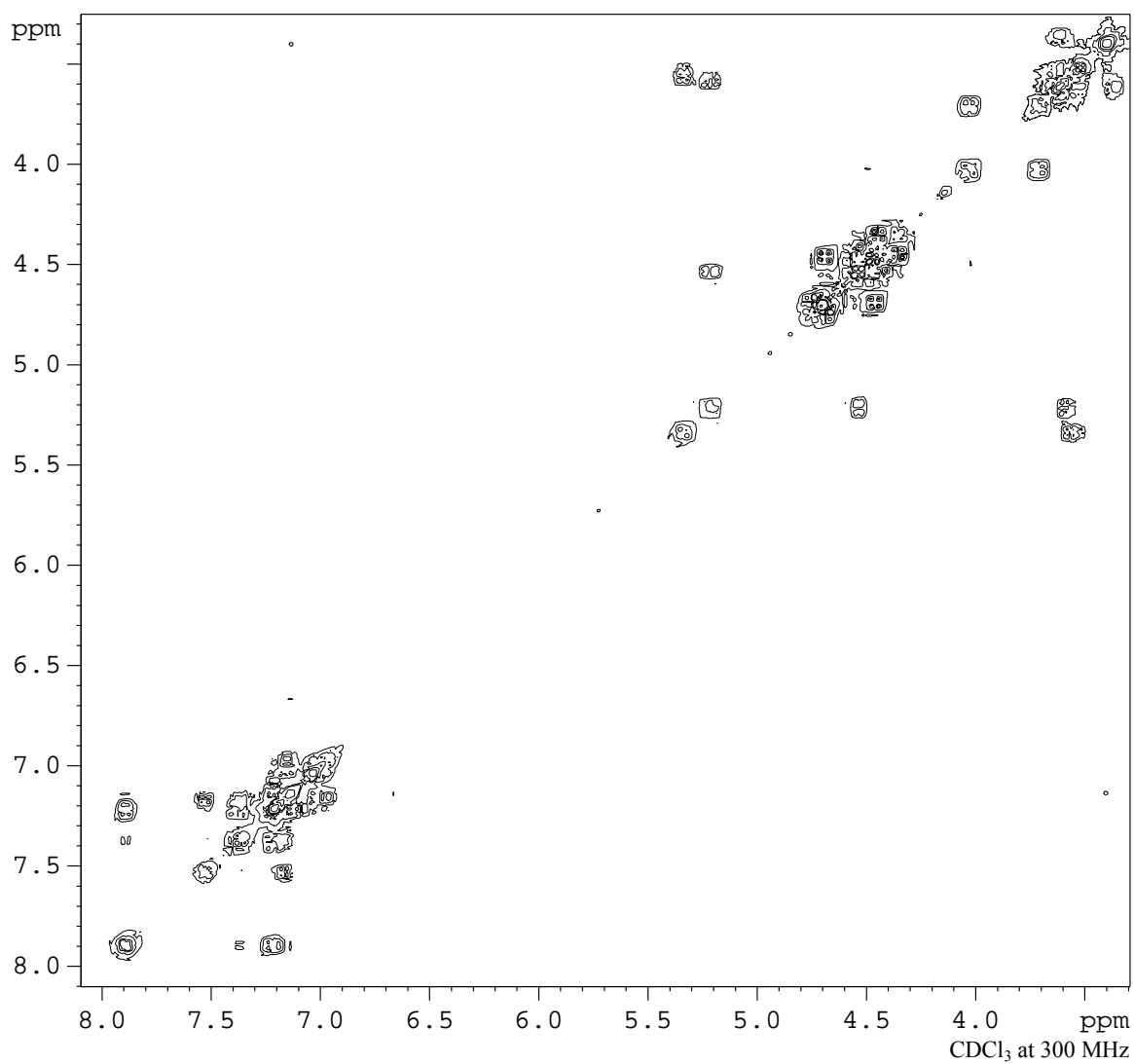
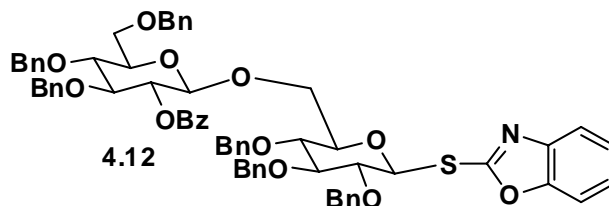


Figure A-36: 2-D NMR COSY spectrum of Benzoxazolyl 6-O-(2-O-benzoyl-3,4,6-tri-O-benzyl- β -D-glucopyranosyl)-2,3,4-tri-O-benzyl-1-thio- β -D-glucopyranoside (**4.12**)

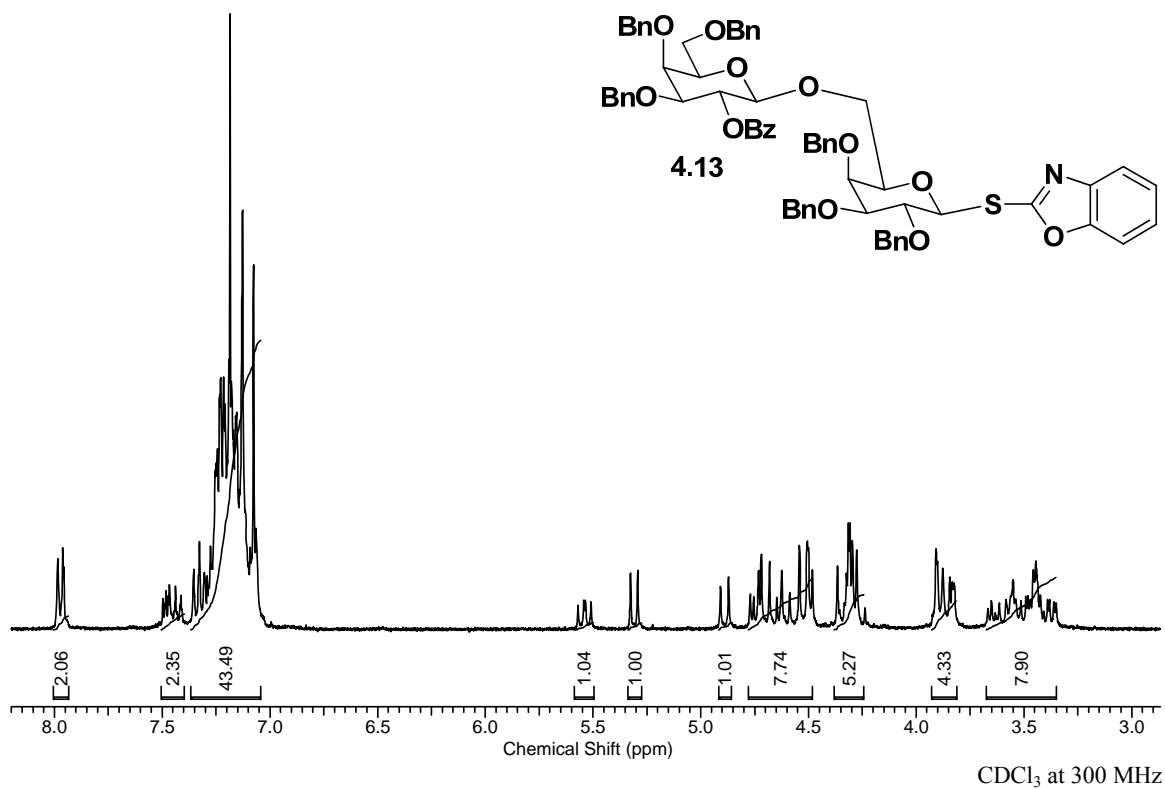


Figure A-37: ¹H NMR spectrum of Benzoxazolyl 6-O-(2-O-benzoyl-3,4,6-tri-O-benzyl-β-D-galactopyranosyl)-2,3,4-tri-O-benzyl-1-thio-β-D-galactopyranoside (**4.13**)

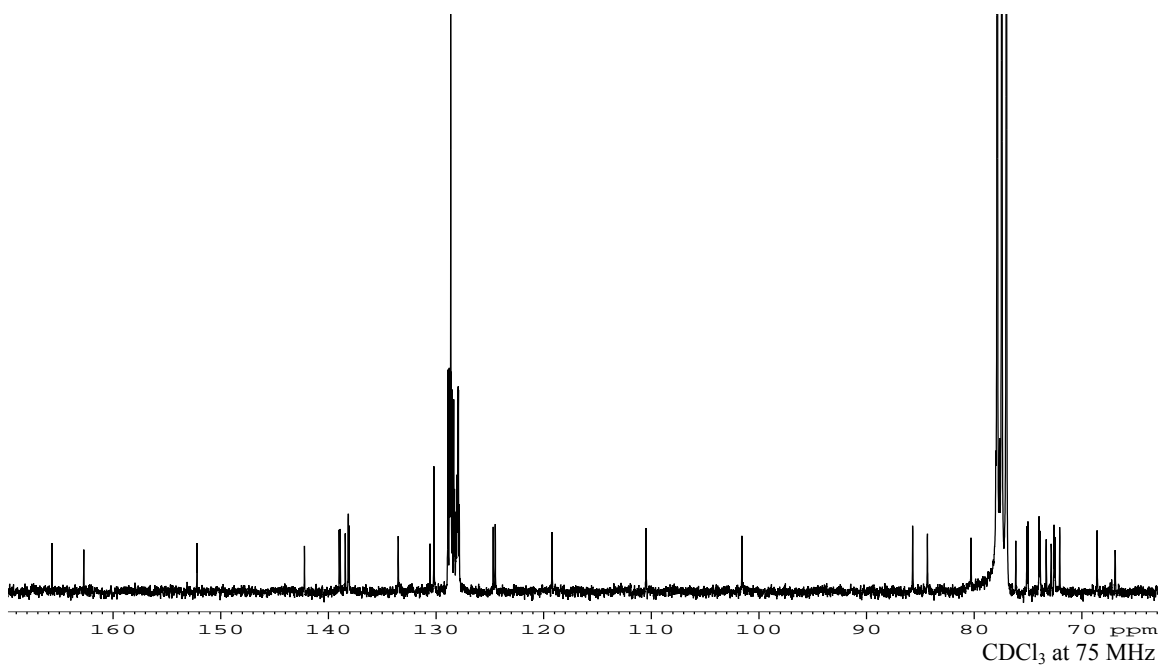


Figure A-38: ^{13}C NMR spectrum of Benzoxazolyl 6-O-(2-O-benzoyl-3,4,6-tri-O-benzyl- β -D-galactopyranosyl)-2,3,4-tri-O-benzyl-1-thio- β -D-galactopyranoside (**4.13**)

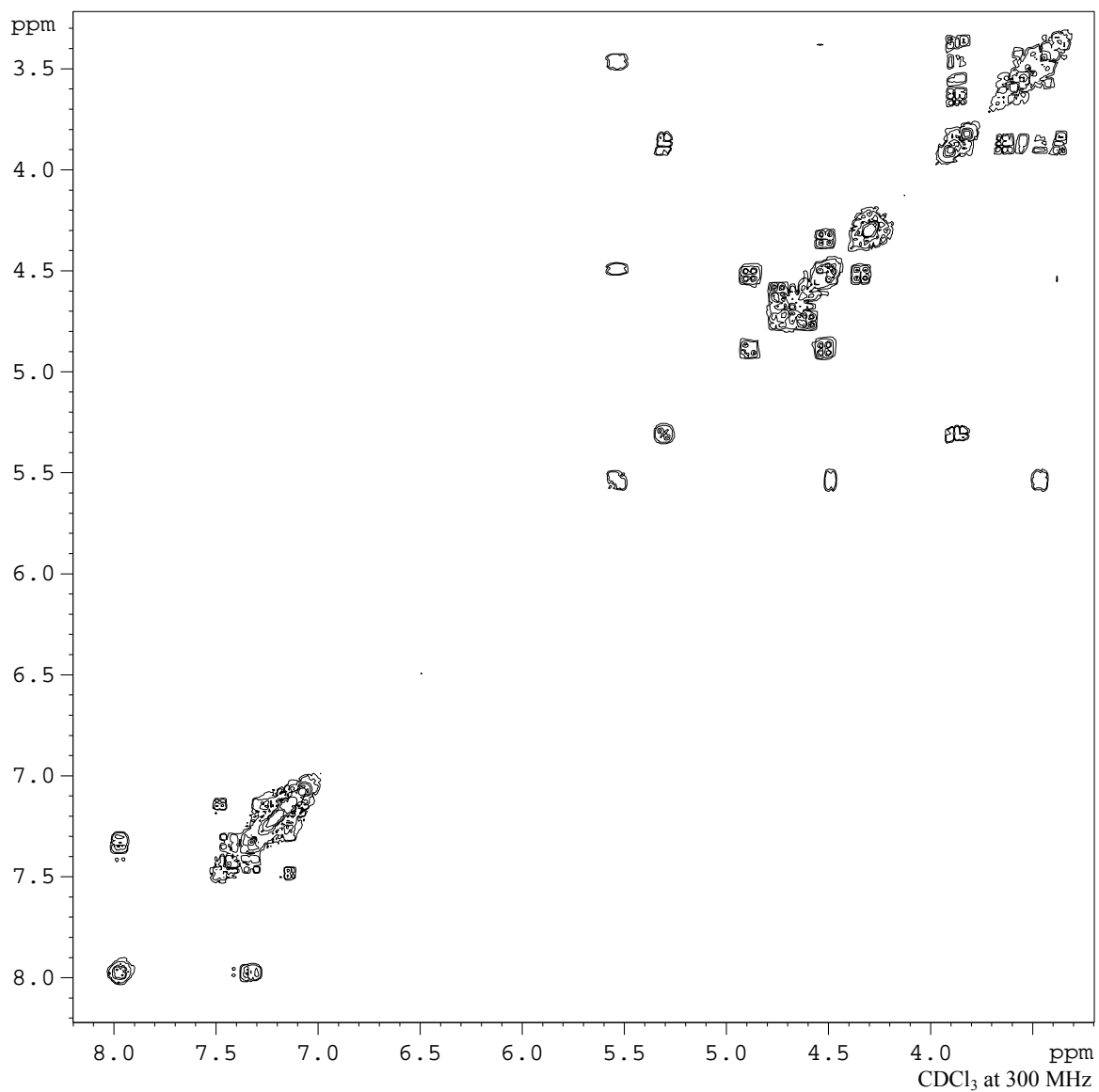
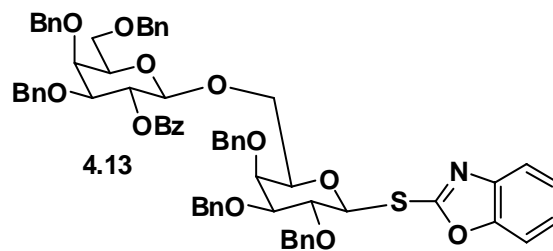


Figure A-39: 2-D NMR COSY spectrum of Benzoxazolyl 6-O-(2-O-benzoyl-3,4,6-tri-O-benzyl- β -D-galactopyranosyl)-2,3,4-tri-O-benzyl-1-thio- β -D-galactopyranoside (**4.13**)

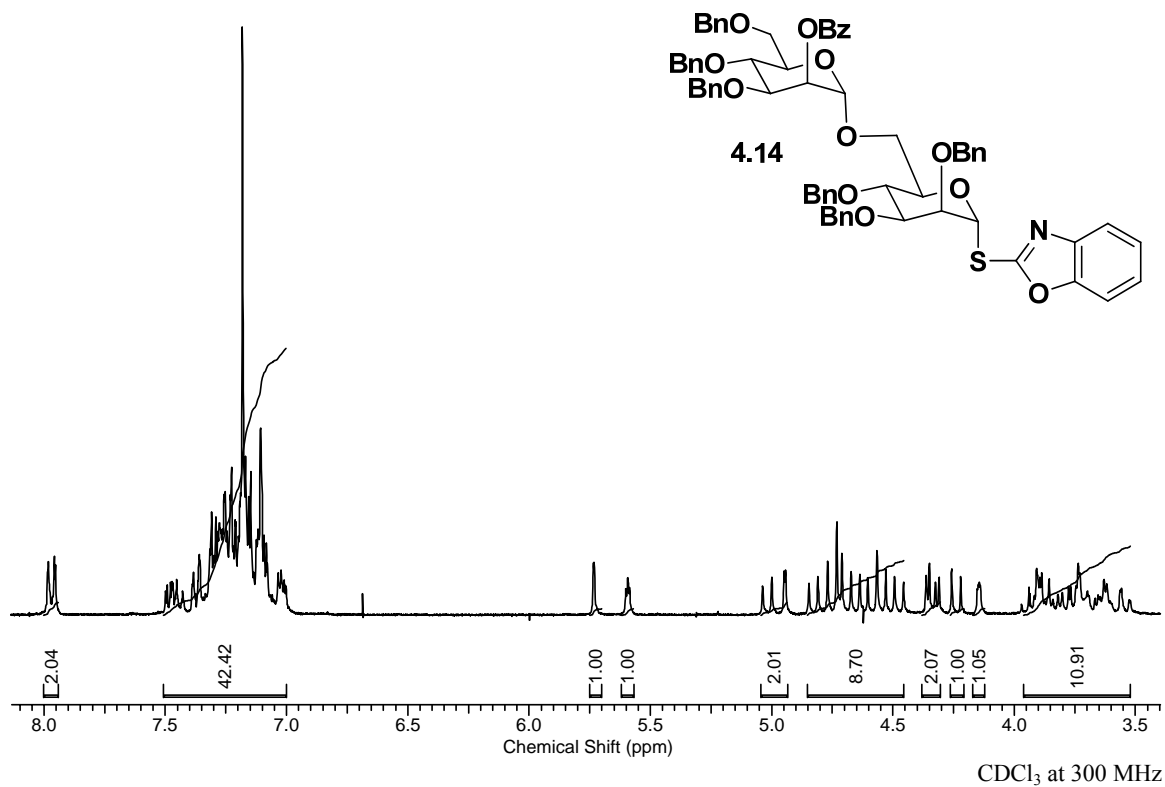


Figure A-40: ¹H NMR spectrum of Benzoxazolyl 6-O-(2-O-benzoyl-3,4,6-tri-O-benzyl- α -D-mannopyranosyl)-2,3,4-tri-O-benzyl-1-thio- α -D-mannopyranoside (**4.14**)

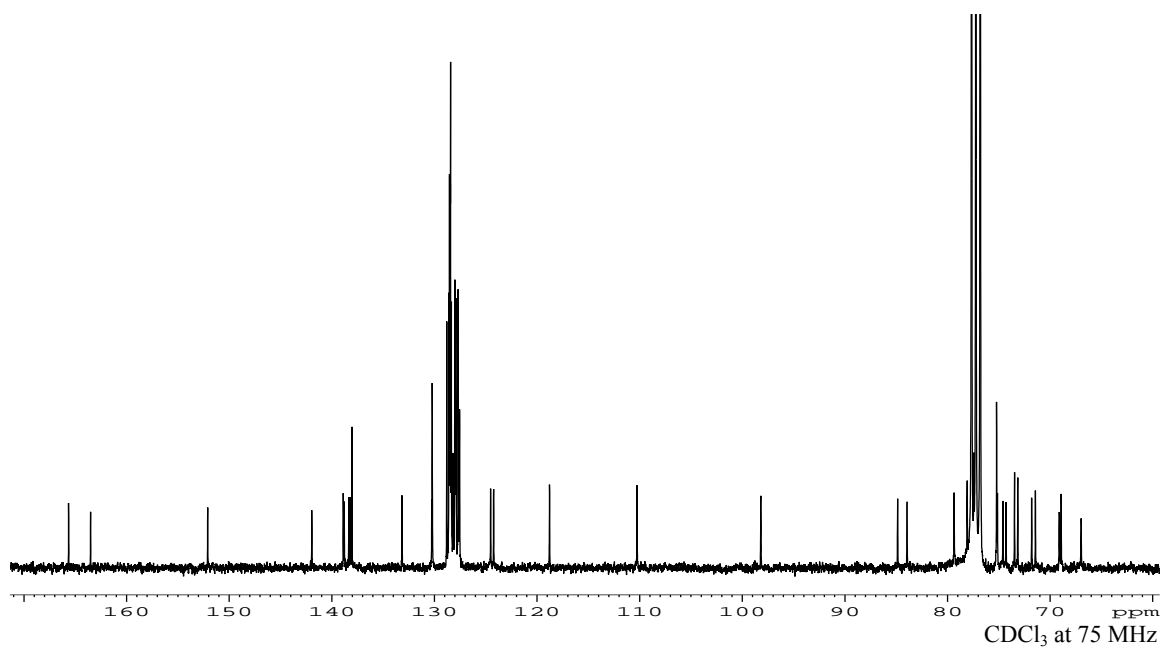


Figure A-41: ^{13}C NMR spectrum of Benzoxazolyl 6-O-(2-O-benzoyl-3,4,6-tri-O-benzyl- α -D-mannopyranosyl)-2,3,4-tri-O-benzyl-1-thio- α -D-mannopyranoside (**4.14**)

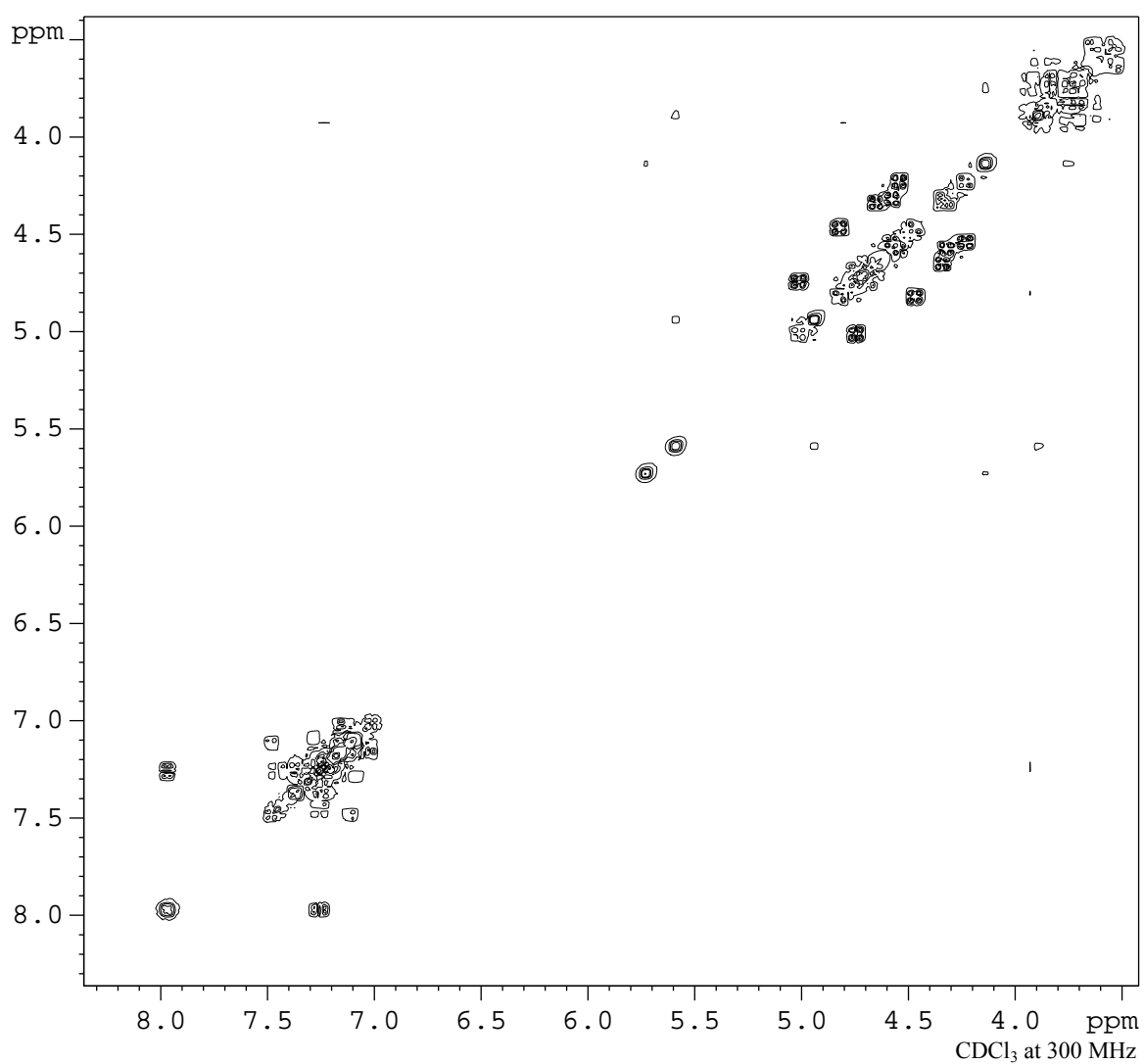
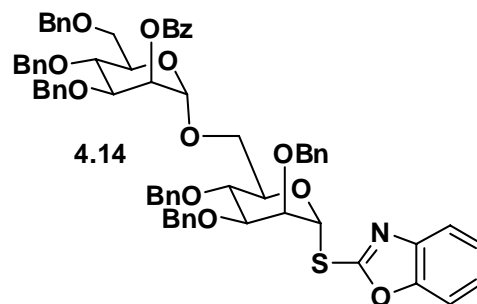


Figure A-42: 2-D NMR COSY spectrum of Benzoxazolyl 6-O-(2-O-benzoyl-3,4,6-tri-O-benzyl- α -D-mannopyranosyl)-2,3,4-tri-O-benzyl-1-thio- α -D-mannopyranoside (**4.14**)

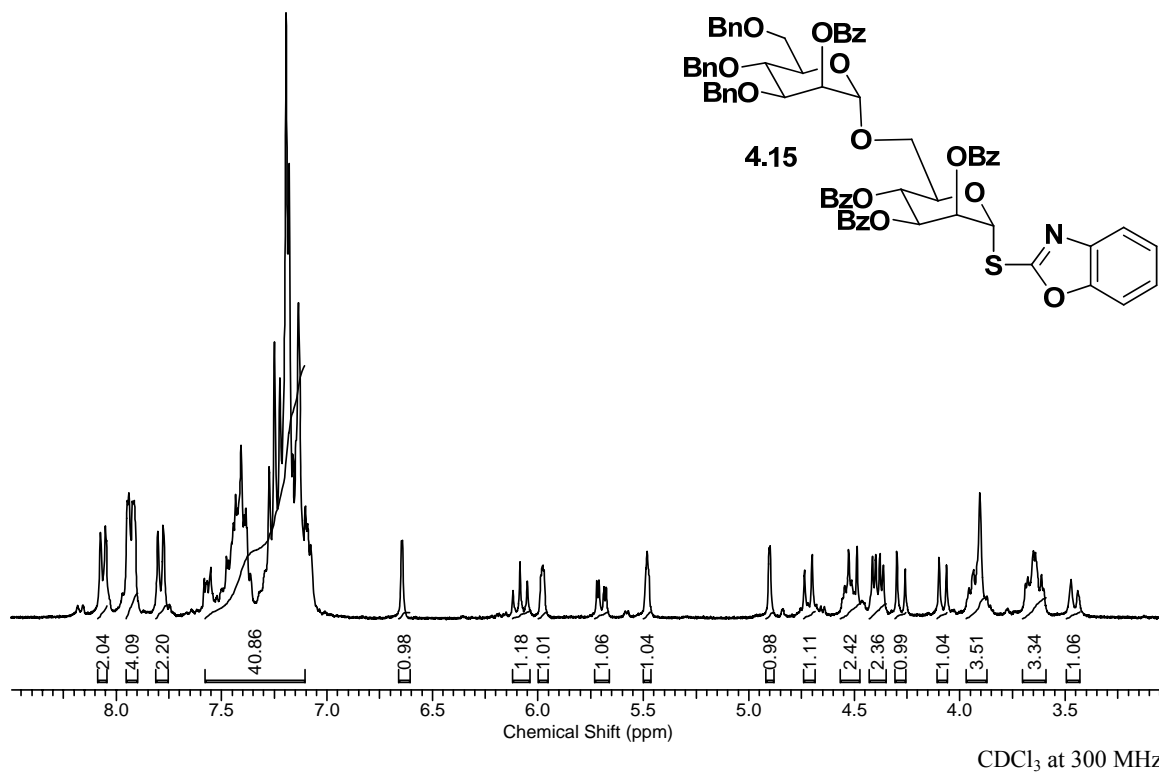


Figure A-43: ¹H NMR spectrum of Benzoxazolyl 2,3,4-tri-O-benzoyl-6-O-(2-O-benzoyl-3,4,6-tri-O-benzyl- α -D-mannopyranosyl)-1-thio- α -D-mannopyranoside (**4.15**)

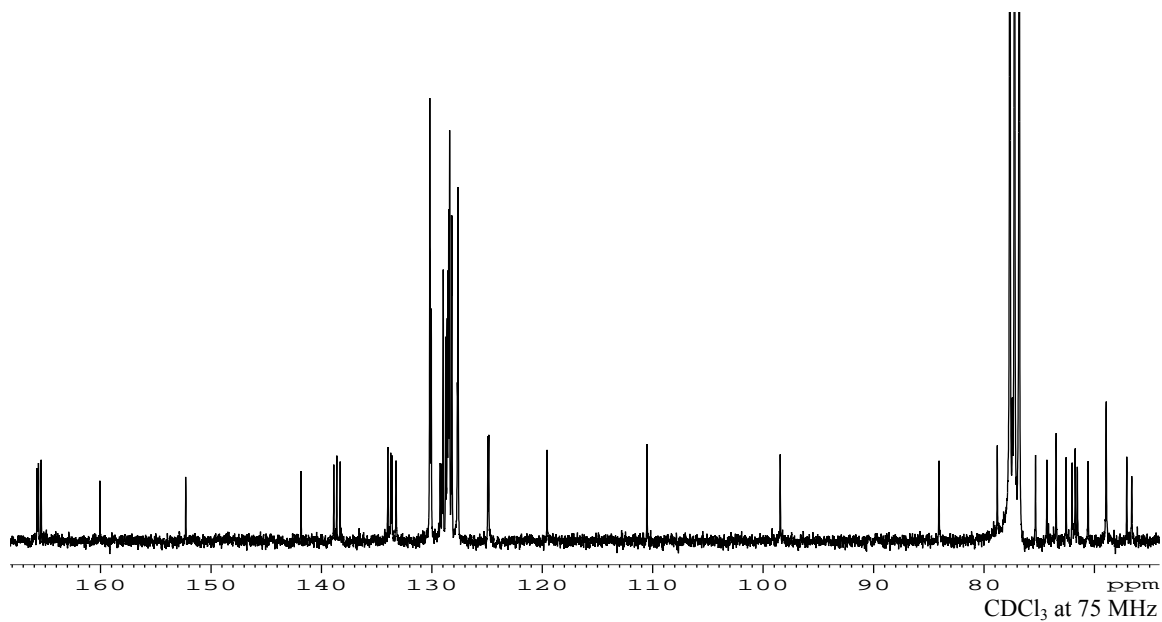


Figure A-44: ^{13}C NMR spectrum of Benzoxazolyl 2,3,4-tri-O-benzoyl-6-O-(2-O-benzoyl-3,4,6-tri-O-benzyl- α -D-mannopyranosyl)-1-thio- α -D-mannopyranoside (**4.15**)

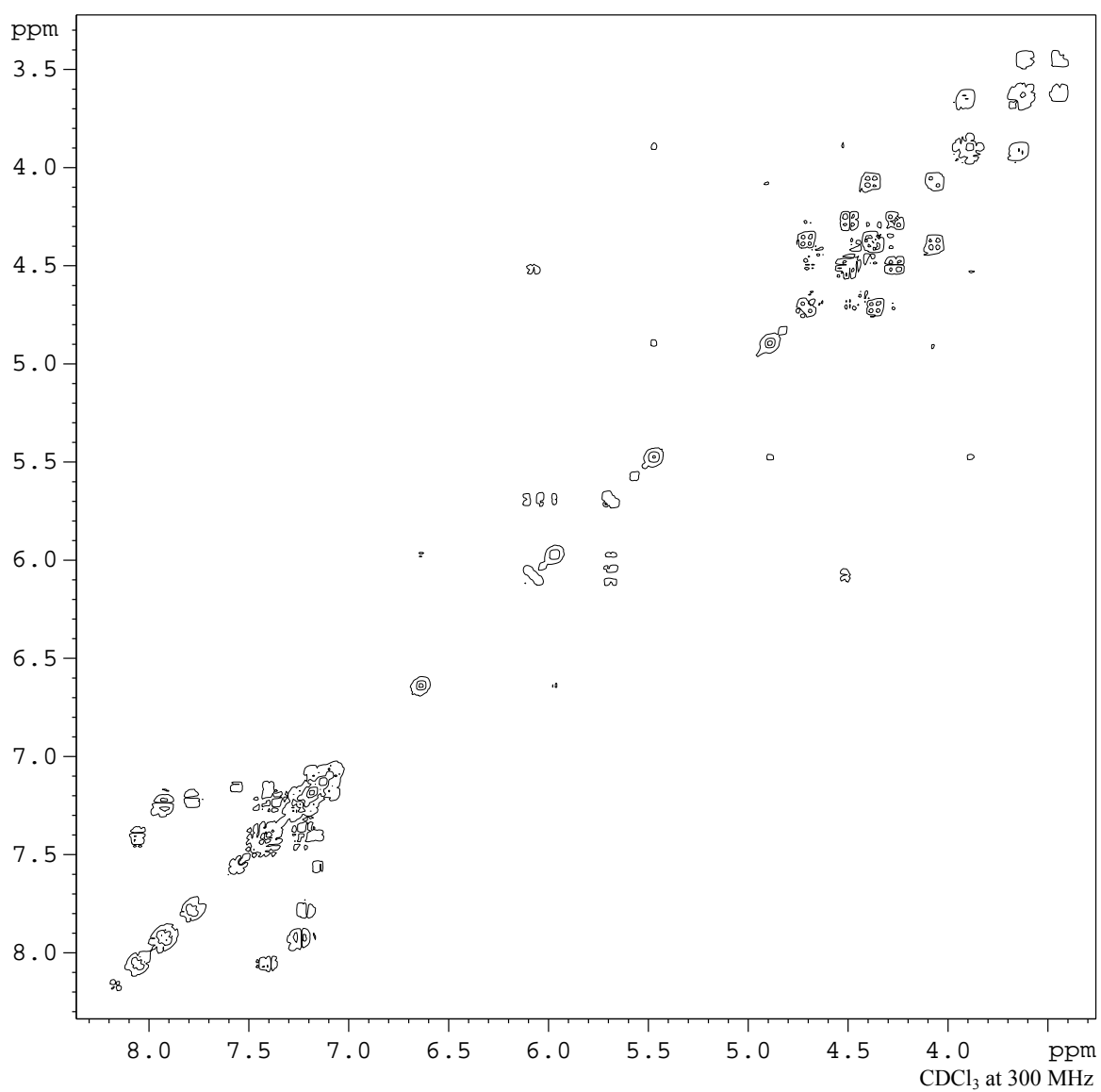
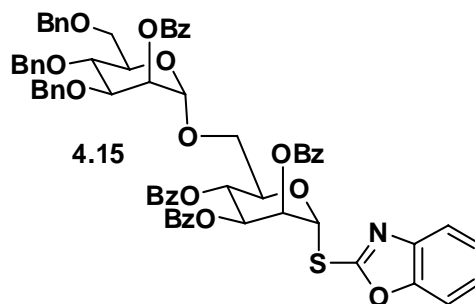


Figure A-45: 2-D NMR COSY spectrum of Benzoxazolyl 2,3,4-tri-O-benzoyl-6-O-(2-O-benzoyl-3,4,6-tri-O-benzyl- α -D-mannopyranosyl)-1-thio- α -D-mannopyranoside (**4.15**)

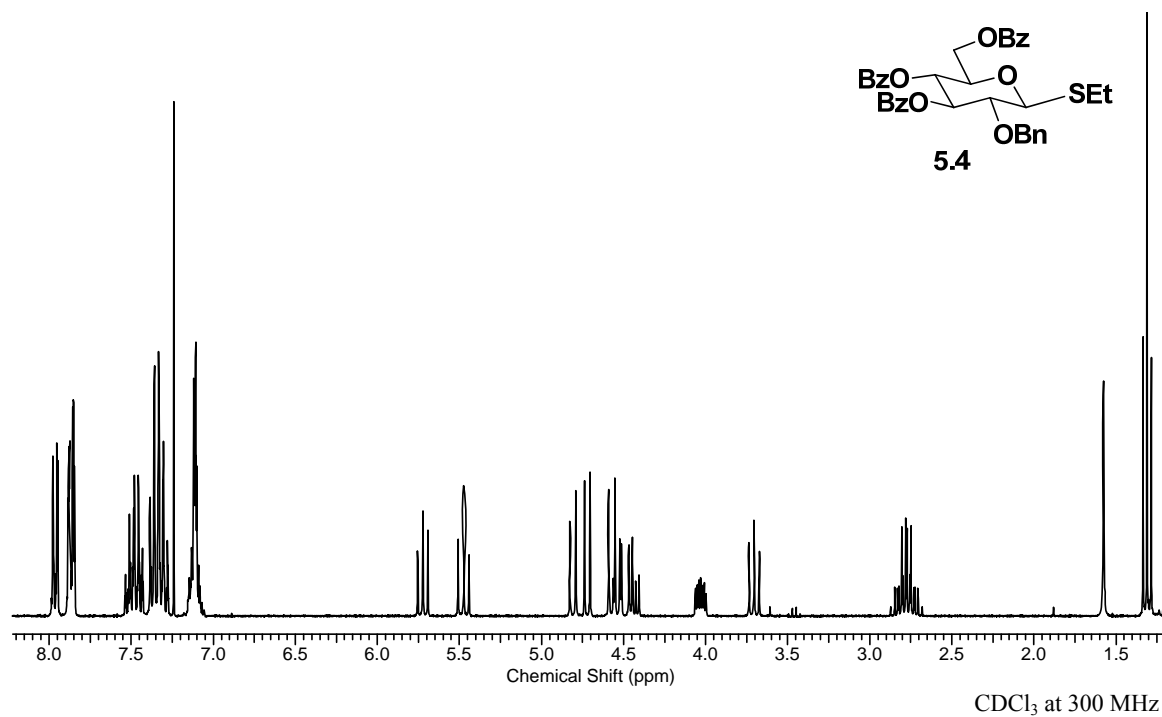


Figure A-46: ¹H NMR spectrum of Ethyl 2-O-benzyl-3,4,6-tri-O-benzoyl-1-thio- β -D-glucopyranoside (**5.4**)

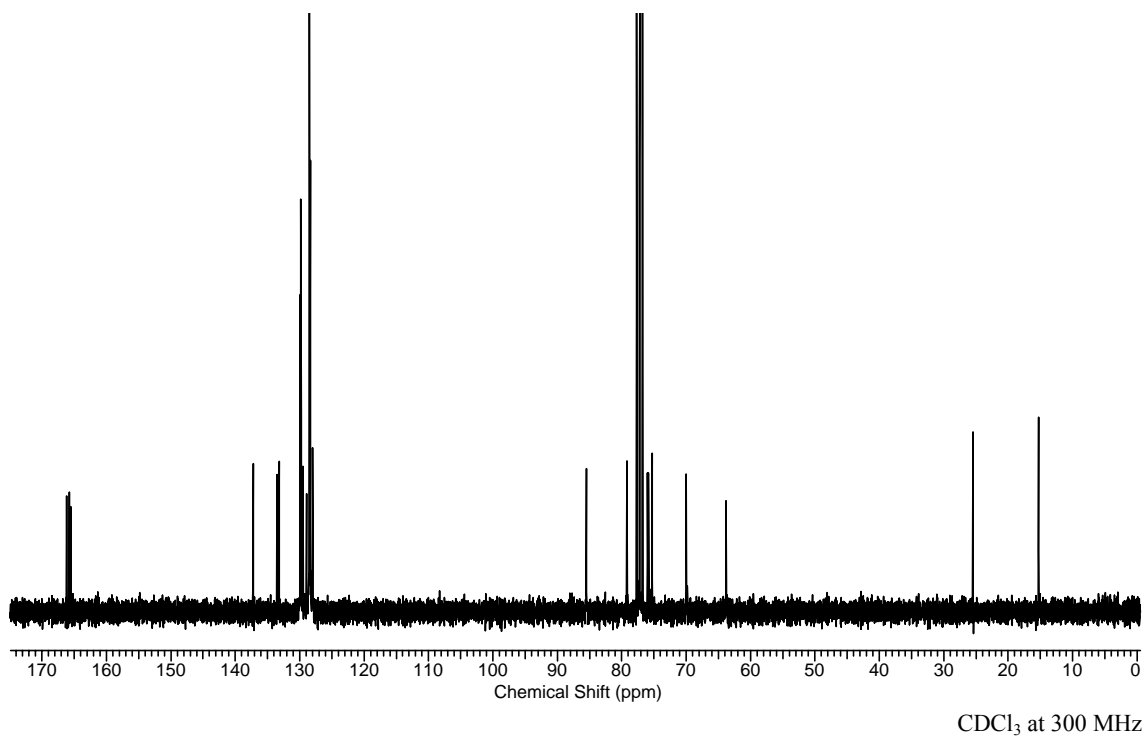
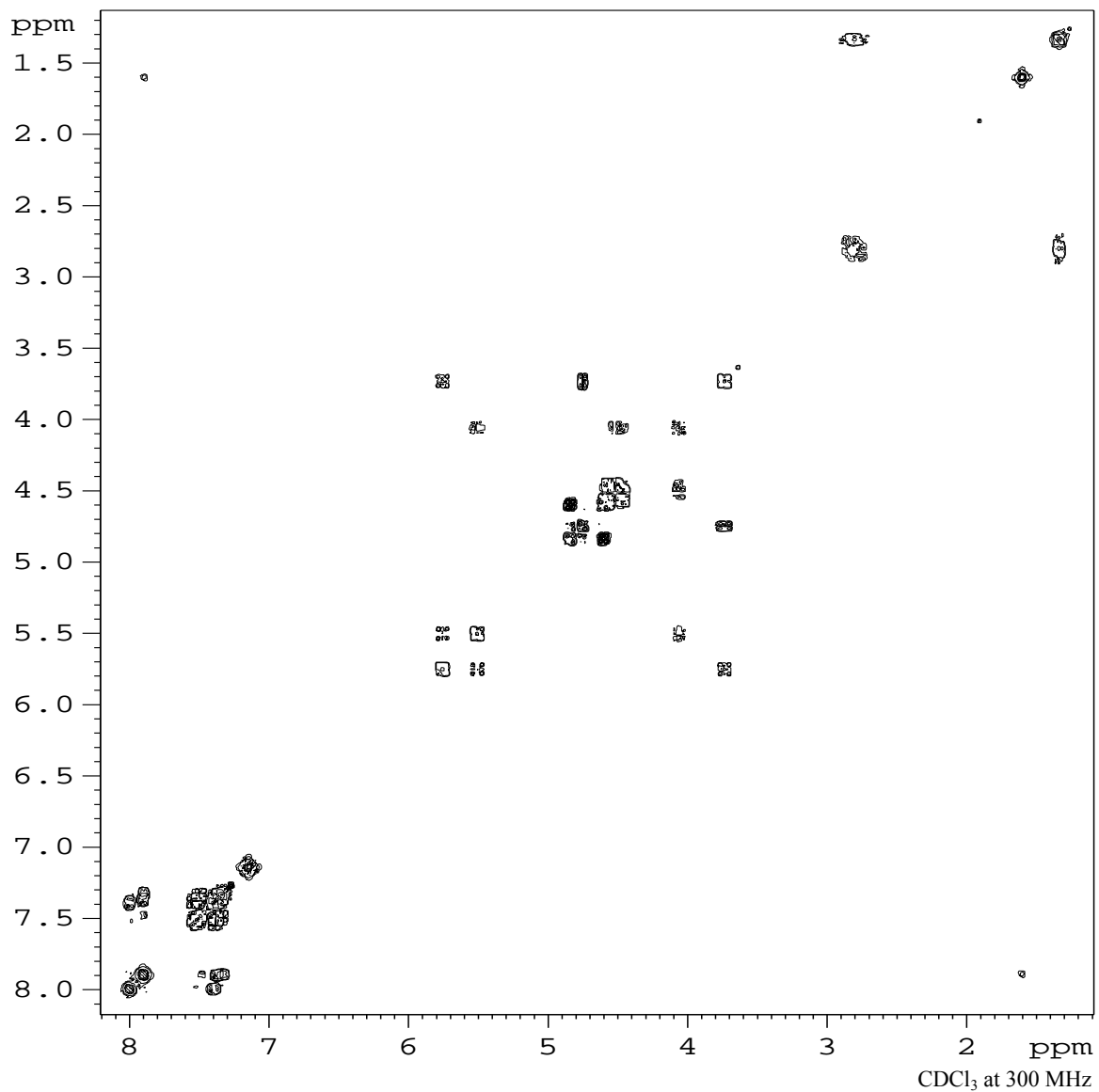
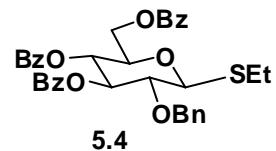


Figure A-47: ^{13}C NMR spectrum of Ethyl 2-O-benzyl-3,4,6-tri-O-benzoyl-1-thio- β -D-glucopyranoside (**5.4**)Figure A-48: 2-D NMR COSY spectrum of Ethyl 2-O-benzyl-3,4,6-tri-O-benzoyl-1-thio- β -D-glucopyranoside (**5.4**)

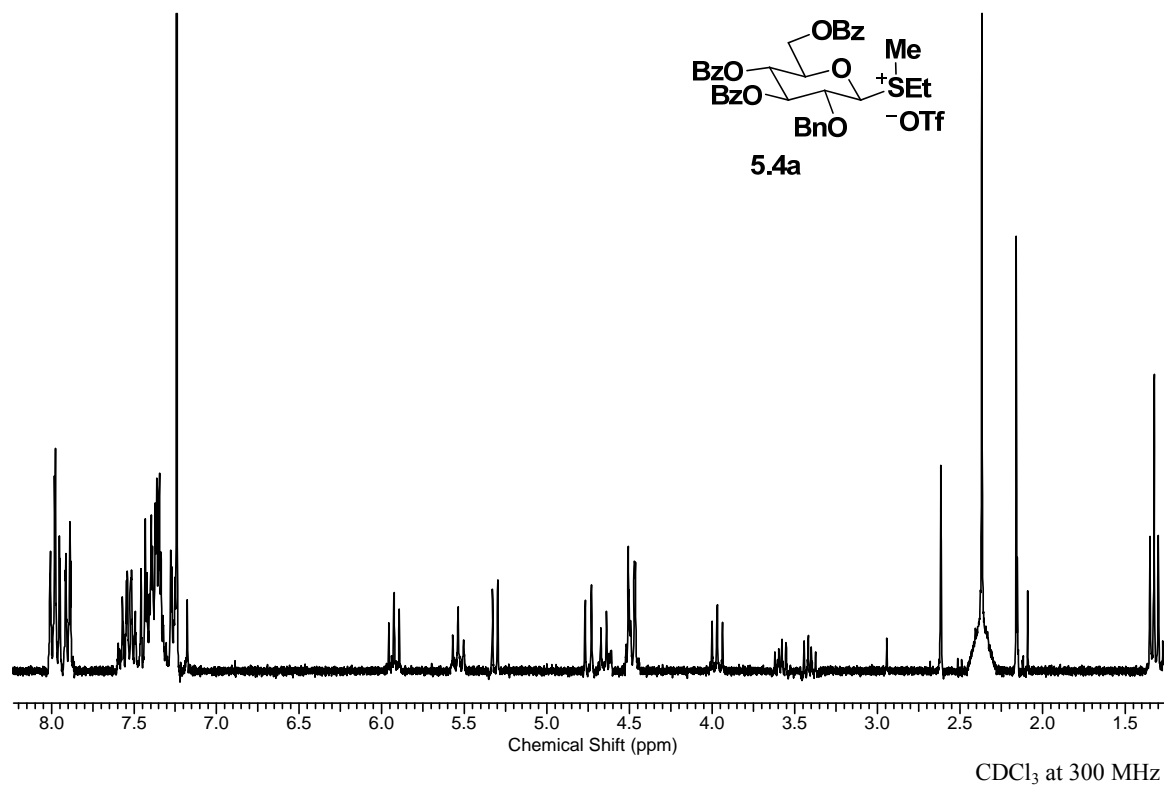


Figure A-49: ¹H NMR spectrum of (2-O-benzyl-3,4,6-tri-O-benzoyl-β-D-glucopyranosyl)ethylmethylsulfonium triflate (**5.4a**)

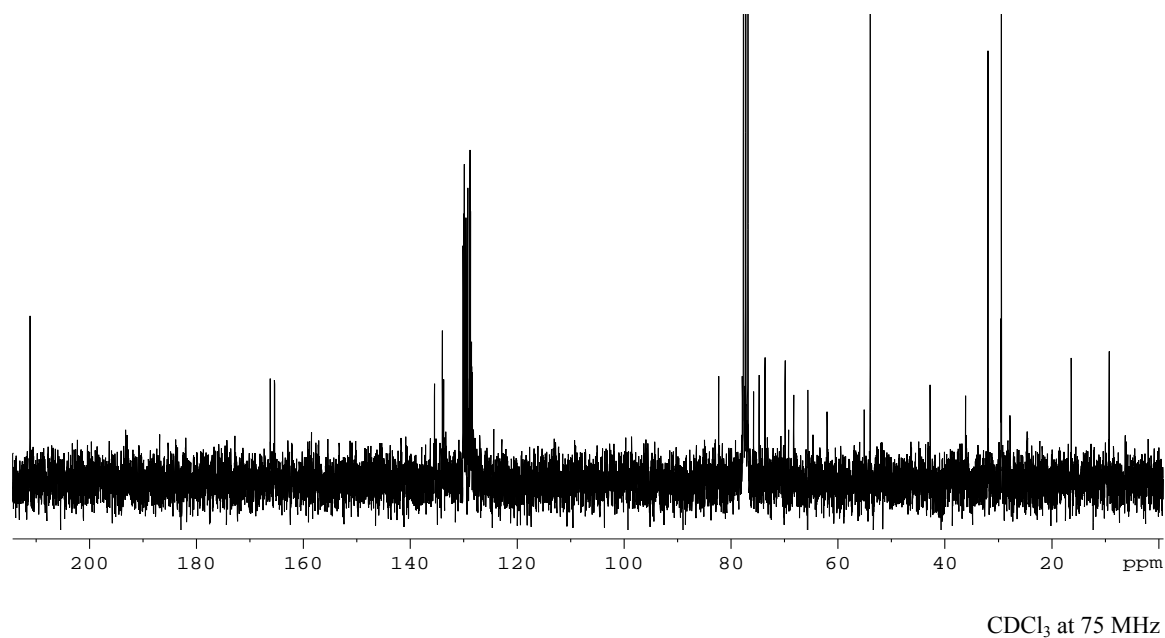
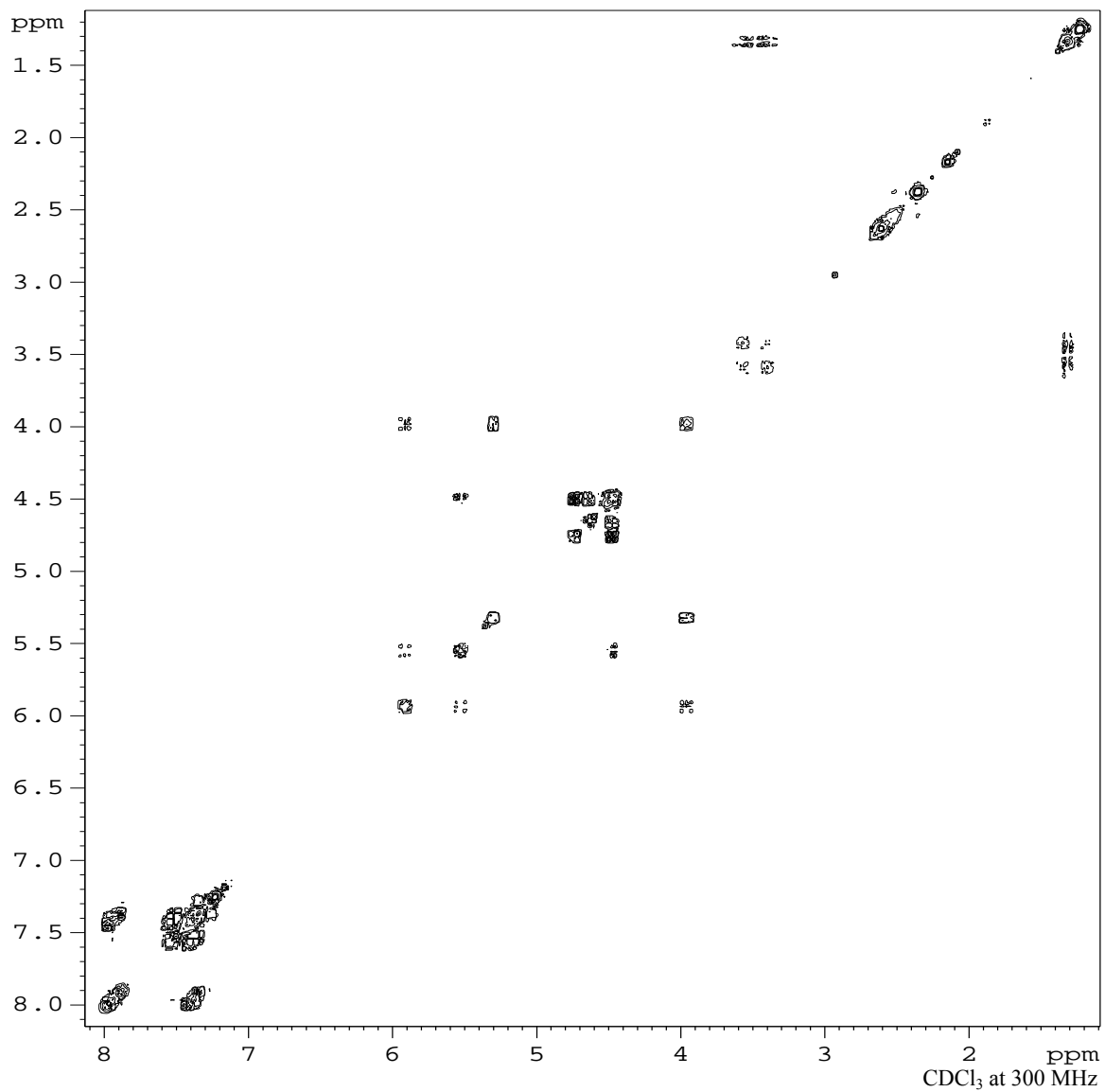
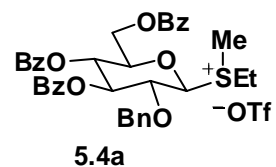


Figure A-50: ^{13}C NMR spectrum of (2-O-benzyl-3,4,6-tri-O-benzoyl- β -D-glucopyranosyl)ethylmethylsulfonium triflate (**5.4a**)Figure A-51: 2-D NMR COSY spectrum of (2-O-benzyl-3,4,6-tri-O-benzoyl- β -D-glucopyranosyl)ethylmethylsulfonium triflate (**5.4a**)

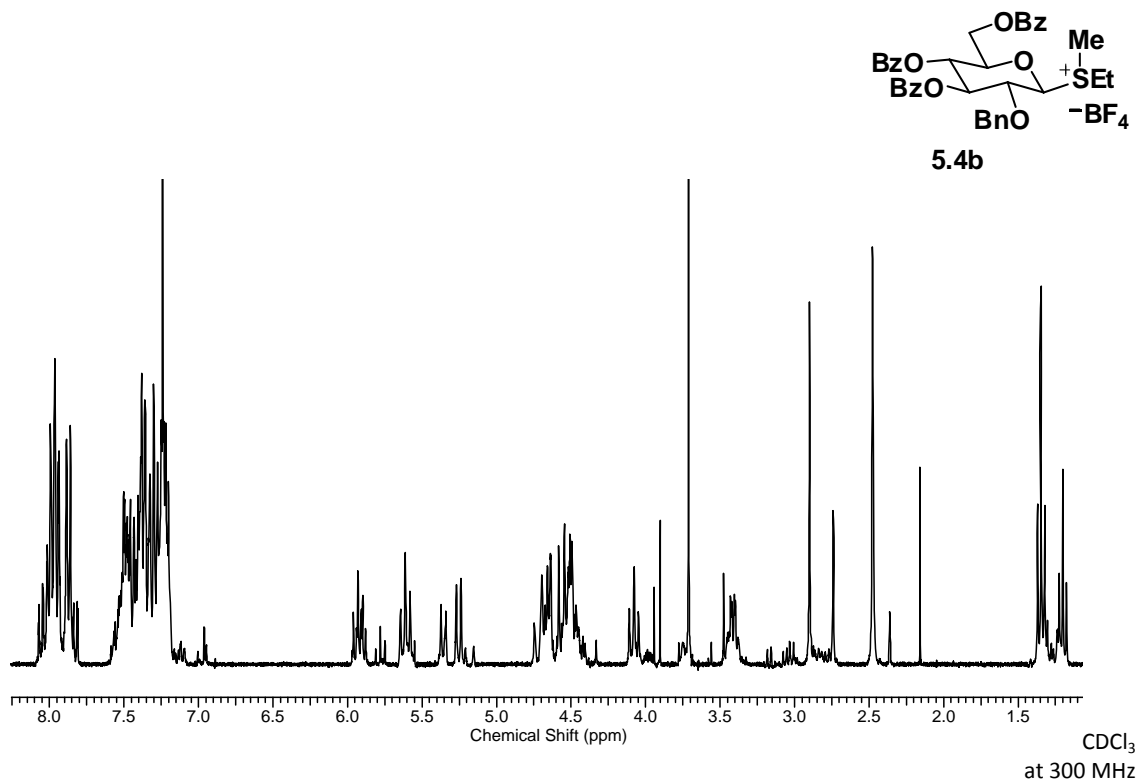


Figure A-52: ¹H NMR spectrum of (2-O-benzyl-3,4,6-tri-O-benzoyl-β-D-glucopyranosyl)ethylmethylsulfonium tetrafluoroborate (**5.4b**)

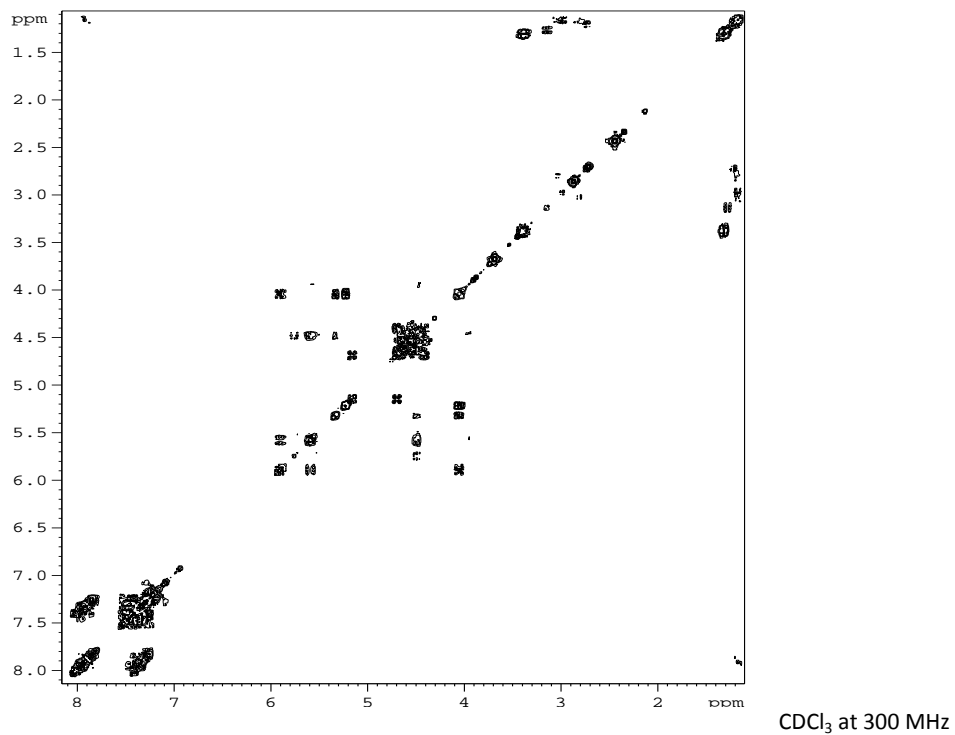


Figure A-53: 2-D NMR COSY spectrum of (2-O-benzyl-3,4,6-tri-O-benzoyl- β -D-glucopyranosyl)ethylmethylsulfonium tetrafluoroborate (**5.4b**)

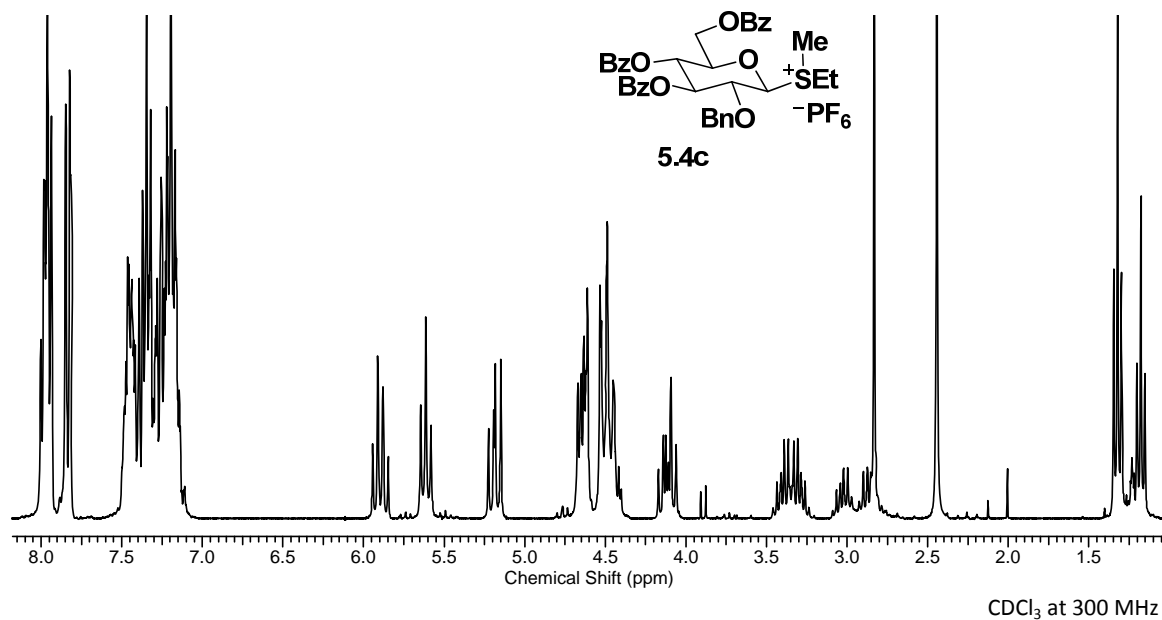


Figure A-54: ¹H NMR spectrum of (2-O-benzyl-3,4,6-tri-O-benzoyl- β -D-glucopyranosyl)ethylmethylsulfonium hexafluorophosphate (**5.4c**)

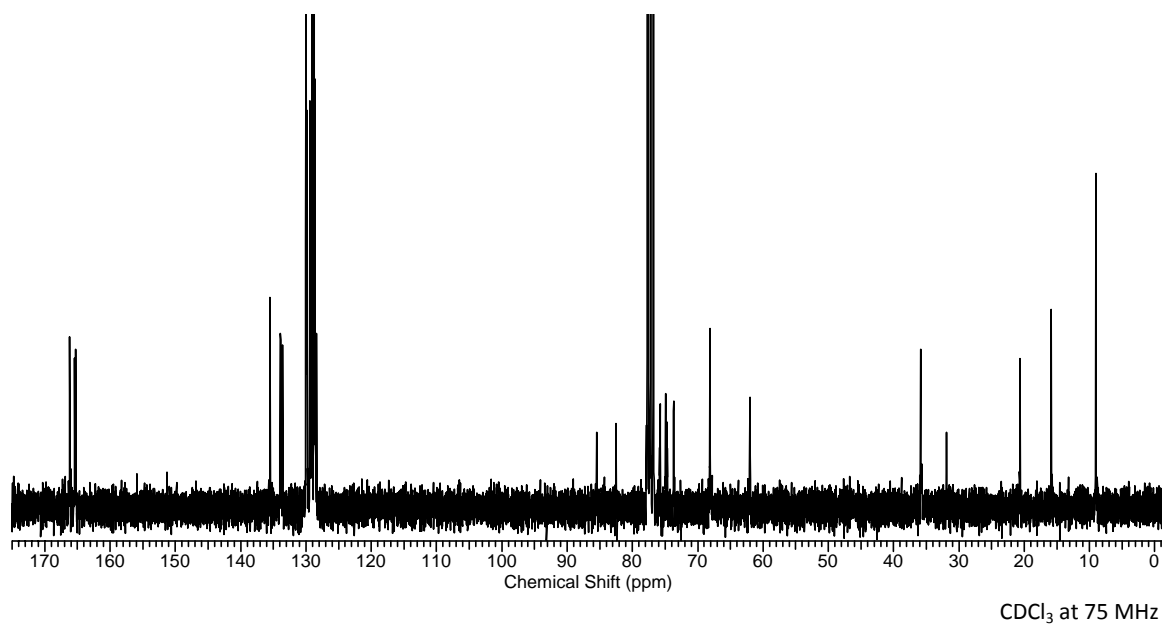


Figure A-55: ^{13}C NMR spectrum of (2-O-benzyl-3,4,6-tri-O-benzoyl- β -D-glucopyranosyl)ethylmethylsulfonium hexafluorophosphate (**5.4c**)

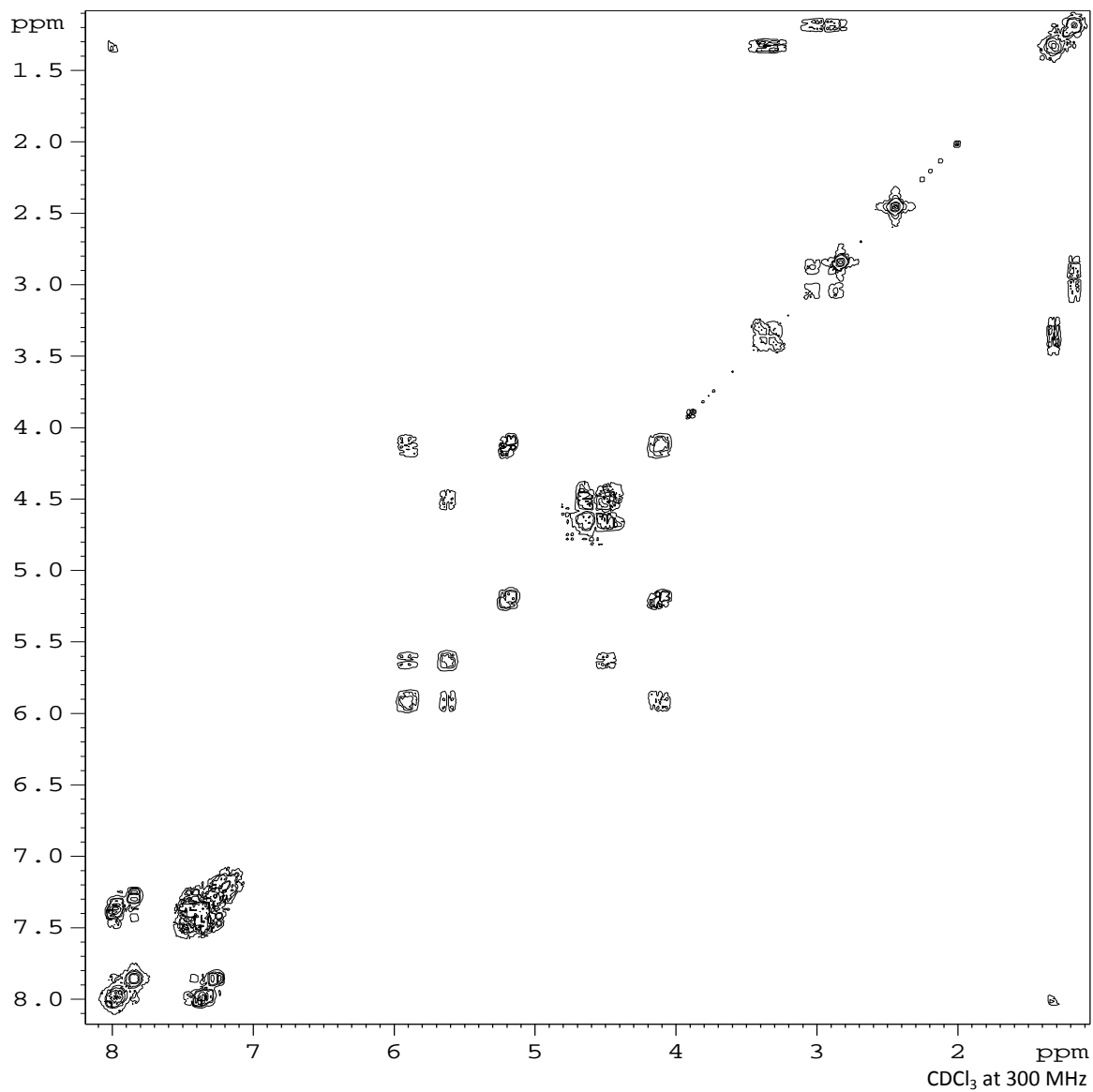
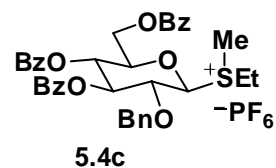


Figure A-56: 2-D NMR COSY spectrum of (2-O-benzyl-3,4,6-tri-O-benzoyl- β -D-glucopyranosyl)ethylmethylsulfonium hexafluorophosphate (**5.4c**)

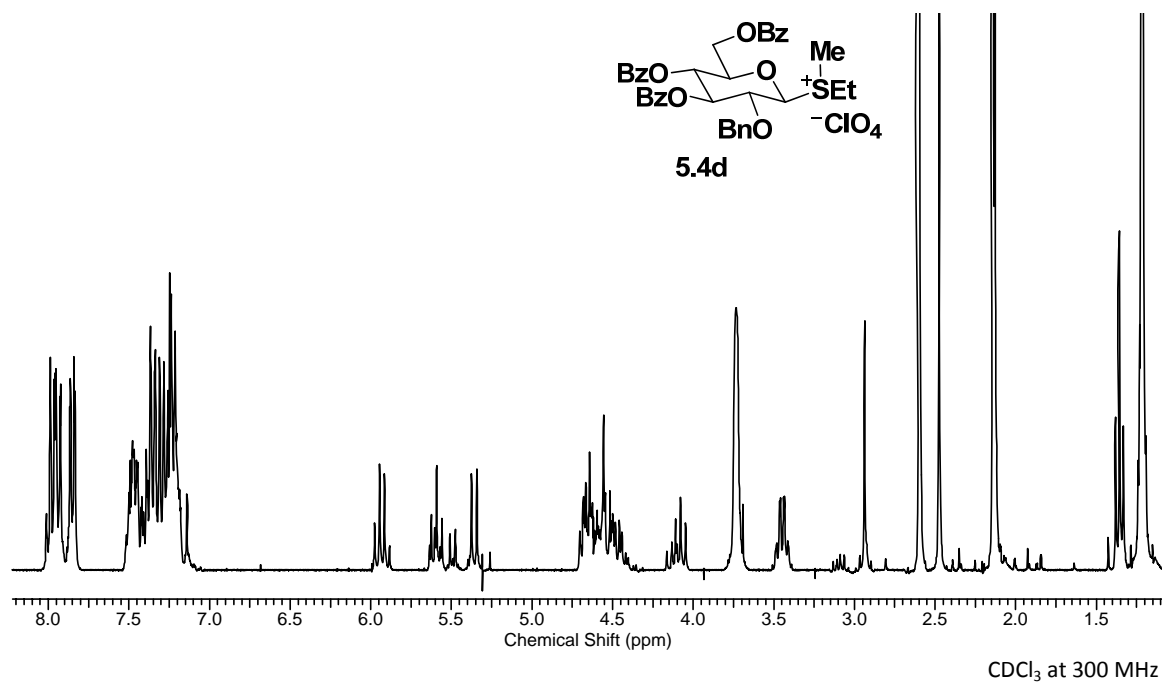


Figure A-57: ¹H NMR spectrum of (2-O-benzyl-3,4,6-tri-O-benzoyl-β-D-glucopyranosyl)ethylmethylsulfonium perchlorate (**5.4d**)

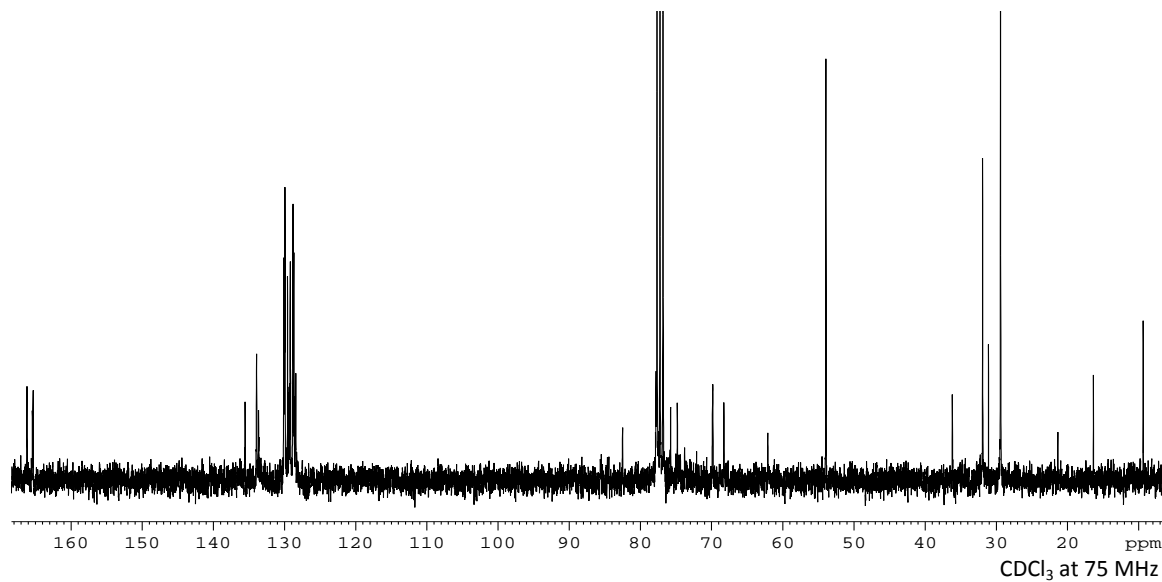


Figure A-58: ¹³C NMR spectrum of (2-O-benzyl-3,4,6-tri-O-benzoyl-β-D-glucopyranosyl)ethylmethylsulfonium perchlorate (**5.4d**)

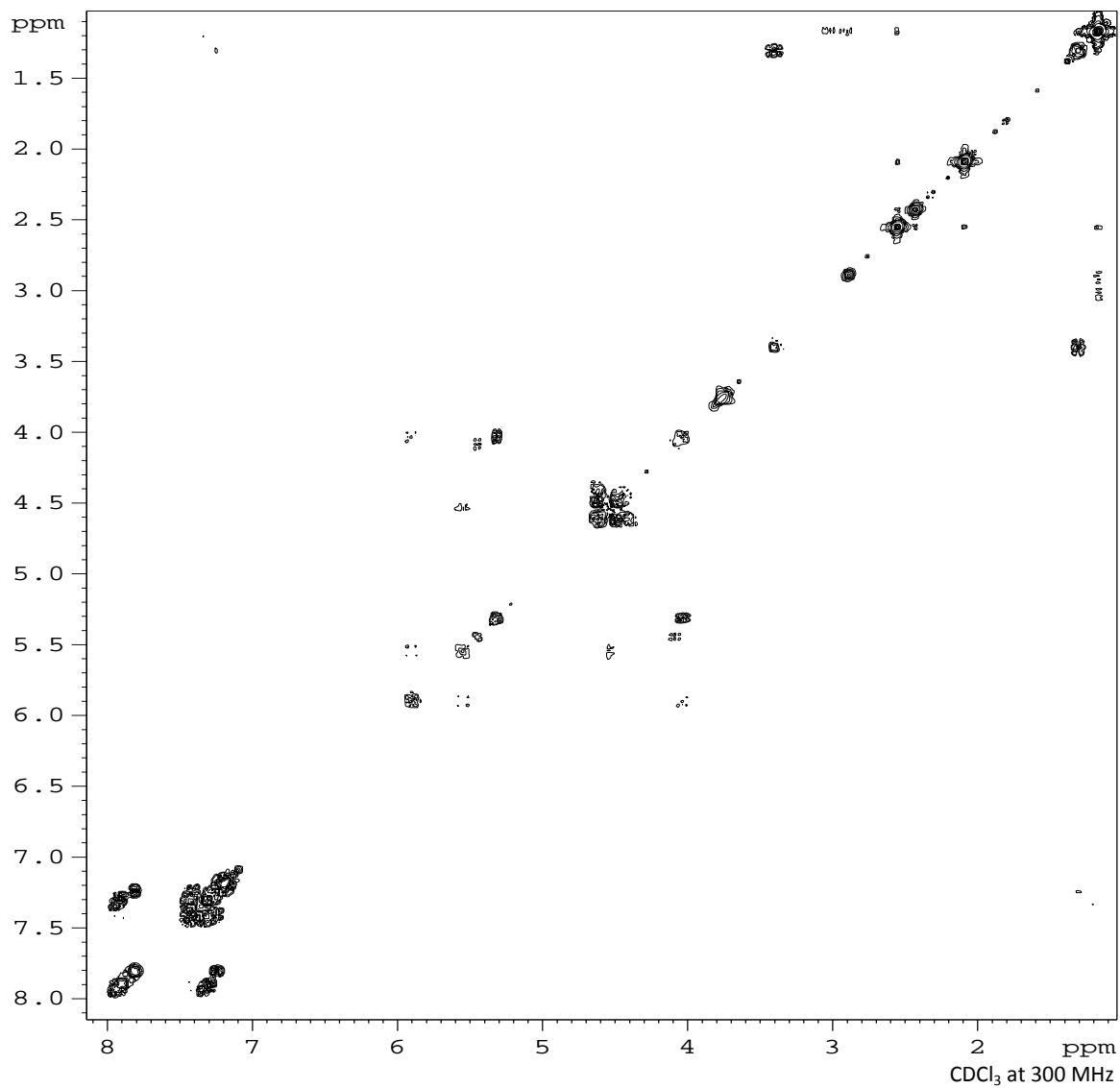
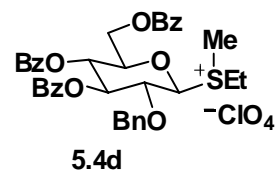


Figure A-59: 2-D NMR COSY spectrum of (2-O-benzyl-3,4,6-tri-O-benzoyl- β -D-glycopyranosyl)ethylmethylyulfonium perchlorate (**5.4d**)

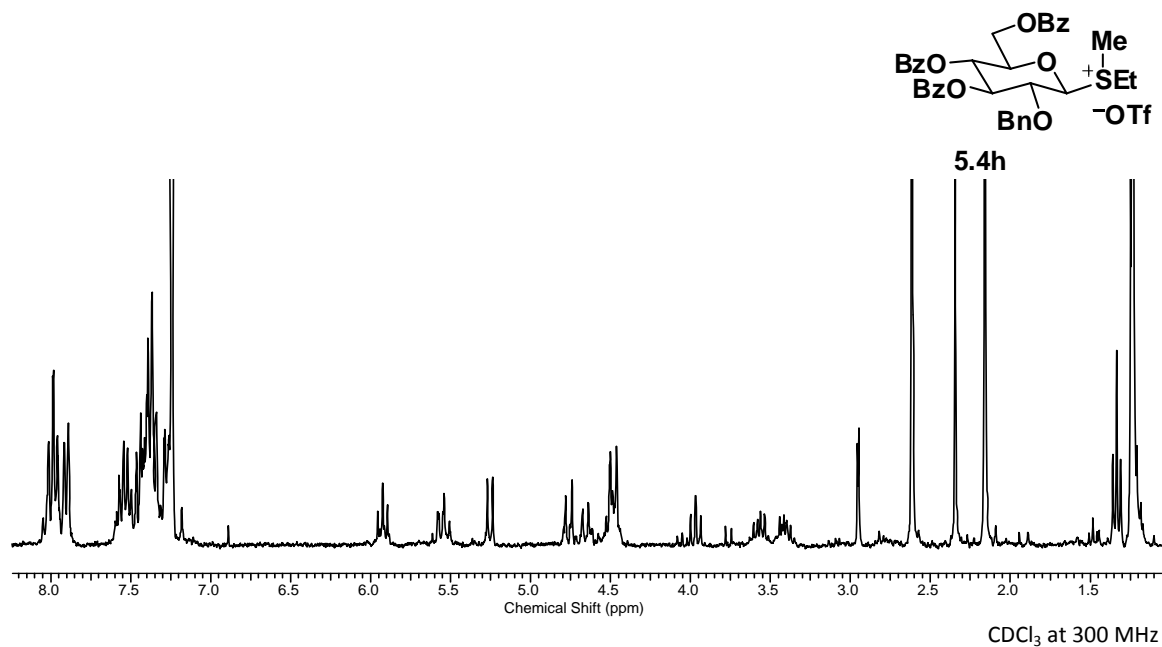


Figure A-60: ¹H NMR spectrum of (2-O-benzyl-3,4,6-tri-O-benzoyl-β-D-glucopyranosyl)ethylmethylsulfonium triflate (**5.4h**)

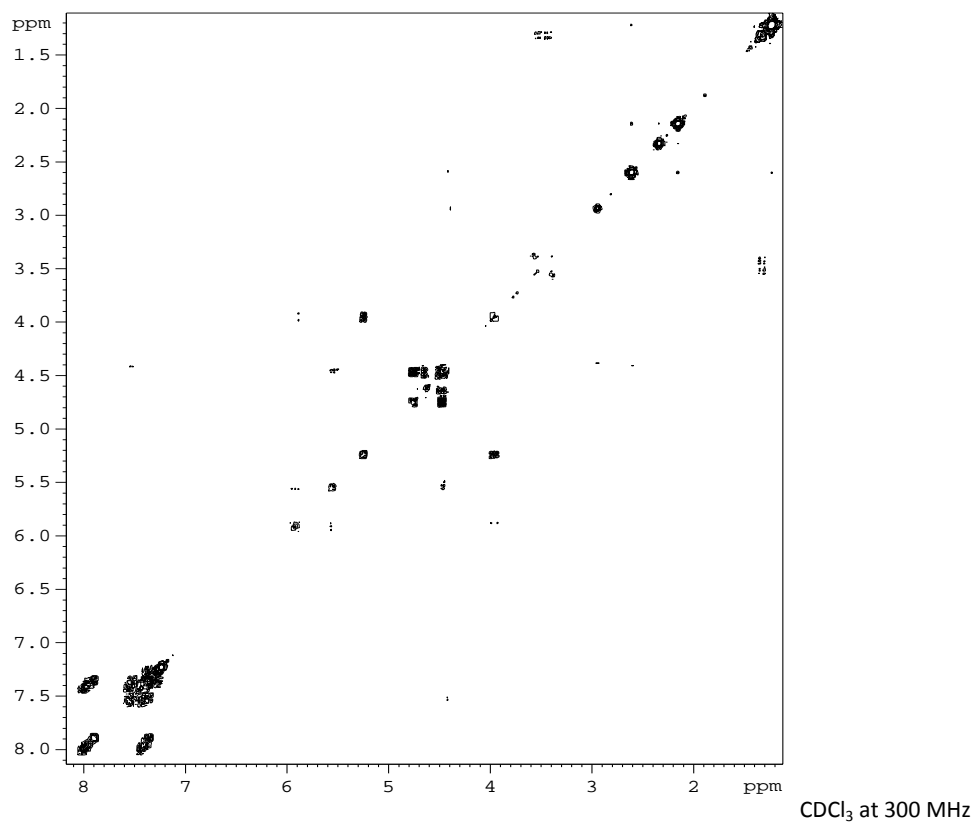


Figure A-61: 2-D NMR COSY spectrum of (2-O-benzyl-3,4,6-tri-O-benzoyl-β-D-glucopyranosyl)ethylmethylsulfonium triflate (**5.4h**)

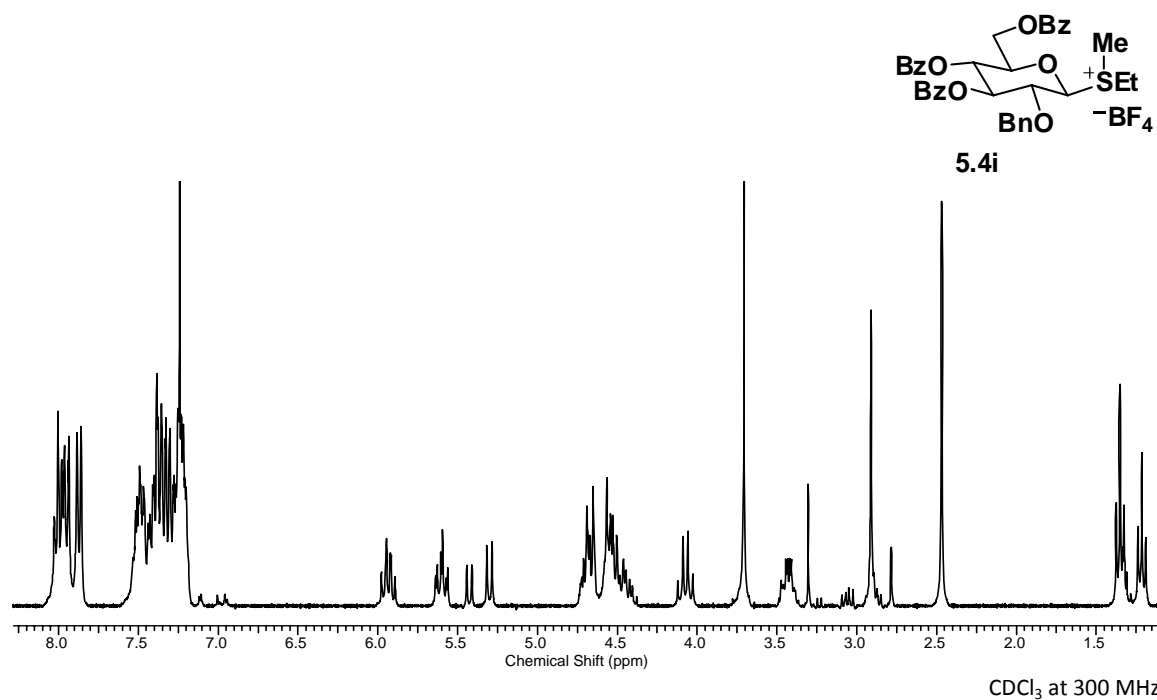


Figure A-62: ¹H NMR spectrum of (2-O-benzyl-3,4,6-tri-O-benzoyl-β-D-glucopyranosyl)ethylmethylium tetrafluoroborate (**5.4i**)

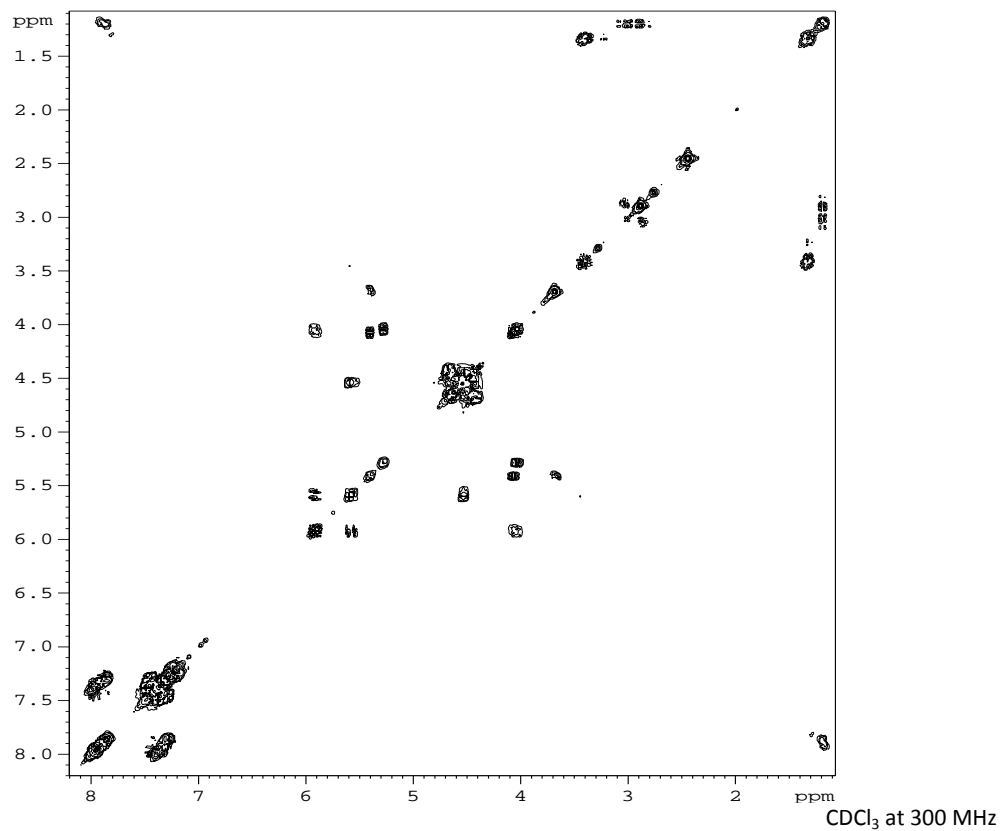


Figure A-63: 2-D NMR COSY spectrum of (2-O-benzyl-3,4,6-tri-O-benzoyl-β-D-glucopyranosyl)ethylmethylium tetrafluoroborate (**5.4i**)

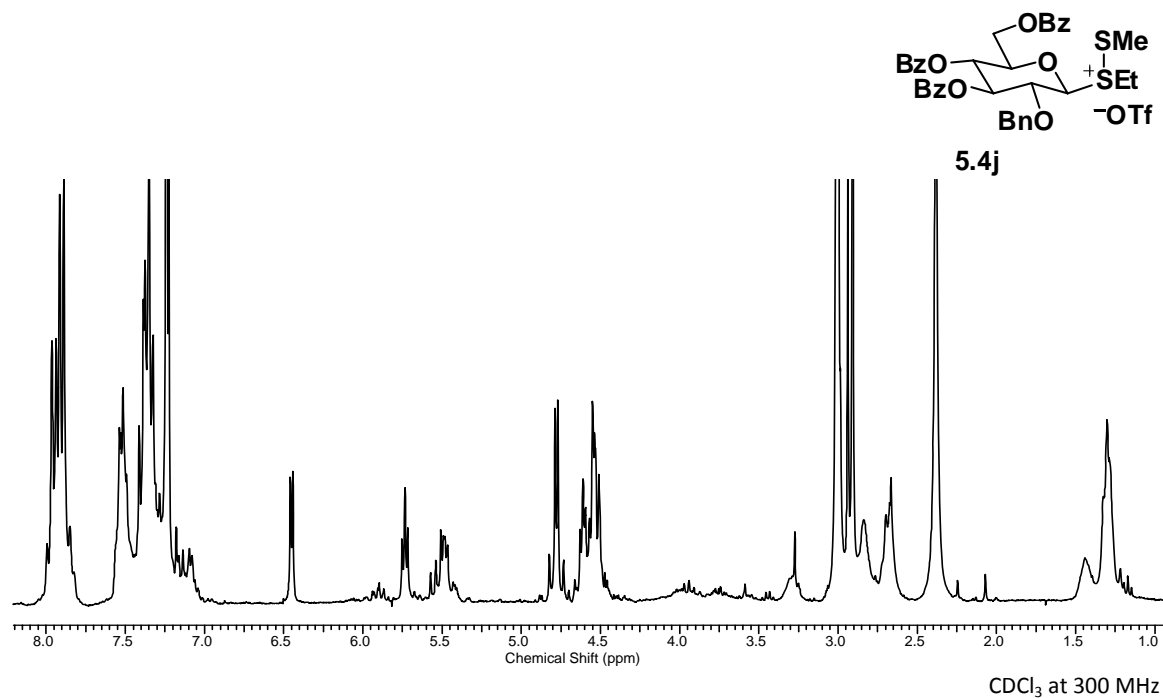


Figure A-64: Crude ¹H NMR spectrum of (2-O-benzyl-3,4,6-tri-O-benzoyl-β-D-glucopyranosyl)ethylthiomethylsulfonium triflate (**5.4j**)

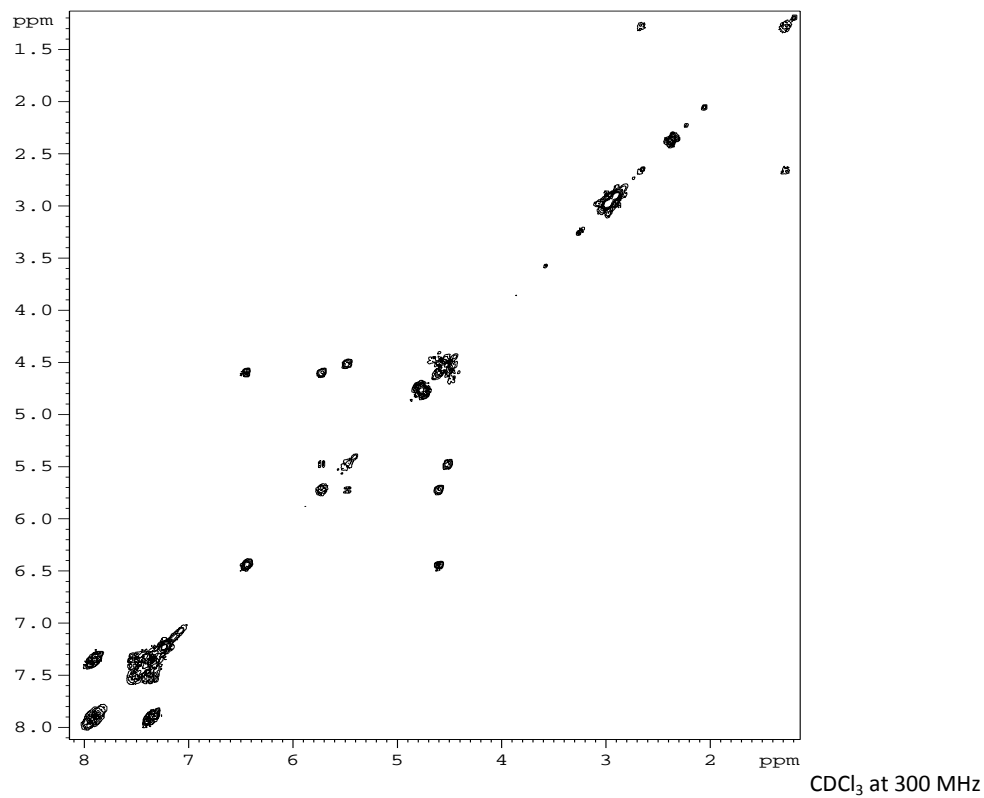


Figure A-65: Crude 2-D NMR COSY spectrum of (2-O-benzyl-3,4,6-tri-O-benzoyl-β-D-glucopyranosyl)ethylthiomethylsulfonium triflate (**5.4j**)

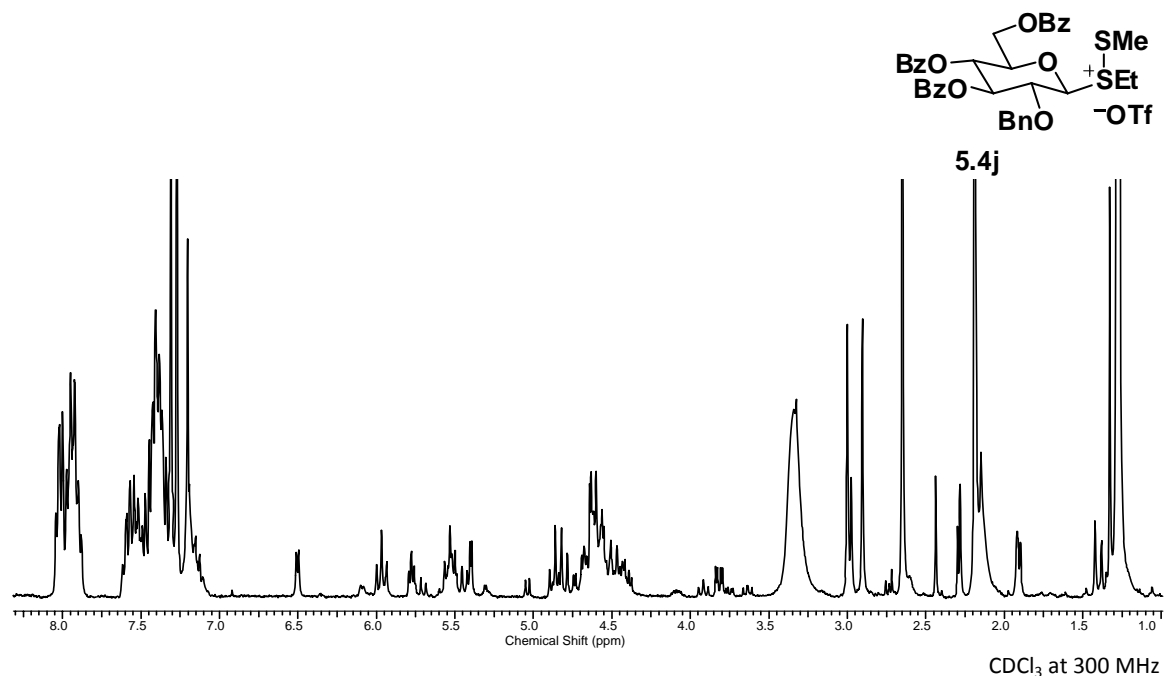


Figure A-66: Purified ^1H NMR spectrum of (2-O-benzyl-3,4,6-tri-O-benzoyl- β -D-glucopyranosyl)ethylthiomethylsulfonium triflate (**5.4j**)

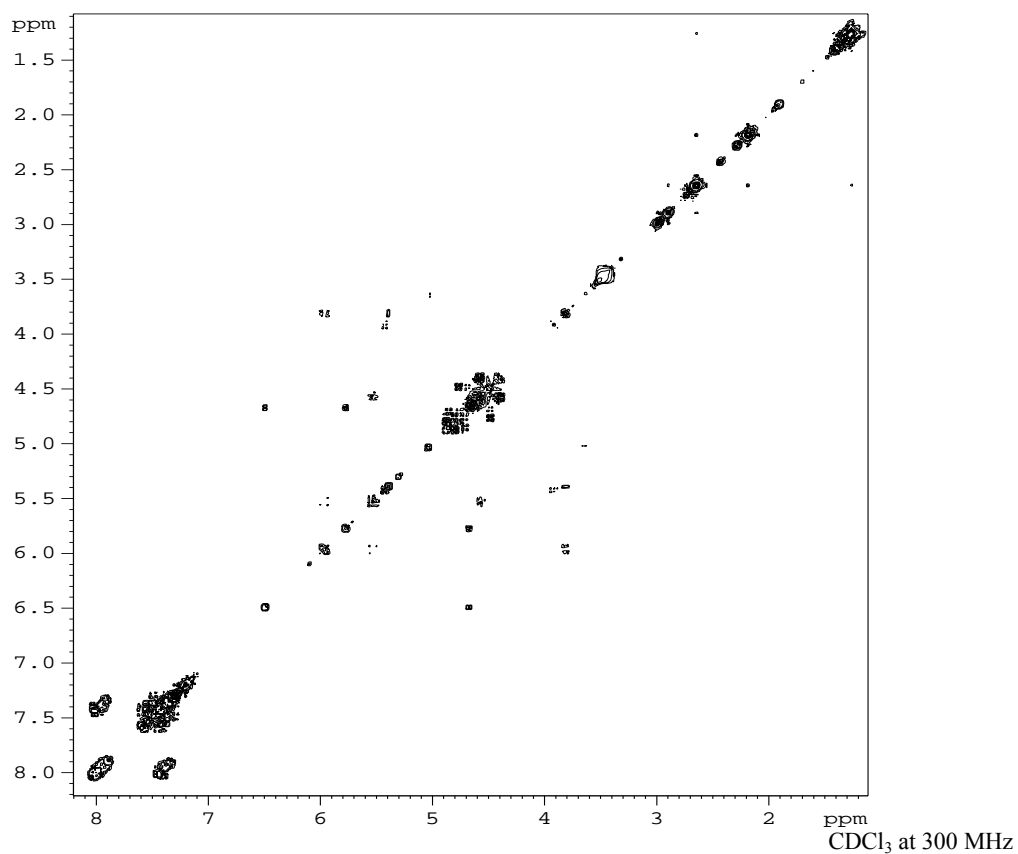


Figure A-67: Purified 2-D NMR COSY spectrum of (2-O-benzyl-3,4,6-tri-O-benzoyl- β -D-glucopyranosyl)ethylthiomethylsulfonium triflate (**5.4j**)

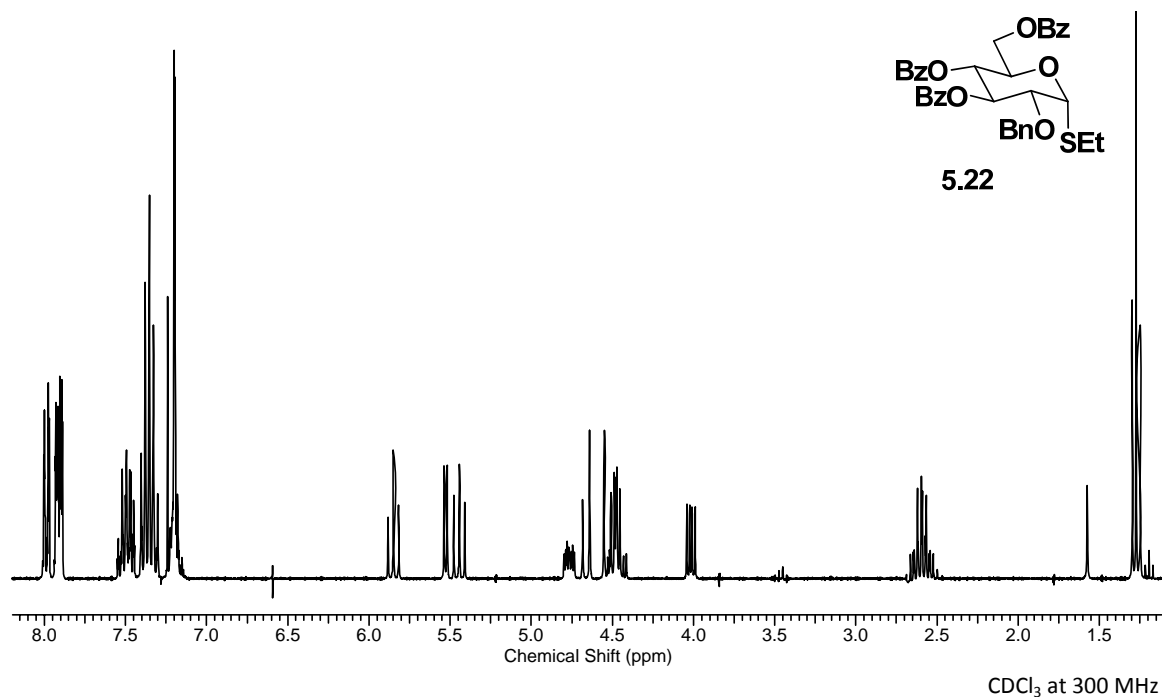


Figure A-68: ¹H NMR spectrum of Ethyl 2-O-benzyl-3,4,6-tri-O-benzyl-1-thio-α-D-glucopyranoside (**5.22**)

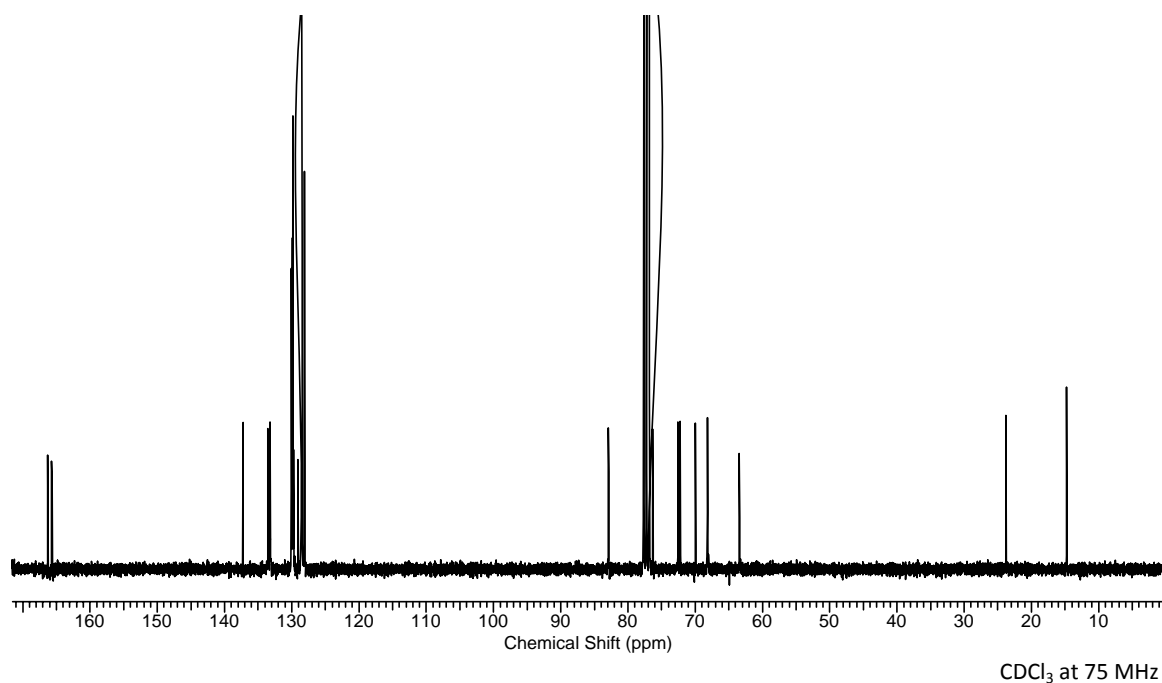


Figure A-69: ¹³C NMR spectrum of Ethyl 2-O-benzyl-3,4,6-tri-O-benzyl-1-thio-α-D-glucopyranoside (**5.22**)

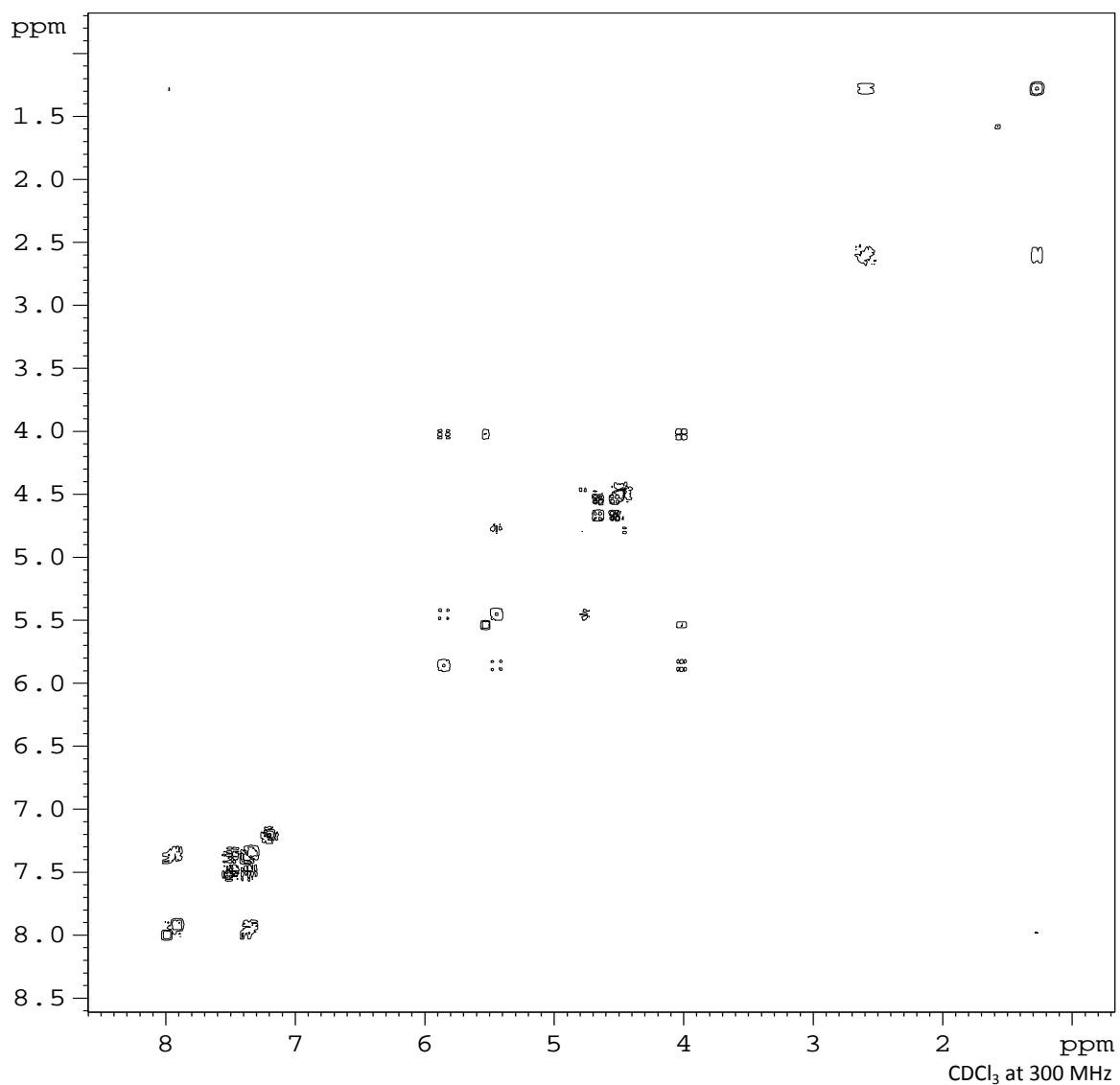
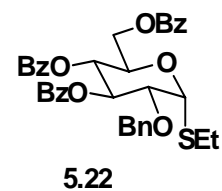


Figure A-70: 2-D NMR COSY spectrum of Ethyl 2-O-benzyl-3,4,6-tri-O-benzyl-1-thio- α -D-glucopyranoside (**5.22**)